AN ANALYTICAL AND EXPERIMENTAL STUDY OF

LARGE STRAIN SOIL CONSOLIDATION

by

Lee, Kuantsai

Linacre College, Oxford

A thesis submitted to the University of Oxford

for the degree of

Doctor of Philosophy

Trinity 1979

This thesis and the effort that went into producing it are dedicated to my parents and my brother Jitsai.

ACKNOWLEDGMENTS

Dr. G.C. Sills suggested this subject to me in 1976 and subsequently supervised me throughout the study. It is the effort, time, and above all, the patience and willingness she devoted to our frequent discussion which made this research a truly educational experience. For this I shall always be grateful.

I wish to mention my parents and my brother Jitsai here not just for their financial support, but mainly for the love and encouragement they have shown in supporting me. Thinking of them has always been a source of inspiration in my work. The dedication of this thesis to them is but a small token of my gratitude.

The staff and technicians in the Engineering Laboratory have provided invaluable help in this study. I owe special thanks to all my collegues in the Oxford Soil Mechanics Group, in particular to Mr. G. Austin for the practical advice he has offered me.

Finally, to Iju, for her patience and understanding during these difficult and not so difficult times.

ABSTRACT

An Analytical and Experimental Study of Large Strain Soil Consolidation

Lee, Kuantsai

Linacre College, Oxford

A thesis submitted to the University of Oxford for the degree of Doctor of Philosophy

Trinity 1979

This thesis is concerned with large strain soil consolidation and a large portion of the work is devoted to the theoretical development in modelling this phenomenon An experimental programme based on a specially designed oedometer is also included.

The governing equations are formulated in Chapter 2, where both the material and the space coordinates are considered. In space coordinate the problem is a moving boundary problem, and special numerical techniques for the idealized case of a thin soil layer are developed in Chapter 3.

In Chapter 4 the consolidation of a normally consolidated stratum and a dredged fill are considered with a linear soil model, and the consolidation of a deposit undergoing continuous sedimentation is considered in Chapter 5. The material coordinate is used in the analysis which also includes the effect of self weight of soil. These problems are again considered in Chapter 6 and Chapter 7 with a nonlinear soil model.

A specially designed oedometer for testing very soft soil is described in Chapter 8, and the experimental results are discussed in Chapter 9. These are compared with the theoretical solutions developed in Chapter 3, and good agreement has been obtained.

TABLE OF CONTENTS

CHAPTER ONE REVIEW OF PREVIOUS WORK ON LARGE STRAIN CONSOLIDATION THEORY AND SCOPE OF PRESENT WORK

1. INTRODUCTION

It is well known that Terzaghi and his consolidation theory brought the fourth dimension - time - into Soil Mechanics in 1923. The idea of effective stress and the consideration of its variation during the flow - coupled - deformation marked the birth of modern Soil Mechanics. The theory postulated that soil, idealized as a fluid saturated skeleton of solid particles, will deform under an external force field in a time-dependent manner. This time-dependent process is governed by the compressibility of the skeleton - which determines the amount of deformation that will take place - and the permeability of the soil, which determines how fast the pore water can seep out to allow deformation to take place. Thus, the theory explains the long term settlement behaviour often observed in engineering structures and provides a basis for an estimation to be made of the rate as well as the magnitude of settlement.

There are, inevitably, simplifications which Terzaghi has used in constructing his theory. The more obvious ones are constant compressibility and permeability - and it is doubtful whether any soil will behave like this when a substantial void ratio change has occured. Accordingly, a great number of efforts have been made to improve this by later workers, resulting in the so-called nonlinear consolidation theories. However, less obvious idealisations in his theory are that the flow and deformation are unlinked - this has been corrected by the linked theory (Biot 1935, Sills 1972) - and that there is a restriction to infinitesimal strain. In recent years the small strain restriction has started attracting attention, and a number of theories have been proposed. These will be briefly reviewed in later sections.

This thesis is concerned with the large strain consolidation theory, with the study being motivated by both practical

and theoretical demands. With the advent of modern technology, engineers now have to work with soils so soft that they would previously have been avoided. As an example, there is now an ever-growing consideration of the usage of reclaimed land. In these areas the soils are usually so soft that preconsolidation is necessary to gain enough strength for supporting building loads. The ability of an engineer to estimate how long the consolidation is going to take will be very valuable, and the best way to acquire such ability, other than experience, is with the aid of a theory. Up till now there are only a few large strain consolidation theories available, and only very simple cases have been considered in these theories. Further theoretical development is therefore in demand, and the bulk of this thesis will be devoted to this.

In this chapter the Terzaghi theory will be described first, with attention drawn to these assumptions restricting the theory to the small strain case. Possible ways of lifting the small strain restrictions will then be discussed in conjunction with a brief review of some previous work. Finally, the scope of the present work is outlined at the end of this chapter.

2. A REVIEW OF THE TERZAGHI THEORY

Terzaghi considered a saturated, homogeneous soil layer of infinite lateral extent with displacement and water flow occuring vertically, see Fig.1.1. When a uniform vertical loading is applied to this layer an initially uniformly distributed excess pore water pressure will be set up which causes water flow towards the drainage boundary.

This outward water flow causes a reduction of the total

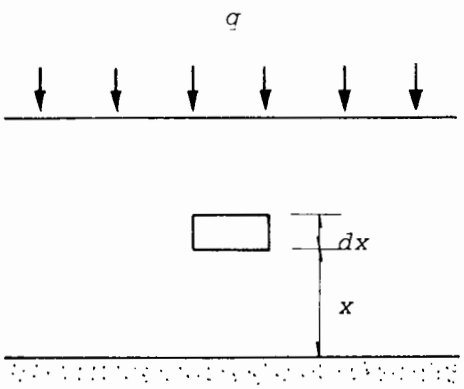

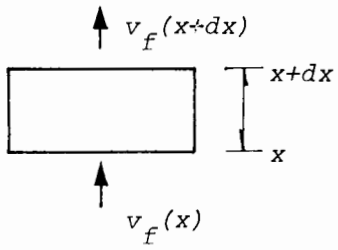

FIG.1.1 (left) A soil layer of infinite lateral extent

FIG.1.2 (right) A soil element with boundaries fixed in space

volume of the soil. In order to describe this mathematically, Terzaghi then proceeded to consider a small soil element within the layer as shown in Fig.1.2. This element has a unit cross sectional area normal to the direction of flow and is bounded by planes having fixed space coordinate x and $x+dx$. The law of mass conservation requires that the difference between the inward and outward water flow across this element be compensated by the change of water volume in this element. Thus :

$$-\frac{\partial v_f}{\partial x} = \frac{\partial V}{\partial t} \qquad (1.1)$$

where v_f is the flow velocity and V is the change of water volume in this element. Eq(1.1) is often referred to as the continuity equation. However, it should be noted that this equation describes only half the process. As flow takes place so does deformation, so there must also be solid particles moving in and out of the element. Otherwise if the total volume of solid particles remained unchanged in this element there can not be any change of the total volume of water, since the element has a fixed total volume. Another equation for the solid phase will be required for a complete description. This is omitted in the Terzaghi theory.

The next step Terzaghi took is to couple the flow velocity to the excess pore water pressure gradient by Darcy's law :

$$v_f = -\frac{k}{\rho_f}\frac{\partial u}{\partial x} \qquad (1.2)$$

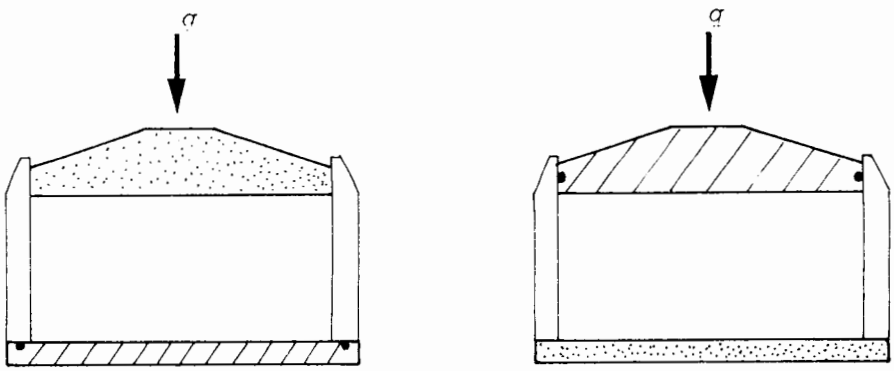

(a) drainage from the top *(b) drainage from the base*

FIG.1.3 Two standard consolidation tests with different drainage arrangements.

in which k is the permeability of the soil, ρ_f is the unit weight of water and u is the excess pore water pressure. Again the solid particle movement is not considered here and the flow velocity is taken as the absolute velocity rather than the relative velocity with respect to the solid skeleton. The fact that it is the relative velocity that should be linked with the excess pore pressure gradient can be demonstrated by a simple example. Fig.1.3 illustrates two standard consolidation tests with different arrangement for drainage. In Fig.1.3(a) the base is sealed and no flow can occur across it, and in Fig.1.3(b) the loading cap is sealed. These undrained faces are characterized by a zero excess pore pressure gradient, and in the case of Fig.1.3(a) no flow occurs in the base. In the case of Fig.1.3(b), however, as soon as the consolidation is started the loading cap will be moved, and so will the pore water and the solid adjacent to it. In other words, in the part near the loading cap the water can flow without the driving of any excess pore pressure gradient, and eq(1.3) is violated. However, if consideration is now given to the relative velocity between the pore water and the skeleton, then in the case of Fig.1.3(a) both the water and solid particles remain stationary in the base and there is no relative velocity between these two. In the case of Fig.1.3(b) both the

water and the solid particles will be moving with the cap in the same velocity, and again the relative velocity between these two is zero.

When eq(1,1) and eq(1.2) are combined together, the velocity term can be eliminated, which results in an equation :

$$\frac{\partial V}{\partial t} = \frac{\partial}{\partial x}\left(\frac{k}{\rho_f}\frac{\partial u}{\partial x}\right) \qquad (1.3)$$

It should be noted that neglecting the solid particle movement in eq(1.1),(1.2) introduces a certain error in each stage with a magnitude dependent upon the amount of strain. However, when these two equations are combined together these errors happened to cancel each other , resulting in a correct expression (Gibson, England and Hussey 1967).

Having obtained this equation, he then postulated that because of the one dimensional condition, the change of water volume equals the strain developed in the element. However, this is only true in the case of infinitesimal Lagrangian strain (the Lagrangian strain is defined as $\Delta l / l_o$). This is because of the assumption that the element has a fixed space coordinate.

The strain is linked to the effective stress by the coefficient of compressibility m_v , and by further assuming that the total stress remains constant the governing equation results :

$$\frac{\partial u}{\partial x} = C_v \frac{\partial^2 u}{\partial x^2} \qquad (1.4)$$

where C_v is the coefficient of consolidation defined as :

$$C_v = \frac{k}{\rho_f m_v} \qquad (1.5)$$

and both the compressibility m_v and the permeability k are assumed to be as constants in this case.

Terzaghi then applied this governing equation(1.4) to the soil layer which is initially bounded by $x = 0$ and $x = h_o$, and found solutions by satisfying the equation within these fixed boundaries. It is obvious that as soon as consolidation starts the whole layer will be compressed, and thus the boundary position will be changed as consolidation proceeds. To take this into account the governing equation should be satisfied in a moving boundary rather than the fixed, initial boundaries. It is only when the total compression is very small that satisfying the governing equation in the initial, fixed boundaries can be used as a reasonable approximation.

In summary, the restriction of small strain to the Terzaghi theory is caused by :

(1) Neglecting the movement of solid particles.
(2) Defining strain in an element of a fixed volume.
(3) Ignoring the boundary movement as consolidation occurs.

Condition (1) and (2) above can be removed by carefully formulating the theory and choosing the correct parameter as the governing variable. The moving boundary nature of the problem, condition (3), appears to be most difficult and previous workers have chosen to use some form of material coordinate to transform the problem into one with a fixed boundary. These will now be described.

3. A BRIEF REVIEW OF SOME PREVIOUS WORK

The small strain restrictions were first removed by McNabb (1960). He defined an entirely different coordinate system as :

".....Let us define z to be the volume of the skeleton of the clay bounded by a cylinder S of unit cross sectional area with its axis in the direction of consolidation, and the two planes ζ, z fixed

relative to the skeleton....."

(McNabb, 1960, p338, line 16-19)

An immediate advantage of using this coordinate system is that, by the fact that the layer always contains the same amount of solid particles, the governing equation so formulated need only be satisfied within a fixed boundary. The problem with solid particle movement is also overcome as there will be no solid particle moving across the material boundaries, and he uses the void ratio as the governing parameter which is directly related to the change of water volume. The governing equation he derived is : (note that some notations have been changed from his original paper in order to confirm with the notations used in this thesis)

$$\frac{\partial e}{\partial t} = -\frac{\partial}{\partial z}\left(\frac{k}{\rho_f(1+e)}\frac{\partial \sigma'}{\partial z}\right) \qquad (1.6)$$

where e is the void ratio, σ' is the effective stress and z is the material coordinate. It should be noted that in this equation the effect of self weight of soil is not included.

Based on this equation McNabb has examined several cases. These include a semi-infinite layer and a standard consolidation test (the thin layer). In the latter case the effect of secondary compression is also considered. Approximate solutions, appropriate for small and large times, have been obtained in most cases.

Three years after McNabb's work Mikasa (1963) proposed a large strain consolidation theory based on a different approach. This approach follows closely that of the Terzaghi theory and the Eulerian strain ε (defined as $\Delta l/l$) is used as the governing parameter. In his theory also the movement of solid particles has been omitted. However, as before, this effect cancels with the incorrect form of Darcy's law to give the final governing equation.

This is :

$$\frac{\partial \varepsilon}{\partial t} = \frac{\partial}{\partial x}\left(c_v \frac{\partial \varepsilon}{\partial x} \right) \qquad (1.7)$$

where c_v has the same definition as eq(1.5). Note that, in this case both the compressibility and the permeability may not necessarily be taken as constants.

Since this equation is formulated in the space coordinate the moving boundary nature of the problem must be considered. This is done by defining a new governing parameter ζ :

$$\zeta = \frac{x}{x_o} \qquad (1.8)$$

which he defines as the consolidation ratio. x and x_o in the equation are respectively the locations (in space) of a particular material point in the initial (undeformed) and current states. The consolidation ratio is related to the Eulerian strain ε by :

$$d\varepsilon = \frac{d\zeta}{\zeta} \qquad (1.9)$$

and the current space coordinate x can be transformed to the initial, undeformed space coordinate x_o by :

$$x = \zeta x_o \qquad (1.10)$$

He can thus reformulate eq(1.7) using ζ and x_o as :

$$\frac{\partial \zeta}{\partial t} = \zeta^2 \frac{\partial}{\partial x_o}\left(c_v \frac{\partial \zeta}{\partial x_o} \right) \qquad (1.11)$$

and a solution is sought in the initial fixed boundaries $x_o = 0$ and $x_o = h_o$.

Mikasa also considered the case including the effect of self weight of soil with the resulting equation :

$$\frac{\partial \zeta}{\partial t} = \zeta^2 \{ C_v \frac{\partial^2 \zeta}{\partial x_o^2} + \frac{d C_v}{d \zeta} (\frac{\partial \zeta}{\partial x_o})^2 - \frac{d}{d\zeta} (C_v m_v (\rho_s - \rho_f)) \frac{\partial \zeta}{\partial x_o} \} \qquad (1.12)$$

Having obtained these equations he then examined several cases numerically, including a thin layer and a thick layer, by a finite difference scheme.

It should be noted that although the coordinate x_o he uses refers to the space position, it is also a type of material coordinate, since reference to a point in space must be traced back to its initial undeformed state which the material at this point previously occupied. The difference between this coordinate x_o and the solid thickness z used by McNabb will depend on the initial distribution of void ratio.

These two approaches by McNabb and Mikasa were later combined by Gibson, England and Hussey (1967), in which the initial undeformed coordinate x_o was used to derive the continuity equation of a material element, and the final governing equation was formulated in the solid thickness z to achieve a more compact formulation. As a very large part of the present work uses this equation, a detailed derivation of this will be referred to the next chapter.

In their theory, Gibson et. al. considered a thin soil layer, i.e. one in which the effect of self weight is not included, and defined therefrom a new coefficient of consolidation C_F . The linear case of a constant C_F and a weakly nonlinear case of a variable C_F have been examined in their work analytically and numerically. The same nonlinear case was later studied by Poskitt (1969) using the technique of perturbation, and Berry and Poskitt (1972) have extended the consideration to include secondary

compression effect. The governing equation has been solved numerically by De Simone and Viggiani (1976) using the finite difference method and by Monte and Krizek (1976) using the finite element method, and in both these cases nonlinear stress-strain and permeability-void ratio relationships have been considered.

4. SCOPE OF PRESENT WORK

The development of large strain consolidation theory up to the time when the present study commenced was dominated by the use of the material coordinate and the analysis has concentrated on the idealized case of a thin soil layer. In the situation where the variation of material properties in space is required, such as the distribution of excess pore water pressure, the transformation from the material to the space coordinate can be difficult. In such situations a theory based on the space coordinate will be more suitable.

It is debatable whether the effect of self weight can be neglected in a theory concerned with large strain. The large strain is mostly likely to occur in a very soft clay, and in such a material the additional stress due to self weight may be appreciable. There is another type of problem where the consolidation is caused entirely by the self weight of the soil, including cases such as the consolidation of a dredged fill or a deposit undergoing continuous deposition. These problems will become more important in the near future and yet there is no solution available. These are theoretical developments which are not currently available and which the present work is intended to consider.

There is also a lack of laboratory evidence to support

the theories. The work of McNabb, Mikasa, and Gibson et al. all pointed out that in a standard consolidation test the settlement of the specimen will behave like $\sqrt{t}$ regardless of the magnitude of strain and the variation of material properties. A well planned experiment will therefore provide invaluable comparison with the theories. However, there was no adequate equipment that can faithfully accomodate a very soft specimen and produce a very large strain.

In view of these, the scope of the present work is :

(1) To formulate a theory based on the space coordinate and to develop solution techniques for the thin layer.
(2) To investigate the effect of self weight on the consolidation behaviour of a stratum and to solve problems using material coordinate with transformation to space coordinate. In particular, these include the consolidation of a dredged fill under its own weight and the consolidation of a deposit undergoing continuous sedimentation.
(3) To develop suitable laboratory equipment for testing very soft specimen to a very large strain.
(4) To compare experimental results with theoretical thin layer solutions.

The organisation of this thesis follows the same sequence as (1) to (4) above. In Chapter 2 governing equations based on the space and the material coordinates will be derived. Numerical techniques for solving the equation based on the space coordinate are developed in Chapter 3 for the particular case of a thin layer. The next four chapters are concerned with the consolidation including the effect of self weight using material coordinate and two soil models will be developed with several cases examined analytically and numerically. Finally, in Chapter 8 and 9 a specially developed oedometer will be described and some experimental results will be compared with available theoretical solutions.

ABSTRACT

The governing equation for the one dimensional consolidation of soil is developed in this chapter. The soil is assumed to be saturated, homogeneous and to obey a generalized Darcy's law which takes into account the movement of solid particles. In the present formulation creep effect of the soil skeleton under a sustained loading is not considered.

The theory is formulated first in terms of a space coordinate and then a material coordinate, associated respectively with the names of Eulerian and Lagrangian. In order that the theory need not be restricted to small strains the governing equation derived in the Eulerian coordinate is satisfied in a moving region due to the compression of the soil layer. To complete the formulation another equation which describes the boundary movement has also been derived. Such a problem does not arise in the Lagrangian coordinate system. Consequently this leads to a more effective formulation, and the governing equation is identical to that of Gibson, England and Hussey (1967). Finally, comparison is made between the two formulations at the end of this chapter.

1. INTRODUCTION

The study of soil consolidation is concerned with the variation of void ratio and other soil parameters with time and space. To understand such a complicated phenomenon it is necessary to develop a proper theoretical model such that the actual behaviour of soil can be predicted and comparisons made. Any deviation of the predictions from the actual observations will therefore lead to further refinement of the theoretical model which may eventually improve the present state of knowledge. This and the following five chapters are concerned with the construction of theoretical models : the governing equation for soil consolidation is derived in this chapter and the subsequent chapters will apply this governing equation to various soil models with different initial and boundary conditions that simulate a wide range of engineering problems.

In order that the theory is not restricted to the classical small strain assumption care must be taken to ensure that a consistent space coordinate system is used. There are two types of space : the Eulerian and the Lagrangian space. The Eulerian space is a global, external space and the Lagrangian space is a local, interior space. This is illustrated by the example of a soil layer shown in Fig.2.1.

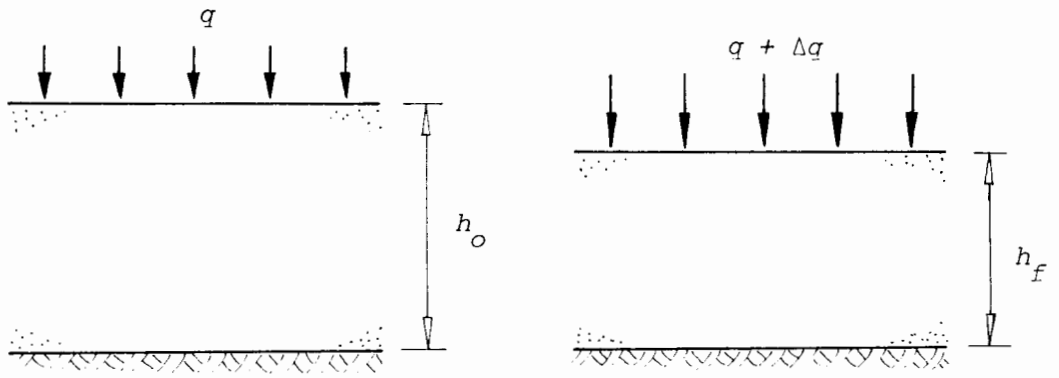

FIG.2.1 A soil layer (a) before (left) and (b) after (right) consolidation.

CHAPTER TWO FORMULATION OF LARGE STRAIN CONSOLIDATION THEORIES

In Fig.2.1(a) the layer is in an equilibrium state and it can be described by either its thickness in space or the number of solid particles in it. In Fig.2.1(b) the same layer is consolidated to a new state of equilibrium, its thickness in space is now different from its original state, Fig.2.1(a), while the number of solid particles it contains still remains the same. The thickness is in fact the coordinate of the soil layer in the Eulerian space, and the number of solid particles is a coordinate in the Lagrangian space. In this particular example it is seen that as the soil layer undergoes deformation its Eulerian coordinate is changing with the deformation while its Lagrangian coordinate remains invariant. As a matter of fact deformation can only be defined and observed in the Eulerian space.

The number of solid particles is just one of the many possible ways of describing the Lagrangian coordinate. For the purpose of analysis it is better to use the concept of solid thickness. A similar concept is very often descibed in textbooks of Soil Mechanics with the definition of void ratio whereby a soil element is conceptually divided into its solid and void components, see Fig.2.2(a). This conceptual division is extended to the soil layer just considered, see Fig.2.2(b), where it can be seen that this solid thickness also remains invariant regardless of the amount of deformation that might occur.

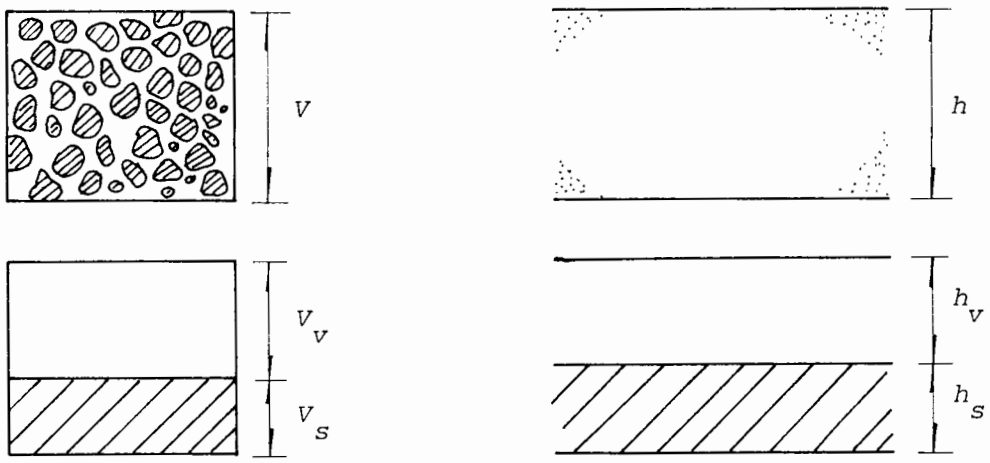

FIG.2.2 (a) left, concept of void ratio

(b) right, concept of the solid thickness of a stratum

The theory of consolidation can be formulated in either of the two coordinates. The Lagrangian coordinate has the advantage of invariance under deformation. However, in practice predictions of consolidation are often required with reference to fixed points in space where the Eulerian coordinate formulation is preferable. For this reason both the Eulerian and the Lagrangian formulations will be developed in this chapter.

When using the Eulerian formulation it is important to realise that the position of the soil layer in space is changing as consolidation proceeds. To take this into account the governing equation is satisfied in a moving region, i.e. that occupied by the soil layer, so that consistency is observed. It may be noted that, in the case of infinitely small strain, the boundary in the Eulerian system is assumed to be fixed at some coordinate value, and the two formulations are then equivalent. In this aspect the classical Terzaghi theory and its nonlinear versions will be inconsistent but approximate only in the small strain case.

2. FORMULATION BASED ON THE EULERIAN COORDINATE

The Eulerian coordinate is a global, external system, i.e. it is so defined that several objects in different locations in space can be located relative to each other. This is the most commonly used system. When considering the deformation of a continuum, the formulation is based on a volume element identified by its position in space. The material that currently occupies this element will change as deformation occurs. In soil consolidation the actual region occupied by the soil will change from time to time as a result of settlement during consolidation. Hence,

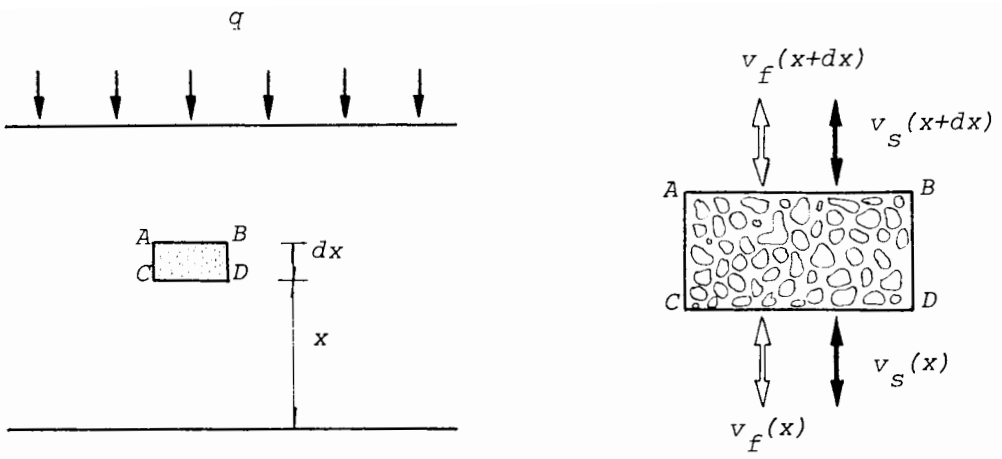

FIG.2.3 A soil layer of infinite lateral extent (left) and a volume element with boundaries fixed in space (right).

the governing equation formulated in this coordinate is valid only within a moving region. The boundary of this moving region is part of the solutions that are sought. This type of problem has been known mathematically as the moving boundary, or the Stefen problem, in which many different physical problems are included. Some examples of this are the melting of ice, freezing of water and solidification of steel (Ockendon and Hodgkins 1975).

Continuity of Solid and Fluid Phase

Consider a saturated, homogeneous soil stratum of infinite lateral extent where drainage and settlement occur one-dimensionally and coincide with the direction of applied stress and gravity. Within this, define a volume element $ABCD$ fixed in space with unit cross sectional area normal to the direction of flow and bounded by planes x and $x + dx$, Fig.2.3. The continuity of solid phase within this element requires the net volumetric flux of solid across the boundaries to be equal to the time rate of change of solid volume within this element, i.e.

$$v_s(x) - v_s(x+dx) = \frac{\partial}{\partial t}[(1-n)dx] \qquad (2.1)$$

where n is the porosity and v_s the apparent velocity of the solid phase.

Expanding the term $v_s(x+dx)$ in eq(2.1) and passing to the limit $dx \to 0$ lead to :

$$\frac{\partial}{\partial x}(v_s) + \frac{\partial}{\partial t}(1-n) = 0 \qquad (2.2)$$

which is the continuity equation of the solid phase.

The continuity equation for the fluid phase can be obtained similarly as :

$$\frac{\partial}{\partial x}(v_f) + \frac{\partial n}{\partial t} = 0 \qquad (2.3)$$

where v_f is the apparent velocity of the fluid phase.

Combining eq(2.2),(2.3) yields a relationship between the apparent solid and fluid velocities :

$$\frac{\partial}{\partial x}(v_s + v_f) = 0 \qquad (2.4)$$

or :

$$v_s + v_f = f(t), \quad 0 \leq x \leq s(t) \qquad (2.4)a$$

where $f(t)$ is a function of time t, and $s(t)$ is the current thickness of the stratum. Clearly, the continuity equations (2.2),(2.3) are also satiafied within this region $0 \leq x \leq s(t)$.

The Generalized Darcy's Law

The flow of water through the soil is governed by Darcy's law, which is :

$$n(\tilde{v}_f - \tilde{v}_s) = - \frac{k}{\rho_f} \frac{\partial u}{\partial x} \qquad (2.5)$$

where k is the permeability, u the excess pore water pressure and $\tilde{v}_s$ and $\tilde{v}_f$ are, respectively, the true velocity of the solid and fluid phases. These are related to the apparent velocities by :

$$n \tilde{v}_f = v_f \qquad (2.6)$$

and :

$$(1-n) \tilde{v}_s = v_s \qquad (2.7)$$

Eq(2.5) can be written in terms of the apparent velocities v_f and v_s as :

$$v_f - n(v_f+v_s) = - \frac{k}{\rho_f} \frac{1}{(1+e)} \frac{\partial u}{\partial x} \qquad (2.8)$$

where e is the void ratio.

Differentiating both sides of eq(2.8) with respect to x leads to :

$$\frac{\partial n}{\partial t} + (v_f+v_s) \frac{\partial n}{\partial x} = \frac{\partial}{\partial x} \left[\frac{k}{\rho_f} \frac{1}{(1+e)} \frac{\partial u}{\partial x} \right] \qquad (2.9)$$

which involves the term (v_f+v_s) . Three different boundary conditions can be distinguished :

(a) Drainage from the moving boundary only, Fig.2.4(a)

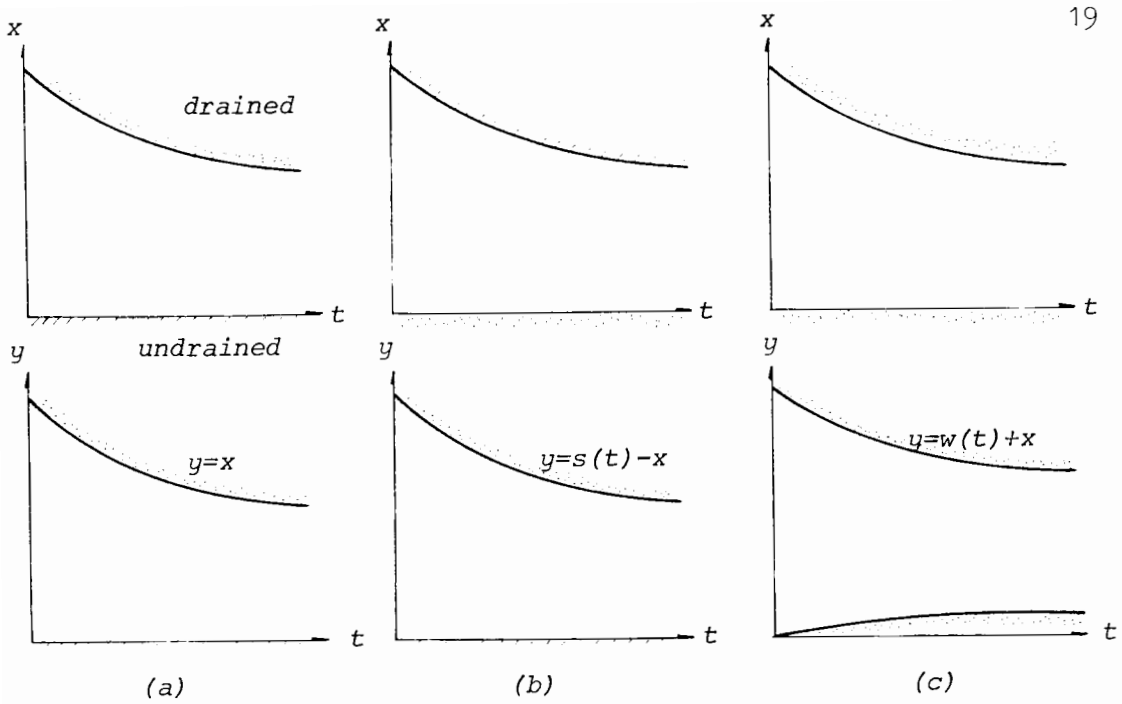

FIG.2.4 Three different arrangements of drainage condition. The lower graphs show the new variable y in terms of which all three cases will have the same governing equation.

In this case consider the fixed (undrained) boundary where both v_s and v_f are zero. It follows from eq$(2.4)_a$ that :

$$v_s + v_f = 0, \quad 0 \leq x \leq s(t)$$

and eq(2.9) becomes :

$$\frac{\partial n}{\partial t} = \frac{\partial}{\partial x}\left[\frac{k}{\rho_f}\,\frac{1}{(1+e)}\,\frac{\partial u}{\partial x}\right] \tag{2.10}$$

(b) Drainage from the fixed boundary only, Fig.2.4(b).

At the fixed boundary, $v_s = 0$, and since this is the only drainage face, the apparent fluid velocity v_f must equal the settlement rate $\dot{s}$. Therefore, eq$(2.4)_a$ becomes,

$$v_f + v_s = \dot{s} \quad , \quad 0 \leq x \leq s(t)$$

from which eq(2.9) becomes :

$$\frac{\partial n}{\partial t} + \dot{s}\,\frac{\partial n}{\partial x} = \frac{\partial}{\partial x}\left[\frac{k}{\rho_f}\,\frac{1}{(1+e)}\,\frac{\partial u}{\partial x}\right] \tag{2.11}$$

This can however be further simplified by defining a new space variable y such that :

$$y = s(t) - x$$

which has the effect of exchanging the two boundaries. Eq(2.11) in terms of this new variable becomes :

$$\frac{\partial n}{\partial t} = \frac{\partial}{\partial y}\left[\frac{k}{\rho_f}\frac{1}{(1+e)}\frac{\partial u}{\partial y}\right] \qquad (2.12)$$

which is identical to eq(2.10). Note that after this transformation y will be in the same region as x, $0 \leq y \leq s(t)$, and the drainage boundary is now located at $y = s(t)$. In this sense the present case is identical to the boundary condition (a).

(c) Drainage from both fixed and moving boundaries, Fig.2.4(c).

Consider again the fixed boundary where $v_s = 0$ and $v_f = -\dot{w}(t)$, where $\dot{w}(t)$ is the rate of fluid flow from this boundary. Thus ;

$$v_s + v_f = -\dot{w}(t), \quad 0 \leq x \leq s(t)$$

and eq(2.9) becomes,

$$\frac{\partial n}{\partial t} - \dot{w}(t)\frac{\partial n}{\partial x} = \frac{\partial}{\partial x}\left[\frac{k}{\rho_f}\frac{1}{(1+e)}\frac{\partial u}{\partial x}\right] \qquad (2.13)$$

A new variable y is defined by :

$$y = x + w(t), \quad w(0) = 0 \qquad (2.14)$$

which will transform the region into one with two moving boundaries $w(t) \leq y \leq w(t)+s(t)$. Eq(2.13) then reads :

$$\frac{\partial n}{\partial t} = \frac{\partial}{\partial y}\left[\frac{k}{\rho_f}\frac{1}{(1+e)}\frac{\partial u}{\partial y}\right] \qquad (2.15)$$

which is again identical to eq(2.10),(2.12). Therefore, in the subsequent analysis it is sufficient to consider eq(2.10) only.

The Governing Equation

Eq(2.10) establishes the relationship between the time rate of change of porosity and the excess pore pressure gradient. From the principle of effective stress :

$$\sigma = \sigma' + p \tag{2.16}$$

where σ and σ' are the total and effective stresses and p is the pore water pressure,

$$p = u + u_h \tag{2.17}$$

where u_h is the hydrostatic pressure. Hence ;

$$\frac{\partial u}{\partial x} = \frac{\partial \sigma}{\partial x} - \frac{\partial \sigma'}{\partial x} - \frac{\partial u_h}{\partial x} \tag{2.18}$$

The total stress within the soil stratum is made up of two components, that arising from the weight of soil and that due to the applied stress $q(x,t)$. Therefore :

$$\frac{\partial \sigma}{\partial x} = - \frac{1}{(1+e)} (G_s + e) \rho_f + \frac{\partial q}{\partial x} \tag{2.19}$$

with x measured against gravity and G_s the specific gravity of the solid particle, this being assumed constant throughout the analysis. The hydrostatic gradient is :

$$\frac{\partial u_h}{\partial x} = - \rho_f \tag{2.20}$$

and it follows that :

$$\frac{\partial u}{\partial x} = -\frac{\partial \sigma'}{\partial x} - \frac{1}{1+e}(\rho_s - \rho_f) + \frac{\partial q}{\partial x} \qquad (2.21)$$

In the absence of secondary time effects, the effective stress will be a unique function of void ratio, thus :

$$\frac{\partial \sigma'}{\partial x} = \frac{d\sigma'}{de}\frac{\partial e}{\partial x} \qquad (2.22)$$

Substituting eq(2.21),(2.22) into eq(2.10) leads to a general governing equation in terms of the porosity n :

$$\frac{\partial n}{\partial t} = -\frac{\partial}{\partial x}\left[\frac{k}{\rho_f}(1+e)\frac{d\sigma'}{de}\frac{\partial n}{\partial x} \right] - \{(G_s-1)$$

$$\frac{d}{dn}[k(1-n)^2] - \frac{\partial q}{\partial n}\frac{d}{dn}\left[\frac{k}{\rho_f}(1-n)\right]\}\frac{\partial n}{\partial x} + \frac{k}{\rho_f}\frac{\partial^2 q}{\partial x^2}(1-n) \qquad (2.23)$$

In the case of a thin soil layer the self weight of soil is negligible compared with the applied stress q which will be uniformly distributed within the specimen. In this situation, eq(2.21) will be replaced by :

$$\frac{\partial u}{\partial x} = \frac{\partial \sigma}{\partial x}$$

and the governing equation is then :

$$\frac{\partial n}{\partial t} = \frac{\partial}{\partial x}\left[\left(-\frac{k}{\rho_f}(1+e)\frac{d\sigma'}{de}\right)\frac{\partial n}{\partial x}\right] \qquad (2.24)$$

It is interesting to note that the term $-\frac{k}{\rho_f}(1+e)\frac{d\sigma'}{de}$ is closely related to the Terzaghi's coefficient of consolidation C_V when the definition of the compressibility m_v is such that :

$$m_v = \frac{d\varepsilon}{d\sigma} = -\frac{1}{1+e}\frac{de}{d\sigma'} \qquad (2.25)$$

where ε is the (Eulerian) strain.

Therefore, eq(2.24) can be abbreviated as :

$$\frac{\partial n}{\partial t} = \frac{\partial}{\partial x}\left(C_v \frac{\partial n}{\partial x} \right) \qquad (2.26)$$

with,

$$C_v = \frac{k}{\rho_f m_v} \qquad (2.27)$$

Although this equation is of the same form as Terzaghi's, two important distinctions can be made. Firstly, the dependent variable is the porosity and variations of permeability and compressibility are included in the coefficient of consolidation and need not be restricted to any particular form. Secondly, the equation will be satisfied within moving boundaries, whose position depends on the final strain, and will be different for different applications.

These differences will produce different solutions in the present case compared with Terzaghi's. When these solutions are used to interpret the coefficient of consolidation C_v from experimental results then a different value from that obtained by Terzaghi's solution will result.

The Moving Boundary

The governing equation derived above is satisfied within a moving region whose boundary location are not yet known and will emerge as part of the solution. In other words, the solution $n(x,t)$ is sought in the region $0 \leq x \leq s(t)$ where $s(t)$ will depend on the solution $n(x,t)$. For a properly posed problem, one or more equations establishing the dependence of $s(t)$ on the solution $n(x,t)$ will be required. To this end, two different possibilities are considered :

(a) Problem with single drainage only.

This includes cases(a),(b) of Fig.2.4. In both cases it has been shown that the drainage boundary can be made to coincide with the moving boundary. On this boundary, the amount of water outflow must equal the amount of volume reduction in the soil :

$$Q = \Delta V$$

This can be shown to be :

$$-\frac{k}{\rho_f}\frac{\partial u}{\partial x} = \frac{ds}{dt} \quad , \quad x = s(t) \tag{2.28}$$

or :

$$-(G_s-1)\, k\, (1-n) + \frac{k}{\rho_f}\frac{\partial q}{\partial x} + C_v \frac{1}{1-n}\frac{\partial n}{\partial x} = \frac{ds}{dt} \quad , \quad x = s(t) \tag{2.29}$$

and for a thin soil layer,

$$C_v \frac{1}{1-n}\frac{\partial n}{\partial x} = \frac{ds}{dt} \quad , \quad x = s(t) \tag{2.30}$$

this, together with the initial condition :

$$s(0) = h_o \tag{2.31}$$

completely defines the problem.

(b) Problem with double drainage.

By a similar argument to the above, it can be shown that :

$$\frac{k}{\rho_f}\frac{\partial u}{\partial x} = \frac{d}{dt}[s(t)+w(t)] \quad , \quad x = s(t)+w(t) \tag{2.32}$$

and

$$\frac{k}{\rho_f}\frac{\partial u}{\partial x} = \frac{dw}{dt} \quad , \quad x = w(t) \tag{2.33}$$

where it has been pointed out in the previous paragraphs that this type of problem involves two moving boundaries $s(t)+w(t)$ and $w(t)$ and requires a seperate equation for each. The transformation to the porosity n can be carried out in a straightforward manner as (a) and will not be reproduced here.

3. FORMULATION BASED ON THE LAGRANGIAN COORDINATE

In contrast to the Eulerian coordinate, the Lagrangian coordinate is fixed in the material thus forming an internal system. There are several possible ways of defining such a system, and in the Introduction section two of these have been given. The formulation is based on an element identified by the material contained within it. The actual position in space of this element will thus be changed as deformation occurs. In other words, the formulation is aiming at a specific point in the material and follows its movement in space. This has the advantage that the governing equation need only be satisfied within a fixed boundary for most applications. In the following paragraphs the governing equation will be derived, and it is seen that this coincides with that of Gibson, England and Hussey (1967).

The Continuity Equation

Consider a stratum in which a point is labelled by the thickness of solid material occupying the space between the point and any convenient datum plane (McNabb 1960). This solid thickness is related to the space (Eulerian) coordinate by :

$$z(x) = \int_0^x \frac{1}{1+e}\, dx \qquad (2.34)$$

or : $$\frac{dz}{dx} = \frac{1}{1+e} \qquad (2.35)$$

A Lagrangian element is defined as one with unit cross sectional area normal to the direction of flow (the z or x axis) and bounded by planes labelled z and $z+dz$. The fact that this element always encloses the same amount of solid particles leads automatically to the continuity of the solid phase. During consolidation the boundaries of this element move with the same velocity as the corresponding (true) solid velocity. Consequently the rate of fluid flow across these boundaries will depend on the relative velocity between the solid and fluid phase :

$$n\ (\ \tilde{v}_f - \tilde{v}_s\ )$$

This consideration leads to the continuity of the fluid phase :

$$\frac{\partial e}{\partial t} = -\frac{\partial}{\partial z}\left[\ n\ (\ \tilde{v}_f - \tilde{v}_s\ )\right] \qquad (2.36)$$

Combining this with the generalized Darcy's law, eq(2.5), yields :

$$\frac{\partial e}{\partial t} = \frac{\partial}{\partial z}\left[\frac{k}{\rho_f}\frac{1}{1+e}\frac{\partial u}{\partial z}\right] \qquad (2.37)$$

The Governing Equation

Eq(2.37) establishes the relationship between the rate of change of void ratio and the excess pore pressure gradient in material space. This is linked to the total and effective stresses by :

$$\frac{\partial u}{\partial z} = \frac{\partial \sigma}{\partial z} - \frac{\partial \sigma'}{\partial z} - \frac{\partial u_h}{\partial z} \qquad (2.38)$$

Two cases can be considered :

(a) A surface loading which is uniformly distributed in the soil layer.

In this case :

$$\frac{\partial \sigma}{\partial x} = -\frac{1}{1+e}(\rho_s + \rho_f e) \tag{2.19}$$

it follows that :

$$\frac{\partial \sigma}{\partial z} = \frac{\partial \sigma}{\partial x}\frac{dx}{dz} = -(\rho_s + \rho_f e) \tag{2.39}$$

Similarly, the hydrostatic pore pressure gradient is :

$$\frac{\partial u_h}{\partial z} = \frac{\partial u_h}{\partial x}\frac{dx}{dz} = -(1+e)\rho_f \tag{2.40}$$

Hence,

$$\frac{\partial u}{\partial z} = -(\rho_s - \rho_f) - \frac{\partial \sigma'}{\partial z} \tag{2.41}$$

Substituting this into eq(2.37) yields,

$$\frac{\partial e}{\partial t} = -\frac{\partial}{\partial z}\left(\frac{k}{\rho_f}\frac{1}{1+e}\frac{d\sigma'}{de}\frac{\partial e}{\partial z}\right) - (\rho_s-\rho_f)\frac{d}{de}\left(\frac{k}{\rho_f(1+e)}\right)\frac{\partial e}{\partial z} \tag{2.42}$$

which is identical to that of Gibson, England and Hussey (1967).

In the case of a thin soil layer, which can be approximated by $\rho_s = \rho_f$, the equation becomes,

$$\frac{\partial e}{\partial t} = -\frac{\partial}{\partial z}\left(\frac{k}{\rho_f}\frac{1}{1+e}\frac{d\sigma'}{de}\frac{\partial e}{\partial z}\right) \tag{2.43}$$

Denoting :

$$C_F = -\frac{k}{\rho_f}\frac{1}{1+e}\frac{d\sigma'}{de} \tag{2.44}$$

by which eq(2.43) can be written as :

$$\frac{\partial e}{\partial t} = \frac{\partial}{\partial z}\left(C_F \frac{\partial e}{\partial z} \right) \tag{2.45}$$

(b) A surface loading which introduces a stress distribution in the soil layer.

In this case an additional term is added to eq(2.39) as :

$$\frac{\partial \sigma}{\partial z} = -(\rho_s + \rho_f e) + \frac{\partial q}{\partial z} \tag{2.46}$$

and eq(2.37) becomes :

$$\frac{\partial e}{\partial t} = \frac{\partial}{\partial z}\left(C_F \frac{\partial e}{\partial z} \right) - (\rho_s - \rho_f)\frac{d}{de}\left[\frac{k}{\rho_f(1+e)}\right]\frac{\partial e}{\partial z} + \frac{\partial}{\partial z}\left(\frac{k}{\rho_f(1+e)}\frac{\partial q}{\partial z}\right) \tag{2.47}$$

In most cases the stress distribution q will be given as a function of the space coordinate x and it will be necessary to perform the transformation from $q(x,t)$ to $q(z,t)$.

4. SOME COMPARISONS BETWEEN THE TWO FORMULATIONS

Governing equations for soil consolidation have been formulated in the Eulerian and the Lagrangian coordinates. In both cases the formulation is not restricted to small strain, and it can be shown that these two formulations are in fact identical to each other. To illustrate this, the simple case of a thin soil layer is used as an example where the governing equations are :

$$\frac{\partial n}{\partial t} = \frac{\partial}{\partial x}\left(C_v \frac{\partial n}{\partial x} \right) \tag{2.26}$$

in the Eulerian coordinate, and :

$$\frac{\partial e}{\partial t} = \frac{\partial}{\partial z}\left(C_F \frac{\partial e}{\partial z} \right) \tag{2.45}$$

in the Lagrangian coordinate.

These two coordinates are related by :

$$z = \int_o^x (1-n)\, dx \tag{2.48}$$

and,

$$x = \int_o^z (1+e)\, dz \tag{2.49}$$

Therefore,

$$\frac{\partial z}{\partial x} = (1-n) \tag{2.50}$$

and,

$$\frac{\partial z}{\partial t} = -\int_o^x \frac{\partial n}{\partial t}\, dx = -\int_o^x \frac{\partial}{\partial x}\left(C_v \frac{\partial n}{\partial x}\right) dx = - C_v \frac{\partial n}{\partial x}\Bigg|_o^x \tag{2.51}$$

Applying the undrained boundary condition to the last term :

$$\left(C_v \frac{\partial n}{\partial x} \right)_{x=0} = 0 \tag{2.52}$$

leads to :

$$\frac{\partial z}{\partial t} = - C_v \frac{\partial n}{\partial x} \tag{2.53}$$

Hence the left hand side of eq(2.26) becomes :

$$\frac{\partial n}{\partial t} = \frac{\partial \tilde{n}}{\partial t} + \frac{\partial \tilde{n}}{\partial z}\frac{\partial z}{\partial t} = \frac{\partial \tilde{n}}{\partial t} - C_v(1-\tilde{n})\left(\frac{\partial \tilde{n}}{\partial t}\right)^2 \qquad (2.54)$$

where : $\tilde{n}(z,t) = n(x,t)$ (2.55)

Similarly the right hand side of eq(2.26) becomes,

$$\frac{\partial}{\partial x}\left(C_v \frac{\partial n}{\partial x}\right) = (1-\tilde{n})^2 C_v \frac{\partial^2 \tilde{n}}{\partial z^2} - C_v(1-\tilde{n})\left(\frac{\partial \tilde{n}}{\partial z}\right)^2 + (1-\tilde{n})^2 \frac{\partial C_v}{\partial z}\frac{\partial \tilde{n}}{\partial z} \qquad (2.56)$$

Equating eq(2.54),(2.56) then yields :

$$\frac{1}{(1-\tilde{n})^2}\frac{\partial \tilde{n}}{\partial t} = C_v \frac{\partial^2 \tilde{n}}{\partial z^2} + \frac{\partial C_v}{\partial z}\frac{\partial \tilde{n}}{\partial z} = \frac{\partial}{\partial z}\left(C_v \frac{\partial \tilde{n}}{\partial z}\right) \qquad (2.57)$$

or:

$$\frac{\partial e}{\partial t} = \frac{\partial}{\partial z}\left(\frac{C_v}{(1+e)^2}\frac{\partial e}{\partial z}\right) = \frac{\partial}{\partial z}\left(C_F \frac{\partial e}{\partial z}\right)$$

which is eq(2.45).

The transformation from eq(2.45) to eq(2.26) can be done in exactly the same manner as above and will not be reproduced here.

While being equivalent to each other, there are, however, significant differences between the two formulations. Taking again the example of a thin soil layer where coefficient of consolidation C_v and C_F are related to each other by :

$$C_F = C_v / (1+e)^2$$

and,

$$C_v = C_F / (1-n)^2$$

Therefore, a linear case in one formulation will correspond to a highly nonlinear case to the other. The choice between the two formulations in a particular application is thus dependent on the behaviour of the soil used.

It is of interest to note that the Eulerian formulation is associated with the Eulerian strain ε :

$$\varepsilon = \frac{l_o - l}{l} = \frac{n_o - n}{1 - n_o}$$

in such a way that the governing equation will remain unchanged when this is used as the dependent variable to replace the porosity. This is also found in the Lagrangian formulation where the Lagrangian strain ε_L :

$$\varepsilon_L = \frac{l_o - l}{l_o} = \frac{e_o - e}{1 + e_o}$$

can be used as the dependent variable.

Another difference between the two formulations is the presence of the moving boundary in the Eulerian formulation. For this reason the Lagrangian formulation will be usually preferred for its fixed boundaries. However, as will be shown in the next chapter, the presence of the moving boundary in the Eulerian formulation does not impose such complications as might at first appear. Indeed, very efficient numerical techniques have been developed especially in the case of a constant c_v . These will be discussed in the next chapter.

CHAPTER THREE SOME SOLUTIONS FOR THE CONSOLIDATION OF A THIN SOIL LAYER

ABSTRACT

The consolidation of a thin soil layer is considered in this chapter. The emphasis has been placed upon solving the moving boundary problem which results from the Eulerian formulation. To this end two numerical methods both using the finite difference approximation and the Crank-Nicolson method are developed. The first is the uniformly deforming grid method in which the space is discretized into equal grids that will deform uniformly as settlement occurs. The second is the modified fixed grid Lagrangian method which allows the boundary to move into the first mesh within each step as a result of settlement, and uses a special Lagrangian interpolation formula for unequally spaced data to approximate the derivatives in the first grid.

To assess the validity of these techniques solutions have been calculated for the C_v constant and the C_F constant cases. In the C_v constant case a comparison is made with a small time approximate solution and a numerical solution obtained for the Lagrangian formulation. In the C_F constant case the anlytical solution obtained by Gibson, England and Hussey (1967) is used to compare with the numerical solutions. In both cases very good agreement is obtained with the modified fixed grid Lagrangian method. Based on this method other solutions have been calculated for different forms of strain dependence of C_v, and the consolidation rates have been examined with reference to the C_v constant and the C_F constant cases. It is concluded from these results that the large strain consolidation behaviour of a thin soil layer will depend on both the final magnitude of strain and the variation of the coefficient of consolidation C_v with strain.

1. INTRODUCTION

In the previous chapter, governing equation for large strain consolidation have been formulated in the Eulerian and the Lagrangian coordinates. For a thin soil layer the equation can be reduced to a simple diffusion type equation as :

$$\frac{\partial n}{\partial t} = \frac{\partial}{\partial x}\left(C_v \frac{\partial n}{\partial x} \right) \tag{3.1}$$

for the Eulerian coordinate x , and :

$$\frac{\partial e}{\partial t} = \frac{\partial}{\partial z}\left(C_F \frac{\partial e}{\partial z} \right) \tag{3.2}$$

for the Lagrangian coordinate z .

There are several occasions where a soil layer can be regarded as a thin layer, and discussion of the effectiveness of this simple approximation in dealing with engineering problems will be deferred until later chapters as general theories are developed. It is also common practice to use the thin layer theory to analyse laboratory experiment results. Very often in these applications solutions corresponding to a step loading are called for, and for this reason, only this simple type of loading will be considered here. The numerical techniques can be easily extended to solve the more complex time dependent type of loading.

In this chapter a thin soil layer is considered with an initially uniform void ratio e_o under an applied loading q . This loading is suddenly increased to $q + \Delta q$ and maintained constant thereafter. The upper surface of this layer is allowed to drain freely, hence its void ratio will immediately reach the new equilibrium state e_1 . The base of this layer is assumed impervious and thus no drainage can occur across it.

A solution for the linear case (C_F constant) of the Lagrangian formulation eq(3.2) has been obtained by Gibson et. al. (1967) as :

$$e(z,t) = e_1 + \frac{4}{\pi}(e_o - e_1) \sum_n \frac{(-1)^n}{2n+1} \sin\left[\frac{(2n+1)}{2}\pi \frac{z}{z_o}\right] \exp\left[-\frac{(2n+1)^2}{4}\pi^2 T_o\right] \quad (3.3)$$

where z_o is the solid thickness of the layer and T_o is a time factor defined as :

$$T_o = \frac{C_F\, t}{z_o^2} \quad (3.4)$$

The degree of settlement S is given by :

$$S(T_o) = \frac{h(0) - h(T_o)}{h(0) - h(\infty)} = 1 - \frac{8}{\pi^2} \sum_n \frac{1}{(2n+1)^2} \exp\left[-\frac{(2n+1)^2}{4}\pi^2 T_o\right] \quad (3.5)$$

An interesting property of this C_F constant case is that the degree of settlement - time factor relationship is strain-invariant i.e. it is not affected by the actual amount of strain occuring.

2. DEVELOPMENT OF NUMERICAL METHODS

With the advent of modern numerical techniques it is possible to deal with any nonlinear case of the Lagrangian formulation, eq(3.2) without great difficulty (see, for example, Crank (1970) for finite difference and other semi-analytical methods, and Mitchell and Gait (1977) for the finite element method). However, the situation is more complicated in the Eulerian formulation because of

the presence of the moving boundary, and special numerical methods must be developed for this.

The governing equation and the initial and boundary conditions in the Eulerian coordinate are :

$$\frac{\partial n}{\partial t} = \frac{\partial}{\partial x}\left(C_v \frac{\partial n}{\partial x} \right) , \; 0 \leq x \leq s(t), \; t \geq 0 \qquad (3.6)$$

$$n(x,0) = n_o$$

$$n(s,t) = n_1 \qquad (3.7)$$

$$\frac{\partial n}{\partial x}(0,t) = 0$$

$$s(0) = h_o \qquad (3.8)$$

$$C_v \frac{1}{1-n_1} \frac{\partial n}{\partial x}(s,t) = \frac{ds}{dt}$$

Using the parameter f defined as :

$$f = \frac{n - n_1}{n_o - n_1} \qquad (3.9)$$

which is a measure of the development of the Eulerian strain during consolidation, eq(3.6-8) can be simplified to :

$$\frac{\partial f}{\partial t} = \frac{\partial}{\partial x}\left(C_v \frac{\partial f}{\partial x} \right) , \; 0 \leq x \leq s(t), \; t \geq 0 \qquad (3.6)_a$$

$$f(x,0) = 1$$

$$f(s,t) = 0$$

$$\frac{\partial f}{\partial x}(0,t) = 0 \qquad (3.7)_a$$

$$s(0) = 0$$

$$C_v \lambda \frac{\partial f}{\partial x}(s,t) = \frac{ds}{dt} \qquad (3.8)_a$$

where λ is the final Lagrangian strain (defined as $\Delta l/l_o$) due to the additional loading Δq .

During the last three decades considerable progress has been made in developing numerical techniques for solving this type of problem. In fact, more than 20 different methods have been reported to be successful (Ockendon and Hodgkins (1975), Rubinstein (1967)). As it is not possible in the present work to experiment with all these methods, only those methods which use the finite difference approximation are considered. In this chapter two methods which have been found most satisfactory will be described and compared. These are respectively the uniformly deforming grid method (UDG) and the modified fixed grid Lagrangian method (MFGL).

The Uniformly Deforming Grid Method

This method has been used by Murray and Landis (1959) in the study of heat conduction problems involving melting and freezing. This uses a transformation of the space variable x to :

$$y = \frac{x}{s(t)} \tag{3.10}$$

which changes the space domain from $0 \leq x \leq s(t)$ to $0 \leq y \leq 1$. The governing equation in terms of this new variable y thus becomes :

$$\frac{\partial f'}{\partial t} = \frac{1}{s^2}\frac{\partial}{\partial y}\left(C_v \frac{\partial f'}{\partial y}\right) + \frac{\dot{s}}{s} y \frac{\partial f'}{\partial y} \quad , \; 0 \leq y \leq 1, \; t \geq 0 \tag{3.11}$$

$$\begin{aligned} f'(y,0) &= 1 \\ f'(1,t) &= 0 \\ \frac{\partial f'}{\partial y}(0,t) &= 0 \\ s(0) &= h_o \end{aligned} \tag{3.12}$$

$$C_v \lambda \frac{\partial f'}{\partial y}(1,t) = - s \frac{ds}{dt} \qquad (3.13)$$

and, $$f'(y,t) = f(x,t) \qquad (3.14)$$

This system is discretized in the space y by the finite difference approximation and the solutions are marched forward by the Crank-Nicolson method. Detailed formulation of this method is included in Appendix A of this chapter.

The Modified Fixed Grid Lagrangian Method

This method is developed from the work of Crank and Gupta (1972a, 1972b), and is essentially a modified version of the fixed grid Lagrangian method of Crank and Gupta (1972b).

In this method, the layer is divided into m equal segments (mesh), and finite differences are used to approximate the derivatives at each node. In the next time level, the boundary is moved into a new position within the first segment and derivatives in the node adjacent to the boundary are approximated by a Lagrangian formula for unequally spaced points. The solution is marched forward in time by the Crank-Nicolson method, and with use of iteration. At the end of each time step the node positions are readjusted to be equally spaced before moving forward to the next time increment, and the functional values at the new nodes are interpolated from the old nodal values by fitting a cubic polynomial within each segment.

The equations resulting from each step of the above mentioned procedure are produced in Appendix B which also contains a more detailed description of the method. This method has been written in a general purpose computer subroutine THIN which is presented in Appendix C of this chapter.

3. COMPARISON OF NUMERICAL SOLUTIONS

In order to assess the validity of the numerical technique developed in the previous section, the calculated solutions are compared with known solutions or solutions obtained by other methods. Two cases, C_v constant and C_F constant have been used for this purpose.

Comparison of Solutions, C_v constant

In this case define a time factor T as :

$$T = \frac{C_v\, t}{h_o^2} \tag{3.15}$$

and the normalized coordinate and boundary position :

$$\chi = \frac{x}{h_o} \tag{3.16}$$

$$\xi = \frac{s}{h_o} \tag{3.17}$$

from which eq(3.6-8)$_2$ reduce to the normalized form :

$$\frac{\partial f}{\partial T} = \frac{\partial^2 f}{\partial \chi^2} \quad , \quad 0 \leq \chi \leq \xi \quad , \; T \geq 0 \tag{3.18}$$

$$\begin{aligned} f(\chi,0) &= 1 \\ f(\xi,T) &= 0 \\ \frac{\partial f}{\partial \chi}(o,T) &= 0 \end{aligned} \tag{3.19}$$

$$\begin{aligned} \xi(0) &= 1 \\ -\lambda \frac{\partial f}{\partial \chi}(\xi,T) &= \frac{d\xi}{dT} \end{aligned} \tag{3.20}$$

In this section solutions to the above equations by the UDG and the MFGL methods will be compared with a small time approximate solution and a numerical solution obtained for the Lagrangian formulation.

(a) Small time approximate solution

During the early stages of consolidation the behaviour of the layer approximates to that of a semi-infinite region. A solution in this case has been obtained by Neumann using similarity methods (see, for example, Carslaw and Jaeger 1959), which in terms of the degree of settlement is :

$$S = \beta \sqrt{T} \qquad (3.21)$$

with,

$$\beta = \frac{2}{\sqrt{\pi}} \frac{exp(-\alpha^2)}{erfc(\alpha)} \qquad (3.22)$$

where α is the root to the transcendental equation :

$$\alpha = \frac{\lambda}{\sqrt{\pi}} \frac{exp(-\alpha^2)}{erfc(\alpha)} \qquad (3.23)$$

with λ the final Lagrangian strain.

It is interesting to note that as $\lambda \to 0$, $\beta \to \frac{2}{\sqrt{\pi}}$ which is the case of the Terzaghi theory (Fox, 1948). Values of β corresponding to different final strains λ have been calculated and given in Table 3.1 . In Chapter 9 this will be used for estimating c_v from experiment results.

(b) Numerical solution of the Lagrangian formulation

The Lagrangian formulation in the case of a constant c_v is :

TABLE 3.1 COEFFICIENT β IN THE C_v CONSTANT SMALL TIME APPROXIMATE SOLUTION $s = \beta\sqrt{T}$

λ	0.00	0.02	0.04	0.06	0.08
0.0	1.1284	1.1430	1.1580	1.1736	1.1896
0.1	1.2063	1.2235	1.2413	1.2597	1.2789
0.2	1.2988	1.3194	1.3409	1.3633	1.3866
0.3	1.4109	1.4363	1.4629	1.4908	1.5200
0.4	1.5506	1.5829	1.6169	1.6528	1.6907
0.5	1.7310	1.7738	1.8193	1.8679	1.9200

$$\frac{\partial e}{\partial t} = \frac{\partial}{\partial z}\left(\frac{C_v}{(1+e)^2}\frac{\partial e}{\partial z}\right), \quad 0 \leq z \leq z_o, \quad t \geq 0 \tag{3.24}$$

$$\begin{aligned} e(z,0) &= e_o \\ e(z_o,t) &= e_1 \\ \frac{\partial e}{\partial z}(0,t) &= 0 \end{aligned} \tag{3.25}$$

Adopting the same time factor as eq(3.15) :

$$T = \frac{C_v t}{h_o^2} = \frac{C_v t}{z_o^2\,(1+e_o)^2} \tag{3.26}$$

and a normalized solid thickness η :

$$\eta = \frac{z}{z_o} \tag{3.27}$$

then eq(3.24,25) can be written in terms of a new variable g :

$$g = \frac{e - e_1}{e_o - e_1}$$

as :

$$\frac{\partial g}{\partial T} = \frac{\partial}{\partial \eta}\left[\frac{1}{(1-\lambda(1-g))^2}\frac{\partial g}{\partial \eta}\right], \quad 0 \leq \eta \leq 1, \; T \geq 0 \qquad (3.24)_a$$

$$g(\eta,0) = 1$$

$$g(1,T) = 0 \qquad (3.25)_a$$

$$\frac{\partial g}{\partial \eta}(0,T) = 0$$

The degree of settlement in this case is :

$$S(T) = 1 - \int_0^1 g(\eta,T)\,d\eta \qquad (3.28)$$

$Eq(3.24)_a$ is discretized in η by the finite difference method and the resulting differential equations are integrated in time by a Variable Step Variable Order algorithm, this algorithm will be described in Chapter 7. The calculated result for $\lambda=0.4$ (i.e. 40% final strain) is given in column 2 of Table 3.2. The first column of this Table is the small time approximate solution, eq(3.21) . It is seen that these two solutions agree with each other to the fourth decimal place within the appropriate range of time factor.

(c) Solution by the UDG method

The solutions are calculated in time steps of 0(0.005) 0.01(0.01)0.02(0.02)0.04(0.03)0.10(0.05)0.20(0.1)0.5(0.2)1.5 . Two discretizations, corresponding to 20 mesh and 40 mesh were calculated with an error bound of 1×10^{-5} and 1×10^{-6} respectively. The results for $\lambda=0.4$ are shown in column 3,4 of Table 3.2. It is seen that even for the finest discretization used (40 mesh) a difference between this and the first two solutions is observed in the third decimal place. This rather disappointing performance of the UDG method may be due partly to the presence of the velocity term $\dot{s}$ in the governing equation. This velocity term is obviously very sensitive to the time step used which may cause error in the solutions.

Time Factor	Small Time Solution	Lagrangian Formulation	UDG n = 20	UDG n = 40	MFGL n = 20	MFGL n = 40
0.005	109646	110400	099456	109265	113664	111070
0.01	155063	155493	153144	156032	158250	156186
0.02	219292	219523	222049	221006	221546	220157
0.04	310126	310237	323190	314157	311734	310780
0.07	410258	410310	428830	415525	411413	410773
0.10	490352	490359	513175	496596	491275	490772
0.15	600557	599924	627217	607263	600524	600291
0.20	693463	689440	723826	693634	689970	689778
0.30	849315	821223	857608	831185	821539	821489
0.50	-	948467	967949	954238	948797	948582
0.90	-	996513	-	997137	997505	996528

TABLE 3.2 COMPARISON OF SOLUTIONS, c_v CONSTANT, 40% FINAL STRAIN, NUMBERS SHOWN ARE DEGREE OF SETTLEMENT X 10^6

(d) Solutions by the MFGL method

The solutions are obtained with the same time step as the UDG method reported above. The first calculation uses 20 mesh and an error bound of $1x10^{-4}$, and the result are presented in column 5 of Table 3.2. The agreement between this and the first two solutions is seen to be within the third decimal place for small times and to the foruth decimal place for large times. As the error bound in this case is $1x10^{-4}$, which is the fourth decimal place, such a close agreement is indeed better than expected. The solution of a finer discretization using 40 mesh and a more rigorous error bound of $1x10^{-6}$ are given in column 6 of the same Table. It can be seen that this agrees with the first two solutions to the fourth decimal place. The computing time required for each case in the ICL 1906A machine is approximately 40 seconds for the Lagrangian formulation, 20 seconds for the UDG method and 15 seconds for the MFGL method.

Comparison of Solutions, C_F constant

The superiority of the MFGL method over the UDG method is clearly demonstrated in the above case. Hence in this section only the solution obtained by the MFGL method will be given and compared with the exact solution, eq(3.5).

The governing equation follows from eq(3.6-8)a , using a time factor T_o which has already been defined in eq(3.4) :

$$T_o = \frac{C_F\, t}{z_o^2} = \frac{C_F\, t}{h_o^2 (1-n_o)^2} \qquad (3.29)$$

and the normalized space variable χ and ξ from eq(3.16,17) :

$$\frac{\partial f}{\partial T_o} = \frac{\partial}{\partial \chi}\left[\frac{1}{(1+\varepsilon_f(1-f))^2}\frac{\partial f}{\partial \chi}\right] , \quad 0 \leq \chi \leq \xi \quad T_o \geq 0 \qquad (3.30)$$

$$f(\chi,0) = 1$$

$$f(\xi,T_o) = 0$$

$$\frac{\partial f}{\partial \chi}(0,T_o) = 0 \qquad (3.31)$$

$$\xi(0) = 1$$

$$-\lambda \frac{\partial f}{\partial \chi}(\xi,T_o) = \frac{d\xi}{dT_o} \qquad (3.32)$$

where ε_f is the final Eulerian strain. This is solved by the MFGL method using 40 mesh and an error bound of 1×10^{-6}. The results for 1%, 10%, 20% and 40% final Lagrangian strain are compared with the exact solution, eq(3.5), in Table 3.3. It can be seen that in most cases the agreement of the numerical solutions with the exact solution is better than the third decimal place.

TABLE 3.3 COMPARISON OF SOLUTIONS, C_F CONSTANT, NUMBERS SHOWN ARE DEGREE OF SETTLEMENT X 10^6.

Time Factor	Exact Solution	Numerical Solutions			
		= 1%	= 10%	= 20%	= 40%
0.01	112838	113276	113154	113015	112916
0.03	195441	195652	195576	195369	194882
0.06	276395	276572	276450	276184	275334
0.10	356823	356960	356833	356523	355377
0.15	436950	437059	436930	436591	435218
0.25	562233	562308	562162	561740	559764
0.41	705247	703462	703326	702906	700733
0.61	820060	818963	818864	818548	816816
0.81	890147	889473	889408	889202	888049
1.01	932935	932521	932480	932351	931624
1.41	975004	975403	974833	974784	974508
2.01	994312	994310	994273	994262	994199

4. THE EFFECT OF STRAIN ON THE CONSOLIDATION BEHAVIOUR

Having thus established confidence in the numerical procedure, this section will investigate the influence of strain on the consolidation behaviour. The MFGL method has been used to perform all the calculations that will be presented below.

In general, the development of strain during a consolidation has two effects on its behaviour; the first being the successive shortening of the drainage path during the consolidation, and the second is that it causes variations of material properties such as the permeability and compressibility. When C_v is held constant, consolidation will be solely dependent on the magnitude of strain . With larger strain, the drainage path will be further shortened, and consolidation is accelerated. This can be seen in the numerical solution, see Fig.3.2(a). When C_v varies with strain, the consolidation will depend on both the mode of variation and the magnitude of strain. Considering firstly C_v increasing monotonically with the (Eulerian) strain, which corresponds to a variation above the C_v constant line in Fig.3.1, then as strain develops, consolidation will be further accelerated. If, on the other hand, C_v decreases monotonically with strain, the reduction of C_v will retard the accelerating process due to the shortening of drainage path that occurs with strain. Eventually there will be one particular combination where the decrease of C_v is just enough to cancel the acceleration due to strain, and a strain-invariant situation results. This is then the case C_F constant, or $C_v \propto (1+\varepsilon)^{-2}$ which is also shown in Fig.3.1. Below this curve, the retardation due to the decrease of C_v will outweigh the acceleration due to strain, and slower consolidation occurs with increased strain.

To illustrate these points, a few examples were calculated with different forms of C_v (see Fig.3.1) :

Curve 1 : $C_v = C_o (1+\varepsilon)^2$

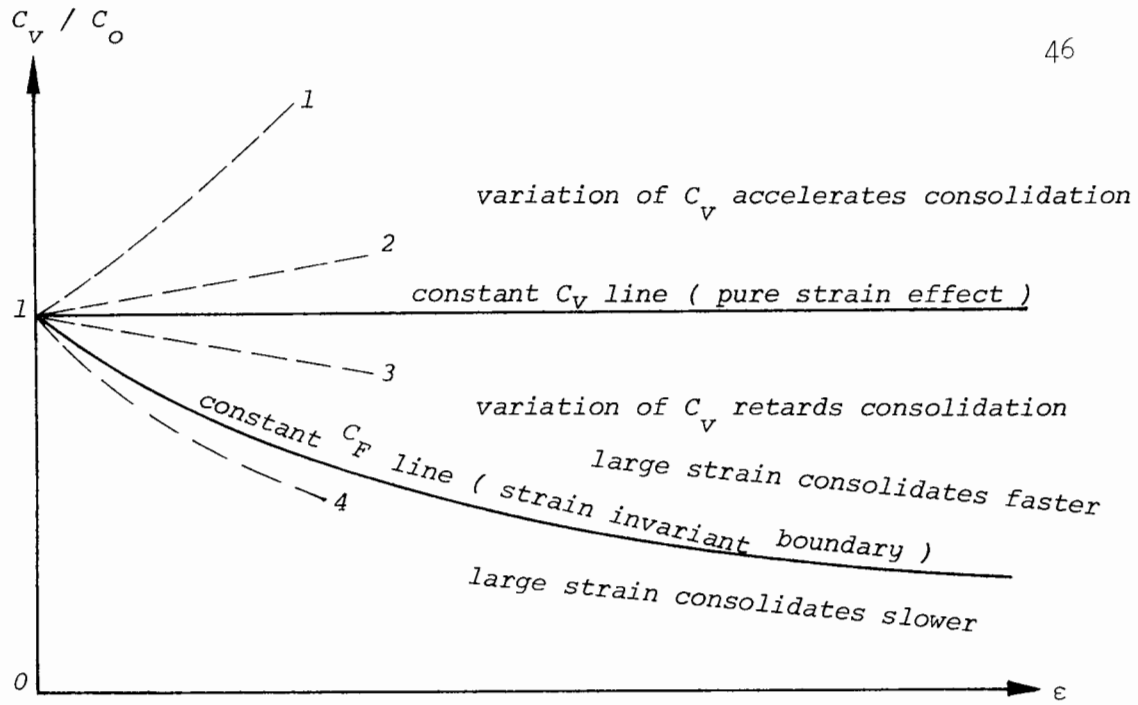

FIG.3.1 Variation of the coefficient of consolidation with the Eulerian starin.

Curve 2 : $C_v = C_o\ (1+0.5\varepsilon)$

Curve 3 : $C_v = C_o\ (1-0.5\varepsilon)$

Curve 4 : $C_v = C_o\ (1+\varepsilon)^{-3}$

where curve1 and 2 are situated above the C_v constant line, curve 3 lies between the C_v constant and the C_F constant line, while curve 4 is completely below the C_F constant line. The solutions are presented in Fig.3.2(b-e) where the degree of settlement S is given as a function of the common time factor T :

$$T = \frac{C_o\ t}{h_o^{\ 2}} \qquad (3.33)$$

Four different values of the final strain are considered in each case. In Fig.3.2(b) where the coefficient of consolidation increases with the square of the current strain, as in curve 1, the consolidation is very much faster for the larger final strains than for the smaller values - comparing, for example, $\lambda = 0.1$ (10%) with $\lambda = 0.4$ (40%). A similar effect, though of smaller magnitude, is observed in Fig.3.2(c) where C_v increases linearly with strain as in curve 2. Fig.3.2(d) shows that the trend in Fig.3.2(b),(c) is continued for C_v decreasing linearly with strain, with the difference between $\lambda = 0.1$ and $\lambda = 0.4$

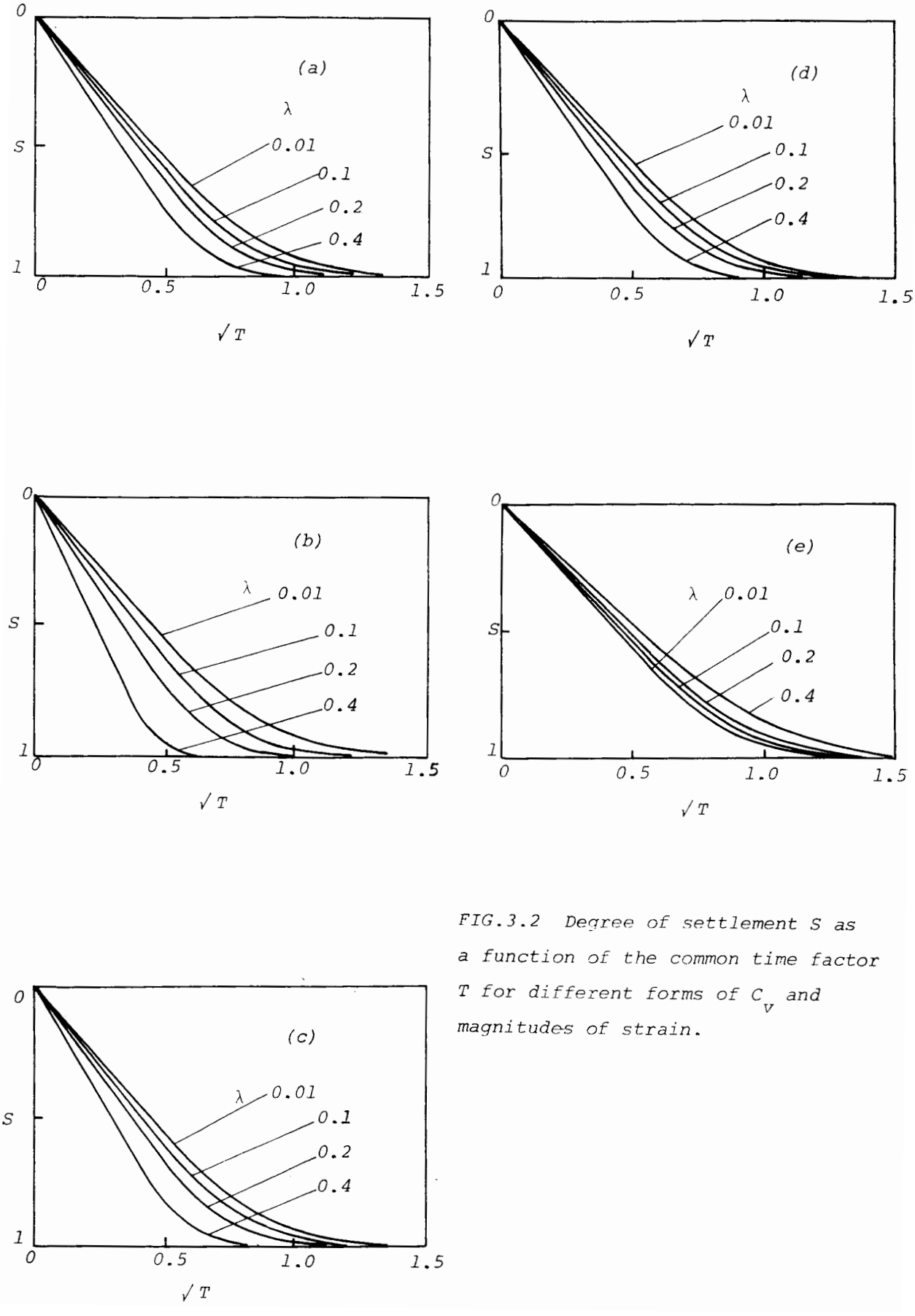

FIG.3.2 Degree of settlement S as a function of the common time factor T for different forms of C_v and magnitudes of strain.

now much reduced. In Fig.3.2(e) the reduction of c_v with strain as in curve 4 has a stronger effect on the consolidation rate than the final strain values and, as predicted, the lowest consolidation rates are associated with the highest values of final strain.

These examples demonstrate the fact that, even for the simple case of a thin soil layer under a step loading, consolidation is a very complex strain-dependent behaviour. It can be seen that the development of strain during consolidation not only changes the length of drainage path but also causes a change in the coefficient of consolidation c_v . In such a complicated situation the particular case of a constant c_F offers the advantage of simplicity due to its strain-invariant property and can therefore be applied as a first approximation to many engineering problems. The following chapters will be concerned with the consolidation including the effect of self weight of this particular case of a constant c_F .

APPENDIX A THE UNIFORMLY DEFORMING GRID METHOD

The governing equation (3.11-13) is discretized in y by the finite difference method as :

$$\left(\frac{\partial f'}{\partial y}\right)_i \simeq \frac{1}{2\Delta y}\left(f'_{i+1} - f'_{i-1}\right)$$

$$\left(\frac{\partial}{\partial y}\left(C_v \frac{\partial f'}{\partial y}\right)\right)_i \simeq \frac{1}{\Delta y^2}\left(\alpha^+ f'_{i+1} - (\alpha^+ + \alpha^-) f'_i + \alpha^- f'_{i-1}\right)$$

where Δy is the grid spacing and f'_i is the nodal functional value in node i , and the coefficients α^+ and α^- are given by :

$$\alpha^+ = C_v\left[\frac{1}{2}\left(f'_i + f'_{i+1}\right)\right]$$

$$\alpha^- = C_v\left[\frac{1}{2}\left(f'_i + f'_{i-1}\right)\right]$$

Thus, eq(3.11-13) reduce to a system of nonlinear ordinary differential equations :

$$\frac{df'_i}{dt} = \left(\frac{1}{s^2}\frac{\alpha^+}{\Delta y^2} + \frac{\dot{s}}{s} y_i \frac{1}{2\Delta y}\right) f'_{i+1} - \frac{1}{s^2}\frac{1}{\Delta y^2}(\alpha^+ + \alpha^-) f'_i$$

$$- \left(\frac{1}{s^2}\frac{\alpha^-}{\Delta y^2} - \frac{\dot{s}}{s} y_i \frac{1}{2\Delta y}\right) f'_{i-1} \qquad i = 2, 3, \ldots, n$$

$$\frac{ds}{dt} = -\frac{\lambda}{s} C_v f'_2/\Delta y \ , \quad f'_1 = 0, \quad f'_{n+1} = f'_{n-1}$$

and the initial conditions are :

$$f'_i(0) = 1$$

$$s(0) = h_o$$

This system is integrated by the Crank-Nicolson method, which requires the solution of a system of nonlinear equations at each time step, and iteration must be applied.

At present the method of successive approximation is used. Thus, the starting values for iteration are :

$$\alpha_{n+1}^{(o)} = \alpha_n$$

$$s_{n+1}^{(o)} = s_n$$

from which the nodal function values $f'^{(o)}_{i,n+1}$ can be calculated. These are then used to calculate the next iterative values of α_{n+1} and s_{n+1}. This is continued until :

$$max \left\{ \left| \frac{f'^{(j)}_{i,n+1} - f'^{(j-1)}_{i,n+1}}{f'^{(j)}_{i,n+1}} \right| , \left| \frac{s^{(j)}_{n+1} - s^{(j-1)}_{n+1}}{s^{(j)}_{n+1}} \right| \right\} < \delta$$

for a successful iteration, or :

$$j \geq N$$

when the number of iteration exceeds that permitted. In the latter case the current time step is halved and a new iteration started by using this smaller time step.

APPENDIX B THE MODIFIED FIXED GRID LAGRANGIAN METHOD

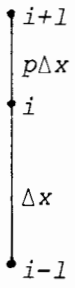

The finite difference approximation for an unequally spaced node as shown in the figure can be obtained by using the Lagrangian interpolation formula, the resulting finite difference equation is shown in eq(B.1) in page 53.

In the present case node $i+1$ is the position of the moving boundary hence $f_{i+1} = 0$. The expression for other equally spaced nodes is obtained by setting $p = 1$ in this equation.

Thus, by using the Crank - Nicolson method and denoting the node next to the moving boundary by M the following system of equations is obtained. (eq(B.2),eq(B.3), page 53).

This gives M equations for the $M+1$ unknowns $f_{i,j+1}$, and p. The unknown p is related to the position of the moving boundary s , and can be calculated from the solutions $f_{i,j+1}$, by the following equation:

$$p = \frac{1}{\Delta x_j} (s_{j+1} - (M-1)\Delta x_j)$$

with,
$$s_{j+1} = \frac{h_o}{\frac{1}{\lambda} - \frac{1}{2} f_M} \left[\frac{\Delta x_j}{2} (f_1 + 2f_2 + \ldots + 2f_{M-1} + f_M) - \frac{1}{2}(M-1)\Delta x_j f_M + \frac{1}{\lambda} - 1 \right]$$

This system is solved by an iteration similar to the UDG method described before. The criteria for terminating the iteration are either :

$$\max \left\{ \left| \frac{f_{i,j+1}^{(n)} - f_{i,j+1}^{(n-1)}}{f_{i,j+1}^{(n)}} \right|_{1 \leq i \leq M} , \left| \frac{p^{(n)} - p^{(n-1)}}{p^{(n)}} \right| \right\} < \delta$$

or: $n \geq N$

or: $p \leq 0.5$

In the latter two cases the time step Δt is halved and the iteration repeated. The restriction of $p \leq 0.5$ is to ensure that within each step the boundary does not move so far as to reduce the accuracy.

At the end of each step the new grid spacing Δx_{j+1} is adjusted to be :

$$\Delta x_{j+1} = \frac{s_{j+1}}{M}$$

which results in a new set of nodes $x_{i,j+1}$. The functional values at the new nodes are interpolated from the old nodal values by fitting a cubic polynomial within the old grid as :

$$f(x) = \alpha_i + \beta_i x + \gamma_i x^2 + \mu_i x^3$$

$$\mu_i = (\ddot{f}_i - \ddot{f}_{i+1}) / 6 \Delta x_j$$

$$\gamma_i = \frac{1}{2} \ddot{f}_i - 3\mu_i x_{i,j}$$

$$\beta_i = \frac{1}{\Delta x_j} (f_i - f_{i+1}) - \gamma_i (x_{i,j} + x_{i+1,j}) - \mu_i (x_{i,j} + x_{i,j} x_{i+1,j} + x_{i+1,j})$$

$$\alpha_i = f_i - \beta_i x_{i,j} - \gamma_i x_{i,j}^2 - \mu_i x_{i,j}^3$$

and the second derivative $\ddot{f}_i$ is approximated by :

$$\ddot{f}_i = \begin{cases} (f_{i-1} - 2f_i + f_{i+1}) / \Delta x_j^2 & 1 \leq i \leq M-1 \\ 2\left(\frac{f_{M-1}}{p+1} - \frac{f_M}{p}\right) / \Delta x_j^2 & i = M \end{cases}$$

The new nodal function value is thus given by :

$$f(x_{i+1,j+1}) = \alpha_i + \beta_i x_{i+1,j+1} + \gamma_i x_{i+1,j+1}^2 + \mu_i x_{i+1,j+1}^3$$

and the solution is now ready to march forward to the next time step $j+2$ by repeating the same procedure as described.

(B.1) $$\frac{\partial}{\partial x}\left(C_v \frac{\partial f}{\partial x}\right)_i \simeq \frac{1}{\Delta x}\{f_{i-1}\left[\frac{C_{v,i+1}}{(p+1)^2} + \frac{1-p}{p+1} C_{v,i} + \frac{p(2+p)}{(p+1)^2} C_{v,i-1}\right] - f_i \left[\frac{C_{v,i+1}}{p^2} - \frac{(p-1)^2}{p^2} C_{v,i} + C_{v,i-1}\right]$$

$$f_{i+1}\left[\frac{2p+1}{p^2(p+1)^2} C_{v,i+1} + \frac{p-1}{p^2(p+1)} C_{v,i} + \frac{1}{(p+1)^2} C_{v,i-1}\right]\}$$

(B.2) $$\frac{1}{\Delta t}\left(f_{M,j+1} - f_{M,j}\right) = \frac{1}{2\,\Delta x_j^2} \{\left[f_{M-1,j}\left(\frac{1}{4} C_{v,M+1,j} + \frac{3}{4} C_{v,M,j}\right) - f_{M,j}\left(C_{v,M+1,j} + C_{v,M,j}\right)\right]$$

$$+ \left[f_{M-1,j+1}\left(\frac{C_{v,M+1,j+1}}{(p+1)^2} + \frac{1-p}{p+1} C_{v,M,j+1} + \frac{p(2+p)}{(p+1)^2} C_{v,M-1,j+1}\right) - f_{M,j+1}\left(\frac{C_{v,m+1,j+1}}{p^2} - \frac{(p-1)^2}{p^2} C_{v,M,j+1}\right.\right.$$

$$\left.\left. + C_{v,M-1,j+1}\right)\right]\}$$

(B.3) $$\frac{1}{\Delta t}\left(f_{i,j+1} - f_{i,j}\right) = \frac{1}{2\Delta x_j^2} \{\left[f_{i-1,j}\left(\frac{1}{4} C_{v,i+1,j} + \frac{3}{4} C_{v,i-1,j}\right) - f_{i,j}\left(C_{v,i+1,j} + C_{v,i-1,j}\right)\right.$$

$$\left. + f_{i+1,j}\left(\frac{3}{4} C_{v,i+1,j} + \frac{1}{4} C_{v,i-1,j}\right)\right] + \left[f_{i-1,j+1}\left(\frac{1}{4} C_{v,i+1,j+1} + \frac{3}{4} C_{v,i-1,j+1}\right)\right.$$

$$\left. - f_{i,j+1}\left(C_{v,i+1,j+1} + C_{v,i-1,j+1}\right) + f_{i+1,j+1}\left(\frac{3}{4} C_{v,i+1,j+1} + \frac{1}{4} C_{v,i-1,j+1}\right)\right]\}$$

where $f_o = f_2$, $C_{v,o} = C_{v,2}$, $1 \leq i \leq M-1$

APPENDIX C A GENERAL PURPOSE SUBROUTINE THIN

SUBROUTINE THIN (FP,F,FO,X,X1,GAMMA,BETA,AWORK,BWORK,CP,COEF,MESH,
ERROR,NTIME,NSTEP,TSTP,STRAIN,FUN,OUTPUT)

This subroutine is written in the ICL1906A Extended Fortran for the solution of the consolidation of a thin soil layer under a step loading and is based on the modified fixed grid Lagrangian method.

This subroutine will calculate the parameter f , defined in eq(3.9), at time intervals specified by the user. The user is required to supply a function FUN which gives the value of the coefficient of consolidation based on the f value given and the final Eulerian strain. This coefficient should be normalized to c_v / c_o where c_o is the initial coefficient of consolidation of the layer.

A subroutine OUTPUT should also be supplied by the user which outputs the results in a required format. Both the function FUN and the subroutine OUTPUT must be declared by an EXTERNAL statement in the main program calling the subroutine THIN.

The parameters used in this subroutine are listed as follows :

(a) Those to be supplied by the user

MESH : an integer, the number of space mesh used.

ERROR : the error bound used to control iteration.

NTIME : an integer, the total number of time steps taken.

NSTEP : an integer, the number of substeps required in each time step.

STRAIN : the final Lagrangian strain.

TSTP(NTIME) : a real array, the time steps used to forward the solution

FUN(A,SNAT) : a function given the coefficient of consolidation from the solution A and the final Eulerian strain SNAT.

OUTPUT(F,X,T,U,MESH) : a subroutine gives the results at the end of each time step, T is the present time factor, U is the degree of settlement.

(b) Those required in the subroutine

FP(MESH) : the solution at the previous time level

F(MESH), FO(MESH) : the present and the previous iterative solutions.

X(MESH),X1(MESH) : the positions of the grids at the present and the next time level.

GAMMA(MESH),BETA(MESH),BWORK(MESH),AWORK(3,MESH) : working spaces.

COEF(MESH),CP(MESH) : the coefficient of consolidation at the present and the previous time level.

This subroutine is written in the single precision algorithm and experiences indicate that an error bound of $1x10^{-6}$ is sufficient for most applications. The core storage requirement and run time depend on the size of discretization and time steps used.

This subroutine is listed in the List of Programs in the form of a microfiche which can be found in the end of this thesis.

CHAPTER FOUR THE CONSOLIDATION OF A LINEAR SOIL MODEL

ABSTRACT

In this chapter the consolidation of a normally consolidated stratum under a surface loading and a dredged fill under its own weight are considered. In both cases the effect of self weight is included in the analysis, and a linear effective stress - void ratio and permeability - void ratio relationship has been assumed for the soil.

The Lagrangian formulation is used for the governing equation. With the particular linear soil model assumed, this reduces to a simple diffusion type equation with a constant coefficient of consolidation C_F . Solution in most cases can therefore be referred to standard references. The consolidation of a normally consolidated stratum is examined and comparison made with the thin layer theory. An example is provided for illustration. Two types of drainage boundary condition have been considered in the consolidation of a dredged fill. It is found that in the case of an impervious base consolidation of the stratum starts from the undrained face. This rather unusual behaviour is explained by studying the dissipation of excess pore water pressure.

1. INTRODUCTION

The thin layer examined in the previous chapter is an idealized situation. In particular, the effect of self weight is ignored in the analysis. In certain applications this can be used as an effective approximation, and in such cases the simplicity resulting from this idealization is really an advantage.

However, there are situations where the effect of self weight must be considered. The first type of problem of this kind is the consolidation of a thick stratum due to surface loading. In this case it is necessary to consider the effect of self weight of soil. Some numerical solutions to this type of problem have been obtained by De Simone and Viggiani (1976). Mikasa (1963) has also considered a similar problem with a surcharge loading and reported some numerical solutions. Owing to the wide acceptance of thin layer solution in engineering practice, it will prove extremely useful to compare the thin layer solution with the solution taking into account the effect of self weight. However, none of the previous work have made such a comparison.

The other type of problem where the effect of self weight has to be considered includes the case of a dredged fill and a deposit undergoing continuous sedimentation. In these cases consolidation is caused entirely by the weight of soil, and the thin layer idealization can no longer apply to this. To model this situation correctly a different approach from the thin layer theory must be taken. The case of a deposit undergoing continuous sedimentation has been considered by Gibson (1958) under the assumptions of small strain and the deposit is accreting at some known rate. Up to the time of writing no published work is yet available in the case of large strain and the case of a dredged fill consolidating under its own weight.

There is therefore a demand for a theory which includes the effect of self weight. Such a theory will be different from the thin layer theory in that not only the complete governing equation (2.23),(2.47) must be used, but also the initial and boundary conditions will be different. Furthermore, in the final equilibrium condition the void ratio distribution within the stratum will follow its effective stress distribution by the appropriate effective stress - void ratio relationship, and the latter distribution will include in this case a part given by the self weight of the soil. Thus it is not sufficient to consider only the variation of the coefficient of consolidation c_F or c_V when analysing such cases. Rather, a theoretical soil model with specified effective stress - void ratio and permeability - void ratio relationships will be required. For this purpose a linear and a nonlinear soil model have been developed in the present study.

This and the next chapter are concerned with the linear model ; the nonlinear model will be discussed in Chapter 6 and Chapter 7. In the analysis the Lagrangian formulation will be used and the coefficient of consolidation c_F has a constant value in the two models. This offers not only the advantage of simplicity, but also the results from these two models can be used to compare with each other and with the thin layer theory.

2. THE LINEAR SOIL MODEL

The choice of a theoretical soil model is very often a compromise between the conflicting requirements of reality and simplicity. Although it is desirable that the model should simulate real soil behaviour as closely as possible, because of the complex nature of soil, it will be difficult, if not impossible, to analyse

such a model. Furthermore, such a model may tend to be too specific in that it may describe well the behaviour of one particular soil while can not be applied to the others.

For the purpose of theoretical development it is thus preferrable to start with a simplified model which can later be extended to a more complex one. Thus, the fundamental behaviour can be understood without involving complicated analysis, and the result can be compared to the more complex model from which the merit of using a complex model can be assessed.

The simplest model is one with a linear effective stress - void ratio and a linear permeability - void ratio relationship. Examining the governing equation of consolidation in the Lagrangian coordinate, eq(2.42) :

$$\frac{\partial e}{\partial t} = -\frac{\partial}{\partial z}\left[\frac{k}{\rho_f(1+e)}\frac{d\sigma'}{de}\frac{\partial e}{\partial z}\right] - (\rho_s-\rho_f)\frac{d}{de}\left(\frac{k}{\rho_f(1+e)}\right)\frac{\partial e}{\partial z} \quad (4.1)$$

suggests that the easiest way of implementing this would be assuming that :

$$\frac{k}{\rho_f} = k_o\,(1+e) \quad (4.2)$$

$$\sigma' = A - \alpha e \quad (4.3)$$

where (4.4)

$$A = \alpha e_i$$

and e_i is the void ratio corresponding to zero effective stress state. The coefficient of consolidation C_F has been defined in Chapter 2 as :

$$C_F = -\frac{k}{\rho_f(1+e)}\frac{d\sigma'}{de} = \alpha k_o \tag{4.5}$$

and will be a constant in the present case. Using these relationships, eq(4.1) can be reduced to :

$$\frac{\partial e}{\partial t} = C_F \frac{\partial^2 e}{\partial z^2} \tag{4.6}$$

which is identical to that of a thin layer with a constant C_F .
It should be noted, however, that the initial and boundary conditions in the present case will be different from that of the thin layer theory. Moreover, the final equilibrium state will also be very different.

In the final equilibrium state the stratum is in equilibrium with its self weight and any surface loading that may be present. To simplify the anlysis the surface loading is assumed to be fully effective within the stratum, i.e. there will be an equal increment of stress to all parts of the stratum. Thus, variation of effective stress in depth will be caused by the weight of the soil only. When expressed in terms of the Lagrangian coordinate a simple expression results :

$$\frac{d\sigma'}{dz} = -(\rho_s - \rho_f) \tag{4.7}$$

where the negative sign indicates that the direction of z is measured against gravity. Hence,

$$\frac{de}{dz} = \frac{de}{d\sigma'}\frac{d\sigma'}{dz} = -\beta \tag{4.8}$$

where

$$\beta = \frac{1}{\alpha}(\rho_s - \rho_f) \tag{4.9}$$

Eq(4.8) can be integrated to give :

$$e(z) = e_s - \beta(z_o - z) \tag{4.10}$$

where e_s is the void ratio in the surface of the stratum and z_o is the solid thickness of the stratum. This shows a linear decrease of void ratio with (solid) depth. The relationship between z_o and the thickness (measured in space) of the stratum h_o can be obtained from the transformation formula between the Eulerian coordinate x and the Lagrangian coordinate z :

$$x(z) = \int_0^z (1+e)dz \tag{4.11}$$

as : $$h_o = (1 + e_s - \frac{1}{2}\beta z_o) z_o \tag{4.12}$$

and, from eq(4.10) :

$$x(z) = (1 + e_s - \beta z_o) z_o + \frac{\beta}{2} z^2 \tag{4.13}$$

Using the normalized coordinate η and χ :

$$\eta = \frac{z}{z_o} \tag{4.14}$$

and $$\chi = \frac{x}{h_o} \tag{4.15}$$

then eq(4.12),(4.13) can be combined to give :

$$\chi = \frac{(1 + e_s - \bar{\beta})\eta + \frac{\bar{\beta}}{2}\eta^2}{(1 + e_s - \frac{1}{2}\bar{\beta})} \tag{4.16}$$

where $$\bar{\beta} = \beta z_o \tag{4.17}$$

Eq(4.16) can be further simplified by using a parameter γ' :

$$\gamma' = \frac{\bar{\beta}}{(1+e_s)} = (\rho_s-\rho_f) z_o [-\frac{1}{1+e_s}\frac{de}{d\sigma'}] \qquad (4.18)$$

as : $$\chi = \frac{1}{1-\frac{\gamma'}{2}} [(1-\gamma')\eta + \frac{\gamma'}{2}\eta^2] \qquad (4.19)$$

or : $$\eta = \frac{1}{\gamma'} \{\sqrt{[(1-\gamma')^2 + 2\gamma'(1-\frac{\gamma'}{2})\chi]} - (1-\gamma)\} \qquad (4.20)$$

This is shown in Fig.4.1.

In the definition of γ' , eq(4.18), the term in the bracket $-\frac{1}{1+e_s}\frac{de}{d\sigma'}$ is the compressibility of the soil and $(\rho_s-\rho_f) z_o$ is the part of the effective stress in the base of the stratum caused by the weight of the soil. Thus, γ' is the (Lagrangian) strain in the base of the stratum due to its self weight. A larger value of γ' is associated with a thick, compressible stratum. Conversely, as γ' approaches zero the stress distribution tends to be more uniform and the stratum approaches the thin layer idealization.

The void ratio distribution in the space coordinate χ can be obtained from the above equations as :

$$e(\chi) = (1+e_s) \sqrt{[(1-\gamma')^2 + 2\gamma'(1-\frac{\gamma'}{2})\chi]} - 1 \qquad (4.21)$$

which is seen to be a function of e_s and γ' . This is shown in Fig.4.2 which also shows the same distribution in the Lagrangian coordinate η .

Having established the equilibrium condition required for a normally consolidated stratum, the next section will consider the consolidation of such a stratum under a surface loading. This is followed by a different problem, namely, a dredged fill consolidating from an initially uniform void ratio to the normally consolidated state.

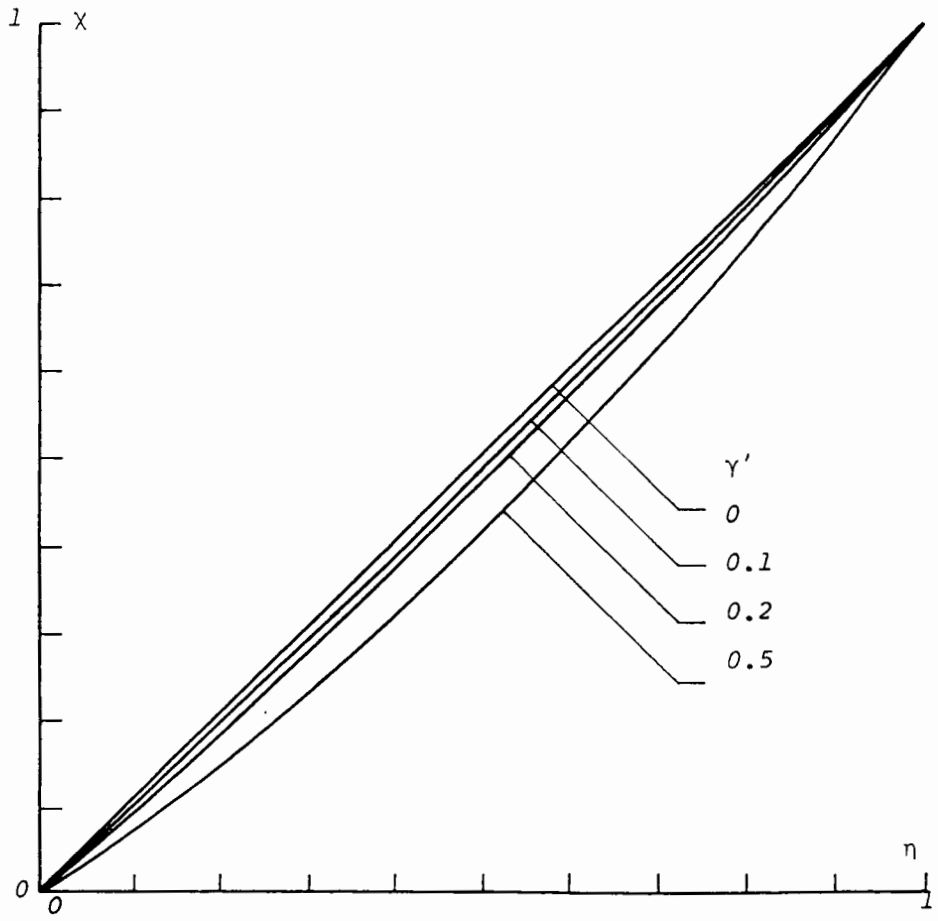

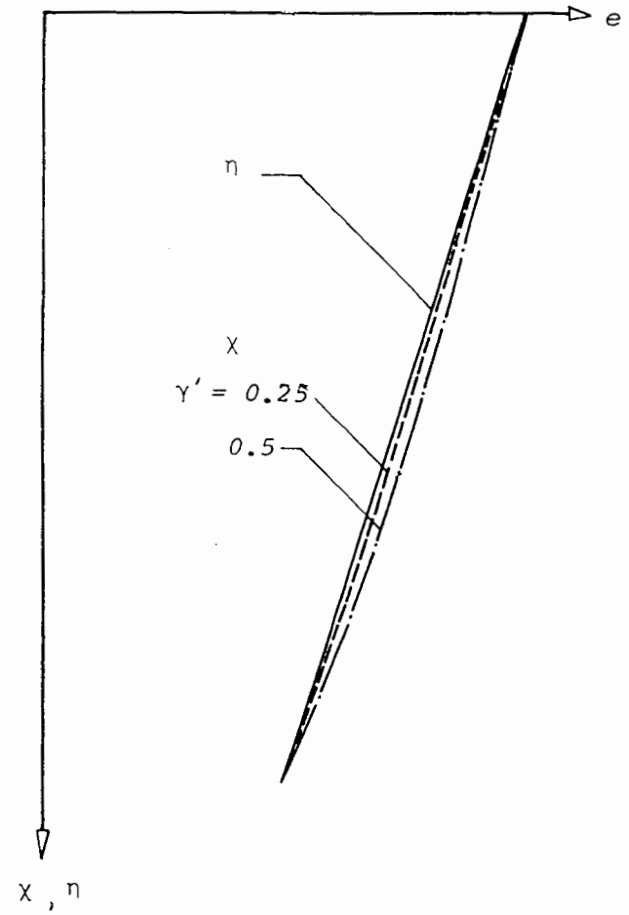

FIG.4.1 (above) Relationship between χ and η in a normally consolidated stratum.

FIG.4.2 (left) Void ratio distribution in a normally consolidated stratum.

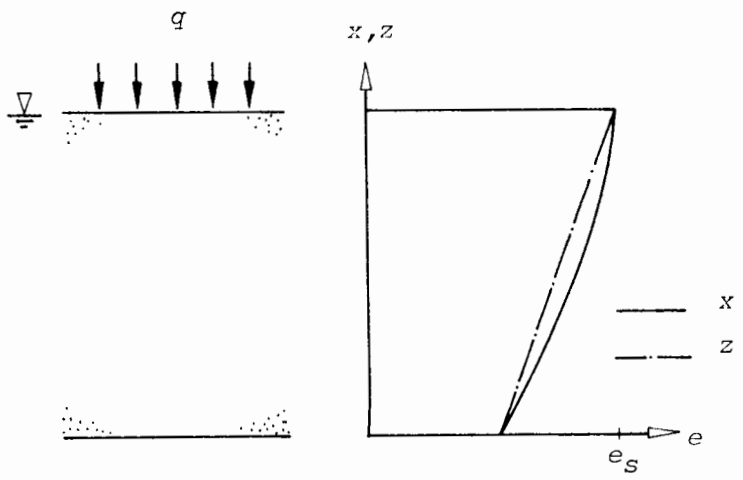

FIG.4.3 A normally consolidated stratum.

3. THE CONSOLIDATION OF A NORMALLY CONSOLIDATED STRATUM UNDER A SURFACE LOADING

Consider a stratum initially in equilibrium with its self weight and a surface loading, Fig.4.3. The void ratio distribution in this stratum is given by eq(4.10) as :

$$e(z,0) = e_s - \beta(z_o - z) \qquad (4.10)$$

where all the notations have the same meaning as before.

At the instant $t = 0$ an additional loading is applied to the surface of the stratum. The governing equation for the consolidation is ,

$$\frac{\partial e}{\partial t} = C_F \frac{\partial^2 e}{\partial z^2} \quad , \quad 0 \leq z \leq z_o \, , \quad t \geq 0 \qquad (4.22)$$

and two types of boundary will be considered :

(a) A drained boundary

The soil in this boundary will respond immediately to the applied loading. Hence :

$$e(0,t) = e_s - \beta z_o - \Delta e \quad \text{in the base} \tag{4.23}$$

$$e(0,t) = e_s - \Delta e \quad \text{in the surface} \tag{4.24}$$

where Δe is the void ratio change caused by the additional loading. Furthermore, the final equilibrium state is simply :

$$e(z,\infty) = e(z,0) - \Delta e \tag{4.25}$$

(b) An undrained boundary

In this type of boundary there will be no flow across it (or, more rigorously, the fluid velocity will be the same as the solid velocity). Thus :

$$\frac{\partial u}{\partial x} = 0 \tag{4.26}$$

Since, $u = \sigma - \sigma' - u_h$ (4.27)

hence, $$\frac{\partial u}{\partial x} = \frac{\partial}{\partial x}(\sigma - \sigma' - u_h) = 0 \tag{4.28}$$

or, $$\frac{\partial \sigma'}{\partial x} = \frac{\partial}{\partial x}(\sigma - u_h) = -\frac{\rho_s - \rho_f}{1+e} \tag{4.29}$$

Transform to the Lagrangian coordinate z :

$$\frac{\partial \sigma'}{\partial z} = \frac{\partial \sigma'}{\partial x}\frac{dx}{dz} = \frac{1}{1+e}\frac{\partial \sigma'}{\partial x} \tag{4.30}$$

therefore, $$\frac{\partial e}{\partial z} = \frac{de}{d\sigma'}\frac{\partial \sigma'}{\partial z} = -\frac{de}{d\sigma}(\rho_s - \rho_f) = \beta \tag{4.31}$$

which is the required boundary condition.

In the analysis it is advantageous to use a new parameter q , the void ratio change, defined as :

$$q(z,t) = e(z,0) - e(z,t) \tag{4.32}$$

which measures the amount of void ratio change that has occured since the start of consolidation. The governing equation in this new parameter is :

$$\frac{\partial q}{\partial t} = C_F \frac{\partial^2 q}{\partial z^2} \quad , \quad 0 \leq z \leq z_o \, , \quad t \geq 0 \tag{4.33}$$

with the initial condition :

$$q(z,0) = 0 \tag{4.34}$$

The drainage boundary condition in the new parameter is simply,

$$q = \Delta e \tag{4.35}$$

and the undrained boundary condition is also simpler :

$$\frac{\partial q}{\partial z} = \frac{\partial e(z,0)}{\partial z} - \frac{\partial e}{\partial z} = 0 \tag{4.36}$$

The use of this new parameter q therefore reduces the initial and boundary conditions to the standard type, and solutions to most cases can be obtained from standard references (see, for example, Carslaw and Jaeger 1959, Chapter 3 ; also Crank 1975, Chapter 4). For this reason only the double drainage case with a step loading will be discussed here, the behaviour of the single drainage case is essentially similar.

The solution for the double drainage case with a step loading is :

$$q(\eta,T) = \Delta e \left[1 - \frac{4}{\pi} \sum_{n} \frac{\sin(n\pi\eta)}{n} \exp(-n^2\pi^2 T) \right] \tag{4.37}$$

$$n = 1, 3, 5, \ldots$$

where η is the normalized material coordinate defined in eq(4.14)

and T is the time factor defined as :

$$T = \frac{C_F t}{z_o^2} \tag{4.38}$$

The degree of settlement S is defined as :

$$S(T) = \frac{h(0) - h(T)}{h(0) - h(\infty)} \tag{4.39}$$

where $h(0)$, $h(T)$ and $h(\infty)$ are respectively the initial, current and final thickness (measured in space) of the stratum. These can be obtained from eq(4.11) and it is found that :

$$S(T) = 1 - \frac{8}{\pi^2} \sum_{n} \frac{1}{n^2} \exp(-n^2\pi^2 T) \tag{4.40}$$

$$n = 1, 3, 5, \ldots.$$

This coincides with the thin layer C_F constant solution, eq(3.5). It should be noted that although in this case the thin layer theory predicts correctly the settlement behaviour of the total stratum, the local settlement behaviour will be different.

To illustrate this, consider the local degree of settlement $\zeta(\eta,T)$, defined as :

$$\zeta(\eta,T) = \frac{x(\eta,0) - x(\eta,T)}{x(\eta,0) - x(\eta,\infty)} \tag{4.41}$$

where $x(\eta,0)$, $x(\eta,T)$ and $x(\eta,\infty)$ are respectively the space coordinates corresponding to η in the initial, current and final states. This corresponds to the settlement plate measurement in field practice : as the settlement plate is installed to a fixed material point, the actual movement observed therefrom is the change in space thickness of that material point. Using eq(4.11) the above equation becomes,

$$\zeta(\eta,T) = \frac{\int_0^{\eta} q(y,T)\,dy}{\int_0^{\eta} q(y,\infty)\,dy} \qquad (4.42)$$

and by virtue of eq(4.37) :

$$\zeta(\eta,T) = \eta - 4 \sum_{n} \frac{1 - \cos(n\pi\eta)}{n^2\pi^2} \exp(-n^2\pi^2 T) \qquad (4.43)$$

$$n = 1, 3, 5, \ldots.$$

This is plotted for η= 0.1(0.1)1.0 in Fig.4.4.

The difference between the thin layer theory and the present theory can now be examined. In practice the location of a settlement plate is specified in the space rather than the material coordinate. Hence, in order to predict or compare with theory the local degree of settlement as measured, a transformation from the space to the material coordinate is required. Obviously this transformation will be different for different theories. Consider a settlement plate installed in the midheight (refer in position to space) of the stratum. According to the thin layer theory the corresponding material coordinate will be the midlayer (η = 0.5) because of the initially uniform void ratio distribution assumed. The predicted local degree of settlement is shown in Fig.4.5 as denoted by γ'=0. According to the present theory, however, this midheight will not correspond to the midlayer because of the heterogenuity introduced by the effect of self weight. Rather, this will depend on the parameter γ' of the stratum, see eq(4.19),(4.20). The predicted results for γ' = 0.2, 0.5 and 0.8 are also shown in Fig.4.5 for comparison with the thin layer theory. It can be seen that the thin layer predicts a faster rate than the present theory. This difference is most pronounced in the early stages and with larger γ' , i.e. a thick, compressible stratum.

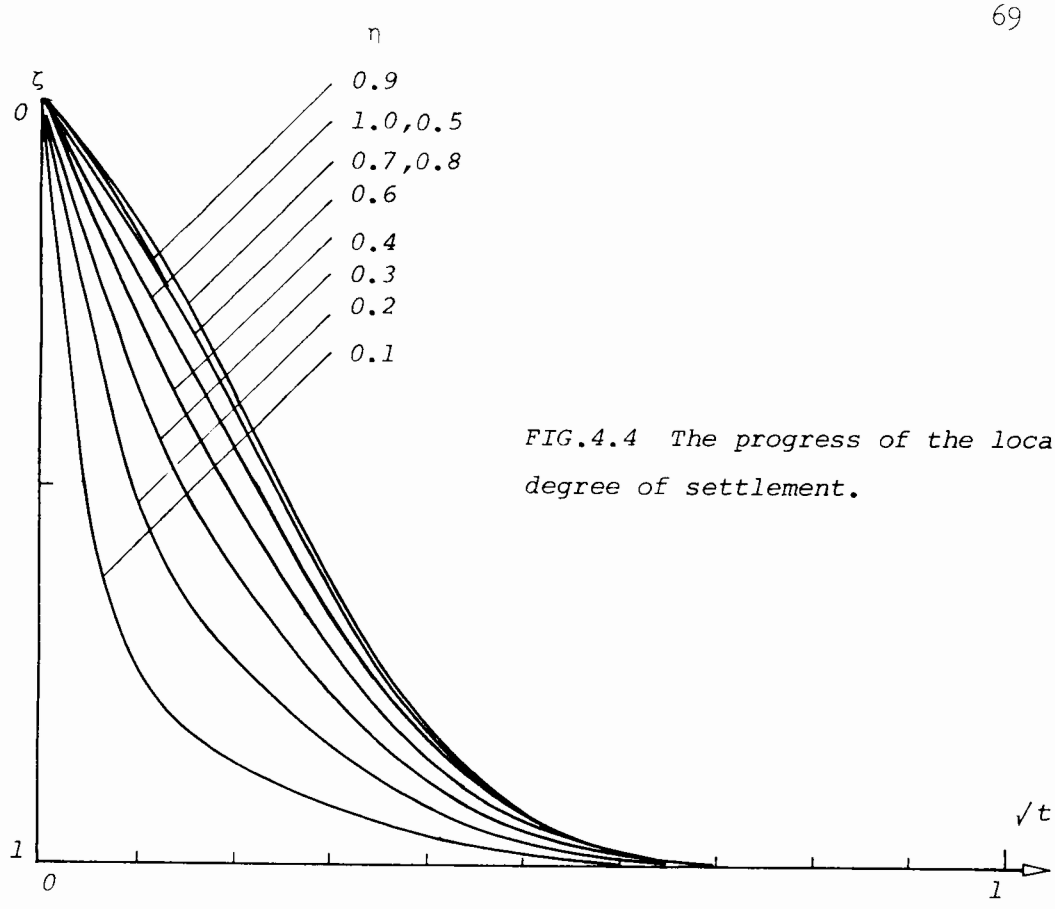

FIG.4.4 The progress of the local degree of settlement.

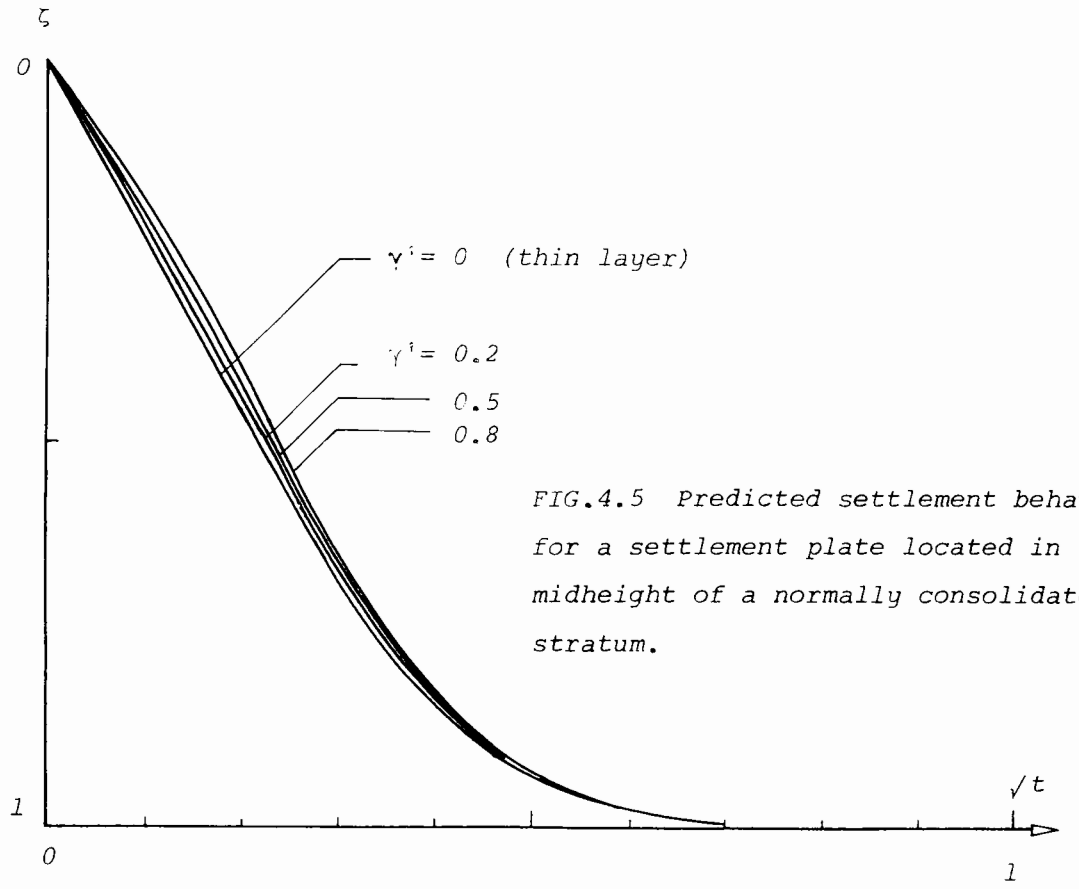

FIG.4.5 Predicted settlement behaviour for a settlement plate located in the midheight of a normally consolidated stratum.

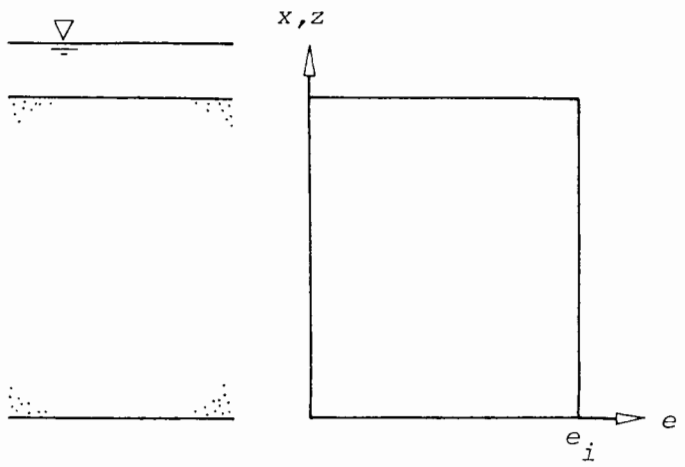

FIG.4.6 A dredged fill of initially uniform density.

4. THE CONSOLIDATION OF A DREDGED FILL UNDER ITS OWN WEIGHT

Consider a dredged fill which has been dumped in situ instantaneously with a uniform void ratio e_i , Fig.4.6. Immediately after this stratum will start consolidating to its normally consolidated state under the action of the self weight of soil. The governing equation is :

$$\frac{\partial e}{\partial z} = C_F \frac{\partial^2 e}{\partial z^2} \quad , \quad o \leq z \leq z_o \, , \quad t \geq o \qquad (4.22)$$

with a uniform initial condition :

$$e(z,0) = e_i \qquad (4.44)$$

The void ratio in the surface will remain in its initial state because no further stress will act upon this,

$$e(z_o,t) = e_i \qquad (4.45)$$

and two types of base will be considered :

(a) A pervious base

The void ratio here will immediately reach its final

equilibrium value, i.e. the normally consolidated state given by :

$$e(z,\infty) = e_i - \beta(z_o - z) \tag{4.46}$$

Hence : (4.47)

$$e(0,t) = e_i - \beta z_o$$

(b) An impervious base

The boundary condition has been obtained in the previous section, see eq(4.31).

The above equations can be written in terms of the normalized material coordinate η , the time factor T and the void ratio change q defined as :

$$\eta = \frac{z}{z_o} \tag{4.48}$$

$$T = \frac{C_F t}{z_o^2} \tag{4.49}$$

$$q(\eta,T) = e_i - e(\eta,T) \tag{4.50}$$

Thus;

$$\frac{\partial q}{\partial T} = \frac{\partial^2 q}{\partial \eta^2} \tag{4.51}$$

$$q(\eta,0) = 0 \tag{4.52}$$

$$q(1,T) = 0 \tag{4.53}$$

$$q(0,T) = \beta z_o \qquad \text{for a pervious base} \tag{4.54}$$

or $$\frac{\partial q}{\partial \eta}(0,T) = -\beta z_o \qquad \text{for an impervious base} \tag{4.55}$$

The two cases of a pervious and an impervious base will now be considered.

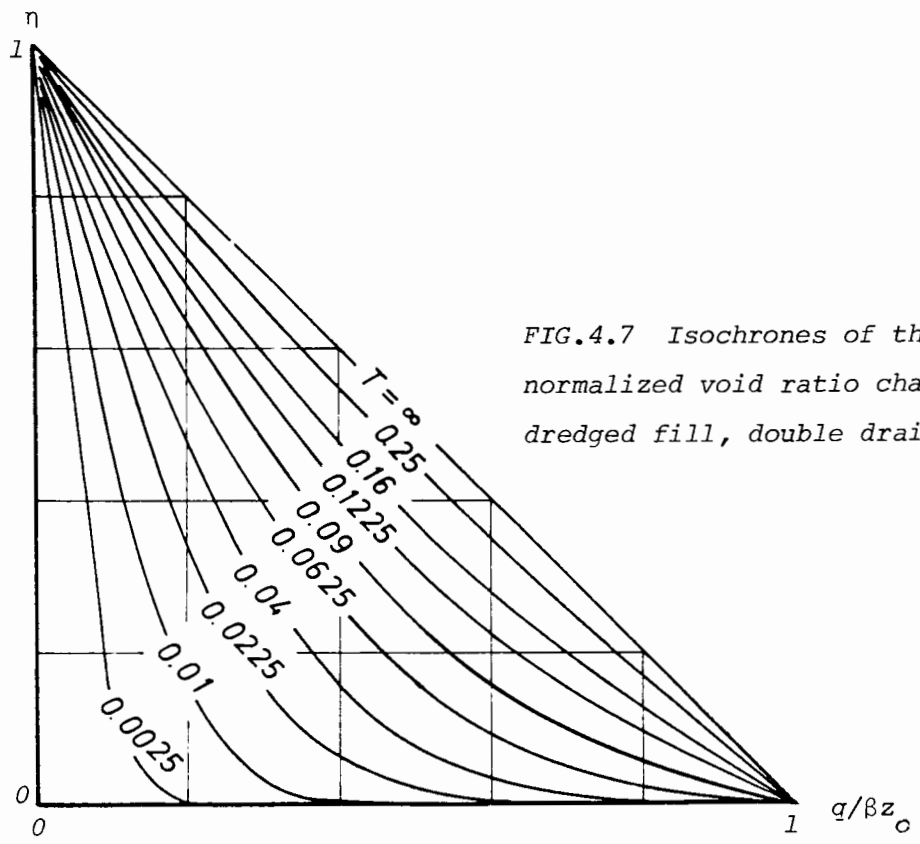

FIG.4.7 Isochrones of the normalized void ratio change, dredged fill, double drain.

Double Drain (Pervious Base)

The solution to eq(4.51-54) can be obtained from standard references (Carslaw and Jaeger 1959, Crank 1975) as :

$$q(\eta,T) = \beta z_o [1-\eta- 2 \sum_n \frac{\sin(n\pi\eta)}{n\pi} \exp(-n^2\pi^2 T)] \qquad (4.56)$$

The degree of settlement S is :

$$S(T) = 1 - 8 \sum_n \frac{1}{n^2\pi^2} \exp(-n^2\pi^2 T) \ , \quad n = 1, 3, 5, \ldots \qquad (4.57)$$

which also coincides with the thin layer solution. It should be noted however, that the present case is an entirely different process to that described by the thin layer theory. Hence, this coincidence should not be considered as a possible application of the thin layer theory.

The isochrones of the void ratio change are shown in Fig.4.7. For clarity of presentation this has been normalized by a factor βz_o .

Surface Drain (Impervious Base)

The equations now comprise eq(2.51-53), eq(2.55), and solution is obtained using the technique of Laplace transform. The transformed solution is,

$$q(\eta,p) = \beta z_o \frac{\sinh[(1-\eta)\sqrt{p}]}{\sqrt{(p)^3}\cosh\sqrt{p}} \qquad (4.58)$$

Using the standard transformation pair (Erdelyl 1954, p.258, pair (5.9.34)) :

$$\mathcal{L}^{-1}\left\{\frac{\sinh[(1-\eta)\sqrt{p}]}{\sqrt{p}\cosh\sqrt{p}}\right\} = 2\sum_n (-1)^n \sin\left[\left(\frac{2n+1}{2}\pi\right)(1-\eta)\right]\exp\left[-\left(\frac{2n+1}{2}\pi\right)^2 T\right] \qquad (4.59)$$

the solution is found as :

$$q(\eta,T) = \beta z_o \left\{1-\eta - 2\sum_n \frac{(-1)^n \sin(m\pi(1-\eta))}{m^2\pi^2}\exp(-m^2\pi^2 T)\right\} \qquad (4.60)$$

$$n = 0, 1, 2, \ldots \qquad m = \frac{1}{2}(2n+1)$$

From which follows the degree of settlement :

$$S(T) = 1 - 4\sum_n \frac{(-1)^n}{m^3\pi^3}\exp(-m^2\pi^2 T) \qquad (4.61)$$

A small time approximate solution for the degree of settlement can be obtained by considering its Laplace transform (Carslaw and Jaeger 1948), which is obtained by integrating eq(4.58) as :

$$S(p) = 2\left[\frac{1}{p^2} - \frac{1}{p^2\cosh\sqrt{p}}\right] \qquad (4.62)$$

where $S(p)$ is the Laplace transform of $S(T)$. As $p \to \infty$, $\cosh \sqrt{p} \to \frac{1}{2}\exp(\sqrt{p})$ and the above equation is approximated by :

$$S(p) \simeq 2 \left[\frac{1}{p^2} - \frac{2}{p^2} \exp(-\sqrt{p}) \right] \tag{4.63}$$

which has the inverse transform :

$$S(T) \simeq 2T + \frac{4}{\sqrt{\pi T}} \exp(-\frac{1}{4T}) - 4T \operatorname{erfc}(\frac{1}{2\sqrt{T}}) \tag{4.64}$$

where $T << 1$.

Since in this case, $\frac{4}{\sqrt{\pi T}} \exp(-\frac{1}{4T}) \to 0$

and : $4T \operatorname{erfc}(\frac{1}{2\sqrt{T}}) \to 0$

thus eq(4.64) can be further simplified to :

$$S(T) \simeq 2T \tag{4.65}$$

which is valid in small value of time factor.

In larger times the first term of the series solution eq(4.61) can be used as an approximate solution, i.e.

$$S(T) \simeq 1 - \frac{32}{\pi^3} \exp(-\frac{\pi^2}{4} T) \tag{4.66}$$

A comparison of this small and large time approximate solutions with the exact solution is provided in Table 4.1.

Time Factor	Exact Solution Eq(4.61)	Small Time Solution Eq(4.65)	Large Time Solution Eq(4.66)
0.0025	0.005000	0.005000	0.010457
0.01	0.019999	0.020000	0.023716
0.0225	0.044999	0.045000	0.046877
0.04	0.079992	0.080000	0.080669
0.0625	0.124808	0.125000	0.124981
0.09	0.178619	0.180000	0.178650
0.16	0.305673	0.320000	0.305673
0.36	0.575459	-	0.575459
1.0	0.912477	-	0.912477
2.25	0.995994	-	0.995994

TABLE 4.1 COMPARISON OF APPROXIMATE SOLUTIONS WITH EXACT SOLUTION

Fig.4.8 shows the isochrones of the void ratio change q, this again has been normalized by βz_o for clarity. An unusual feature that can be seen from this is that consolidation of the stratum starts from the part near the undrained base. This can be explained by considering the dissipation of excess pore water pressure within the stratum.

Referring to eq(4.27), it is found that in the present case :

$$\sigma - u_h = (\rho_s - \rho_f)(z_o - z) \tag{4.67}$$

and,

$$\sigma' = \alpha(e_i - e) = \alpha q = \frac{(\rho_s - \rho_f)}{\beta} q \tag{4.68}$$

Hence the excess pore water pressure :

$$u = 2(\rho_s - \rho_f) z_o \sum_n \frac{(-1)^n \sin(m\pi(1-\eta))}{m^2\pi^2} \exp(-m^2\pi^2 T) \tag{4.69}$$

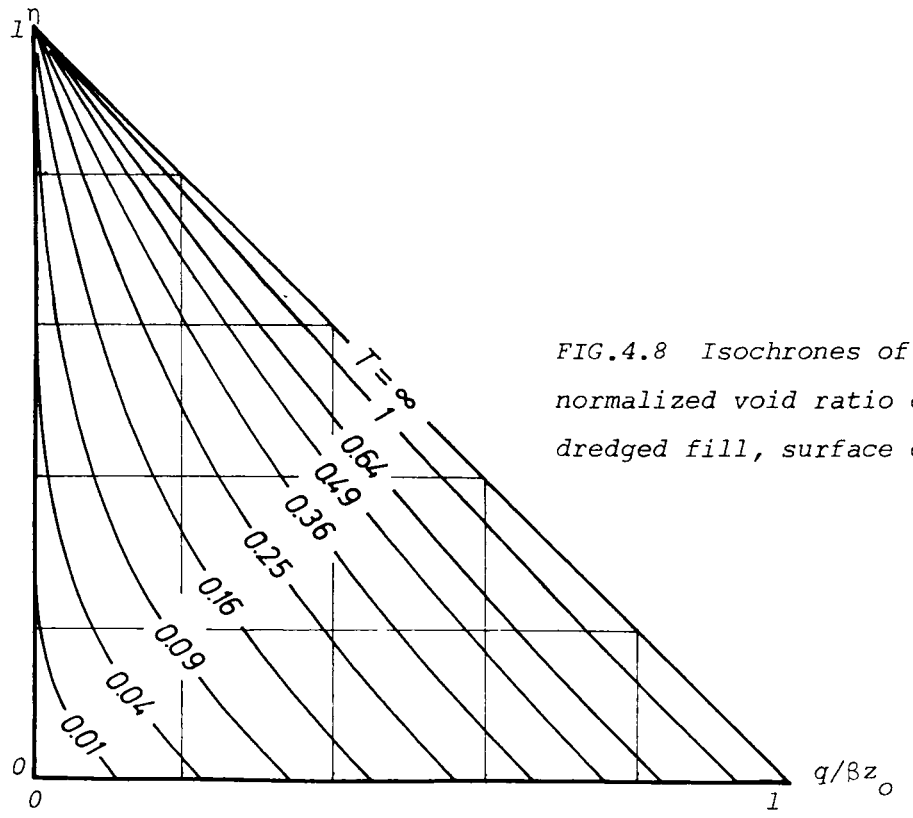

FIG.4.8 Isochrones of the normalized void ratio change, dredged fill, surface drain.

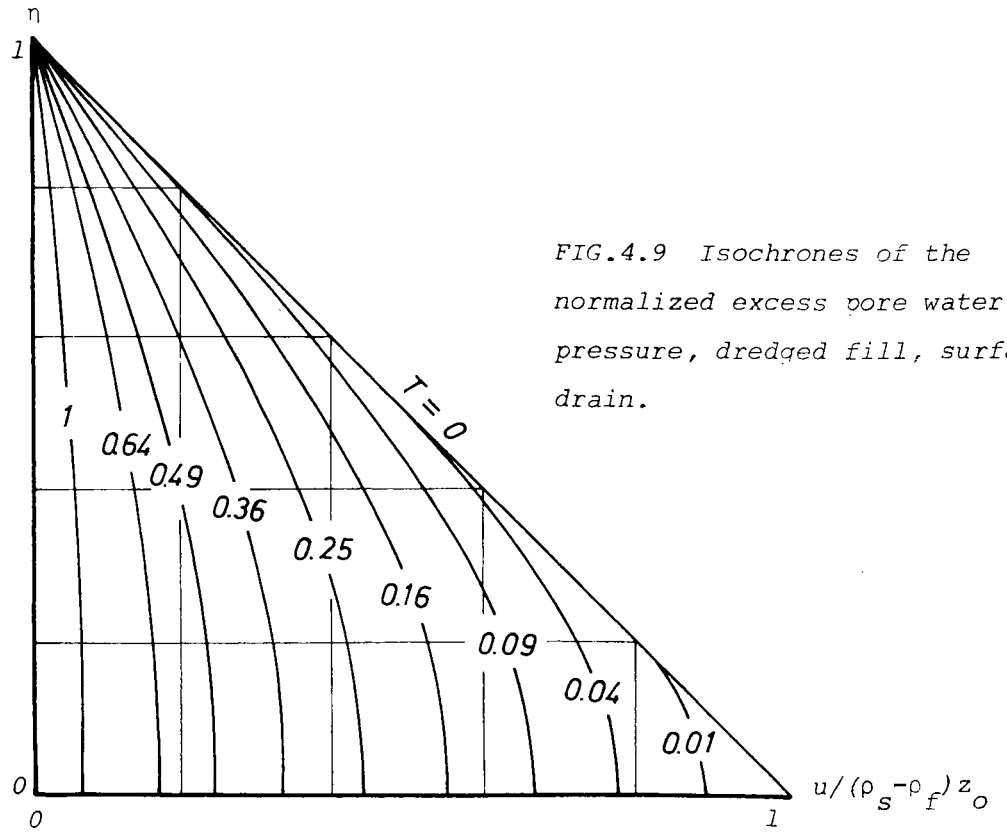

FIG.4.9 Isochrones of the normalized excess pore water pressure, dredged fill, surface drain.

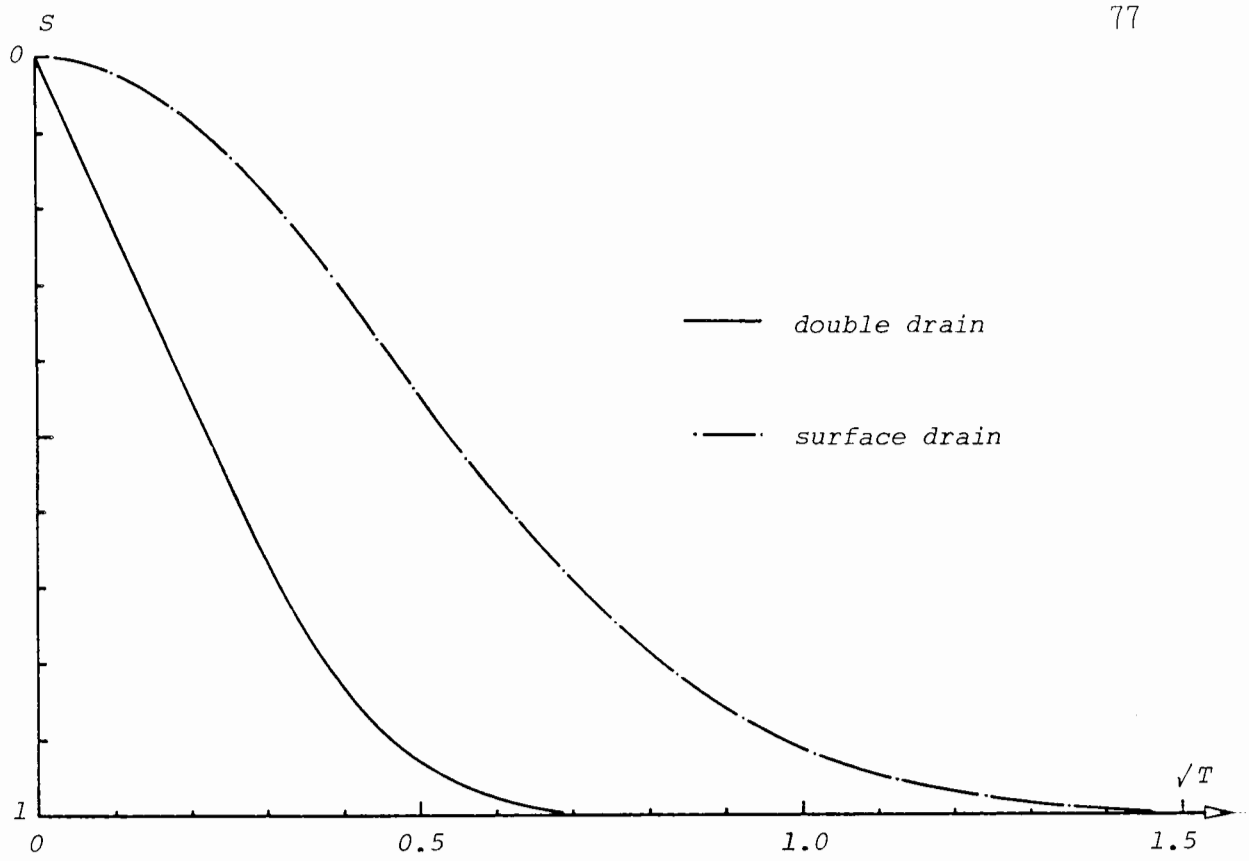

FIG.4.10 Degree of settlement versus the square root of time factor, dredged fill.

The isochrones are shown in Fig.4.9. It can be seen that the maximum excess pore water pressure occurs in the base. Therefore, in order that a continuous outward water flow from the stratum during consolidation can be maintained the excess pore water pressure in the base must be dissipated first. This can be seen in this figure. As a consequence, an earlier consolidation in this part is observed.

Finally, the degree of settlement of the present and the double drainage cases are shown in Fig.4.10.

CHAPTER FIVE THE CONSOLIDATION DURING AND AFTER THE DEPOSITION OF A LINEAR SOIL

ABSTRACT

The consolidation accompanying the formation of a deposit by continuous sedimentation is considered in this chapter. In the absence of other external forces, the consolidation is caused by the weight of the soil itself that varies as deposition proceeds. This process is further complicated by the change of the drainage length as the deposit builds up and is compressed. Consequently the mathematical model is more complicated than those treated in the previous chapters. Analytical solutions are thus limited to two types of deposition in the present study.

The first type of deposition assumes that the material in the deposit is increased in proportional to the square root of time. This boundary value problem is solved either by the Fourier method, or alternatively by the method of generalized potential. The latter method yields a system of Voltera equation of the second kind, for which a simple solution can be obtained in this particular case. The agreement between the two solutions is seen to be very good.

The second type considered is a constant rate of deposition. The corresponding boundary value problem can be reduced to a singular integral equation of the Fredholm type and subsequently solved.

The present problem is then linked to those treated in the previous chapters by defining a time factor in a similar manner. From this a unique time - settlement relationship is shown to exist for each of the two cases considered.

The consolidation after deposition has ceased is considerably simpler as only fixed boundaries are involved. Solutions have been obtained by the Fourier method for the constant rate of deposition. Finally, at the end of this chapter the theory is applied to analyse the consolidation with different dumping rate of a dredged fill.

1. INTRODUCTION

In the last chapter the consolidation of a dredged fill was analysed assuming that all the material was dumped instantaneously. This is an idealization which can only be applied to a small number of engineering problem. A real filling operation, especially if the area to be covered is large, will normally take some considerable time to complete. During the operation, the deposit has already started compressing while the weight of additional material will cause further compression. The drainage path is increased as more material is deposited. However, there will also be a reduction in drainage path as the deposit is compressed by the newly deposited material. Hence, the ability of the deposit to consolidate will depend not only on its consolidation characteristics but will also be influenced by the deposition rate.

A similar problem, largely with geological applications is the formation of seabed by sedimentation. Apart from the different time scale involved, the basic mechanism of these processes is identical and can therefore be studied in the same category.

Within the framework of the linear soil model, the governing equation is :

$$\frac{\partial e}{\partial t} = C_F \frac{\partial^2 e}{\partial t^2} \qquad (5.1)$$

where z is the material coordinate which will be bounded by a time dependent domain :

$$0 \leq z \leq s(t) \qquad (5.2)$$

with $s(t)$ defined as the solid thickness at present time t , this is a measure of the deposited material.

The boundary condition in the surface of the deposit is :

$$e(s,t) = e_i \tag{5.3}$$

where e_i is the assumed initial state of the soil, i.e. the zero effective stress state.

The boundary condition in the base of the deposit depends on its drainage condition, i.e.:

$$\frac{\partial e}{\partial z}(0,t) = \beta \qquad \text{for an impervious base} \tag{5.4}$$

and $$e(0,t) = e_i - \beta s(t) \qquad \text{for a pervious base} \tag{5.5}$$

where β has been originally defined in the last chapter as $\frac{1}{a}(\rho_s - \rho_f)$ (see eq(4.9),eq(4.31)).

Eq(5.1-5) thus constitute the mathematical model for the present problem. This is a moving boundary problem with prescribed boundary movement, and the existence of a solution with a well behaved boundary movement $s(t)$ can be established by the method of generalized potential. A brief description of this is appended at the end of this chapter.

It is noticed that similar problems have been attempted by several previous workers and treated most successfully by Gibson (1958). These formulations were based on the small strain theory and the studies were restricted to a clay layer accreting in thickness with time. These are therefore very different from the present study. Despite this, the solutions emerging from the present study are in some ways strikingly similar to these obtained by Gibson (1958).

2. DEPOSITION PROPORTIONAL TO THE SQUARE ROOT OF TIME

General Consideration

The first case considered is when the deposition proceeds in proportion to the square root of time, i.e. :

$$s(t) = pt^{\frac{1}{2}} \tag{5.6}$$

where $s(t)$ is the amount of solid material deposited up to the time t and p is a constant. Accordingly, the rate of deposition of the present case is given by :

$$\frac{ds}{dt} = \frac{1}{2} pt^{-\frac{1}{2}} \tag{5.7}$$

It can be seen that initially the deposition rate is very large which approaches infinity as $t \to 0$; and in large times this becomes very small and eventually ceases as $t \to \infty$. Although this particular deposition behaviour is unlikely to occur naturally, it is a possible idealization for the dumping of dredged fill, and an analytical solution can be obtained which possesses certain interesting properties as will be seen later.

The equations describe this situation are :

$$\frac{\partial e}{\partial t} = C_F \frac{\partial^2 e}{\partial z^2} \qquad 0 \leq z \leq pt^{\frac{1}{2}} \qquad t \geq 0 \tag{5.8}$$

$$e(pt^{\frac{1}{2}}, t) = e_i \tag{5.9}$$

$$e(0,t) = e_i - \beta pt^{\frac{1}{2}} \qquad \text{for a pervious base} \tag{5.10}$$

or :

$$\frac{\partial e}{\partial z}(0,t) = \beta \qquad \text{for an impervious base} \tag{5.11}$$

It is more convenient to work with a new variable q defined as (see eq(4.50)) :

$$q(z,t) = e_i - e(z,t)$$

This, as described in the previous chapters, is the void ratio change from its initial state.

Using this new variable eq(5.8-11) will now appear as :

$$\frac{\partial q}{\partial t} = C_F \frac{\partial^2 q}{\partial z^2} \qquad 0 \leq z \leq pt^{\frac{1}{2}} \qquad t \geq 0 \qquad (5.8)_a$$

$$q(pt^{\frac{1}{2}},t) = 0 \qquad (5.9)_a$$

$$q(0,t) = \beta pt^{\frac{1}{2}} \qquad \text{for a pervious base} \qquad (5.10)_a$$

or : $$\frac{\partial q}{\partial z}(0,t) = -\beta \qquad \text{for an impervious base} \qquad (5.11)_a$$

This will be solved firstly by the Fourier method and then by the method of generalized potential in the following sections.

Solution by the Fourier Method (Seperation of Variables)

In this method the moving boundary $s(t)$ is fixed by the use of a new variable y :

$$y = z/pt^{\frac{1}{2}} \qquad (5.12)$$

From which the governing equation becomes :

$$t\frac{\partial q}{\partial t} = \frac{C_F}{p^2}\frac{\partial^2 q}{\partial y^2} + \frac{y}{2}\frac{\partial q}{\partial y} \qquad 0 \leq y \leq 1 \qquad t > 0 \qquad (5.13)$$

with the boundary conditions :

$$q(1,t) = 0 \tag{5.14}$$

$$q(0,t) = \beta p t^{\frac{1}{2}} \qquad \text{for a pervious base} \tag{5.15}$$

or :
$$\frac{\partial q}{\partial y}(0,t) = -\beta p t^{\frac{1}{2}} \qquad \text{for an impervious base} \tag{5.16}$$

By the method of seperation of variables,

$$q(y,t) = F(y)G(t)$$

Substituting in eq(5.13) yields two equations for $F(y)$ and $G(t)$ as:

$$t \frac{dG_\lambda}{dt} = \lambda G_\lambda(t) \tag{5.17}$$

and
$$\frac{d^2F_\lambda}{dy^2} + \frac{p^2}{C_F}\left(\frac{y}{2} \frac{dF_\lambda}{dy} - \lambda F_\lambda \right) = 0 \tag{5.18}$$

where the value of λ varies for different solutions and the subscript λ denotes the eigenfunction with respect to λ . The solution to eq(5.17) is simply,

$$G_\lambda(t) = t^\lambda \tag{5.19}$$

In integrating eq(5.18) it is apparent that a solution can only exist for $\lambda = \frac{1}{2}$, thus:

$$\frac{d^2F}{dy^2} + \frac{p^2}{2C_F}\left(y\frac{dF}{dy} - F \right) = 0 \tag{5.20}$$

This can be written as:

$$\frac{d^2F}{dy^2} + \frac{\nu^2}{2}\left(y\frac{dF}{dy} - F \right) = 0 \tag{5.20}_a$$

where $$\nu = \frac{1}{2} p C_F^{-\frac{1}{2}} \tag{5.21}$$

The function :

$$F_1(y) = By \tag{5.22}$$

with arbitrary constant B satisfies eq(5.20) and therefore is a first solution. From this the second solution can be constructed by setting :

$$F_2(y) = F_1(y)u(y)$$

which yields the following differential equation for $u(y)$:

$$\frac{d^2u}{dy^2} + \left(\frac{2}{y} + \frac{\nu^2}{2} y \right) \frac{du}{dy} = 0 \tag{5.23}$$

Let,

$$w(y) = \frac{du}{dy} \tag{5.24}$$

then,

$$\frac{dw}{dy} = - \left(\frac{2}{y} + \frac{\nu^2}{2} y \right) w \tag{5.25}$$

Hence,

$$w(y) = y^{-2} \exp(-\nu^2 y^2) \tag{5.26}$$

and finally,

$$u(y) = \exp(-\nu^2 y^2)/y + \pi^{\frac{1}{2}} \nu \operatorname{erf}(\nu y) \tag{5.27}$$

The second solution is therefore,

$$F_2(y) = A \left(\exp(-\nu^2 y^2) + \pi^{\frac{1}{2}} \nu y \operatorname{erf}(\nu y) \right) \tag{5.28}$$

and the complete solution is obtained from linear superposition :

$$F(y) = A(\exp(-\nu^2 y^2) + \pi^{\frac{1}{2}} \nu y \operatorname{erf}(\nu y)) + By \tag{5.29}$$

Thus a solution to the partial differential equation (5.13) is :

$$q(y,t) = [A(\exp(-\nu^2 y^2) + \pi^{\frac{1}{2}}\nu y\,\mathrm{erf}(\nu y)) + By]\ t \qquad (5.30)$$

with constants A , B to be determined from the boundary conditions.

(a) Pervious base

The complete solution is determined from the boundary conditions eq(5.14,15) as :

$$q(y,t) = \beta p t^{\frac{1}{2}} \{ \exp(-\nu^2 y^2) + \pi^{\frac{1}{2}}\nu y\,\mathrm{erf}(\nu y) - [\exp(-\nu^2) + \pi^{\frac{1}{2}}\nu\,\mathrm{erf}(\nu)]y \} \qquad (5.31)$$

(b) Impervious base

The complete solution is determined from the boundary conditions eq(5.14,16) as :

$$q(y,t) = \beta p t^{\frac{1}{2}} \{ \frac{\exp(-\nu^2 y^2) + \pi^{\frac{1}{2}}\nu y\,\mathrm{erf}(\nu y)}{\exp(-\nu^2) + \pi^{\frac{1}{2}}\nu\,\mathrm{erf}(\nu)} - y \} \qquad (5.32)$$

Eq(5.31),(5.32) can be written in terms of the original variables z,t by using the transformation eq(5.12). At the moment, however, it is more interesting to normalize the variable $q(y,t)$ by dividing it by $\beta p t^{\frac{1}{2}}$, which is the largest void ratio change that can be experienced in the deposit at current time t . Thus,

the normalized void ratio change $\bar{q}(y,t) = \dfrac{q(y,t)}{\beta p t^{\frac{1}{2}}}$ (5.33)

This, for a pervious base is,

$$\bar{q}_{pervious} = \exp(-\nu^2 y^2) + \pi^{\frac{1}{2}}\nu y\,\mathrm{erf}(\nu y) - [\exp(-\nu^2) + \pi^{\frac{1}{2}}\nu\,\mathrm{erf}(\nu)]y \qquad (5.34)$$

and for an impervious base :

$$\bar{q}_{impervious} = \frac{exp(-\nu^2 y^2) + \pi^{\frac{1}{2}}\nu y erf(\nu y)}{exp(-\nu^2) + \pi^{\frac{1}{2}}\nu erf(\nu)} - y \qquad (5.35)$$

Surprisingly, the $\bar{q}$ for both pervious and impervious bases are functions of y only. In other words, if one attempts to plot the isochrone for the normalized void ratio change with the normalized space variable y, there is only one curve for each different value of ν. This is shown in Fig.5.1. This demonstrates that the parameter ν, defined for $\frac{1}{2} p/C_F^{\frac{1}{2}}$, will determine the consolidation behaviour during this particular deposition. In its physical meaning, the parameter p is a measure of the deposition rate, i.e. the larger it is, the faster the deposition will be. When combined with the coefficient of consolidation C_F, the new parameter ν is a measure of the relative speed of the two processes. When the deposition is faster than the mud can consolidate, as characterized by a large ν, very little consolidation can occur. This can be seen in Fig.5.1, when $\nu=5$ virtually no void ratio change occurs in the stratum. Conversely, in a very slow deposition, which corresponds to a small value of ν, the deposit will be close to its fully consolidated state. In Fig.5.1 when $\nu=0.25$ with a pervious base, the difference from the fully consolidated state has become so small that it can not be distinguished in the drawing.

An alternative way of describing the present state of consolidation is to consider the behaviour of surface settlement. To this end, a new variable, the degree of settlement is defined as :

Degree of Settlement $S(t)$

$$= \frac{\text{(the settlement that has occured at present, i.e. substract the present mud thickness from its fully unconsolidated thickness)}}{\text{(the settlement that would eventually occur if the deposition suddenly ceased at this moment)}}$$

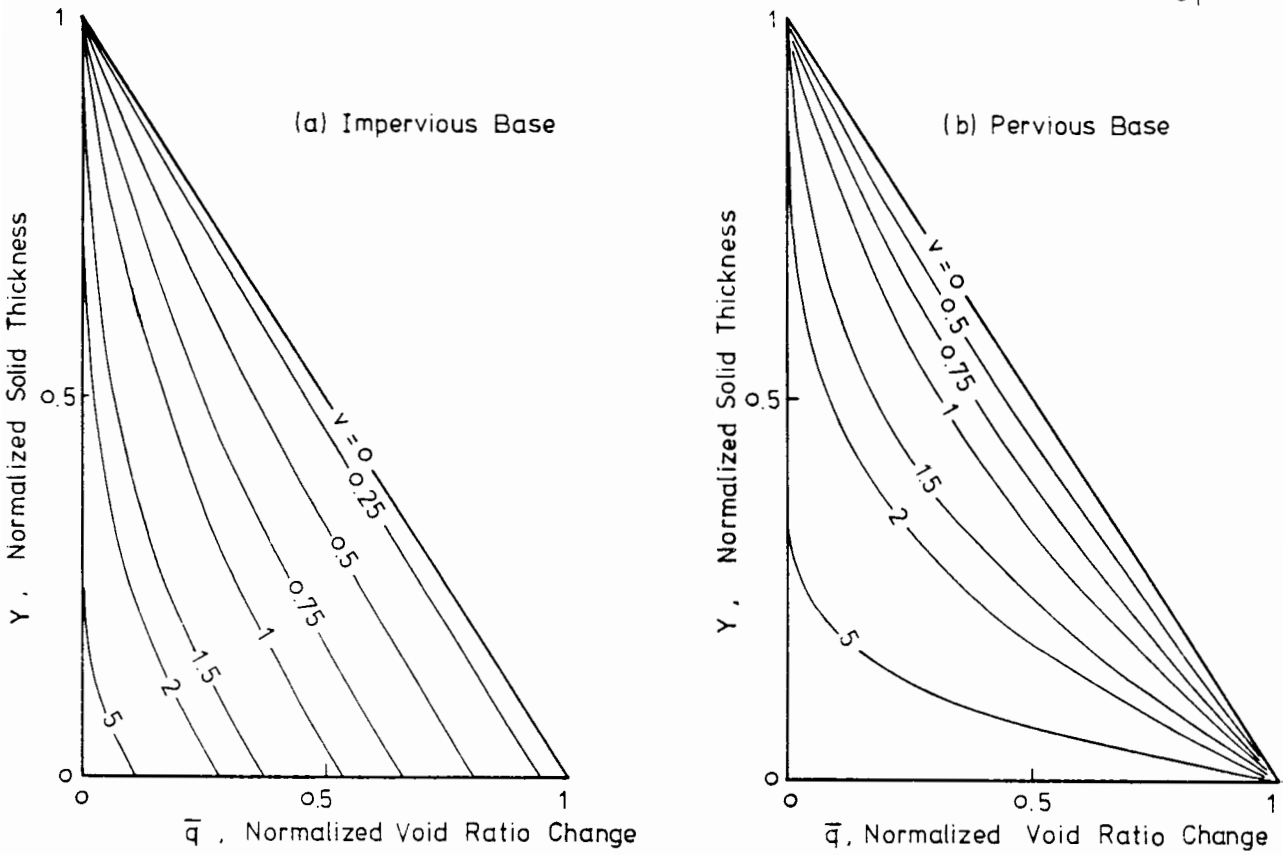

FIG.5.1 Isochrones of the normalized void ratio change in a square root time deposition.

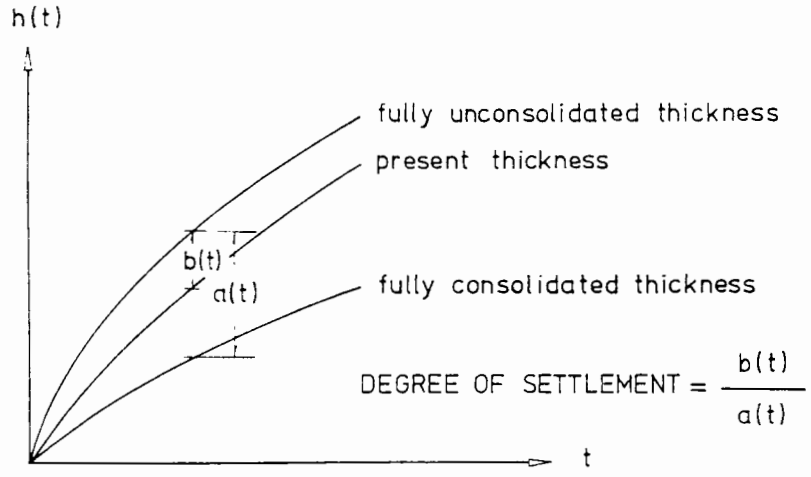

FIG.5.2 The degree of settlement.

This concept, as is illustrated in Fig.5.2, is more difficult than that of the previous chapters. It can be shown that $S(t)$ is given by this expression :

$$S(t) = \frac{\int_0^{pt} q(y,t)\,dy}{\frac{1}{2}\beta p^2 t} \qquad (5.36)$$

and it is found that :

$$S_{pervious} = \frac{\pi^{\frac{1}{2}}}{\nu} erf(\nu) - \frac{1}{\nu}\gamma\left(\frac{3}{2}, \nu^2\right) - exp(-\nu^2) \qquad (5.37)$$

and, $$S_{impervious} = S_{pervious} / [exp(-\nu^2) + \pi^{\frac{1}{2}}\nu erf(\nu)] \qquad (5.38)$$

where $\gamma(a,x)$ is the incomplete Gamma function defined as :

$$\gamma(a,x) = \int_0^x t^{a-1} exp(-t)\,dt \qquad (5.39)$$

whose numerical values are tabulated, see, for instance, Abramowitz and Stegun (1965).

It can be seen in eq(5.37),(5.38) that for a given ν , the function $S(t)$ has a constant value. That is, in a particular deposition characterized by ν , the degree of settlement remains the same throughout the process. This behaviour has also been observed by Gibson (1958) in studying the consolidation of clay accumulating thickness in proportion to the square root of time. It appears that this particular behaviour can be attributed to this particular rate of the square root of time.

The ratio of the degree of settlement for a pervious and an impervious base is given by $(exp(-\nu^2)+\pi^{\frac{1}{2}}\nu erf(\nu))^{-1}$ in eq(5.38) and is very close to unity for small values of ν .

The degree of settlement for different values of ν is listed in the following Table for both pervious and impervious bases.

ν	0.1	0.2	0.5	1.0	2.0
Pervious Base	0.9970	0.9868	0.9225	0.7468	0.4410
Impervious Base	0.9872	0.9491	0.7457	0.4017	0.1243

Solution by the Method of Generalized Potential

(a) Pervious base

The governing equation and the boundary conditions are given by eq$(5.8\text{-}10)_a$, to which a solution can be constructed by combining two double layer potentials (see Appendix A of this chapter) as :

$$q(z,t) = \frac{1}{2}(\pi C_F)^{-\frac{1}{2}} \int_0^t (t-\tau)^{-\frac{3}{2}} z\, \Phi(\tau)\, exp[-\frac{z^2}{4C_F(t-\tau)}]\, d\tau$$

$$+ \frac{1}{2}(\pi C_F)^{-\frac{1}{2}} \int_0^t (t-\tau)^{-\frac{3}{2}} (z - p\tau^{\frac{1}{2}})\, \Psi(\tau) exp[-\frac{(z - p\tau^{\frac{1}{2}})^2}{4C_F(t-\tau)}]d\tau \qquad (5.40)$$

This satisfies the governing equation (5.8)a for arbitrary functions $\Phi(t)$ and $\Psi(t)$, these are determined from the boundary conditions eq(5.9,10)a.

Substituting eq(5.40) into the boundary conditions eq(5.9)a and eq(5.10)a, applying a lemma by Holmgren (1903) in the integrals as $z \to 0$ and $z \to pt^{\frac{1}{2}}$ respectively, these reduce to a system of Volterra equations of the second kind for the two unknown functions :

$$\Phi(t) = \beta p t^{\frac{1}{2}} + \pi^{-\frac{1}{2}}\nu \int_0^t \Psi(\tau)\, K_1(t,\tau)d\tau \qquad (5.41)$$

and $$\Psi(t) = \pi^{-\frac{1}{2}}\nu \int_0^t \Phi(\tau)K_2(t,\tau)d\tau + \pi^{-\frac{1}{2}}\nu \int_0^t \Psi(\tau)K_3(t,\tau)d\tau \qquad (5.42)$$

with the kernel functions :

$$K_1(t,\tau) = \tau^{\frac{1}{2}}(t-\tau)^{-\frac{3}{2}} \exp[-\nu^2\tau/(t-\tau)] \tag{5.43}$$

$$K_2(t,\tau) = t^{\frac{1}{2}}(t-\tau)^{-\frac{3}{2}} \exp(-\nu^2\, t/(t-\tau)] \tag{5.44}$$

$$K_3(t,\tau) = (t^{\frac{1}{2}} - \tau^{\frac{1}{2}})(t-\tau)^{-\frac{3}{2}} \exp[-\nu^2\,(t^{\frac{1}{2}}-\tau^{\frac{1}{2}})^2/(t-\tau)] \tag{5.45}$$

where the parameter ν has already been defined in eq(5.21).

This system can be solved by the method of successive approximation, for, letting,

$$\Phi(t) = \sum_n \omega^n a_n(t) \tag{5.46}$$

$$\Psi(t) = \sum_n \omega^n b_n(t) \tag{5.47}$$

$$\omega = \pi^{-\frac{1}{2}}\nu \tag{5.48}$$

Substituting into eq(5.41),(5.42) and comparing corresponding power of ω , the following expressions for $a_n(t)$ and $b_n(t)$ are obtained :

$$\begin{aligned}
a_o(t) &= \beta p t^{\frac{1}{2}} \\
b_o(t) &= 0 \\
a_1(t) &= 0 \\
b_1(t) &= \int_o^t a_o(\tau)K_2(t,\tau)d\tau \\
a_2(t) &= \int_c^t b_1(\tau)K_1(t,\tau)d\tau \quad , \quad b_2(t) = \int_o^t b_1(\tau)K_3(t,\tau)d\tau \\
a_i(t) &= \int_o^t b_{i-1}(\tau)K_1(t,\tau)d\tau \\
b_i(t) &= \int_o^t a_{i-1}(\tau)K_2(t,\tau)d + \int_o^t b_{i-1}(\tau)K_3(t,\tau)d\tau
\end{aligned} \tag{5.49}$$

Thus, to obtain $b_1(t)$,

$$b_1(t) = \beta p t^{\frac{1}{2}} \int_0^t \tau^{\frac{1}{2}} (t-\tau)^{-\frac{3}{2}} \exp[-\nu^2 t/(t-\tau)]\, d\tau \qquad (5.50)$$

using a new variable $u=\tau/t$ in the integral, this becomes :

$$b_1(t) = \beta p t^{\frac{1}{2}} \int_0^1 u^{\frac{1}{2}} (1-u)^{-\frac{3}{2}} \exp[-\nu^2/(1-u)]\, du \qquad (5.51)$$

Since the integral now involves only the parameter u and is independent of t, it follows that,

$$b_1(t) = c t^{\frac{1}{2}} \qquad (5.52)$$

where c is a constant.

Similar arguments can be applied to the subsequent functions $a_i(t)$ and $b_i(t)$, say,

$$\begin{aligned} a_i(t) &\propto t^{\frac{1}{2}} \\ b_i(t) &\propto t^{\frac{1}{2}} \\ i &= 0,1,2,3,\ldots. \end{aligned} \qquad (5.53)$$

It follows that the original functions $\Phi(t)$, $\Psi(t)$, which are linear superpositions of $a_i(t)$ and $b_i(t)$, must therefore be proportional to $t^{\frac{1}{2}}$:

$$\begin{aligned} \Phi(t) &= m_1 t^{\frac{1}{2}} \\ \Psi(t) &= m_2 t^{\frac{1}{2}} \end{aligned} \qquad (5.54)$$

The constants m_1 and m_2 are determined by substituting eq(5.54) into the original integral equations (5.41,42). Application of the transformation $u=\tau/t$ in the integrals then yields the simultaneous algebraic equations :

$$m_1 = \beta p + \omega F_1(\nu) m_2$$
$$m_2 = \omega F_2(\nu) m_1 + \omega F_3(\nu) m_2 \qquad (5.55)$$

The functions :

$$F_1(\nu) = \int_0^1 u(1-u)^{-\frac{3}{2}} \exp[-\nu^2 u/(1-u)]du$$
$$F_2(\nu) = \int_0^1 u^{\frac{1}{2}}(1-u)^{-\frac{3}{2}} \exp[-\nu^2/(1-u)]du \qquad (5.56)$$
$$F_3(\nu) = \int_0^1 u^{\frac{1}{2}}(1-u^{\frac{1}{2}})(1-u)^{-\frac{3}{2}} \exp[-\nu^2(1-u^{\frac{1}{2}})^2/(1-u)]du$$

can not be related to exact functions at present. However, numerical schemes are available to integrate these.

The solution to the simultaneous equation is given by :

$$m_1 = \beta p/[1-(\omega^2 F_1 F_2/(1-\omega F_3))]$$
$$m_2 = \beta p\left(\frac{\omega F_2}{1-\omega F_3}\right)/[1-(\omega^2 F_1 F_2/(1-\omega F_3))] \qquad (5.57)$$

and the complete solution to the original boundary value problem follows :

$$q(z,t) = \frac{1}{2} m_1 (\pi C_F)^{-\frac{1}{2}} \int_0^t \tau^{\frac{1}{2}}(t-\tau)^{-\frac{3}{2}} z \exp[-z^2/(4C_F(t-\tau))]d\tau$$
$$+ \frac{1}{2} m_2 (\pi C_F)^{-\frac{1}{2}} \int_0^t \tau^{\frac{1}{2}}(t-\tau)^{-\frac{3}{2}}(z-p\tau^{\frac{1}{2}}) \exp[-(z-p\tau^{\frac{1}{2}})^2/(4C_F(t-\tau))]d\tau \qquad (5.58)$$

This can be normalized as before, using the space variable y defined in eq(5.12) and the normalized void ratio change $\bar{q}$ defined in eq(5.33). After some manipulation, including a change of variable in the integrals, this becomes,

$$\bar{q}(y,t) = \omega F_4(y,\nu)/[1-\omega^2 F_1 F_2/(1-\omega F_3))]$$

$$+ \frac{\omega^2 F_2}{1-\omega F_3} F_5(y,\nu)/[1-\omega^2 F_1 F_2/(1-\omega F_3))] \qquad (5.59)$$

This is, as in the last section, a function of y and ν only, and is independent of t. The functions F_4 and F_5 are defined by the integrals,

$$F_4(y,\nu) = \int_0^1 y u^{\frac{1}{2}}(1-u)^{-\frac{3}{2}} exp[-\nu^2 y^2/(1-u)]du$$

$$F_5(y,\nu) = \int_0^1 (y-u^{\frac{1}{2}})u^{\frac{1}{2}}(1-u)^{-\frac{3}{2}} exp[-\nu^2(y-u^{\frac{1}{2}})^2/(1-u)]du \qquad (5.60)$$

These integrals have been computed using a special Gaussian quadrature and the solution obtained from eq(5.59) is compared to the sclution by the Fourier method, eq(5.34), in the following Table for $\nu = 1$.

y	0.1	0.3	0.5	0.7	0.9
eq(5.34)	0.823831	0.530216	0.309318	0.150517	0.040718
eq(5.59)	0.823831	0.530215	0.309311	0.150517	0.040786

It can be seen that the agreement between these two solutions is very good.

The degree of settlement is found to be :

$$S(t) = \nu^{-1}\pi^{-\frac{1}{2}}\{(\alpha-F_6(\nu))/[1-\omega^2 F_1 F_2/(1-\omega F_3)]$$

$$+ \frac{\omega F_2}{1-\omega F_3} (F_7(\nu)-F_8(\nu))/[1-\omega^2 F_1 F_2/(1-\omega F_3)]\} \qquad (5.61)$$

where,

$$\alpha = \int_0^1 u^{\frac{1}{2}}(1-u)^{\frac{1}{2}}du = \frac{\pi}{2}$$

$$F_6(\nu) = \int_0^1 u^{\frac{1}{2}}(1-u)^{\frac{1}{2}} exp[-\nu^2/(1-u)]du$$

$$F_7(\nu) = \int_0^1 u^{\frac{1}{2}}(1-u)^{\frac{1}{2}} exp[-\nu^2 u/(1-u)]du \qquad (5.62)$$

$$F_8(\nu) = \int_0^1 u^{\frac{1}{2}}(1-u)^{\frac{1}{2}} exp[-\nu^2(1-u^{\frac{1}{2}})^2/(1-u)]du$$

Which again demonstrates that the degree of settlement is a function of ν only and is independent of t. The integrals in eq(5.62) have again to be integrated numerically, from which eq(5.61) can be compared with the solution from the Fourier method, eq(5.37) in the following Table.

ν	0.2	0.5	1.0	2.0
eq(5.37)	0.98680	0.92256	0.74683	0.44104
eq(5.61)	0.98688	0.92256	0.74682	0.44104

(b) Impervious base

The governing equation and the boundary conditions in this case are given by eq(5.8,9.11)a, and the solution can be constructed from a single and a double layer potential as :

$$q(z,t) = \frac{1}{2}(\pi C_F)^{-\frac{1}{2}} \int_0^t \Phi(\tau)(t-\tau)^{-\frac{1}{2}} exp[-z^2/(4C_F(t-\tau))]d\tau$$

$$+ \frac{1}{2}(\pi C_F)^{-\frac{1}{2}} \int_0^t \Psi(\tau)(z-p\tau^{\frac{1}{2}})(t-\tau)^{-\frac{3}{2}} exp[-(z-p\tau^{\frac{1}{2}})^2/(4C_F(t-\tau))]d\tau \qquad (5.63)$$

Applying the boundary conditions eq(5.9)a,(5.11)a leads to a system of Volterra equation of the second kind for $\Phi(t)$ and $\Psi(t)$. The solution is found by following a similar argument as for eq(5.46) to eq(5.53) and appears as :

$$\Phi(t) = n_1 = constant$$
$$\Psi(t) = n_2 t^{\frac{1}{2}} \qquad (5.64)$$

where,

$$n_1 = \beta p^2/2\nu^2/[1- F_9(\tfrac{1}{2}F_{10} - \nu^2 F_{11})/\pi/(1-\nu\pi^{-\frac{1}{2}}F_3)] \qquad (5.65)$$

$$n_2 = \beta p F_9/2\nu\pi^{\frac{1}{2}}/(1-\nu\pi^{-\frac{1}{2}}F_3)/[1-F_9(\tfrac{1}{2}F_{10}-\nu^2F_{11})/(1-\nu\pi^{-\frac{1}{2}}F_3)]$$

with

$$\begin{aligned} F_9(\nu) &= \int_0^1 (1-u)^{-\frac{1}{2}} exp[-\nu^2/(1-u)]du \\ F_{10}(\nu) &= \int_0^1 u^{\frac{1}{2}}(1-u)^{-\frac{3}{2}} exp[-\nu^2u/(1-u)]du \\ F_{11}(\nu) &= \int_0^1 u^{\frac{3}{2}}(1-u)^{-\frac{5}{2}} exp[-\nu^2u/(1-u)]du \end{aligned} \qquad (5.66)$$

and $F_3(\nu)$ has already been defined in eq(5.56).

It will be more convenient to write

$$n_1' = n_1/(\beta p^2) \qquad (5.67)$$

and

$$n_2' = n_2/(\beta p)$$

The normalized void ratio change follows as :

$$\bar{q}(y,\nu) = n_1'\pi^{-\frac{1}{2}}\nu F_{12}(y,\nu) + n_2'\pi^{-\frac{1}{2}}\nu F_5(y,\nu) \qquad (5.68)$$

where,

$$F_{12}(y,\nu) = \int_0^1 (1-u)^{-\frac{1}{2}} exp[-\nu^2y^2/(1-u)]du \qquad (5.69)$$

and F_5 is defined in eq(5.60). This is compared with the Fourier method solution eq(5.35) in the following Table for $\nu = 1$.

y	0.0	0.2	0.4	0.6	0.8
eq(5.35)	0.537193	0.358539	0.220923	0.119764	0.048531
eq(5.68)	0.537193	0.358539	0.220923	0.119764	0.048530

Finally, the degree of settlement is found to be :

$$S(t) = n_1' \int_0^1 erf[\nu(1-y)^{-\frac{1}{2}}]dy + n_2' (F_7-F_8)/(\nu\pi^{\frac{1}{2}}) \qquad (5.70)$$

This is compared in the following Table with the Fourier method solution eq(5.38).

ν	0.2	0.5	1.0	2.0
eq(5.38)	0.94909	0.74395	0.40119	0.12435
eq(5.70)	0.94912	0.74395	0.40119	0.12435

Numerical values of the functions F_1 to F_{12} have been tabulated in Appendix B for further reference. Examination of these Tables suggests that, for large values of ν, the degree of settlement may be approximated to the fifth decimal place by the expression :

$$S_{pervious} \simeq \pi^{\frac{1}{2}}/2\nu$$

$$S_{impervious} \simeq 1/2\nu^2 \qquad \nu \geq 3$$

Such expressions could also be obtained by considering the behaviour of eq(5.37,38) as $\nu \to \infty$.

The more important case of a constant rate of deposition will now be considered in the rest of this chapter.

3. DEPOSITION WITH A CONSTANT RATE

General Consideration

The study of soil undergoing deposition and subsequent consolidation is relevant to practical questions such as :

(i) Does there exist an optimum procedure for placing dredged fill or similar material over a reclaimed area when the main interest is the time required before this land can be utilized ?

(ii) How will the rate of deposition and the soil characteristics affect the state of consolidation at the end of a long period of a slow deposition ?

Neither of these questions can be expected to have a simple answer. However, the study of a constant rate deposition may be expected to provide valuable information and this will now be investigated.

Pervious Base

(a) Development of solution

Assuming the deposition proceeds at a constant rate m then the material (solid thickness) in the deposit at any time t during the deposition is given by mt . The governing equation and the boundary conditions are therefore,

$$\frac{\partial q}{\partial t} = C_F \frac{\partial^2 q}{\partial z^2} \qquad 0 \leq z \leq mt \qquad t \geq 0 \tag{5.71}$$

$$q(mt,t) = 0 \tag{5.72}$$

$$q(0,t) = \beta mt \tag{5.73}$$

A non-trivial solution which satisfies eq(5.71) and eq(5.73) is,

$$q_1(z,t) = \frac{1}{2}\beta m\,(\pi C_F)^{-\frac{1}{2}} \int_0^t \tau(t-\tau)^{-\frac{3}{2}} z\, exp[-z^2/(4C_F(t-\tau))]d\tau \qquad (5.74)$$

This is, in terms of the theory of generalized potential, the result given by considering a source at $z=0$ with strength βmt . That eq(5.74) satisfies the boundary condition (5.73) can be confirmed by applying the Holmgren's lemma as $z \to 0$.

In order to satisfy the other boundary condition at $z=mt$ another solution has to be sought which must not upset the boundary condition at $z=0$ as well. This can be done by considering the solution,

$$q_2(z,t) = t^{-\frac{1}{2}} \int_0^\infty f(\xi)\ \{exp[-(z-\xi)^2/(4C_F t)]-exp[-(z+\xi)^2/(4C_F t)]\}\ d\xi \qquad (5.75)$$

This function combines two symmetric (to the axis $z=0$) source distributions at $t \to 0$, so that these will cancel with each other at $z=0$, i.e.

$$q_2(0,t) = 0$$

Superposition of these two solutions leads to,

$$\begin{aligned} q(z,t) &= q_1(z,t) + q_2(z,t) \\ &= \frac{1}{2}\beta m(\pi C_F)^{-\frac{1}{2}} \int_0^t \tau(t-\tau)^{-\frac{3}{2}} z\, exp[-z^2/(4C_F(t-\tau))]d\tau \\ &\quad + t^{-\frac{1}{2}} \int_0^\infty f(\xi)\ \{exp[-(z-\xi)^2/(4C_F t)]-exp[-(z+\xi)^2/(4C_F t)]\}\ d\xi \end{aligned} \qquad (5.76)$$

This will be a solution to the original equations (5.71-73) if the function $f(\xi)$ can be so chosen that the other boundary condition eq(5.72) is satisfied.

Hence, it is required that :

$$t^{-\frac{1}{2}}\int_0^\infty f(\xi)\{\exp[-(mt-\xi)^2/(4C_Ft)]-\exp[-(mt+\xi)^2/(4C_Ft)]\}d\xi$$

$$+\frac{1}{2}\beta m(\pi C_F)^{-\frac{1}{2}}\int_0^t \tau(t-\tau)^{-\frac{3}{2}} mt\ \exp[-m^2t^2/(4C_F(t-\tau))]d\tau = 0 \qquad (5.77)$$

After the second integral has been evaluated using the technique of change of variable and replacing the terms within the bracket of the first integral by the identity :

$$\exp[-(x-\xi)^2/(4C_Ft)] - \exp[-(x+\xi)^2/(4C_Ft)]$$
$$= 2\ \exp[-x^2/(4C_Ft)]\exp[-\xi^2/(4C_Ft)]\sinh[x\xi/(2C_Ft)] \qquad (5.78)$$

eq(5.77) then becomes,

$$2t^{-\frac{1}{2}}\int_0^\infty f(\xi)\exp[-m^2t/(4C_F)]\exp[-\xi^2/(4C_Ft)]\sinh[m\xi/(2C_F)]d\xi$$
$$= \beta m^2t^{\frac{3}{2}}(\pi C_F)^{-\frac{1}{2}}\exp[-m^2t/(4C_F)] - (\beta mt+\beta m^3t^2/(2C_F))\operatorname{erfc}[\frac{m}{2}(t/C_F)^{\frac{1}{2}}] \qquad (5.79)$$

which is a singular integral equation of the Fredholm type.

This equation can be greatly simplified by adopting the following change of variable :

$$p = (4C_Ft)^{-1} \quad , \quad r = \xi^2$$
$$F(r) = \frac{f(\xi)}{2\xi}\sinh[m\xi/(2C_F)] \qquad (5.80)$$

after which it becomes,

$$\int_0^\infty F(r)\exp(-pr)dr = \frac{1}{32}\beta m^2p^{-2}\pi^{-\frac{1}{2}}C_F^{-\frac{5}{2}}$$
$$-(\frac{1}{16}\beta m(pC_F)^{-\frac{3}{2}} + \frac{1}{128}\beta m^3p^{-\frac{5}{2}}C_F^{-\frac{7}{2}})\exp[m^2/(16pC_F^2)]$$
$$\operatorname{erfc}[m/(4C_Fp^{\frac{1}{2}})] \qquad (5.81)$$

The right hand side of this equation involves the variable p only

and the left hand side is a standard form of the Laplace transform from the variable r to p, hence standard Tables can be consulted to give, (Erdelyi 1954 , p267, pair(5.12.21))

$$\mathcal{L}^{-1}\{ \frac{1}{32} \beta m^2 \pi^{-\frac{1}{2}} C_F^{-\frac{5}{2}} p^{-2} \} = \frac{1}{32} \beta m^2 \pi^{-\frac{1}{2}} C_F^{-\frac{5}{2}} r \tag{5.82}$$

$$\mathcal{L}^{-1}\{ \frac{1}{16} \beta m (pC_F)^{-\frac{3}{2}} exp[m^2/(16pC_F^2)] erfc[m/(4C_F p^{\frac{1}{2}})]\}$$

$$= \frac{1}{4} \beta (\pi C_F)^{-\frac{1}{2}} (1-exp[mr^{\frac{1}{2}}/(2C_F)]) \tag{5.83}$$

$$\mathcal{L}^{-1}\{ \frac{1}{128} \beta m^3 C_F^{-\frac{7}{2}} p^{-\frac{5}{2}} exp[m^2/(16pC_F^2)] erfc[m/(4C_F p^{\frac{1}{2}})]\}$$

$$= \frac{1}{32} \beta m^2 \pi^{-\frac{1}{2}} C_F^{-\frac{5}{2}} \int_0^r (1-exp(-mx^{\frac{1}{2}}/(2C_F)))dx \tag{5.84}$$

the last integral can be evaluated by a change of variable followed by an integration by parts to give,

$$\int_0^r (1-exp(-mx^{\frac{1}{2}}/(2C_F)))dx$$

$$= r - 8C_F^2 m^{-2} [1-exp(-mr^{\frac{1}{2}}/(2C_F)) - (mr^{\frac{1}{2}}/2C_F) exp(-mr^{\frac{1}{2}}/2C_F)] \tag{5.85}$$

From these equations a surprisingly simple expression for $F(r)$ follows,

$$F(r) = - \frac{1}{8} mr^{\frac{1}{2}} \pi^{-\frac{1}{2}} C_F^{-\frac{3}{2}} exp[-mr^{\frac{1}{2}}/2C_F] \tag{5.86}$$

and hence the unknown function $f(\xi)$ is,

$$f(\xi) = \frac{1}{4} \beta m \xi^2 \pi^{-\frac{1}{2}} C_F^{-\frac{3}{2}} [\, 1 - coth(m\xi/2C_F)] \tag{5.87}$$

From which follows the required solution as :

$$q(z,t) = \frac{1}{2}\beta m(\pi t)^{-\frac{1}{2}}C_F^{-\frac{3}{2}}\exp[-z^2/(4C_F t)]\int_o^\infty \xi^2(1-\coth(m\xi/2C_F))\sinh(z\xi/2C_F t)$$
$$\exp(-\xi^2/4C_F t)d\xi + (m\beta t + m\beta z^2/2C_F)\operatorname{erfc}[z/2(C_F t)^{\frac{1}{2}}] \qquad (5.88)$$
$$- m\beta z(t/\pi C_F)^{\frac{1}{2}}\exp(-z^2/4C_F t)$$

The expression can be simplified by evaluating the integral. This is detailed in Appendix C of this chapter. It is found that :

$$q(z,t) = \beta m\ \{(z^2/2C_F + t) - \frac{1}{2}(\pi t)^{-\frac{1}{2}}C_F^{-\frac{3}{2}}\exp(-z^2/4C_F t)$$
$$\int_o^\infty \xi^2\coth(m\xi/2C_F)\sinh(z\xi/2C_F t)\exp(-\xi^2/4C_F t)d\xi\} \qquad (5.89)$$

(b) The normalized void ratio change and the degree of settlement

Eq(5.89) is written in terms of the real variable z, t. To simplify further this expression the normalized space variable is chosen as :

$$y = z/mt \qquad (5.90)$$

and the normalized void ratio change is chosen as ,

$$\bar{q}(y,t) = q(y,t)/q(0,t) \qquad (5.91)$$

Thus, eq(5.89) becomes,

$$\bar{q}(y,t) = 1 + \frac{1}{2}y^2(m^2t/C_F) - \frac{1}{2}\pi^{-\frac{1}{2}}(m^2t/C_F)^{\frac{3}{2}}\exp(-y^2m^2t/4C_F)$$
$$\int_o^\infty \xi^2\coth(\xi m^2t/2C_F)\sinh(\xi y m^2t/2C_F)\exp(-\xi^2m^2t/4C_F)d\xi \qquad (5.92)$$

this suggests a time factor of the form :

$$T = m^2 t/C_F \tag{5.93}$$

and hence,

$$\bar{q}(y,T) = 1 + \frac{1}{2}y^2T - \frac{1}{2}\pi^{-\frac{1}{2}}T^{\frac{3}{2}}\exp(-y^2T/4)\int_0^\infty \xi^2 \coth(\xi T/2)\sinh(\xi Ty/2)\exp(-\xi^2 T/4)\,d\xi \tag{5.94}$$

Note that the effect of this time factor is to scale the real time by a factor m^2/C_F . Since m is a measure of the deposition speed and C_F represents the characteristic of the soil consolidation, this parameter is analogous to the factor $\frac{1}{2}pC_F^{-\frac{1}{2}}$ introduced in the analysis of the square roct time deposition. In both cases, therefore, a small change in the consolidation characteristic (i.e. a change in C_F) will have less effect than correspondingly small changes in rate of deposition, i.e. m or p .

The degree of settlement in the present case is given by,

$$S(t) = 2\,\beta^{-1}(mt)^{-2}\int_0^{mt} q(z,t)\,dz \tag{5.95}$$

or in the normalized variables,

$$S(T) = 2T^{-1}\int_0^1 \bar{q}(y,T)\,dy \tag{5.96}$$

This is evaluated in Appendix C from which it can be shown that :

$$S(T) = 2 + \frac{T}{3} - \frac{T}{2}\int_0^\infty \xi^2 \coth(\xi T/2)\,\{\,2\,\mathrm{erf}(\tfrac{1}{2}\xi T^{\frac{1}{2}}) + \mathrm{erf}(\tfrac{1}{2}(1-\xi)T^{\frac{1}{2}}) - \mathrm{erf}(\tfrac{1}{2}(1+\xi)T^{\frac{1}{2}})\}\,d\xi \tag{5.97}$$

This depends solely on the time factor T which is scaled to the real time t by a factor m^2/c_F. Physically, this suggests that the consolidation state of a low permeability, soft clay (which exhibits a small c_F value) under a slow deposition is similar to that of a highly permeable stiff clay (which is associated with a large c_F value) under a fast deposition because the factor m^2/c_F in both cases are of comparable magnitude.

(c) Some remarks on practical computation

The solutions obtained thus far involve singular integrals in an infinite region. While this can not be expressed in terms of known functions, numerical techniques for this type of integral are readily applicable.

In the course of the present study three different techniques were suggested, these are :

(i) Transform into a finite region by splitting the range (Squire 1970) :

In this method the integral

$$\int_0^\infty f(x)dx$$

is split into :

$$\int_0^s f(x)dx + \int_s^\infty f(x)dx$$

and telescoping both integrals into the range (0,1) by a change of variable which results in :

$$s \int_0^1 [f(st) + t^{-2} f(s/t)]dt \qquad (5.98)$$

then a quadrature of the Gaussian type can be applied.

(ii) Application of simple trapezoidal rule (Goodwin 1949) :

In this case the integral is approximated by :

$$\int_0^\infty f(x)dx = \Delta x \sum_0^N f(n\Delta x), \quad \left| f(N\Delta x) \right| \leq \delta \qquad (5.99)$$

with a predetermined error bound δ . It has been reported (Goodwin 1949) that such a method yields high accuracy especially when the integrand is decaying as $exp(-x^2)$, which is approximately the present case.

(iii) Combination of simple trapezoidal rule with Romberg's correction procedure (Squire 1970) :

The three techniques were compared by some preliminary numerical experiments, of which 20 points Gaussian quadrature combined with 40 points Kronrod quadrature was used in (i) and a simple trapezoidal rule using

$$\Delta x = \begin{cases} 0.2 & T > 1 \\ 0.5 & T \leq 1 \end{cases}$$

and

$$\delta = 10^{-18}$$

was used. The degree of settlement was computed by both methods for selected values of T . The results are compared in the following Table :

T	0.2	2.0	20	90
eq(5.98)	0.9683	0.7709	0.3327	0.1585
eq(5.99)	0.9683	0.7709	0.3326	0.1506

Except at large T , the agreement between both methods appears to be reasonable, while the simple trapezoidal rule is obviously more efficient in terms of computing time. In this example the computing time for the simple trapezoidal rule is about $\frac{2}{3}$ of the Gaussian quadrature.

Although at present there is no way of judging which of these two methods is more accurate, the merit of the trapezoidal rule can be assessed by applying the Romberg correction procedure and studying its convergency. This is done by evaluating the integral in eq(5.94), the results is shown in the following Table.

(I) $x = 0.5$ $T = 1.0$ $\delta = 2.8 \times 10^{-14}$

$\Delta y = 1.0$	1.5024161			
		1.5024173		
$\Delta y = 0.5$	1.5024170		1.5024170	
		1.5024170		1.5024170
$\Delta y = 0.25$	1.5024170		1.5024170	
		1.5024170		
$\Delta y = 0.125$	1.5024170			

(II) $x = 0.5$ $T = 0.01$ $\delta = 4.2 \times 10^{-12}$

$\Delta y = 4.0$	17.6697672		
		17.6697672	
$\Delta y = 2.0$	17.6697672		17.6697672
		17.6697672	
$\Delta y = 1.0$	17.6697672		

It can be seen that the simple trapezoidal rule is far better than one would have imagined judging from its crude nature. In any event it does not even require the Romberg correction procedure if a modest subinterval Δy has been chosen properly. It was therefore decided to carry out the computation by this simple technique. The results are shown in Fig.5.3 for the degree of settlement and in Fig.5.4 for the isochrones of the normalized void ratio change.

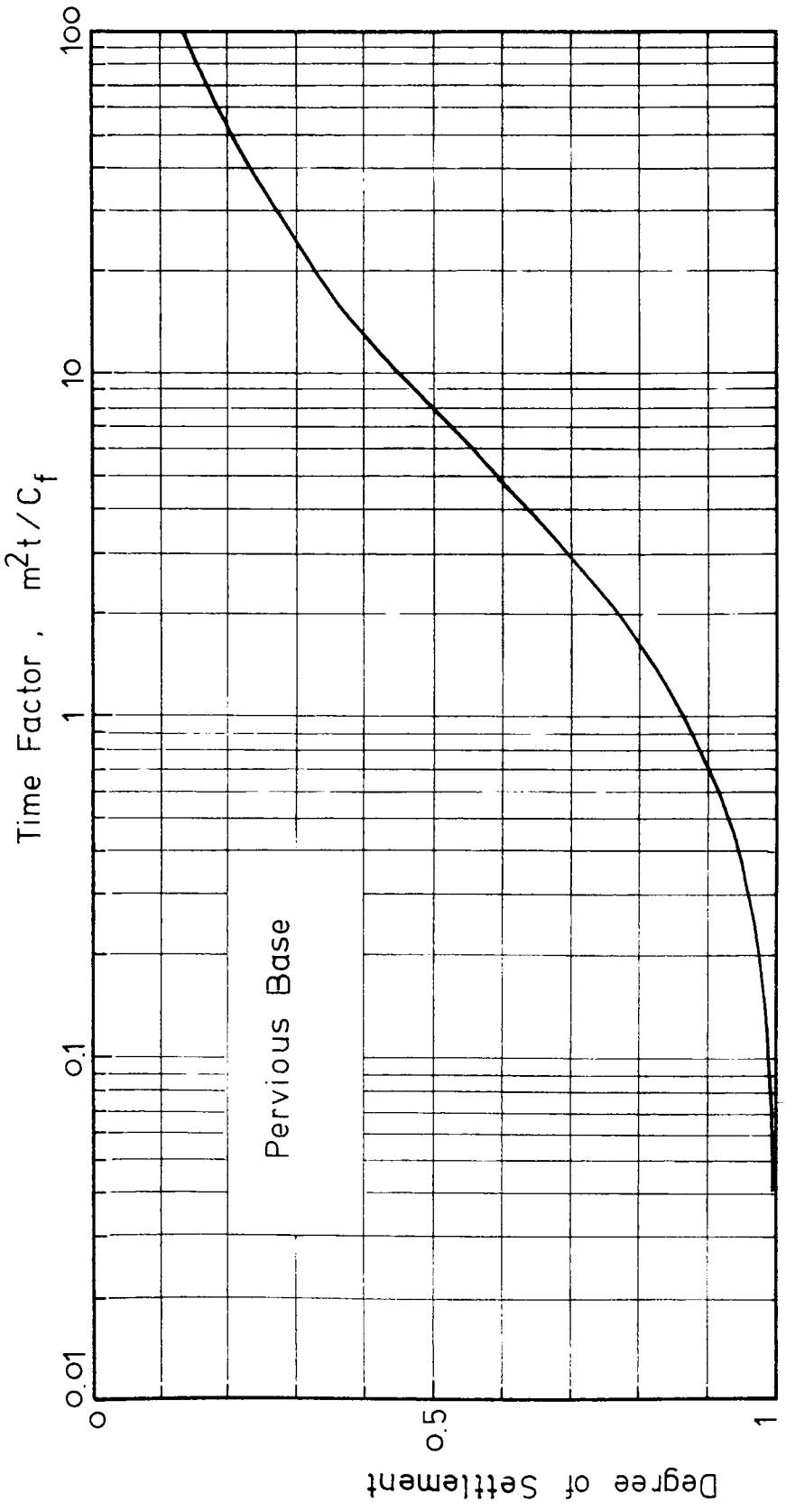

FIG.5.3 Degree of settlement versus the time factor during a constant rate of deposition.

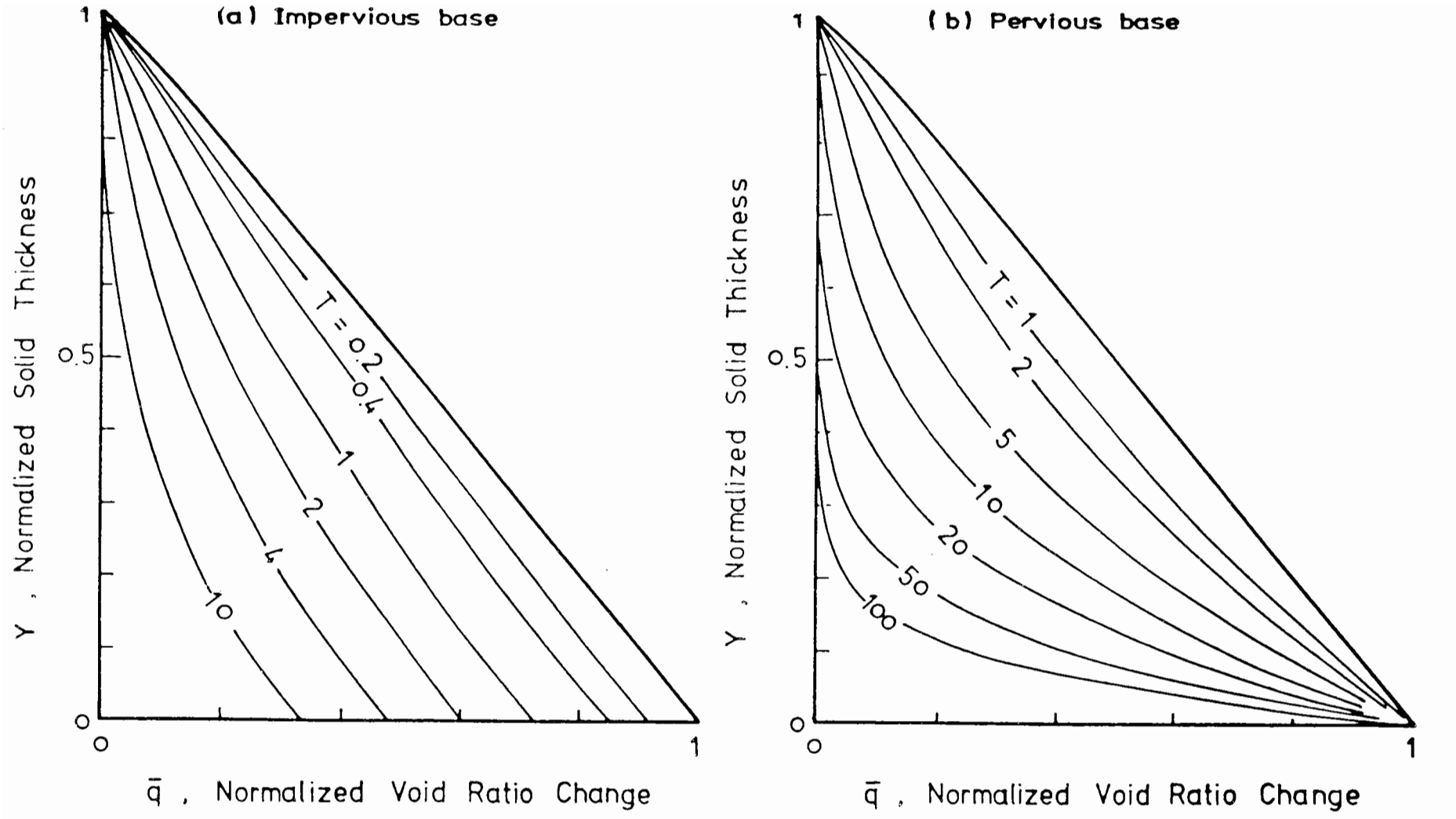

FIG.5.4 Isochrones of the normalized void ratio change during a constant rate of deposition.

Impervious Base

The case of an impervious base can be treated in a similar manner to that of a pervious base. The governing equation and the boundary conditions are :

$$\frac{\partial q}{\partial t} = C_F \frac{\partial^2 q}{\partial z^2} \qquad 0 \leq z \leq mt \qquad t \geq 0 \tag{5.71}$$

$$q(mt,t) = 0 \tag{5.72}$$

$$\frac{\partial q}{\partial z}(0,t) = -\beta \tag{5.100}$$

The first non-trivial solution to satisfy eq(5.71),(5.100) can be constructed by considering a simple layer potential acting at $z = 0$. This is given by :

$$q_1(z,t) = \beta(C_F/\pi)^{\frac{1}{2}} \int_0^t (t-\tau)^{-\frac{1}{2}} exp[-z^2/(4C_F(t-\tau))]d\tau \tag{5.101}$$

The second solution to be added to this which will not disturb the condition at $z = 0$ is,

$$q_2(z,t) = t^{-\frac{1}{2}} \int_0^\infty f(\xi)\{exp[-(z-\xi)^2/4C_F t]+exp[-(z+\xi)^2/4C_F t]\}d\xi \tag{5.102}$$

which is a combination of two anti-symmetric source distributions at $t \to 0$. By simple differentiation it can be shown that :

$$\frac{\partial q_2}{\partial t}(0,t) = 0$$

Hence the boundary condition at $z=0$ is not disturbed.

Superposition of these two solutions leads to :

$$q(z,t) = t^{-\frac{1}{2}} \int_0^\infty f(\xi)\{exp[-(z-\xi)^2/4C_F t] + exp[-(z+\xi)^2/4C_F t]\}d\xi$$

$$+ \beta(C_F/\pi)^{\frac{1}{2}} \int_0^t (t-\tau)^{-\frac{1}{2}} exp[-z^2/(4C_F(t-\tau))]d\tau \qquad (5.103)$$

This will be a solution to the boundary value problem if the function $f(\xi)$ satisfies the integral equation :

$$t^{-\frac{1}{2}} \int_0^\infty f(\xi)\{exp[-(mt-\xi)^2/4C_F t] + exp[-(mt+\xi)^2/4C_F t]\}d\xi \qquad (5.104)$$

$$= -\beta(C_F/\pi)^{\frac{1}{2}} \int_0^t (t-\tau)^{-\frac{1}{2}} exp[-m^2t^2/(4C_F(t-\tau)]d\tau$$

The integral in the right hand side can be evaluated using a change of variable followed by an integration by parts to give :

$$\beta(C_F/\pi)^{\frac{1}{2}} \int_0^t (t-\tau)^{-\frac{1}{2}} exp[-z^2/(4C_F(t-\tau))]d\tau$$

$$= 2\beta(C_F t/\pi)^{\frac{1}{2}} exp(-z^2/4C_F t) - \beta z erfc[\frac{z}{2}(C_F t)^{-\frac{1}{2}}] \qquad (5.105)$$

From which eq(5.104) reduces to :

$$2t^{-\frac{1}{2}} exp(-m^2 t/4C_F) \int_0^\infty f(\xi) exp(-\xi^2/4C_F t) cosh(m\xi/2C_F)d\xi \qquad (5.106)$$

$$= -2\beta(C_F t/\pi)^{\frac{1}{2}} exp(-m^2 t/4C_F) + \beta m terfc[\frac{m}{2}(C_F/t)^{-\frac{1}{2}}]$$

Using a change of variable :

$$p = (4C_F t)^{-1} \quad , \quad r = \xi^2$$

$$F(r) = 2f(\xi)\xi^{-1} cosh(m\xi/2C_F) \qquad (5.107)$$

Again a standard form of the Laplace transform is recovered :

$$\int_0^\infty F(r) exp(-pr)dr = \frac{1}{16}\beta m(C_F p)^{-\frac{3}{2}} exp(m^2/4C_F{}^2 p) erfc(m/4C_F p^{\frac{1}{2}})$$

$$- \frac{1}{4}\beta(C_F\pi)^{-\frac{1}{2}} p^{-1} \qquad (5.108)$$

The inverse transform is not very different from that of the pervious

base and hence eq(5.81) can be applied which yields the required solution :

$$F(r) = -\frac{\beta}{4}(C_F\pi)^{-\frac{1}{2}} exp(-mr^{\frac{1}{2}}/2C_F) \qquad (5.109)$$

then,

$$f(\xi) = -\frac{\beta}{2}\xi(C_F\pi)^{-\frac{1}{2}}(1-\tanh(m\xi/2C_F)) \qquad (5.110)$$

and finally,

$$q(z,t) = 2\beta(C_F t/\pi)^{\frac{1}{2}} exp(-z^2/4C_F t) - \beta z erfc[\frac{z}{2}(C_F t)^{-\frac{1}{2}}]$$

$$- \beta(\pi C_F t)^{-\frac{1}{2}} exp(-z^2/4C_F t) \int_o^\infty \xi(1-\tanh(m\xi/2C_F)) \cosh(x\xi/2C_F t) exp(-\xi^2/4C_F t) d\xi \qquad (5.111)$$

Part of this integral can be evaluated in the same way as its counterpart for the pervious base which has already beer detailed in Appendix C, it can be shown that :

$$q(z,t) = \beta(\pi C_F t)^{-\frac{1}{2}} exp(-z^2/4C_F t) \int_o^\infty \xi \tanh(m\xi/2C_F) \cosh(z\xi/2C_F t)$$

$$exp(-\xi^2/4C_F t) d\xi - \beta z \qquad (5.112)$$

Introducing, as before, the normalized space variable defined in eq(5.90) and the time factor defined in eq(5.93) the solution now becomes,

$$q(y,T) = \beta(C_F/m)T \{(T/\pi)^{\frac{1}{2}} exp(-\frac{1}{4}y^2 T) \int_o^\infty \xi \tanh(\xi T/2) \cosh(\xi y T/2)$$

$$exp(-\xi^2 T/4) d\xi - y \} \qquad (5.113)$$

and hence the normalized void ratio change follows,

$$\bar{q}(y,T) = (T/\pi)^{\frac{1}{2}} exp(-y^2 T/4) \int_o^\infty \xi \tanh(\xi T/2) \cosh(\xi y T/2) exp(-\xi^2 T/4) d\xi - y \qquad (5.114)$$

The degree of settlement is found as :

$$S(T) = 2\pi^{-\frac{1}{2}} \int_0^\infty \xi \tanh(\xi T/2)\left[\operatorname{erf}(T^{\frac{1}{2}}(1-\xi)/2)+\operatorname{erf}(T^{\frac{1}{2}}(1+\xi)/2)\right]d\xi - 1 \qquad (5.115)$$

Again, this is evaluated by the simple trapezoidal rule. The results are shown in Fig.5.5. The isochrones of the normalized void ratio change are shown in Fig.5.4.

The other curve appears in Fig.5.5 is the normalized void ratio change for the impervious base. This represents the local consolidation state there, which can be seen to be faster than the degree of settlement, which is a measure of the average consolidation through the layer. It can also be inferred from the isochrones, Fig.5.4 that that region closest to the impervious base is the most consolidated part of the deposit. A similar observation has been reported in the last chapter with the consolidation of a dredged fill under its own weight.

4. DISCUSSION OF RESULTS

So far in this chapter two different types of deposition have been considered. The solutions are expressed in terms of the normalized void ratio change and the degree of settlement. The former measures the local variation of the state of consolidation in the deposit, and the latter is an indication of the average consolidation state of the deposit.

In the first type of deposition considered, i.e. that which is proportional to the square root of time, it is seen that both the distribution of the normalized void ratio change and the degree of

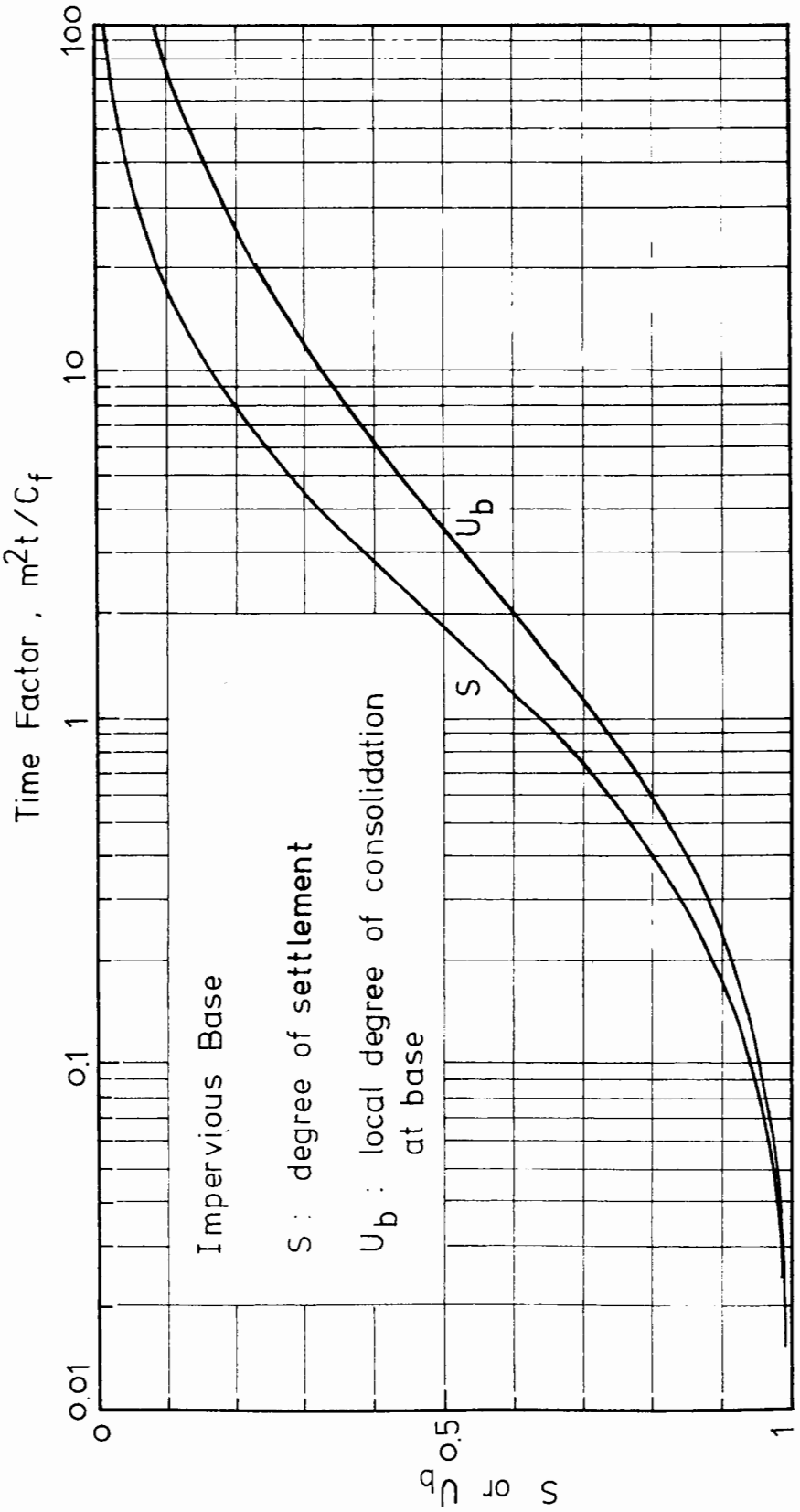

FIG.5.5 The degree of settlement and the local degree of consolidation (normalized void ratio change) at base versus the time factor during a constant rate of deposition.

settlement remain unchanged during the deposition. These are determined by a parameter ν, defined as $\frac{1}{2}pC_F^{-\frac{1}{2}}$, where p is the proportional constant in the deposition rate and C_F is the coefficient of consolidation of the soil. The relationship between the degree of settlement and ν is shown in Fig.5.6.

In the constant rate of deposition case, a time factor m^2t/C_F has been defined with m being the proportional canstant of the deposition rate, and it has been shown that both the normalized void ratio change and the degree of settlement vary with the time factor, see Fig.5.3,5.4,5.5. From thess figures it can be seen that the average consolidation of the deposit decreases with increasing time factor. Since this time factor is proportional to the square of the deposition rate m^2 and the reciprocal of the coefficient of consolidation C_F, the progress of consclidation in real time is determined by this proportional constant. In other words, during this particular process the state of consolidation of the deposit will move along the curves in Fig.5.3,5.5, and its actual position in these curves at a given time will be determined by the ccnstant m^2t/C_F which is a characteristic of the process.

As an example, consider the same soil being deposited at different speeds m_1 and m_2, the degree cf settlement in both cases after a period of time t will be different as each will then correspond to different time factors m_1^2t/C_F and m_2^2t/C_F. For the slower deposition, which is associated with smaller m, the time factor will also be smaller, and consequently more consolidation can be achieved.

The two deposition prccesses therefore yield different cansclidation behaviour. In the square root time deposition the state of consolidation of the deposit remains unchanged with its actual magnitude being determined by the parameter ν. In the constant rate of deposition the state of consolidation of the deposit will decrease as deposition proceeds. In the last chapter it is seen that

for an instantaneously dumped dredged fill the state of consolidation is improved with time. From the three cases it appears that the progress of consolidation with time in the deposit is dictated by the mode of deposition.

In the theory of consolidation of an existing stratum treated in the previous chapters it is seen that the consolidation of such cases is determined by a time factor defined as :

$$\text{time factor} = \frac{(\text{coefficient of consolidation of the soil}) \times (\text{time})}{(\text{square of the solid thickness of the stratum})}$$

It is possible to modify this definition to include the deposition-consolidation process treated in this chapter, and such a modified definition will be :

$$\text{time factor} = \frac{(\text{coefficient of consolidation of the soil}) \times (\text{time})}{(\text{square of the present solid thickness of the deposit})}$$

From which the time factor for an instantaneously dumped dredged fill is,

$$\text{time factor} = C_F t / z_o^2$$

For the square root time deposition this is,

$$\text{time factor} = C_F t / (pt^{\frac{1}{2}})^2 = C_F / p^2 = (4v^2)^{-1}$$

which will be a constant for a particular process.
For the constant rate of deposition this is,

$$\text{time factor} = C_F t / (mt)^2 = C_F / m^2 t$$

which is the reciprocal of the time factor adopted in the analysis.

With this time factor so defined its relationship with the degree of settlement for the three caess are given in Fig.5.7. It is seen that a unique time factor - degree of settlement relationship

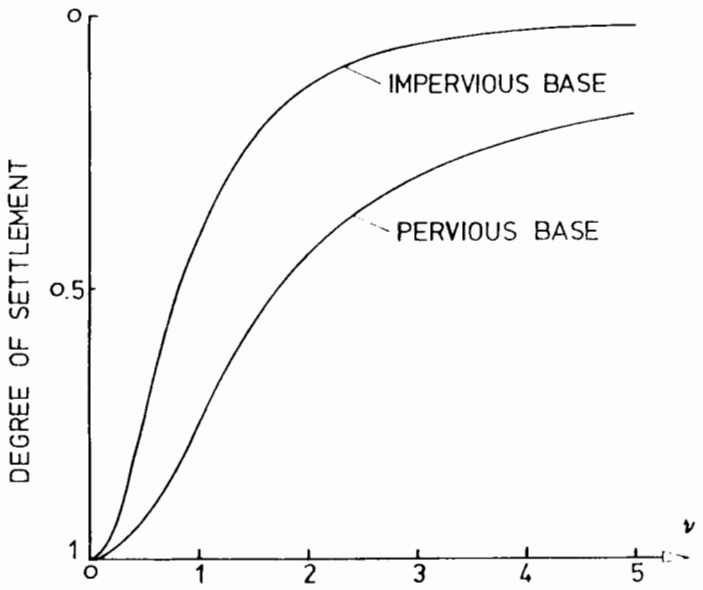

FIG.5.6 (above)

FIG.5.7 (right) The degree of settleemnt versus the time factor, the time factors are deifined in a consistent manner, see p.114 for the definitions.

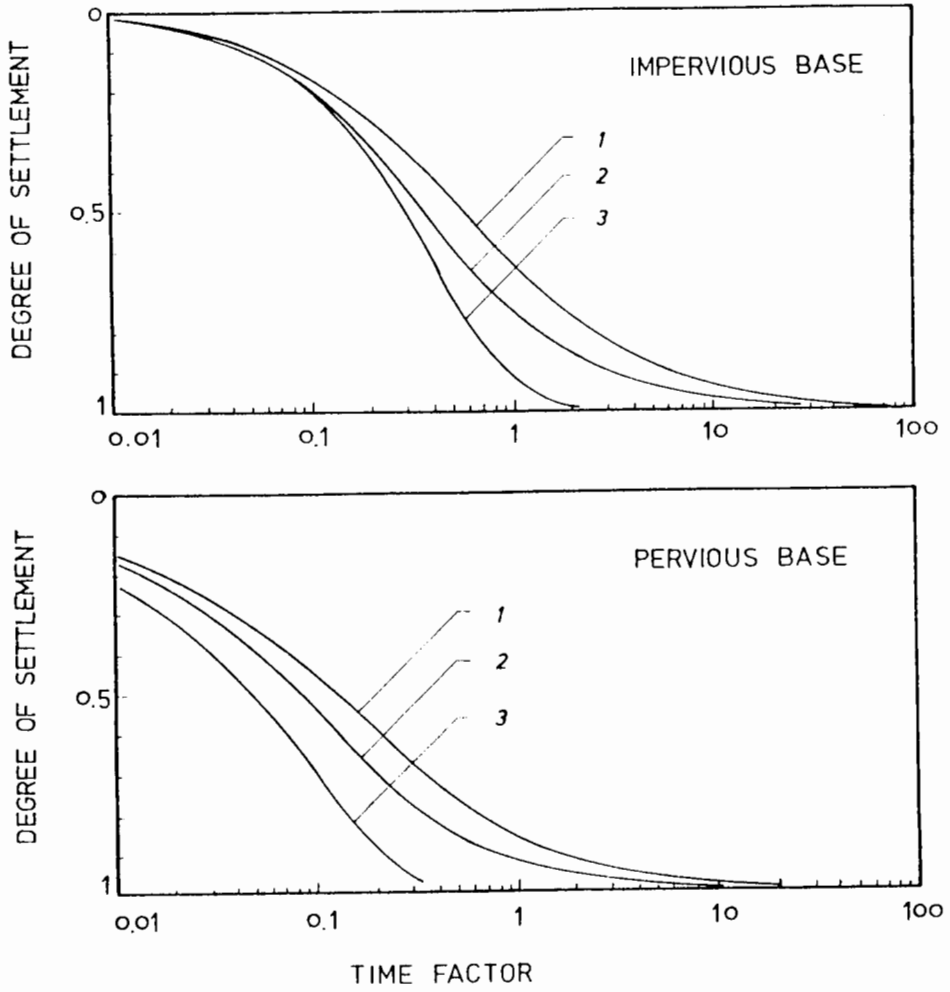

1 constant rate deposition

2 root time deposition

3 instantaneously dumping

exists in each case, and the state of consolidation improves with increasing time factor. In this aspect the deposition - consolidation behaviour is similar to the consolidation of an existing stratum : that there exists a unique time factor - state of consolidation relationship, with higher consolidation associated with a larger time factor. The unexpected behaviour during the square root time deposition can now be explained as its associated time factor is constant during the deposition, and since this corresponds to a particular consolidation state, its state of consolidation will thus remain unchanged.

Referring to Fig.5.7, in the constant rate of deposition the real time travels in the opposite direction to the time factor. Hence although the state of consolidation in this case worsens with time, an improvement is observed with the progress of the time factor.

For the instantaneously dumped dredged fill the real time travels in the same direction as the time factor. In the square root time deposition the real time and the time factor are independent. The relationship between the real time and the time factor therefore provides useful criterion in determining whether during a particular deposition process the state of consolidation in the deposit will be improved as deposition proceeds. When the mode of deposition is such that the time factor obtained will travel in the same direction as the real time, improvement of the consolidation will result as deposition proceeds. When the time factor travels in the opposite direction to the real time, such as the constant rate of deposition, the state of consolidation worsens as deposition proceeds.

5. CONSOLIDATION AFTER DEPOSITION HAS TERMINATED

The consolidation of the deposit after deposition has terminated differs very little from the treatment in the last chapter of a dredged fill consolidated under its own weight. Here, only fixed material boundaries are involved and consolidation is due only to self weight. The difference, however, lies in the initial void ratio distribution. In the dredged fill case this is uniform whereas in the present case this distribution is determined by the previous deposition condition.

Assuming that the deposition ceased at time t_1, during which the material (solid thickness) of the deposit is $s(t_1)$, and a void ratio distribution given by $g(z)$. The governing equation and boundary conditions for the subsequent consolidation, assuming there is no surface loading, will be :

$$\frac{\partial e}{\partial t} = C_F \frac{\partial^2 e}{\partial z^2} \qquad 0 \leq z \leq s(t_1) \qquad t \geq t_1 \qquad (5.121)$$

$$e(z,t_1) = g(z) \qquad (5.122)$$

$$e(s(t_1),t) = e_i \qquad (5.123)$$

and $$e(0,t) = e_i - \beta s(t_1) \qquad \text{for a pervious base} \qquad (5.124)$$

or $$\frac{\partial e}{\partial z}(0,t) = \beta \qquad \text{for an impervious base} \qquad (5.125)$$

When working in terms of the void ratio change $q(z,t)$ as defined in eq(5.12), the above equations become,

$$\frac{\partial q}{\partial t} = C_F \frac{\partial^2 q}{\partial z^2} \qquad 0 \leq z \leq s(t_1) \qquad t \geq t_1 \qquad (5.121)a$$

$$q(z,t_1) = f(z) \tag{5.122)a}$$

$$q(s(t_1),t) = 0 \tag{5.123)a}$$

and $$q(0,t) = \beta s(t_1) \qquad \text{for a pervious base} \tag{5.124)a}$$

or $$\frac{\partial q}{\partial z}(0,t) = -\beta \qquad \text{for an impervious base} \tag{5.125)a}$$

In general, this type of equation can be solved by the Fourier method with, perhaps, some difficulty in evaluating the Fourier coefficients. In the present study only the consolidation after a constant rate of deposition will be considered.

Pervious Base

Following the terminology used in the previous sections the governing equation and the initial and boundary conditions are :

$$\frac{\partial q}{\partial t} = C_F \frac{\partial^2 q}{\partial z^2} \qquad 0 \leq z \leq mt_1 \qquad t \geq t_1 \tag{5.126}$$

$$q(z,t_1) = f(z) \tag{5.127}$$

$$q(mt_1,t) = 0 \tag{5.128}$$

$$q(0,t) = \beta mt_1 \tag{5.129}$$

where the initial distribution $f(z)$ can be obtained by replacing t by t_1 in eq(5.89).

Let,

$$\tau = t - t_1 \tag{5.130}$$

and normalize the boundary conditions by defining :

$$q_2(z,t) = \beta(mt_1 - z) \tag{5.131}$$

and let, $$q(z,t) = q_1(z,t) + q_2(z,t) \tag{5.132}$$

Then eq(5.126-129) can be written down for the new variable q_1 with the simple boundary conditions :

$$\frac{\partial q_1}{\partial \tau} = C_F \frac{\partial^2 q_1}{\partial z^2} \qquad 0 \leq z \leq mt_1 \qquad \tau \geq 0$$

$$q_1(z,0) = f(z) - q_2(z) \tag{5.133}$$

$$q_1(0,\tau) = q_1(mt_1,\tau) = 0$$

The solution is obtained by the Fourier method as,

$$q_1(z,\tau) = \sum_n b_n \sin(n\pi z/mt_1) \exp[-(n\pi/mt_1)^2 C_F \tau] \tag{5.134}$$

with the Fourier coefficients,

$$b_n = \frac{2}{mt_1} \int_o^{mt_1} (f(x)-q_2(x)) \sin(n\pi x/mt_1) dx \tag{5.135}$$

and the complete solution is,

$$q(z,t) = \beta(mt_1-z) + \frac{2}{mt_1} \sum_n \sin(n\pi z/mt_1) \exp[-(n\pi/mt_1)^2 C_F (t-t_1)] \int_o^{mt_1} (f(x)- (mt_1-x)) \sin(n\pi x/mt_1) dx \tag{5.136}$$

where $f(x)$ is, from eq(5.89),

$$f(x) = \beta m \{(x^2/2C_F + t_1) - \frac{1}{2} (\pi t_1)^{-\frac{1}{2}} C_F^{-\frac{3}{2}} \exp(-x^2/4C_F t_1)) \int_o^{\infty} \xi^2 \coth(m\xi/2C_F) \sinh(x\xi/2C_F t_1) \exp(-\xi^2/4C_F t_1) d\xi\} \tag{5.137}$$

Using the following change of variable,

$$\eta = z/mt_1$$

$$T = m^2 t/C_F \qquad (5.138)$$

$$T_1 = m^2 t_1/C_F$$

and,

$$T_v = (T-T_1)/T_1^2$$

eq(5.136) can be written in the normalized form :

$$\bar{q}(\eta,T_v) = \frac{q(\eta,T_v)}{\beta m t_1} = 1 - \eta - 2 \sum_n b_n \sin(n\pi\eta)\exp(-n^2\pi^2 T_v) \qquad (5.139)$$

with the coefficients b_n given by,

$$b_n = \int_o^1 \{\frac{1}{2}x^2T_1 + x - \frac{1}{2}\pi^{-\frac{1}{2}}T_1^{-\frac{3}{2}}\exp(-x^2T_1/4) \int_o^\infty y^2\cosh(yT_1/2) \sinh(yT_1x/2)\exp(-y^2T_1/4)dy\}\sin(n\pi x)dx \qquad (5.140)$$

By the identity :

$$\int_o^1 x\sin(n\pi x)dx = -\frac{(-1)^n}{n\pi}$$

$$\int_o^1 x^2\sin(n\pi x)dx = -\frac{(-1)^n}{n\pi} - \frac{2(1-(-1)^n)}{n^3\pi^3}$$

eq(5.140) can be reduced to :

$$b_n = -\frac{(-1)^n}{n\pi}\left(\frac{1}{2}T_1 + 1\right) - \frac{(1-(-1)^n)}{n^3\pi^3} - \frac{1}{2}\pi^{-\frac{1}{2}}T_1^{-\frac{3}{2}} \int_o^1 \int_o^\infty y\cosh(yT_1/2)\sinh(yT_1x/2)\exp(-(x^2+y^2)T_1/4)\sin(n\pi x)dydx \qquad (5.141)$$

Numerical integration now has to be applied. This was achieved using the trapezoidal rule for the inner integral followed by a special quadrature for the outer integral. The computation become very tedious for larger values of n due to the periodic nature of the sine function in the integrand. Fortunately, the series in

eq(5.139) decays fairly fast and thus only the first few values of b_n will be required.

The degree of settlement is given by,

$$S(T_v) = 1 + \frac{8}{\pi} \sum_n \frac{b_{2n-1}}{(2n-1)} \exp(-(2n-1)^2\pi^2 T_v) \qquad (5.142)$$

This has been calculated for several different T_1 and plotted in terms of the original time factor m^2t/C_F in Fig.5.8.

Impervious Base

The development of a solution for the impervious base is essentially parallel to the pervious base case, and hence only a brief description will be given here.

The solution is constructed from a cosine series given by :

$$q(z,t) = \beta(mt_1-z) + \frac{2}{mt_1} \sum_n a_n \cos[(\frac{2n-1}{2})\pi z/mt_1] \exp[-(\frac{2n-1}{2})^2 \frac{\pi^2}{m^2t_1^2} C_F(t-t_1)] \qquad (5.143)$$

with the Fourier coefficients,

$$a_n = \int_o^{mt_1} (f(x)-\beta(mt_1-x)) \cos[(\frac{2n-1}{2})\pi x/mt_1]dx \qquad (5.144)$$

and $f(x)$ given by,

$$f(x) = \beta(\pi C_F t_1)^{-\frac{1}{2}} \exp(-x^2/4C_F t_1) \int_o^{\infty} y \tanh(my/2C_F) \cosh(xy/2C_F t_1) \exp(-y^2/4C_F t_1)dy - \beta x \qquad (5.145)$$

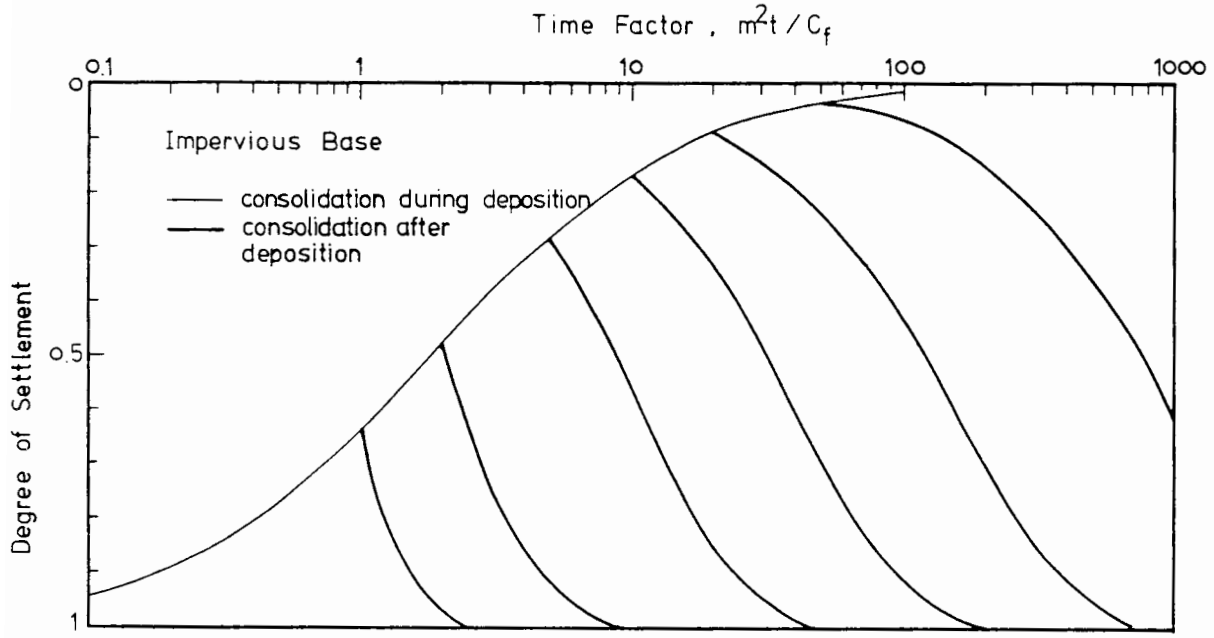

FIG.5.8 Consolidation during and after a constant rate of deposition
(above) impervious base
(below) pervious base

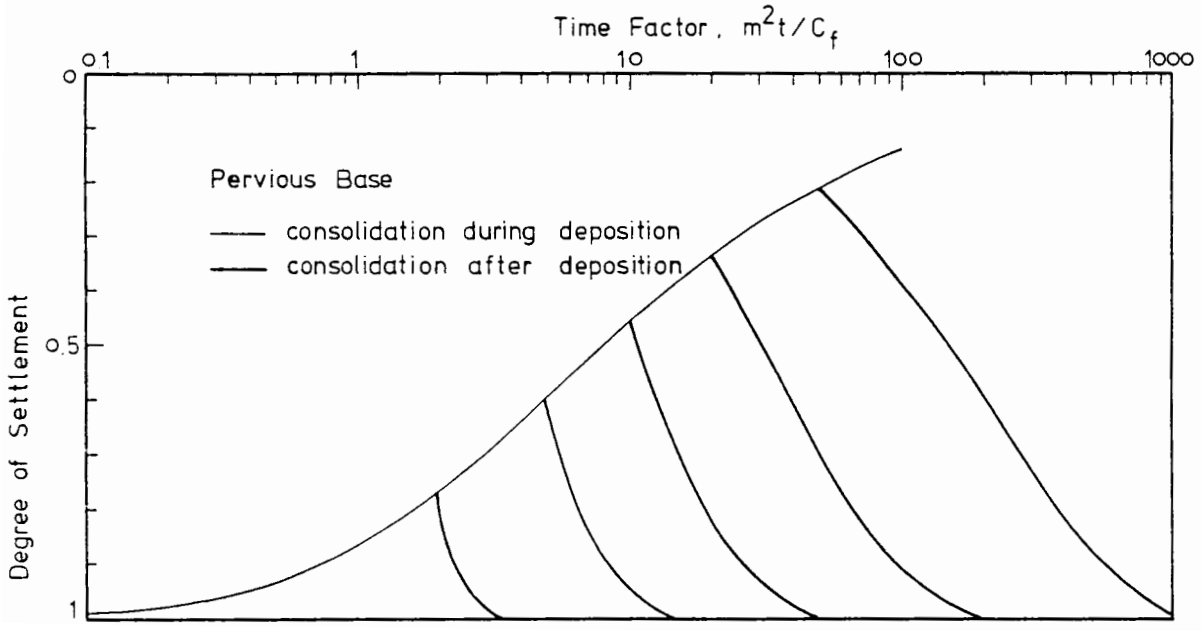

Introducing the change of variable as in eq(5.138), and writing in terms of the normalized void ratio change, it is found that :

$$\bar{q}(\eta,T_v) = 1 - \eta + 2 \sum_n c_n \cos[(\frac{2n-1}{2})\pi\eta]\exp[-(\frac{2n-1}{2})^2\pi^2 T_v] \qquad (5.146)$$

where,

$$c_n = (-1)^n \frac{2}{(2n-1)\pi} + (T_1/\pi)^{\frac{1}{2}} \int_0^1 \int_0^\infty y\tanh(yT_1/2)\cosh(xyT_1/2) \exp[-(x^2+y^2)T_1/4]\cos[(\frac{2n-1}{2})\pi x \, dydx \qquad (5.147)$$

The degree of settlement is found to be :

$$S(T_v) = 1 + \frac{8}{\pi} \sum_n \frac{(-1)^n}{2n-1} c_n \exp[-(\frac{2n-1}{2})^2\pi^2 T_v] \qquad (5.148)$$

This has been evaluated using similar algorithms to the pervious base case and presented in Fig.5.8.

6. A THEORETICAL ANALYSIS OF THE CONSOLIDATION DURING AND AFTER THE FILLING OPERATION OF A DREDGED FILL

In the begining of section 3 of this chapter it is asked how the coefficient of consolidation and filling speed affect the consolidation of a dredged fill and whether there exists an optimum situation. In the light of the solutions obtained in this chapter it is now possible to analyse this situation thecretically assuming the soil behaves linearly and a constant rate of deposition.

It is assumed that an amount of scil *MA* is to be dumped

in a filling site, where A is the total area of the site. The unit of M is thus solid volume per unit area of the filling site. Let the coefficient of consolidation of the soil be a constant denoted by C_F, and a reference time is defined as :

$$t_o = M^2/C_F$$

which corresponds to a time factor $C_F t_o/M^2 = 1$

A reference dumping rate is defined as :

$$m_r = M/t_o$$

which is the rate at which the total soil will be dumped in the time t_o.

The position in space of the mud surface during and after the filling can be calculated using the solutions obtained. This is done for several different deposition rates and the results are shown in Fig.5.9 for a pervious and an impervious base. In these figures the ratio shown for the unconsolidated and final thickness are quite arbitrary. It is seen that the faster the filling the earlier the total fill reaches full consolidation. This can be interpreted on the basis of Fig.5.7 that, although the state of consolidation during a constant rate of deposition worsens with time, as soon as the deposition terminates then its consolidation will be governed by a different law giving improved consolidation with time. Hence, the earlier this transfer takes place the faster will the stratum reach full consolidation.

Also shown in Fig.5.9 denoted by $m=\infty$ are the idealized situation that the soil is dumped instantaneously, which is the case analysed in the previous chapter. The difference between this and the fast deposition cases is seen to be greater for the pervious base case than the impervious base case. This is attributed to the behaviour close to the base. In the idealized situation this region will be subjected to the full loading which in the pervious base case can immediately drain and consolidate. However, if deposition

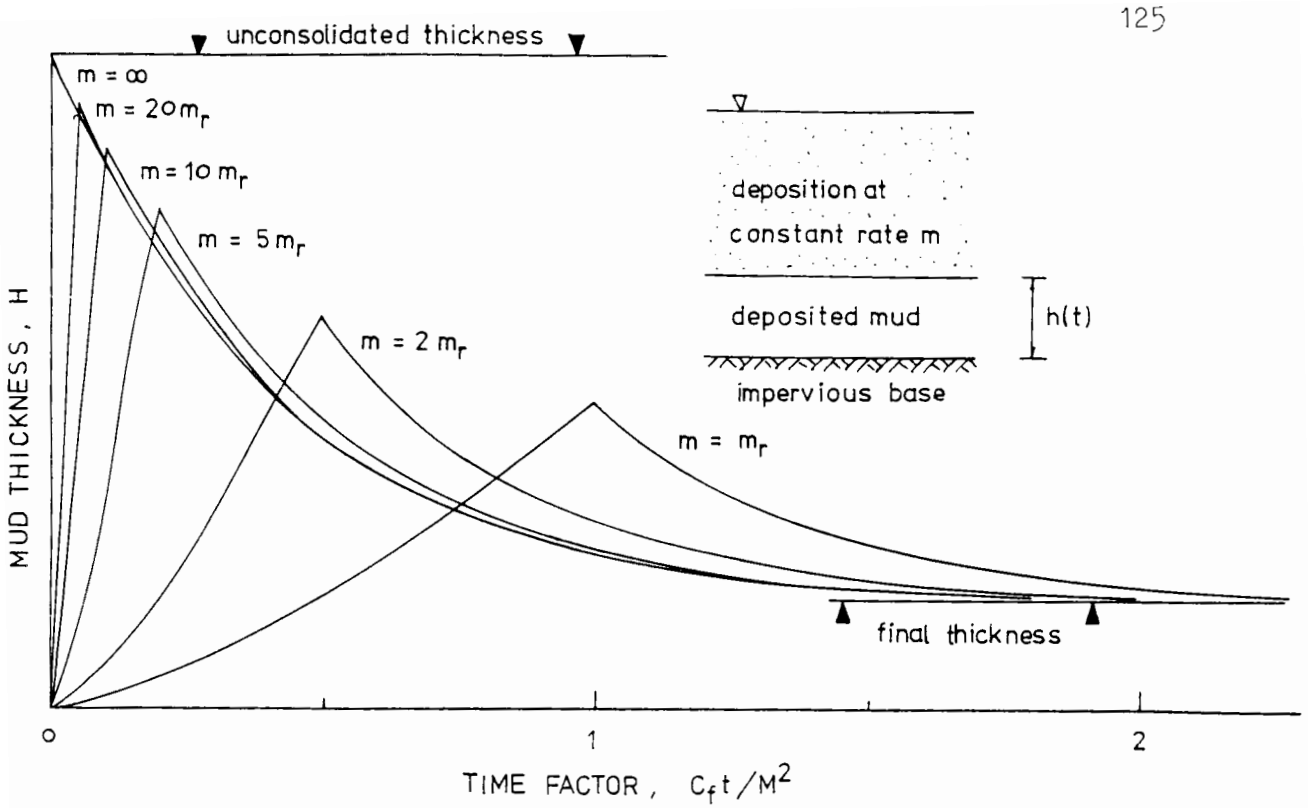

FIG.5.9 Consolidation of dredged fills being deposited at different speed.

(above) impervious base

(below) pervious base

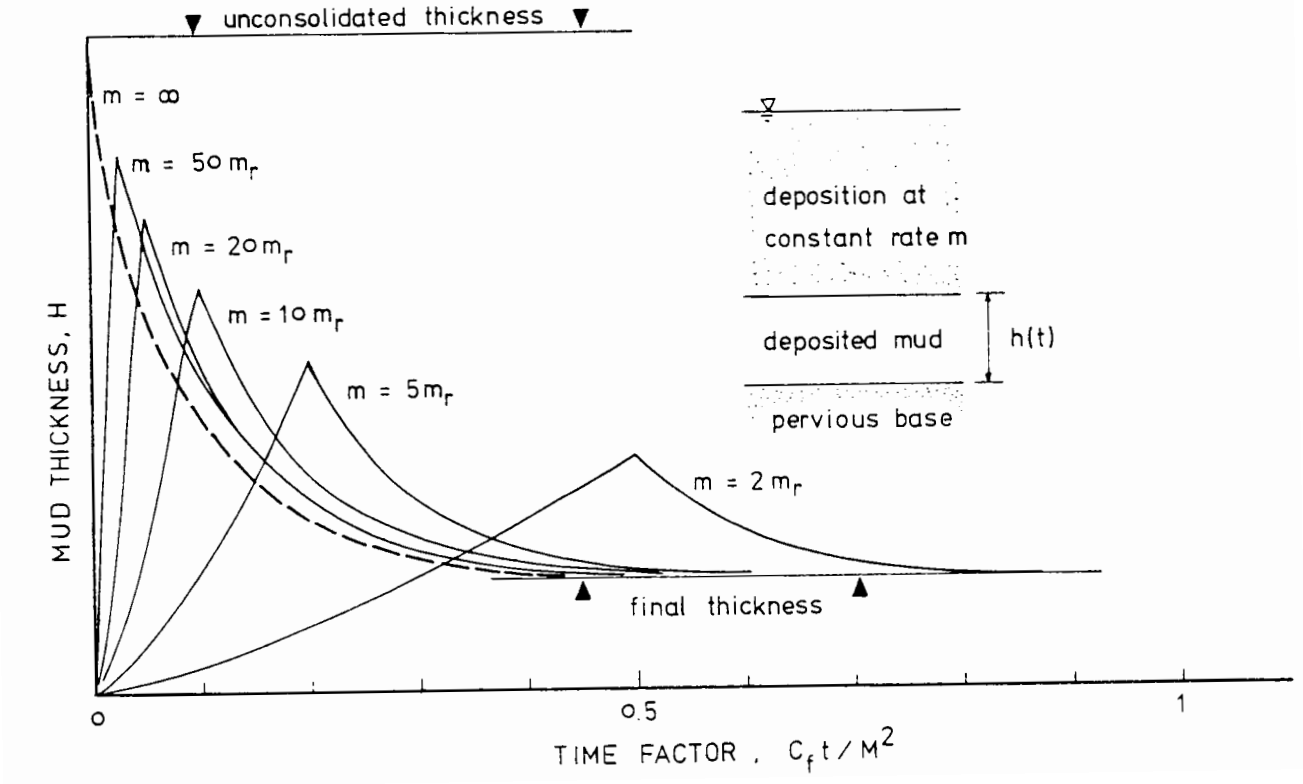

occurs over a period of time, the full loading is not realized until the end of deposition and a slower consolidation is resulted.

It can be noticed from Fig.5.9 that for both pervious and impervious base conditions the faster deposition rates give a comparable time for the final thickness to be achieved. For the pervious base, this is true for $m \geq 5m_r$, and for the impervious base it is true for $m \geq 10m_r$. When comparing these curves it should be noted that the time scales are different.

It is concluded from the analysis that earlier consolidation is achieved with a faster deposition rate. However, there exists an optimum speed for each drainage boundary condition such that a higher deposition rate does not lead to a substantially increased rate of consolidation.

APPENDIX A A BRIEF DESCRIPTION OF THE METHOD OF GENERALIZED POTENTIAL

The application of the method of generalized potential is to reduce a boundary value problem to an integral equation. Detailed development can be found in Smirnov (1964).

Consider the partial differential equation :

$$\frac{\partial q}{\partial t} = a \frac{\partial^2 q}{\partial x^2} \qquad (A.1)$$

where q is defined in the domain (x,t) . A principal (singular) solution for this equation is,

$$q = \frac{1}{2a} (\pi(t-\tau))^{-\frac{1}{2}} exp[-(\zeta-x)^2/(4a^2(t-\tau))] \qquad (A.2)$$

which corresponds to a source located at the point $x = \zeta$ at the instant $t = \tau$.

Differentiating with respect to ζ and adding the constant $2a^2$ the solution corresponding to a dipole is obtained :

$$q = \frac{1}{2a} \pi^{-\frac{1}{2}} (t-\tau)^{-\frac{3}{2}} (x-\zeta) exp[-(\zeta-x)^2/(4a^2(t-\tau))] \qquad (A.3)$$

Multiplying this with some function $\phi(t)$ and integrating with respect to τ from $\tau = 0$ to $\tau = t$, the resulting function :

$$q = \int_0^t \frac{1}{2a} \phi(\tau) \pi^{-\frac{1}{2}} (t-\tau)^{-\frac{3}{2}} (x-\zeta) exp[-(\zeta-x)^2/(4a^2(t-\tau))] d\tau \qquad (A.4)$$

is again a solution to eq(A.1) and this corresponds to a dipole at $x = \zeta$ acting from the instant $\tau = 0$ with strength $\phi(\tau)$. It can be proved that :

$$q(\zeta+0,\ t) = \phi(t) \quad , \quad q(\zeta-0,\ t) = -\phi(t) \tag{A.5}$$

this is achieved by a change of variable :

$$\alpha = \frac{1}{2a}\,(x-\zeta)\,(t-\tau)^{-\frac{1}{2}} \tag{A.6}$$

Consider now the domain in (x,t) as bounded from below by $t=b$ and at the sides by the two curves ι_1 and ι_2 defined by : (see Fig.A.1)

$$x = \iota_1(t) \ , \quad x = \iota_2(t) \ , \ \iota_1(t) \leq \iota_2(t) \tag{A.6}$$

The method of generalized potential is to consider a source or dipole located along $x= \iota_1(t)$ or $x= \iota_2(t)$ acting from $t = b$ with unknown strength $\phi_1(t)$, $\phi_2(t)$.

The solution constructed by a source (simple layer potential) is thus :

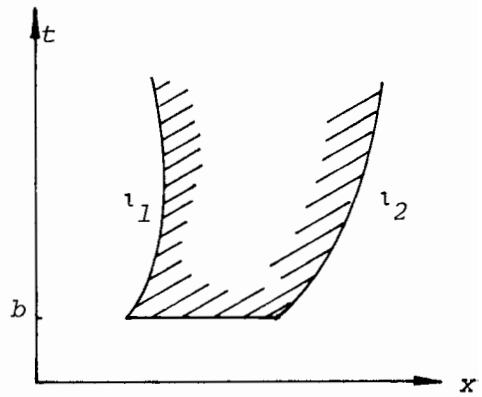

FIG.A.1

$$q_i(x,t) = \frac{1}{2a}\pi^{-\frac{1}{2}} \int_b^t \phi_i(\tau)\,(t-\tau)^{-\frac{1}{2}} exp[-(\iota_i(\tau)-x)^2/4a^2(t-\tau))]\ d\tau \tag{A.7}$$

and a dipole (double layer potential) :

$$q_i(x,t) = \frac{1}{2a}\pi^{-\frac{1}{2}} \int_b^t \phi_i(\tau)\,(x-\iota_i(\tau))\,(t-\tau)^{-\frac{3}{2}} exp[-(\iota_i(\tau)-x)^2/4a^2(t-\tau)]\ d\tau \tag{A.8}$$

It can be shown that the solutions $q_i(x,t)$ thus constructed is bounded and is continuous as far as $\iota_i(t)$. Invoking a lemma by Holmgren (1903) the integral eq(A.8) has different limit as (x,t) tends to the point (x_o,t_o) on ι_i :

$$\lim_{(x,t)\to(x_o,t_o)} q_i(x,t) = \pm \phi_i(t_o) + q_i(x_o,t_o) \qquad (A.9)$$

where the positive sign is taken if (x,t) approaching (x_o,t_o) from the right of ι_i and vice visa.

Hence, the boundary value problem with boundary conditions,

$$\lim_{(x,t)\to \iota_1} q(x,t) = w_1(t) \quad , \quad \lim_{(x,t)\to \iota_2} q(x,t) = w_2(t) \qquad (A.10)$$

can be reduced to integral equations by constructing the solutions with arbitrary combinations of the potentials eq(A.7),(A.8). The case of derived and mixed boundary conditions can be treated similarly.

To demonstrate the existence of solution corresponds to the boundary value problem eq(A.1),(A.10), a solution is sought by combining two double layer potentials as :

$$q(x,t) = \frac{1}{2a}\pi^{-\frac{1}{2}} \sum_i \int_b^t \phi_i(\tau)(x-\iota_i(\tau))(t-\tau)^{-\frac{3}{2}} \exp[-(\iota_i(\tau)-x)^2/4a^2(t-\tau)]\, d\tau$$

The unknown strength functions $\phi_i(t)$ have to satisfy the integral equations obtained from the boundary conditions :

$$w_1(t) = \phi_1(t) + \frac{1}{2a}\pi^{-\frac{1}{2}} \sum_i \int_b^t \phi_i(\tau)(\iota_1(t)-\iota_i(\tau))(t-\tau)^{-\frac{3}{2}} \exp[-\frac{(\iota_i(\tau)-\iota_1(t))^2}{4a^2(t-\tau)}]\, d\tau$$

$$w_2(t) = -\phi_2(t) + \frac{1}{2a}\pi^{-\frac{1}{2}} \sum_i \int_b^t \phi_i(\tau)(\iota_2(t)-\iota_i(\tau))(t-\tau)^{-\frac{3}{2}} \exp[-\frac{(\iota_i(\tau)-\iota_2(t))^2}{4a^2(t-\tau)}]\, d\tau$$

The kernel functions in the above equations are continuous and hence the method of successive approximation can be applied to form a uniformly convergent series solution for the unknown functions $\phi_1(t)$ and $\phi_2(t)$. A proof of this can be found in Smirnov (1964).

APPENDIX B TABLES OF NUMERICAL VALUES OF SOME FUNCTIONS

TABLE B-I Numerical values of function $F_1(\nu)$ for $\nu = 0.1(0.1)5.0$

$$F_1(\nu) = \int_0^1 y(1-y)^{-\frac{3}{2}} \exp[-\nu^2 y/(1-y)]\, dy$$

TABLE B-II Numerical values of function $F_2(\nu)$ for $\nu = 0.1(0.1)4.0$

$$F_2(\nu) = \int_0^1 y^{\frac{1}{2}}(1-y)(1-y)^{-\frac{3}{2}} \exp[-\nu^2/(1-y)]\, dy$$

TABLE B-III Numerical values of function $F_3(\nu)$ for $\nu = 0.1(0.1)5.0$

$$F_3(\nu) = \int_0^1 y^{\frac{1}{2}}(1-y^{\frac{1}{2}})(1-y)^{-\frac{3}{2}} \exp[-\nu^2(1-y^{\frac{1}{2}})^2/(1-y)]\, dy$$

TABLE B-IV Numerical values of function $F_6(\nu)$ for $\nu = 0.1(0.1)4.0$

$$F_6(\nu) = \int_0^1 y^{\frac{1}{2}}(1-y)^{-\frac{1}{2}} \exp[-\nu^2/(1-y)]\, dy$$

TABLE B-V Numerical values of function $F_7(\nu)$ for $\nu = 0.1(0.1)5.0$

$$F_7(\nu) = \int_0^1 y^{\frac{1}{2}}(1-y)^{-\frac{1}{2}} \exp[-\nu^2 y/(1-y)]\, dy$$

TABLE B-VI Numerical values of function $F_8(\nu)$ for $\nu = 0.1(0.1)5.0$

$$F_8(\nu) = \int_0^1 y^{\frac{1}{2}}(1-y)^{-\frac{1}{2}} \exp[-\nu^2(1-y^{\frac{1}{2}})^2/(1-y)]\, dy$$

TABLE B-VII Numerical values of function $F_9(\nu)$ for $\nu = 0.1(0.1)4.0$

$$F_9(\nu) = \int_0^1 (1-y)^{-\frac{1}{2}} \exp[-\nu^2/(1-y)]\, dy$$

TABLE B-VIII Numerical values of function $F_{10}(\nu)$ for $\nu = 0.1(0.1)5.0$

$$F_{10}(\nu) = \int_0^1 y^{\frac{1}{2}}(1-y)^{-\frac{3}{2}} \exp[-\nu^2 y/(1-y)]\, dy$$

TABLE B-IX Numerical values of function $F_{11}(\nu)$ for $\nu = 0.1(0.1)5.0$

$$F_{11}(\nu) = \int_0^1 y^{\frac{3}{2}}(1-y)^{-\frac{5}{2}} \exp[-\nu^2 y/(1-y)]\, dy$$

TABLE B-X Numerical values of function $\int_0^1 erf[\nu(1-x)^{-\frac{1}{2}}]\, dx$

for $\nu = 0.1(0.1)4.0$

TABLE B-XI Numerical values of function $F_4(x,\nu)$

for $x = 0.1(0.1)0.9$, $\nu = 0.1(0.1)1.0(0.2)2.0(0.5)5.0$

$$F_4(x,\nu) = \int_0^1 xy^{\frac{1}{2}}(1-y)^{-\frac{3}{2}} \exp[-\nu^2 x^2/(1-y)]\, dy$$

TABLE B-XII Numerical values of function $F_5(x,\nu)$

for $x = 0.1(0.1)0.9$, $\nu = 0.1(0.1)1.0(0.2)2.0(0.5)5.0$

$$F_5(x,\nu) = \int_0^1 (x-y^{\frac{1}{2}})y^{\frac{1}{2}}(1-y)^{-\frac{3}{2}} \exp[-\nu^2(x-y^{\frac{1}{2}})^2/(1-y)]\, dy$$

TABLE B-XIII Numerical values of function $F_{12}(x,\nu)$

for $x = 0.1(0.1)0.9$, $\nu = 0.1(0.1)1.0(0.2)2.0(0.5)5.0$

$$F_{12}(x,\nu) = \int_0^1 (1-y)^{-\frac{1}{2}} \exp[-\nu^2 x^2/(1-y)]\, dy$$

TABLE B-I Function $F_1(v)$ in 10^{-6}

v	0.1	0.2	0.3	0.4	0.5	0.6	0.7	0.8	0.9	1.0
0.0	14 207072	5 743329	3 121371	1 923503	1 273848	885035	636758	470688	355617	273616
1.0	213824	169373	135773	110003	089983	074250	061757	051743	043646	037047
2.0	031629	027150	023424	020305	017681	015460	013573	011960	010577	009385
3.0	008354	007459	006679	005997	005399	004873	004408	003997	003633	003308
4.0	003019	002760	002528	002320	002132	001963	001810	001672	001546	001432

TABLE B-II Function $F_2(v)$ in 10^{-6}

v	0.1	0.2	0.3	0.4	0.5	0.6	0.7	0.8	0.9	1.0
0.0	14 759896	6 072823	3 290488	1 980205	1 254383	816476	539000	358038	238069	157879
1.0	104145	068196	044259	028432	018060	011333	007021	004291	002586	001536
2.0	000899	000518	000294	000164	000090	000049	000026	000014	000007	000004
3.0	000002	000001	000001	-	-	-	-	-	-	-

TABLE B-III Function $F_3(v)$ in 10^{-6}

v	0.1	0.2	0.3	0.4	0.5	0.6	0.7	0.8	0.9	1.0
0.0	857494	854770	850279	844094	836313	827055	816457	804666	791839	778137
1.0	763716	748731	733327	717639	701790	685889	670035	654308	638780	623508
2.0	608539	593908	579644	565767	552289	539219	526558	514307	502461	491013
3.0	479957	469281	458976	449029	439430	430164	421222	412589	404255	396207
4.0	388433	380923	373666	366650	359867	353306	346957	340813	334864	329102

TABLE B-IV Function $F_6(v)$ in 10^{-6}

v	0.1	0.2	0.3	0.4	0.5	0.6	0.7	0.8	0.9	1.0
0.0	1 246541	978063	758447	581046	439601	328330	241999	175962	126180	089206
1.0	062158	042676	028863	019225	012608	008139	005171	003233	001988	001203
2.0	000715	000419	000241	000136	000076	000041	000022	000012	000006	000003
3.0	000002	000001	-	-	-	-	-	-	-	-

TABLE B-V Function $F_7(v)$ in 10^{-6}

v	0.1	0.2	0.3	0.4	0.5	0.6	0.7	0.8	0.9	1.0
0.0	1 259069	1 017979	829873	681864	564459	470605	395019	333709	283641	242486
1.0	208446	180124	156423	136482	119618	105284	093042	082541	073492	065664
2.0	058863	052934	047745	043188	039173	035523	032476	029678	027183	024951
3.0	022951	021153	019533	018070	016746	015546	014455	013462	012555	011727
4.0	010969	010272	009633	009045	008503	008003	007540	007112	006715	006347

TABLE B-VI Function $F_8(v)$ in 10^{-6}

v	0.1	0.2	0.3	0.4	0.5	0.6	0.7	0.8	0.9	1.0
0.0	1 569338	1 564985	1 557802	1 547896	1 535409	1 520515	1 503417	1 484332	1 463496	1 441147
1.0	1 417525	1 392865	1 367391	1 341316	1 314835	1 288126	1 261347	1 234638	1 208120	1 181895
2.0	1 156048	1 130651	1 105759	1 081417	1 057656	1 034501	1 011966	990060	968786	948142
3.0	928122	908717	889916	871705	854070	836995	820463	804459	788963	773961
4.0	759433	745364	731736	718534	705742	693344	681326	669672	658369	647404

TABLE B-VII Function $F_9(v)$ in 10^{-6}

v	0.1	0.2	0.3	0.4	0.5	0.6	0.7	0.8	0.9	1.0
0.0	1 665476	1 370489	1 113876	893769	707710	552776	425737	323202	241769	178148
1.0	129266	092341	064923	044914	030567	020461	013468	008716	005545	003467
2.0	002130	001286	000763	000444	000254	000143	000079	000043	000023	000012
3.0	000006	000003	000002	000001	-	-	-	-	-	-

TABLE B-VIII Function $F_{10}(v)$ in 10^{-6}

v	0.1	0.2	0.3	0.4	0.5	0.6	0.7	0.8	0.9	1.0
0.0	14 908236	6 320659	3 600368	2 323793	1 610659	1 170279	879818	679013	535157	429160
1.0	349248	287835	239858	201844	171346	146604	126333	109574	095607	083878
2.0	073961	065524	058302	052088	046714	042043	037966	034392	031247	028469
3.0	026007	023817	021863	020115	018546	017134	015861	014709	013665	012717
4.0	011854	011066	010346	009686	009081	008525	008013	007541	007105	006702

TABLE B-IX Function $F_{11}(v)$ in 10^{-6}

v	0.1	0.2	0.3	0.4	0.5	0.6	0.7	0.8	0.9	1.0
0.0	871 31869	104 457706	29 222852	11 523503	5 479156	2 932624	1 703934	1 051899	680518	457066
1.0	316587	225028	163522	121125	091240	069760	054051	042385	033600	026901
2.0	021733	017706	014536	012019	010005	008379	007059	005979	005090	004354
3.0	003741	003229	002797	002433	002124	001861	001635	001442	001275	001130
4.0	001005	000896	000801	000717	000644	000580	000523	000472	000428	000388

TABLE B-X $\int_0^1 erf[v(1-x)^{-\frac{1}{2}}]\,dx$ in 10^{-6}

v	0.1	0.2	0.3	0.4	0.5	0.6	0.7	0.8	0.9	1.0
0.0	206427	377346	517158	630094	720141	790979	845939	887979	919671	943210
1.0	960429	972831	981625	987761	991974	994819	996708	997942	998734	999234
2.0	999544	999734	999847	999913	999952	999974	999986	999993	999996	999998
3.0	999999	999999	1 000000	1 000000	1 000000	1 000000	1 000000	1 000000	1 000000	1 000000

TABLE B-XI Function $F_4(x,v)$ in 10^{-6}

v \ x	0.1	0.2	0.3	0.4	0.5	0.6	0.7	0.8	0.9
0.1	17 415691	17 103126	16 798003	16 496252	16 198035	15 903353	15 612203	15 324581	15 040480
0.2	8 551563	8 248125	7 951677	7 662290	7 379948	7 104625	6 836290	6 574906	6 320433
0.3	5 599334	5 301118	5 013493	4 736417	4 469821	4 213622	3 967717	3 731987	3 506295
0.4	4 124063	3 831145	3 552312	3 287453	3 036411	2 798990	2 574952	2 364020	2 165886
0.5	3 239607	2 951979	2 681893	2 429129	2 193389	1 974293	1 771391	1 584164	1 412038
0.6	2 650559	2 368208	2 106811	1 865993	1 645244	1 443924	1 261280	1 096459	948524
0.7	2 230315	1 953226	1 700450	1 471404	1 265279	1 081097	917706	773823	648070
0.8	1 915573	1 643727	1 399495	1 182010	990103	822344	677095	552564	446857
0.9	1 671164	1 404541	1 168765	962616	784465	632350	504055	397206	309357
1.0	1 475990	1 214565	987146	792082	627191	489885	377300	286431	214262
1.2	1 184104	932997	721962	548229	408238	297905	212905	148931	101917
1.4	976613	735700	540549	386912	269500	182490	120019	076601	047408
1.6	821863	591005	411172	276282	179019	111699	067025	038635	021371
1.8	702270	481308	316175	198603	119034	067945	036873	018997	009278
2.0	607282	396041	244943	143215	078940	040918	019902	009067	003862
2.5	438678	250877	131736	063152	027502	010836	003849	001229	000352
3.0	329049	163295	071421	027278	009030	002575	000629	000131	000023
3.5	253056	107800	038499	011373	002749	000539	000085	000011	000001
4.0	198021	071608	020459	004533	000768	000098	000009	000001	000000
4.5	156893	047614	010656	001717	000196	000016	000001	000000	000000
5.0	125438	031576	005418	000615	000045	000002	000000	000000	000000

TABLE B-XII Function $F_5(x,v)$ in -10^{-6}

v \ x	0.1	0.2	0.3	0.4	0.5	0.6	0.7	0.8	0.9
0.1	14 434981	14 684890	14 991612	15 372534	15 701765	15 575459	14 702759	16 817299	22 829665
0.2	5 949193	6 159291	6 374934	6 597111	6 815247	7 031556	7 348840	7 421170	8 014481
0.3	3 290154	3 464542	3 644573	3 830090	4 020939	4 219616	4 411252	4 672944	4 392077
0.4	2 062953	2 208546	2 360255	2 518021	2 681836	2 851268	3 028346	3 200124	3 345703
0.5	1 389923	1 512349	1 641078	1 776033	1 917100	2 064187	2 216859	2 374127	2 580127
0.6	982341	1 085991	1 195920	1 312104	1 434121	1 562043	1 695559	1 835367	2 001604
0.7	718880	807206	901646	1 002053	1 108225	1 219916	1 336848	1 458707	1 587520
0.8	540440	616171	697768	785048	877762	975606	1 078229	1 185146	1 292160
0.9	415222	480533	551415	627647	708935	794924	885214	979369	1 073953
1.0	324845	381483	443371	510253	581793	657591	737206	820190	905282
1.2	207831	251086	298936	351063	407060	466457	528760	593471	660631
1.4	139448	173109	210746	251990	296381	343414	392579	443400	495484
1.6	097199	123839	153899	186972	222566	260167	299287	339497	380389
1.8	069918	091324	115663	142501	171336	201668	233051	265128	297629
2.0	051652	069087	089036	111049	134627	159303	184690	210503	236561
2.5	026609	037594	050292	064251	079031	094284	109779	125383	141028
3.0	015207	022555	031076	040355	050046	059924	069873	079846	089825
3.5	009396	014546	020506	026916	033522	040197	046891	053589	060287
4.0	006169	009916	014225	018797	023459	028145	032835	037525	042216
4.5	004250	007060	010261	013614	017007	020407	023808	027209	030611
5.0	003046	005205	007638	010158	012694	015233	017772	020311	022850

TABLE B-XIII Function $F_{12}(x,v)$ in 10^{-6}

v \ x	0.1	0.2	0.3	0.4	0.5	0.6	0.7	0.8	0.9
0.1	1 964749	1 929902	1 895452	1 861403	1 827753	1 794501	1 761648	1 729194	1 697136
0.2	1 929902	1 861403	1 794501	1 729194	1 665476	1 603342	1 542785	1 483797	1 426369
0.3	1 895452	1 794501	1 697136	1 603342	1 513096	1 426369	1 343127	1 263329	1 186929
0.4	1 861403	1 729194	1 603342	1 483797	1 370489	1 263329	1 162209	1 067005	977576
0.5	1 827753	1 665476	1 513096	1 370489	1 237487	1 113876	999400	893769	796657
0.6	1 794501	1 603342	1 426369	1 263329	1 113976	977576	853921	742333	642177
0.7	1 761648	1 542785	1 343127	1 162209	999400	853921	724864	611216	511888
0.8	1 729194	1 483797	1 263329	1 067005	893769	742333	611216	498801	403379
0.9	1 697136	1 426369	1 186929	977576	796657	642177	511888	403379	314155
1.0	1 665476	1 370489	1 113876	893769	707710	552776	425737	323202	241769
1.2	1 603342	1 263329	977576	742333	552776	403379	288285	201661	138002
1.4	1 542785	1 162209	853921	611216	425737	288285	189598	121008	074891
1.6	1 483797	1 067005	742333	498801	323202	201661	121008	069751	038583
1.8	1 426369	977576	642177	403379	241769	138002	074891	038583	018845
2.0	1 370489	893769	552776	323202	178148	092341	044914	020461	008716
2.5	1 237487	707710	371621	178148	077583	030567	010858	003467	000993
3.0	1 113876	552776	241769	092341	030567	008716	002130	000444	000079
3.5	999400	425737	152046	044914	010858	002130	000337	000043	000004
4.0	893769	323202	092341	020461	003467	000444	000043	000003	000000
4.5	796657	241769	054109	008716	000993	000079	000004	000000	000000
5.0	707710	178148	030567	003467	000254	000012	000000	000000	000000

APPENDIX C EVALUATION OF SOME DEFINITE INTEGRALS IN EQ(5.88), EQ(5.96)

C-1 The integral in eq(5.88) is,

$$I = \frac{1}{2}\beta m(\pi t)^{-\frac{1}{2}} C_F^{-\frac{3}{2}} \exp(-z^2/4C_F t) \int_0^\infty \xi^2 (1-\coth(m\xi/2C_F)) \sinh(z\xi/2C_F t) \exp(-\xi^2/4C_F t)\, d\xi$$

$$= \frac{1}{2}\beta m(\pi t)^{-\frac{1}{2}} C_F^{-\frac{3}{2}} [\, I_1 - \exp(-z^2/4C_F t) I_2]$$

where,

$$I_1 = \int_0^\infty \xi^2 \exp[-(z-\xi)^2/4C_F t]\, d\xi - \int_0^\infty \xi^2 \exp[-(z+\xi)^2/4C_F t]\, d\xi$$

set, $y = (z-\xi)/(2(C_F t)^{\frac{1}{2}})$ in the first integral

and $y = (z+\xi)/(2(C_F t)^{\frac{1}{2}})$ in the second integral

this leads to :

$$I_1 = \int_{-\infty}^{\infty} 2(C_F t)^{\frac{1}{2}} [z^2 - 4(C_F t)^{\frac{1}{2}} zy + 4C_F t y^2] \exp(-y^2)\, dy$$

$$- 2 \int_{z/(2(C_F t)^{\frac{1}{2}})}^{\infty} 2(C_F t)^{\frac{1}{2}} (z^2 - 4(C_F t)^{\frac{1}{2}} zy + 4C_F t y^2) \exp(-y^2)\, dy$$

which can be decompcsed as :

$$I_{11} = \int_{-\infty}^{\infty} 2(C_F t)^{\frac{1}{2}} z^2 \exp(-y^2)\, dy = 2(\pi C_F t)^{\frac{1}{2}} z^2$$

$$I_{12} = \int_{z/(2(C_F t)^{\frac{1}{2}})}^{\infty} 4(C_F t)^{\frac{1}{2}} z^2 \exp(-y^2)\, dy = 2(\pi C_F t)^{\frac{1}{2}} z^2 \operatorname{erfc}[z/(2(C_F t)^{\frac{1}{2}})]$$

$$I_{13} = 8C_F tz \int_{-\infty}^{\infty} y \exp(-y^2)\, dy = 0$$

$$I_{14} = 16C_F tz \int_{z/(2(C_F t)^{\frac{1}{2}})}^{\infty} y \exp(-y^2)\, dy = 8C_F tz \exp(-z^2/4C_F t)$$

and

$$I_{15} = 8(C_F t)^{\frac{3}{2}} \int_{-\infty}^{\infty} y^2 \exp(-y^2)\, dy = 4\pi^{\frac{1}{2}} (C_F t)^{\frac{3}{2}}$$

To evaluate the integral,

$$I_{16} = 16(C_F t)^{\frac{3}{2}} \int_{z/(2(C_F t)^{\frac{1}{2}})}^{\infty} y^2 \exp(-y^2)\, dy$$

one starts from the identity,

$$\int_{z/(2(C_F t)^{\frac{1}{2}})}^{\infty} \exp(-y^2) dy = \frac{1}{2}\pi^{\frac{1}{2}} \operatorname{erfc}[z/(2(C_F t)^{\frac{1}{2}})]$$

hence,

$$\int_{z/(2(C_F t)^{\frac{1}{2}})}^{\infty} \exp(-ay^2)\, dy = \frac{1}{2}\left(\frac{\pi}{a}\right)^{\frac{1}{2}} \operatorname{erfc}\left[\frac{z}{2}\left(\frac{a}{C_F t}\right)^{\frac{1}{2}}\right]$$

Therefore,

$$\int_{z/(2(C_F t)^{\frac{1}{2}})}^{\infty} y^2 \exp(-ay^2)\, dy = -\frac{d}{da}\left\{\int_{z/(2(C_F t)^{\frac{1}{2}})}^{\infty} \exp(-ay^2)\, dy\right\}$$

$$= \frac{1}{4} a^{-\frac{3}{2}} \pi^{\frac{1}{2}} \operatorname{erfc}\left[\frac{z}{2}\left(\frac{a}{C_F t}\right)^{\frac{1}{2}}\right] + \frac{1}{4a} z(C_F t)^{-\frac{1}{2}} \exp[-az^2/4C_F t]$$

Put $a = 1$ it then follows that,

$$\int_{z/(2(C_F t)^{\frac{1}{2}})}^{\infty} y^2 \exp(-y^2)\, dy = \frac{\pi^{\frac{1}{2}}}{4} \operatorname{erfc}[z/(2(C_F t)^{\frac{1}{2}})] + \frac{z}{4}(C_F t)^{-\frac{1}{2}} \exp(-z^2/4C_F t)$$

Combining I_{11} to I_{16}, it is found that :

$$I_1 = 2(\pi C_F t)^{\frac{1}{2}} z^2 + 4(C_F t)^{\frac{3}{2}} \pi^{\frac{1}{2}} - 2(\pi C_F t)^{\frac{1}{2}} z^2 \exp(-z^2/4C_F t)$$

$$+ 4(C_F t)^{\frac{3}{2}} \pi^{\frac{1}{2}} \operatorname{erfc}[z/(2(C_F t)^{\frac{1}{2}})] + 4C_F t z \exp(-z^2/4C_F t)$$

substituting this into eq(5.88) thus results to eq(5.89).

C-2 The integral in eq(5.96) is,

$$I = \int_0^1 \sinh(yT\eta/2)\exp(-\eta^2 T/4)\, d\eta$$

$$= \frac{1}{2}\left\{ \int_0^1 \exp(-\eta^2 T/4 + yT\eta/2)\, d\eta - \int_0^1 \exp(-\eta^2 T/4 - yT\eta/2)\, d\eta \right\}$$

let, $x = \frac{1}{2} T^{\frac{1}{2}}(\eta - y)$ in the first integral

and $x = \frac{1}{2} T^{\frac{1}{2}}(\eta + y)$ in the second integral

Thus,

$$I = T^{-\frac{1}{2}} \exp(y^2 T/4) \left\{ \int_{-T^{\frac{1}{2}}y/2}^{T^{\frac{1}{2}}(1-y)/2} \exp(-x^2)dx - \int_{T^{\frac{1}{2}}y/2}^{T^{\frac{1}{2}}(1+y)/2} \exp(-x^2)dx \right\}$$

$$= T^{-\frac{1}{2}}\exp(y^2 T/4) \left\{ 2\,\mathrm{erf}(T^{\frac{1}{2}}y/2) + \mathrm{erf}(T^{\frac{1}{2}}(1-y)/2) - \mathrm{erf}(T^{\frac{1}{2}}(1+y)/2) \right\}$$

from which eq(5.97) follows.

CHAPTER SIX THE CONSOLIDATION OF A NONLINEAR SOIL MODEL

(continued on next page)

ABSTRACT

The consolidation of a particular nonlinear soil model is considered in this chapter. An exponential stress - void ratio and a parabolic permeability - void ratio relationships are assumed in this model, whereby the coefficient of consolidation of the soil C_F remains constant and the governing equation reduces to a linear one. The void ratio distribution in a normally consolidated stratum which is composed of such a soil varies nonlinearly as a result of the weight of the soil causing the effective stress to increase with depth. This variation of void ratio is best described by a parameter, defined as the stratum coefficient γ . This parameter is of fundamental importance in the present theory.

The first part of this chapter is devoted to the consolidation of a normally consolidated stratum under a surface loading. Analytical and approximate solutions have been obtained with various drainage conditions in the step loading case. The solutions reveal that, when drainage is allowed in both the surface and the base, a stratum with larger γ value will consolidate faster. The difference between the solutions with up to a moderate γ (< 1) and the thin layer solution of Gibson et.al. (1967) is of the order of a few percent. This, however, does not apply equally well to the single drain conditions. It is found that a stratum with a surface drain always consolidates faster than that with a base drain. The difference in consolidation speed of the two drainage conditions is a result of the nonlinear void ratio distribution in a normally consolidated stratum which calls for different void ratio changes in the surface and the base. The consolidation under a time dependent loading is briefly discussed and the general solution is given. These solutions are applied to the analysis of the particularly important case of a linear ramp loading in which some charts considered to be of practical interest are produced.

The consolidation of a dredged fill under its own weight

is then considered in the second part of this chapter. This differs significantly from that of the first part in that no surface loading is involved and the consolidation is caused by the self weight which creates a stress that increases with depth. Analytical and approximate solutions are developed for double drain and surface drain conditions, and it is found that faster consolidation is achieved with larger ν. The dissipation of excess pore water pressure is also analysed in both cases.

1. INTRODUCTION TO THE NONLINEAR SOIL MODEL

The preceeding chapters have considered a linear soil model in which simple stress - void ratio and permeability relationships are assumed. This simple model has the advantage of reducing the mathematical complexities involved, although at the cost of adopting a highly idealized material behaviour. When a stratum of sufficient thickness, or one which is composed of soft clay is considered, the soil can be expected to behave nonlinearly during the consolidation. In such cases the need for a better model that will cope with the nonlinear nature of the soil behaviour becomes apparent. This chapter is concerned with such a model, which simulates real soil behaviour to a reasonable extent while at the same time keeping to a minimum the mathematical complexities involved.

In the governing equation of consolidation :

$$\frac{\partial e}{\partial t} = \frac{\partial}{\partial z}\left(C_F \frac{\partial e}{\partial z} \right) - \beta \frac{\partial e}{\partial z} \qquad (6.1)$$

$$\beta = (\rho_s - \rho_f) \frac{d}{de} \left(\frac{k}{\rho_f (1+e)} \right)$$

where both C_F and β are functions of the void ratio. In the linear model C_F is a constant and β equals zero. If a nonzero constant value is assumed for β , then eq(6.1) will be a linear equation and the effective stress - void ratio and permeability relationships have the following nonlinear forms :

$$k = \rho_f (\alpha e + \alpha_1)(1 + e) \qquad (6.2)$$

and

$$\sigma' = A - \frac{C_F}{\alpha} ln[e + \frac{\alpha_1}{\alpha}] \qquad (6.3)$$

where α is a soil constant given by :

$$\alpha = \frac{\beta}{\rho_s - \rho_f} \qquad (6.4)$$

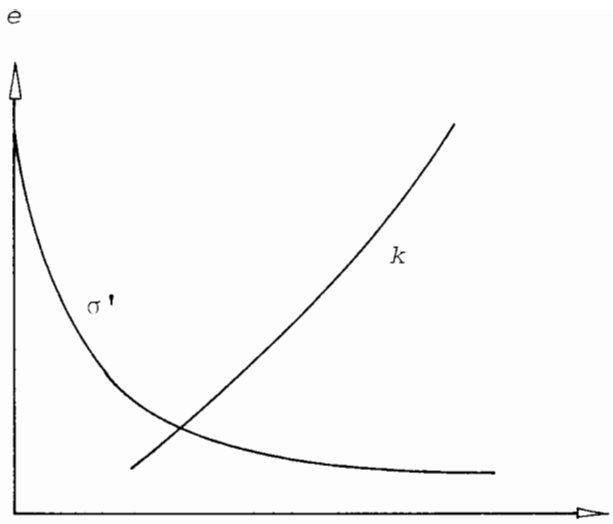

FIG.6.1 The nonlinear soil model

and α_1 and A are integration constants. From eq(6.2), α_1 corresponds to the permeability of the soil when the void ratio equals zero, and hence must also equal zero. In practice, however, such a constant may exist as a result of fitting experimental data with eq(6.2) in a specific void ratio range. For the sake of simplicity it will be assumed that $\alpha_1=0$ in the following analysis. It can be proved that such an assumption has no effect on the consolidation behaviour of the soil.

The constant A appearing in eq(6.3) is obtained when σ' equals zero, i.e.

$$A = \frac{C_F}{\alpha} \ln\left[e_i + \frac{\alpha_1}{\alpha} \right] \qquad (6.5)$$

where e_i is the void ratio of the soil when it is in a no effective stress state. In nature this will probably depend on the previous stress history of the particular soil. And in practice this can be obtained by fitting experimental data to eq(6.3). It will be seen later that the actual magnitude of this does not affect the consolidation behaviour.

The effective stress - void ratio relationship, eq(6.3), and the permeability law, eq(6.2) are shown schematically in Fig.6.1.

In a normally consolidated stratum, i.e. one which is in equilibrium under its own weight, the void ratio distribution must

be such that the stress - void ratio relationship is satisfied. From eq(6.3) this is found to be :

$$e(z) = e_b \exp[\frac{\beta}{C_F} z \,] \tag{6.6}$$

where e_b is the void ratio at the base of the stratum and z is the material coordinate (solid thickness) measured against gravity. For a stratum with known total solid thickness z_o this equation can be expressed in terms of the normalized coordinate $\eta = z / z_o$ as :

$$e(\eta) = e_b \exp(\gamma\eta) \tag{6.7}$$

where γ is a dimensionless parameter, called the stratum ccefficient which is defined as :

$$\gamma = \frac{\beta}{C_F} z_o \tag{6.8}$$

Substituting eq(6.2-4) into this yields :

$$\gamma = [(\rho_s - \rho_f) z_o][- \frac{1}{e} \frac{de}{d\sigma'}] \tag{6.9}$$

The first part of this expression $(\rho_s-\rho_f)z_o$ is the effective stress exerted on the base of the stratum by the weight of its superimposed soil, while the second part of this expressior is analogous to the compressibility. Hence, this stratum coefficient γ is a measure of the strain induced in the base of the stratum by its own weight. Later in this chapter it will be seen that this parameter is of fundamental importance in the consolidation of a stratum. It is therefore useful to record typical values of γ of natural strata. A direct method is to make use of eq(6.8). This will require the knowledge of the soil constant β and C_F as well as the solid thickness of the stratum z_o, and neither of these can be easily interpreted from published data. Therefore, approximate methods must

be used. This is to measure the ratio of the void ratios in the surface and the base of the stratum, and this ratio is related to γ by virtue of eq(6.7) as :

$$\frac{e_s}{e_b} = exp(\gamma) \tag{6.10}$$

where e_s and e_b are the void ratio in the surface and the base respectively.

Eq(6.10) can also be written in terms of the water content, which is mostly found in published data, by assuming that the stratum is fully saturated. Hence,

$$\frac{w_s}{w_b} = \frac{e_s}{e_b} = exp(\gamma) \tag{6.11}$$

where w_s and w_b are the water content in the surface and the base of the stratum. This equation applies only to the theoretical model. In practice, as a result of nonhomogenuity, desiccation near the surface and the effect of previous loading, very seldom will a stratum have its maximun water content near the surface, nor will the minimum water content occur near the base. Thus, further approximation to the above equation must be applied.

The most sensible approximation is to measure the ratio of the maximum to the minimum water content and use this ratio to replace w_s / w_b in eq(6.11). It is expected that this method will probably underestimate the true γ value. In the present study seven sites from five case records were examined with results given in Table 6.1. It is seen from this Table that the γ so interpreted range from 0.4 to 1.4. According to this the discussion in this chapter will be confined to a range of γ from 0.1 to 2.0.

The material coordinate adopted in the present analysis is related to the space coordinate x by the transformation :

Soil Description	$\frac{w_{max}}{w_{min}}$	γ	Source
Mexico city clay 25m thick	1.71	0.54	Girault (1972)
Mexico city clay 25m thick	1.75	0.56	Girault (1972)
Grey clayey silt (Bay mud) 33m thick	1.47	0.4	Taylor and Buchignani (1972)
Grey silty clay with decayed vegetation 20m thick	3.45	1.2	Sanglerat et.al. (1974)
Grey plastic clay with thin layers of decayed vegetation, thickness 27m	4.19	1.4	Sanglerat et. al. (1974)
Normally consolidated lacustrine clay more than 50m thick	1.91	0.65	D'Elia and Grisclia (1974)
Soft sensitive marine illitic clay 8m thick	2.0	0.7	Ladd (1972)

TABLE 6.1 ESTIMATED STRATUM COEFFICIENT BASED ON FIVE CASE RECORDS

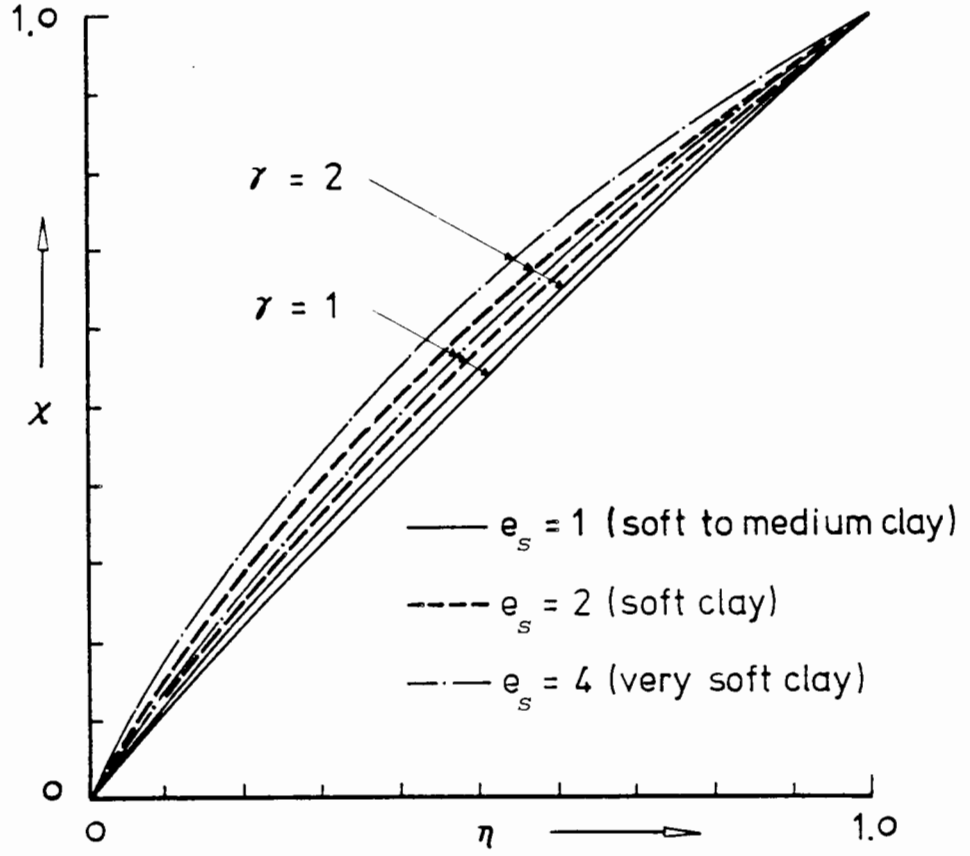

FIG.6.2 The relationship between the normalized space and material coordinates.

$$x(z) = \int_0^z (1 + e) \, dz \tag{6.12}$$

where x is measured in the same direction as z . In a normally consolidated stratum with the void ratio distribution given by eq(6.7) the above equation becomes,

$$x(\eta) = z_o \{\eta + \frac{e_s}{\gamma} [\exp[-\gamma(1-\eta)] - \exp(-\gamma)]\} \tag{6.13}$$

where the normalized material coordinate η is used here for clarity. The space coordinate can also be normalized to give,

$$\chi = \frac{x}{h_o} = \frac{\eta + \frac{e_s}{\gamma} [\exp[-\gamma(1-\eta)] - \exp(-\gamma)]}{1 + \frac{e_s}{\gamma} [1 - \exp(-\gamma)]} \tag{6.14}$$

where h_o is the initial thickness (in space) of the stratum. This relationship between the normalized space and material coordinate is shown in Fig.6.2 for different values of γ and e_s .

The void ratio distribution in the space coordinate is obtained by using eq(6.7) in the above equation, thus :

$$\chi = \frac{\gamma + \ln\left(\frac{e}{e_s}\right) + e - e_b}{\gamma + e_s - e_b} \qquad (6.15)$$

which is implicit. This is shown in Fig.6.3 for different values of γ and e_s . For comparison, Fig.6.4 shows the same distribution in the normalized material coordinate. Note that in this case only the value of γ will be needed to determine the distribution.

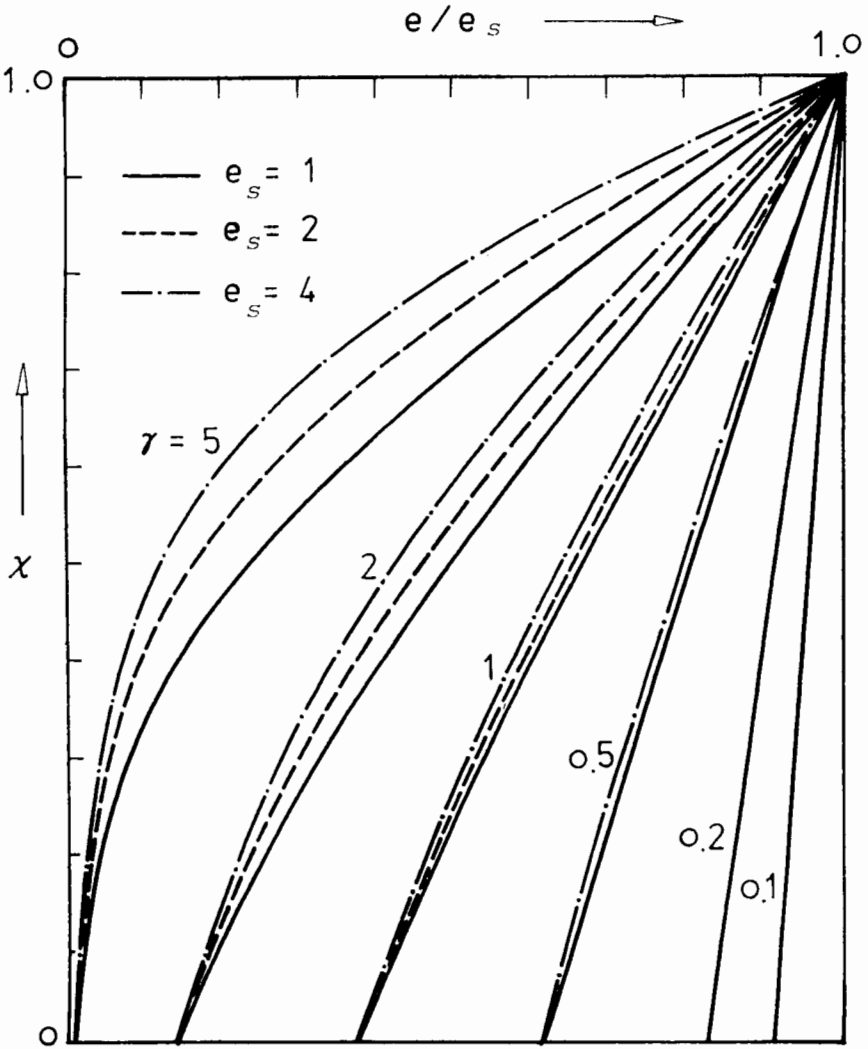

FIG.6.3 Distribution of void ratio in space coordinate in a normally consolidated stratum

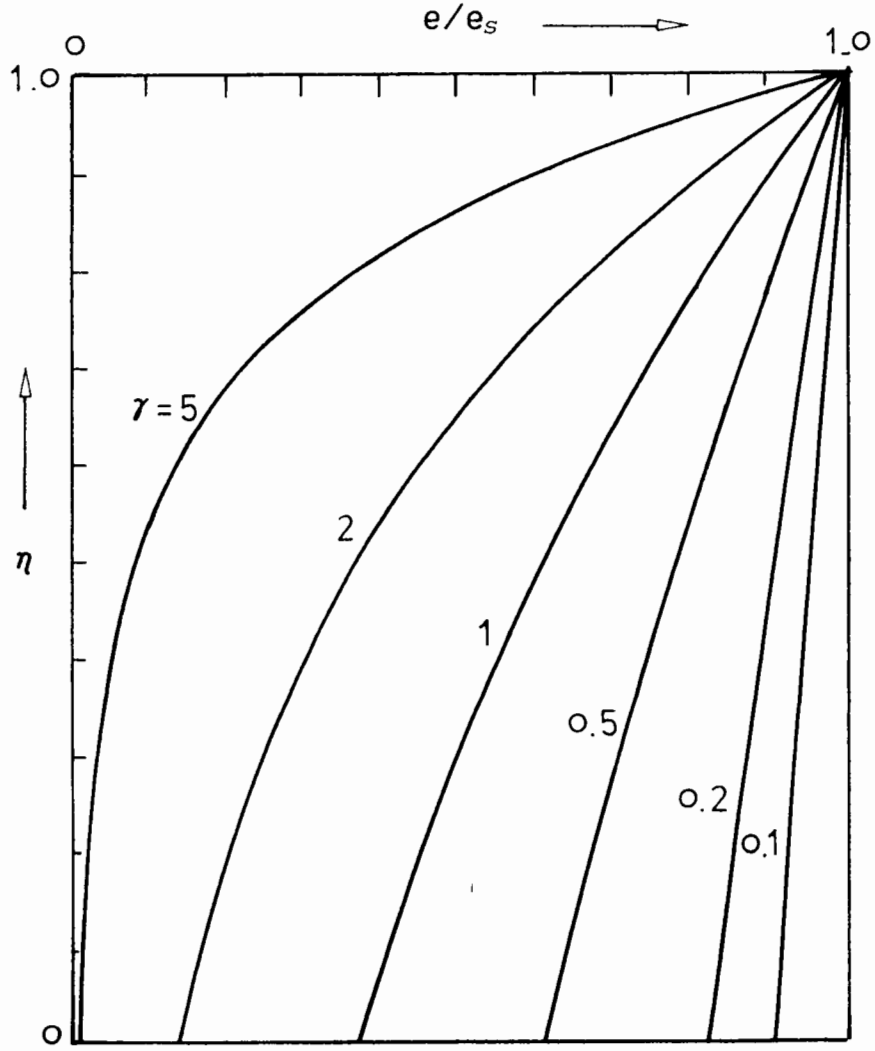

FIG.6.4 Distribution of void ratio in material coordinate in a normally consolidated stratum

2. MATHEMATICAL FORMULATION OF THE CONSOLIDATION OF THE NONLINEAR SOIL MODEL

The governing equation for the consolidation of the nonlinear model is,

$$\frac{\partial e}{\partial t} = C_F \frac{\partial^2 e}{\partial z^2} - \beta \frac{\partial e}{\partial z}, \quad 0 \leq z \leq z_o, \quad t \geq 0 \tag{6.16}$$

where both C_F and β reamin constant during consolidation throughout the soil. With the normalized material coordinate η :

$$\eta = \frac{z}{z_o} \tag{6.17}$$

and the time factor T :

$$T = \frac{C_F\, t}{z_o^2} \tag{6.18}$$

eq(6.16) becomes,

$$\frac{\partial e}{\partial T} = \frac{\partial^2 e}{\partial \eta^2} - \gamma \frac{\partial e}{\partial \eta}, \quad 0 \leq \eta \leq 1, \quad T \geq 0 \tag{6.19}$$

where γ is the stratum coefficient defined in eq(6.8).

There are two types of soil stratum that will be dealt with in this chapter :

(a) A normally consolidated stratum subjected to a surface loading.

The stratum is initially in a normally consolidated state with its void ratio distribution given by eq(6.7). Consolidation in this case is caused by a loading applied to the surface of the stratum. This loading is assumed to be fully effective within the stratum,

i.e. it causes an equal amount of stress increment to all parts of the stratum. The drainage boundary conditions are therefore given by :

in the surface : $$e(1,T) = e_s - \Delta e(1,T) \tag{6.20}$$

in the base : $$e(0,T) = e_b - \Delta e(1,T)\ exp(-\gamma) \tag{6.21}$$

where $\Delta e(1,T)$ is the void ratio change in the surface caused by the applied loading. In the undrained boundary where no excess pore water pressure gradient exists, the condition is given by :

$$\frac{\partial u}{\partial x} = 0 \tag{6.22}$$

where u is the excess pore water pressure induced by the applied loading and x is the space coordinate. This equation can be written in terms of the void ratio e and the normalized material coordinate η as :

$$\frac{\partial e}{\partial \eta} = \gamma e \tag{6.23}$$

(b) A dredged fill consolidated under its own weight.

In this case a dredged fill of an initially uniform density is considered. Consolidation is caused by the weight of the fill itself. Thus, the initial condition is :

$$e(\eta,0) = e_i \tag{6.24}$$

Since there is no loading other than its own weight acting on this stratum, the void ratio in the surface will remain in its initial state :

$$e(1,T) = e_i \tag{6.25}$$

If the stratum were undrelaid by a pervious base, the condition there is given by :

$$e(0,T) = e_i exp(-\gamma) \tag{6.26}$$

In the case of an impervious base the boundary condition is given by eq(6.23).

In both (a) and (b) it will be convenient to use a new variable q , the void ratio change, defined as :

$$q(\eta,T) = e(\eta,0) - e(\eta,T) \tag{6.27}$$

An obvious advantage of using this variable is that a simple initial condition is achieved :

$$q(\eta,0) = 0 \tag{6.28}$$

while the governing equation retains the same form :

$$\frac{\partial q}{\partial T} = \frac{\partial^2 q}{\partial \eta^2} - \gamma \frac{\partial q}{\partial \eta} \tag{6.29}$$

With this new variable the drainage boundary conditions become,

normally consolidated stratum :

$$q(1,T) = \Delta e(1,T) \tag{6.20)a}$$

$$q(0,T) = \Delta e(0,T)\ exp(-\gamma) \tag{6.21)a}$$

dredged fill :

$$q(1,T) = 0 \tag{6.25)a}$$

$$q(0,T) = e_i[\ 1 - exp(-\gamma)] \tag{6.26)a}$$

And the undrained boundary conditions are, respectively,

normally consolidated stratum $$\frac{\partial q}{\partial \eta} = \gamma q \qquad (6.23)a$$

dredged fill $$\frac{\partial q}{\partial \eta} = \gamma q - \gamma e_i \qquad (6.30)$$

A less obvious advantage of using this variable is that the settlement of a stratum during consolidation can be simply calculated by :

$$\text{settlement} = h(0) - h(T) = z_o \int_0^1 q(\eta,T)\,d\eta \qquad (6.31)$$

This is obtained since the thickness of the stratum at any time can be calculated from the transformation equation (6.12) as :

$$h(T) = z_o \int_0^1 [\,1 + e(\eta,T)\,]\,d\eta \qquad (6.32)$$

and the initial thickness of the stratum is,

$$h(0) = z_o \int_0^1 [\,1 + e(\eta,0)\,]\,d\eta \qquad (6.33)$$

and eq(6.31) is obtained by substracting eq(6.32) from eq(6.33).

For the purpose of analysis, it is advantageous to use the degree of settlement defined as :

$$S(T) = \frac{h(0) - h(T)}{h(0) - h(\infty)} \qquad (6.34)$$

where $h(\infty)$ is the thickness of the stratum when consolidation has completed. The degree of settlement is related to the void ratio change by :

$$S(T) = \frac{\int_0^1 q(\eta,T)\,d\eta}{\int_0^1 q(\eta,\infty)\,d\eta} \tag{6.35}$$

where $q(\eta,\infty)$ is the total void ratio change that has occured during the consolidation.

In the following sections the consolidation of the two different types of stratum will be considered. In both cases this will require solving the governing equation (6.29) with appropriate initial and boundary conditions, and this is accomplished by the Laplace transform method. The governing equation (6.29) has been known in other fields as the general diffusion, or the Plank-Fokker equation. This is often arised in the theory of stochastic processes , particularly in subjects such as the diffusion processes, Brownian motion and random walk. For a brief introduction to these see Feller (1966) Vol.1 Chapter 14, p311-337 and Vol.2, Chapter 10, p.321-336. Some solutions in the cases of a semi-infinite region and simple boundary conditions can be found in Cox and Miller (1965).

PART I THE CONSOLIDATION OF A NORMALLY CONSOLIDATED STRATUM UNDER A SURFACE LOADING

3. DEVELOPMENT OF SOLUTIONS CORRESPONDING TO A STEP LOADING

The Double Drainage Boundary

The governing equation is,

$$\frac{\partial q}{\partial T} = \frac{\partial^2 q}{\partial \eta^2} - \gamma \frac{\partial q}{\partial \eta} \quad , \quad 0 \leq \eta \leq 1 \quad , \quad T \geq 0 \qquad (6.29)$$

Initially the stratum is in equilibrium with its own weight and a surface loading and is described by the equation :

$$q(\eta, 0) = 0 \qquad (6.28)$$

At the instant $T=0$ an additional loading is applied to the surface which causes void ratio change in both the surface and the base of the stratum as :

$$q(0, T) = a \qquad (6.35)$$

$$q(1, T) = b \qquad (6.36)$$

where $a = b \exp(-\gamma)$ in this case.

(a) The formal solution

The Laplace transform $\bar{q}(\eta, p)$ to the required solution $q(\eta, T)$ is,

$$\bar{q}(\eta,p) = \int_0^\infty q(\eta,T)\, exp(-pT)dT \tag{6.37}$$

by which the governing equation becomes,

$$p\bar{q} = \frac{d^2\bar{q}}{d\,\eta^2} - \gamma\frac{d\bar{q}}{d\eta} \tag{6.38}$$

The solution to this is,

$$\bar{q} = A_1 exp(m_1\eta) + A_2 exp(m_2\eta) \quad , \quad \begin{matrix} m_1 \\ m_2 \end{matrix} = \frac{\gamma}{2} \pm \sqrt{\left(\frac{\gamma^2}{4}+p\right)} \tag{6.39}$$

and the constants A_1 , A_2 are determined from the boundary condition :

$$\bar{q}(0,p) = \frac{a}{p} \tag{6.40}$$

$$\bar{q}(1,p) = \frac{b}{p} \tag{6.41}$$

as :

$$A_1 = \frac{b - a\, exp(m_1)}{p[\, exp(m_2) - exp(m_1)\,]} \tag{6.42}$$

and

$$A_2 = \frac{a\, exp(m_2) - b}{p[\, exp(m_2) - exp(m_1)\,]} \tag{6.43}$$

Hence,

$$\bar{q}(\eta,p) = -a exp\left(\frac{\gamma}{2}\eta\right)\frac{sinh[(\eta-1)\sqrt{\left(\frac{\gamma^2}{4}+p\right)}]}{psinh\sqrt{\left(\frac{\gamma^2}{4}+p\right)}} + b exp\left[\frac{\gamma}{2}(\eta-1)\right]\frac{sinh[\eta\sqrt{\left(\frac{\gamma^2}{4}+p\right)}}{psinh\sqrt{\left(\frac{\gamma^2}{4}+p\right)}} \tag{6.44}$$

Using the standard transformation pair (Erdelyl 1954 p.259, pair (5.9.39)) :

$$\mathcal{L}^{-1}\left\{\frac{1}{p-iw}\,\frac{\sinh(x\sqrt{p})}{\sinh\sqrt{p}}\right\} = \frac{\sinh(x\sqrt{(iw)})}{\sinh\sqrt{(iw)}}\exp(iwT) + 2\pi\sum_n \frac{(-1)^n n\sin(n\pi x)}{n^2\pi^2+iw}\exp(-n^2\pi^2 T) \tag{6.45}$$

the inverse transformation to eq(6.44) is found to be :

$$q(\eta,T) = a\left\{\frac{1-\exp[\gamma(\eta-1)]}{1-\exp(-\gamma)} - 2\sum_n \frac{n\pi\sin(n\pi\eta)}{n^2\pi^2+\frac{\gamma^2}{4}}\exp\left[-\left(n^2\pi^2+\frac{\gamma^2}{4}\right)T+\frac{\gamma}{2}\eta\right]\right\} \tag{6.46}$$

$$+ b\left\{\frac{\exp(\gamma\eta)-1}{\exp(\gamma)-1} + 2\sum_n \frac{(-1)^n n\pi\sin(n\pi\eta)}{n^2\pi^2+\frac{\gamma^2}{4}}\exp\left[-\left(n^2\pi^2+\frac{\gamma^2}{4}\right)T+\frac{\gamma}{2}(\eta-1)\right]\right\}$$

which is the required solution. In the present case, appropriate values of a , b are substituted into the above equation to yield :

$$q(\eta,T) = b\left\{\exp[\gamma(\eta-1)] - 2\sum_n \left[1-(-1)^n\exp\left(\frac{\gamma}{2}\right)\right]\right. \frac{n\pi\sin(n\pi\eta)}{n^2\pi^2+\frac{\gamma^2}{4}}\left.\exp\left[-\left(n^2\pi^2+\frac{\gamma^2}{4}\right)T+\frac{\gamma}{2}\eta-\gamma\right]\right\} \tag{6.47}$$

where b is the void ratio change in the base of the stratum. A new variable, the local degree of consolidation, defined as :

$$f(\eta,T) = \frac{q(\eta,T)}{q(\eta,\infty)} \tag{6.48}$$

can be derived from the solution. The final equilibrium state in the present case is,

$$q(\eta,\infty) = b\exp[\gamma(\eta-1)] \tag{6.49}$$

Hence,

$$f(\eta,T) = 1 - 2\sum_n \left[1-(-1)^n\exp\left(\frac{\gamma}{2}\right)\right]\frac{n\pi\sin(n\pi\eta)}{n^2\pi^2+\frac{\gamma^2}{4}} \tag{6.50}$$

$$\exp\left[-\left(n^2\pi^2+\frac{\gamma^2}{4}\right)T-\frac{\gamma}{2}\eta\right]$$

The degree of settlement is found from eq(6.47),(6.49) as :

$$S(T) = 1 - \frac{2}{exp(\gamma)-1} \sum_n \{ [1-(-1)^n exp(\frac{\gamma}{2})] \frac{n\pi}{n^2\pi^2 + \frac{\gamma^2}{4}} \}^2 \qquad (6.51)$$

$$exp[-(n^2\pi^2 + \frac{\gamma^2}{4})T]$$

It can be seen that both the local degree of consolidation, eq(6.50) and the degree of settlement, eq(6.51) are strain - invariant, i.e. unaffected by the actual magnitude of the void ratio change.

Strain - invariant solutions have also been obtained in the thin layer and the linear theory discussed in the previous chapters. These results, and the solutions that will appear in later sections, suggest that this is a property associated with the assumption of a constant C_F .

The stratum coefficient γ has appeared in the solutions eq(6.50,51) , and different consolidation behaviour will therefore be expected in strata with different γ values. The limiting case when $\gamma \to 0$, which may be a result of either $z_o \to 0$,i.e. a very thin stratum, or $\rho_s \to \rho_f$, i.e. in cases where the weight of the soil is negligible, is therefore equivalent to the thin layer idealization. Since,

$$\lim_{\gamma \to 0} \frac{\gamma}{exp(\gamma) - 1} = 1 \qquad (6.52)$$

it follows that :

$$\lim_{\gamma \to 0} S(T) = 1 - \frac{8}{\pi^2} \sum_m \frac{1}{m^2} exp(-m^2\pi^2 T) \qquad (6.53)$$

$$m = 1,3,5,...$$

which, as can be expected, agrees with the thin layer solution.

(b) Approximate solutions

In practical computation it is sometimes desirable to have approximate solutions to the settlement behaviour in order to obtain numerical values easily. One possibility of achieving this is to consider seperately the early and later stages of consolidation, and the behaviour in the whole time span is approximated by matching the two solutions.

For the small time solution consider the Laplace transform of the degree of settlement :

$$S(p) = \frac{\int_0^1 q(\eta,p)d\eta}{\int_0^1 q(\eta,\infty)d\eta} \qquad (6.54)$$

where $S(p)$ is the Laplace transform of $S(T)$ and $q(\eta,p)$ has been given in eq(6.44). It follows that :

$$S(p) = \frac{\gamma}{exp(\gamma)-1}\left\{[1-exp(-\gamma)]\frac{\gamma}{2p^2} + [1+exp(\gamma)]\frac{\sqrt{(\frac{\gamma^2}{4}+p)}}{p^2 tanh\sqrt{(\frac{\gamma^2}{4}+p)}} - 2\frac{exp(\frac{\gamma}{2})\sqrt{(\frac{\gamma^2}{4}+p)}}{p^2 sinh\sqrt{(\frac{\gamma^2}{4}+p)}}\right\} \qquad (6.55)$$

As $p \to \infty$

$$tanh\sqrt{(\frac{\gamma^2}{4}+p)} \to 1$$

and $$sinh\sqrt{(\frac{\gamma^2}{4}+p)} \to \infty$$

Thus for small γ the third term in eq(6.55) can be omitted and the following approximation results :

$$S(p) \simeq \frac{\gamma}{exp(\gamma)-1}\left\{[1-exp(-\gamma)]\frac{\gamma}{2p^2} + [1+exp(\gamma)]\frac{\sqrt{(\frac{\gamma^2}{4}+p)}}{p^2}\right\} \qquad (6.56)$$

$p \to \infty$

The inverse transform of the second term in the above expression is obtained from the standard transformation pair (Erdelyi, 1954) as:

$$\mathcal{L}^{-1}\{\frac{\sqrt{(\frac{\gamma^2}{4}+p)}}{p^2}\} = \int_0^T \frac{exp(-\frac{\gamma^2}{4}t)}{\sqrt{(\pi t)}}\,dt + \frac{\gamma}{2}\int_0^T erf(\frac{\gamma}{2}\sqrt{t})dt \qquad (6.57)$$

The first integral is related to the incomplete Gamma function and can be expressed as (Lebedev 1965) as :

$$\int_0^T \frac{exp(-\frac{\gamma^2}{4}t)}{\sqrt{(\pi t)}}\,dt = \frac{2}{\gamma\sqrt{\pi}}\sum_k \frac{(-1)^k\,(\frac{\gamma^2}{4}T)^{\frac{1}{2}+k}}{k!\,(k+\frac{1}{2})} \qquad (6.58)$$

$$= 2\sqrt{(\frac{T}{\pi})}\,[\,1 - \frac{\gamma^2}{12}T + \cdots\cdots\,]$$

Neglecting the higher order terms as $T \to 0$ this becomes,

$$\int_0^T \frac{exp(-\frac{\gamma^2}{4}t)}{\sqrt{(\pi t)}}\,dt \simeq 2\sqrt{(\frac{T}{\pi})} - \frac{\gamma^2}{6\sqrt{\pi}}\sqrt{(T)^3} \qquad (6.59)$$

The second integral in eq(6.57) involves the error function in the integrand which can be approximated by $\gamma(\frac{t}{\pi})^{\frac{1}{2}}$ as $t \to 0$.
Thus,

$$\int_0^T erf(\frac{\gamma}{2}\sqrt{t})dt \simeq \int_0^T \gamma\sqrt{(\frac{t}{\pi})}\,dt = \frac{2}{3}\frac{\gamma T^2}{\sqrt{(\pi T)}} \qquad (6.60)$$

Therefore,

$$\mathcal{L}^{-1}\{\frac{\sqrt{(\frac{\gamma^2}{4}+p)}}{p^2}\} \simeq 2\sqrt{(\frac{T}{\pi})} + \frac{\gamma^2}{2\sqrt{\pi}}\sqrt{(T)^3} \qquad (6.61)$$

And finally,

$$S(T) \simeq \frac{\gamma}{exp(\gamma)-1}\{2[exp(\gamma)+1]\sqrt{(\frac{T}{\pi})} - \frac{\gamma}{2}[exp(\gamma)-1]T \qquad (6.62)$$

$$+ \frac{\gamma^2}{6}[exp(\gamma)+1]\sqrt{(\frac{T^3}{\pi})}\}$$

Stratum Coefficient	Time Factor	Degree of settlement x 10^4		
		Exact Solution	Small Time Approximation	Large Time Approximation
0.1	0.0001	0230	0226	-
	0.0025	1129	1129	-
	0.0100	2258	2258	2287
	0.0400	4514	4515	4514
	0.0900	6667	6772	6667
	0.1600	8330	9028	8330
	0.4900	9936	-	9936
1.0	0.0001	0248	0244	-
	0.0025	1209	1209	-
	0.0100	2394	2394	2430
	0.0400	4699	4700	4699
	0.0900	6831	6930	6831
	0.1600	8441	9097	8441
	0.4900	9945	-	9945
2.0	0.0001	0299	0294	-
	0.0025	1433	1435	-
	0.0100	2773	2773	2829
	0.0400	5204	5205	5204
	0.0900	7270	7356	7270
	0.1600	8729	9285	8729
	0.4900	9955	-	9955

TABLE 6.2 COMPARISON OF SMALL AND LARGE TIME APPROXIMATE SOLUTIONS WITH EXACT SOLUTION, NORMALLY CONSOLIDATED STRATUM, DOUBLE DRAIN

In the later stages of consolidation which associated with large time factor T, it is seen that the series in the formal solution eq(6.51) converges very fast as a result of the exponential term in the series. It can be expected therefore that using the first few terms in the series will result in an efficient approximation in this stage.

The small and large time approximate solutions are compared with the formal solution in Table 6.2, the first five terms of the series of eq(6.51) have been used for large time approximate solution in this case. The agreement is seen to be very good.

The Single Drainage Boundary

In situations where drainage is only allowed at one of the two boundaries of the stratum, the progress of consolidation will be retarded. In the theory of a linear soil model and the thin layer the actual location of this boundary, whether it is in the surface or the base, does not affect the settlement rate of the stratum. This is because identical void ratio changes occur at both boundaries. In the present theory, however, the void ratio changes in both boundaries will be different. Consequently, a difference in the settlement rate is expected for different locations of the drainage boundary. This will be confirmed in this section by the solutions developed for each case.

(a) Surface drain

The boundary conditions in this case are :

$$q(1,T) = \Delta e \tag{6.63}$$

$$\frac{\partial q}{\partial \eta}(0,T) = \gamma q(0,t) \tag{6.64}$$

Using the Laplace transform it is found that :

$$\bar{q}(\eta,p) = A_1 \exp(m_1\eta) + A_2 \exp(m_2\eta) \quad , \quad \begin{matrix} m_1 \\ m_2 \end{matrix} = \frac{\gamma}{2} \pm \sqrt{(\frac{\gamma^2}{4} + p)} \tag{6.65}$$

with,

$$A_1 = \frac{B\ \Delta e}{p[\ \exp(m_2) - B\exp(m_1)\ ]} \tag{6.66}$$

$$A_2 = \frac{\Delta e}{p[\ \exp(m_2) - B\exp(m_1)\ ]} \tag{6.67}$$

and $$B = \frac{m_2 - \gamma}{m_1 - \gamma} \tag{6.68}$$

The Laplace transform of the local degree of consolidation is given by :

$$\bar{f}(\eta,p) = \frac{\bar{q}(\eta,p)}{q(\eta,\infty)} \tag{6.69}$$

After some manipulation, this is found to be :

$$\bar{f}(\eta,p) = \frac{\exp[-\frac{\gamma}{2}(\eta-1)]\ \{\sqrt{(\frac{\gamma^2}{4}+p)}\ \cosh[\eta\sqrt{(\frac{\gamma^2}{4}+p)}] + \frac{\gamma}{2}\sinh[\eta\sqrt{(\frac{\gamma^2}{4}+p)}]\}}{p\ \{\sqrt{(\frac{\gamma^2}{4}+p)}\cosh[\sqrt{(\frac{\gamma^2}{4}+p)}] + \frac{\gamma}{2}\sinh[\sqrt{(\frac{\gamma^2}{4}+p)}]\}} \tag{6.70}$$

The inverse transformation is evaluated in Appendix A from which it is found that :

$$f(\eta,T) = 1 - 2\sum_n \frac{(-1)^n[\beta_n\cos(\beta_n\eta) + \frac{\gamma}{2}\sin(\beta_n\eta)]}{\sqrt{(\beta_n^2+\frac{\gamma^2}{4})}\ [\beta_n+\frac{\gamma^2}{4\beta_n}+\frac{\gamma}{2\beta_n}]}\ \exp[-(\beta_n^2+\frac{\gamma^2}{4})T - \frac{\gamma}{2}(\eta-1)] \tag{6.71}$$

where the β_ns are the zeroes of

$$\beta_n\cos\beta_n + \frac{\gamma}{2}\sin\beta_n \tag{6.72}$$

The expression for the void ratio change q can be obtained by :

$$q(\eta,T) = \Delta e\ \exp[\gamma(\eta-1)]\ f(\eta,T) \tag{6.73}$$

The degree of settlement is found to be :

$$S(T) = 1 - \frac{2\gamma}{1-exp(-\gamma)} \sum_n \frac{exp[-(\beta_n^2 + \frac{\gamma^2}{4})T]}{(\beta_n^2 + \frac{\gamma^2}{4})(1 + \frac{\gamma^2}{4\beta_n^2} + \frac{\gamma}{2\beta_n^2})} \qquad (6.74)$$

The small time approximation to this can be obtained by considering the behaviour of the Laplace transform, which is :

$$S(p) = \frac{\gamma}{p[1-exp(-\gamma)]} \frac{1}{\sqrt{(\frac{\gamma^2}{4} + p)}coth[\sqrt{(\frac{\gamma^2}{4}+p)} + \frac{\gamma}{2}}} \qquad (6.75)$$

As $p \to \infty$, $coth\sqrt{(\frac{\gamma^2}{4} + p)} \to 1$

it follows that :

$$S(p) \simeq \frac{\gamma}{1-exp(-\gamma)} \frac{1}{p[\sqrt{(\frac{\gamma^2}{4} + p)} + \frac{\gamma}{2}]} \qquad p \to \infty \qquad (6.76)$$

Since,

$$\mathcal{L}^{-1}\{\frac{1}{p[\sqrt{(\frac{\gamma^2}{4} + p)} + \frac{\gamma}{2}]}\} = \mathcal{L}^{-1}\{\frac{\sqrt{(\frac{\gamma^2}{4} + p)}}{p^2}\} - \frac{\gamma}{2}T \qquad (6.77)$$

It follows from eq(6.61) that,

$$S(T) \simeq \frac{\gamma}{1-exp(-\gamma)} [\, 2\sqrt{(\frac{T}{\pi})} - \frac{\gamma}{2}T + \frac{\gamma^2}{6\sqrt{\pi}}\sqrt{T^3}\,] \qquad T \to 0 \qquad (6.78)$$

In large time an approximate solution can again be obtained

Time Factor	Degree of Settlement x 10^4		
	Exact Solution	Small Time Approximation	Large Time Approximation
0.0001	0176	0178	-
0.0025	0872	0873	-
0.0100	1707	1707	1811
0.0400	3266	3266	3268
0.0900	4683	4683	4683
0.1600	5968	5970	5968
0.2500	7108	7133	7108
0.4900	8790	9130	8790
1.0000	9809	-	9809

TABLE 6.3 COMPARISON OF SMALL AND LARGE TIME APPROXIMATIONS WITH EXACT SOLUTION, NORMALLY CONSOLIDATED STRATUM, SURFACE DRAIN.

by taking the first few terms of the series solution, eq(6.74). A comparison of the small and large time approximation (up to the third term in the series) with the exact solotion is shown in Table 6.3 for a typical value of $\gamma=1$. The agreement is seen to be very good.

(b) Base drain

The boundary conditions for this case are :

$$q(0,T) = \Delta e \exp(-\gamma) \tag{6.79}$$

$$\frac{\partial q}{\partial \eta}(1,T) = \gamma q(1,T) \tag{6.80}$$

Using the Laplace transform it is found that :

$$\bar{q}(\eta,p) = \frac{\Delta e\ exp(\frac{\gamma}{2}\eta - \gamma)}{p} \left[\sqrt{(\frac{\gamma^2}{4} + p)}\cosh[(1-\eta)\sqrt{(\frac{\gamma^2}{4}+p)}] - \frac{\gamma}{2}\right.$$

$$\left.\sinh[(1-\eta)\sqrt{(\frac{\gamma^2}{4}+p)}]\right] / \left[\sqrt{(\frac{\gamma^2}{4}+p)}\cosh\sqrt{(\frac{\gamma^2}{4}+p)} - \frac{\gamma}{2}\sinh\sqrt{(\frac{\gamma^2}{4}+p)}\right] \quad (6.81)$$

and,

$$\bar{f}(\eta,p) = \frac{exp(-\frac{\gamma}{2}\eta)}{p} \frac{\sqrt{(\frac{\gamma^2}{4}+p)}\cosh[(1-\eta)\sqrt{(\frac{\gamma^2}{4}+p)}] - \frac{\gamma}{2}\sinh[(1-\eta)\sqrt{(\frac{\gamma^2}{4}+p)}]}{\sqrt{(\frac{\gamma^2}{4}+p)}\cosh\sqrt{(\frac{\gamma^2}{4}+p)} - \frac{\gamma}{2}\sinh\sqrt{(\frac{\gamma^2}{4}+p)}} \quad (6.82)$$

The inverse transform of this is also evaluated in Appendix A of this chapter, from which it is found that :

$$f(\eta,T) = 1 - 2 \sum_n \frac{(-1)^n[\alpha_n\cos\alpha_n(1-\eta) - \frac{\gamma}{2}\sin\alpha_n(1-\eta)]}{(\alpha_n + \frac{\gamma^2}{4})(\alpha_n^2 + \frac{\gamma^2}{4\alpha_n} - \frac{\gamma}{2\alpha_n})} exp[-(\alpha_n^2 + \frac{\gamma^2}{4})T - \frac{\gamma}{2}\eta] \quad (6.83)$$

and the degree of settlement is :

$$S(T) = 1 - \frac{2\gamma}{exp(\gamma) - 1} \sum_n \frac{exp[-(\alpha_n^2 + \frac{\gamma^2}{4})T]}{(\alpha_n^2 + \frac{\gamma^2}{4})(1 + \frac{\gamma^2}{4\alpha_n^2} - \frac{\gamma}{2\alpha_n^2})} \quad (6.84)$$

where the α_ns are the zeroes of

$$\alpha_n\cos\alpha_n - \frac{\gamma}{2}\sin\alpha_n \quad (6.85)$$

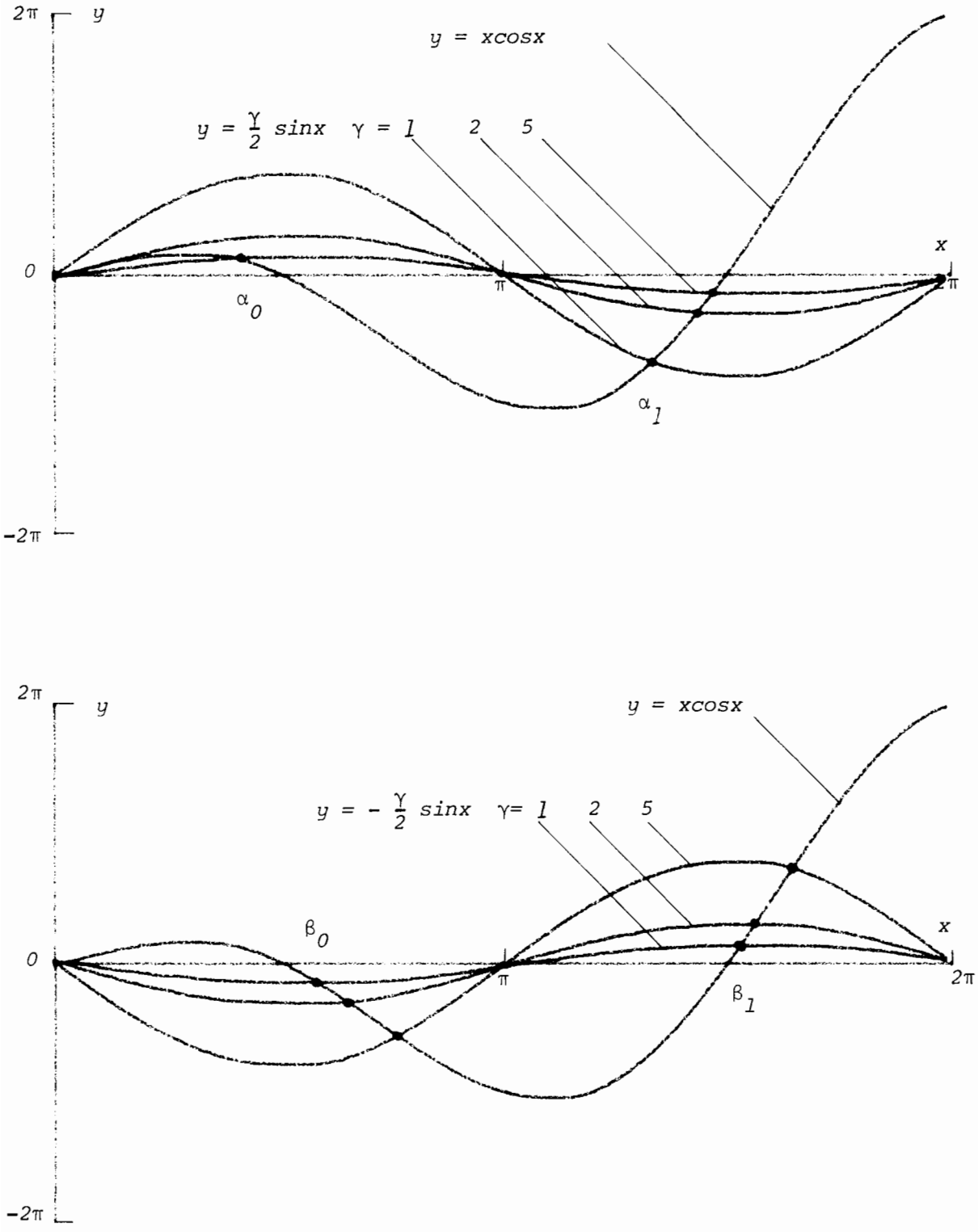

FIG.6.5 Characteristic roots α_n *of eq(6.85), (top), and* β_n *of eq(6.72), (above).*

The locations of this are shown in Fig.6.5, which also shows the locations of the β_n of the surface drain case. These can be calculated by the Newton's method. It should be noted that for large γ the determination of the first root α_0 becomes extremely difficult, and a practical upper limit is about $\gamma=2$ before this difficulty becomes serious.

The small time approximation to the degree of settlement is obtained by considering its Laplace transform :

$$\bar{S}(p) = \frac{\gamma}{p[\exp(\gamma)-1]} \frac{1}{\sqrt{(\frac{\gamma^2}{4}+p)}\coth\sqrt{(\frac{\gamma^2}{4}+p)} - \frac{\gamma}{2}} \qquad (6.86)$$

As $p \to \infty$, $\coth\sqrt{(\frac{\gamma^2}{4}+p)} \to 1$

it follows that :

$$S(p) \simeq \frac{\gamma}{\exp(\gamma)-1} \frac{1}{p[\sqrt{(\frac{\gamma^2}{4}+p)} - \frac{\gamma}{2}]} \qquad (6.87)$$

The inverse transform of this is, approximately,

$$S(T) \simeq \frac{\gamma}{\exp(\gamma)-1} [2\sqrt{(\frac{T}{\pi})} + \frac{\gamma}{2}T - \frac{\gamma^2}{6}\frac{1}{\sqrt{\pi}}\sqrt{T^3}] \qquad (6.88)$$

It is worth noting that by adding this to the expression for the surface drain case :

$$S_{base} + S_{surface} \simeq \frac{\gamma}{\exp(\gamma)-1}[2(1+\exp(\gamma))\sqrt{(\frac{T}{\pi})} - \frac{\gamma}{2}(\exp(\gamma)-1)T + \frac{\gamma^2}{6}(1+\exp(\gamma))\frac{1}{\sqrt{\pi}}\sqrt{T^3}] \qquad (6.89)$$

Time Factor	Degree of Settlement x 10^4		
	Exact Solution	Small Time Approximation	Large Time Approximation
0.0001	0066	0066	-
0.0025	0336	0336	0482
0.0100	0686	0686	0726
0.0400	1434	1434	1435
0.0900	2247	2247	2247
0.1600	3126	3127	3126
0.2500	4066	4079	4066
0.4900	5968	6210	5968
1.0000	8225	-	8225

TABLE 6.4 COMPARISON OF SMALL AND LARGE TIME APPROXIMATIONS WITH THE EXACT SOLUTION, NORMALLY CONSOLIDATED STRATUM, BASE DRAIN

resulting in the expression for the double drainage case. In other words, during the early stages the consolidation occurs mostly near the drained boundaries. Thus summing the two cases of single drainage in the early stages is equivalent to the double drainage case.

In later stages the solution can be approximated by using the first three terms of the series solution, eq(6.84). Table 6.4 shows the comparison of the small and large time approximations with the exact solution for a typical value of $\gamma=1$. The agreement is again very good.

4. DISCUSSION OF SOLUTIONS

The solutions of the consolidation of a normally consolidated stratum under a step loading have been developed in the previous section. In this section particular attention will be paid to the effect of the stratum coefficient γ on the consolidation behaviour of such case.

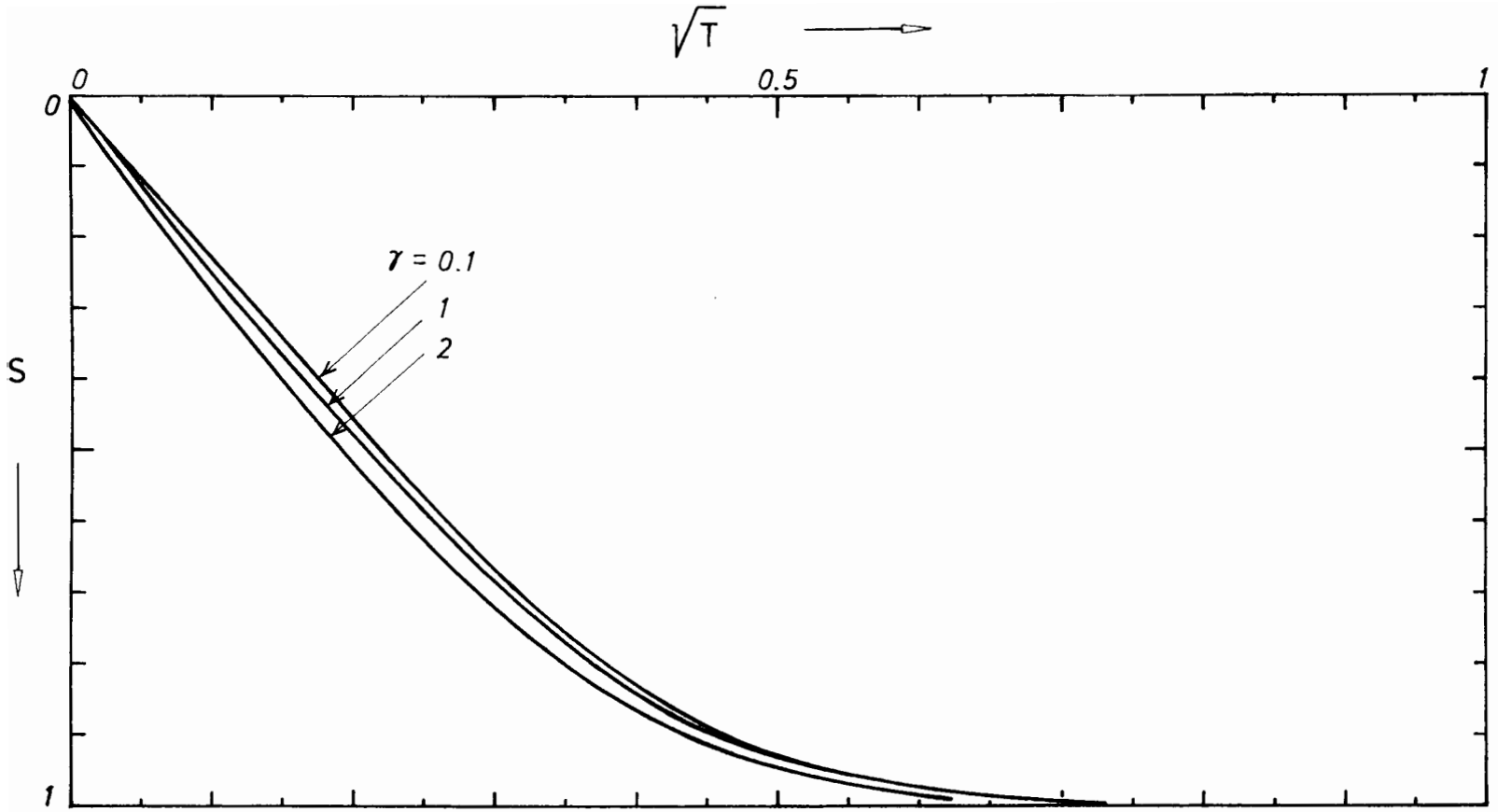

FIG 6.6 The degree of settlement versus the square root of time factor for the consolidation of a normally consolidated stratum under a step loading with double drainage.

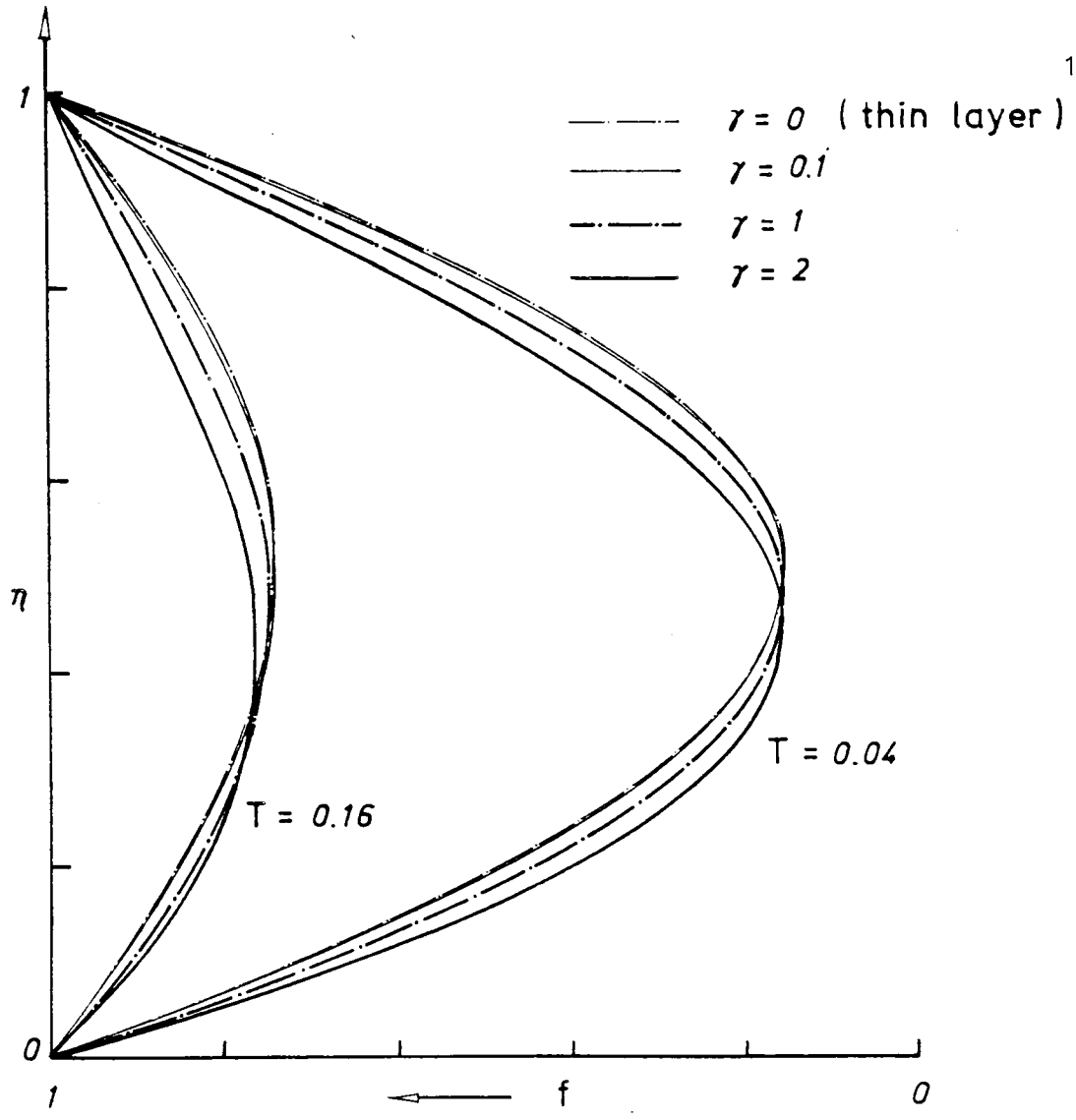

FIG.6.7 Variations of the local degree of consolidation.

The Double Drainage Boundary

The progress of the degree of settlement with the square root of time factor is shown in Fig.6.6. It is seen that a fast consolidation occurs with increasing values of γ. The term fast is used here with respect to the time factor, and does not imply a similar sense in real time. It is found that within the range of γ considered, the use of the thin layer solution by Gibson et. al. (1967) gives an approximation with an error of the order of a few percent.

The variation of the local degree of consolidation in the stratum at different time factors is shown in Fig.6.7 for different values of γ. Also shown in this figure is that of the thin layer solution, in

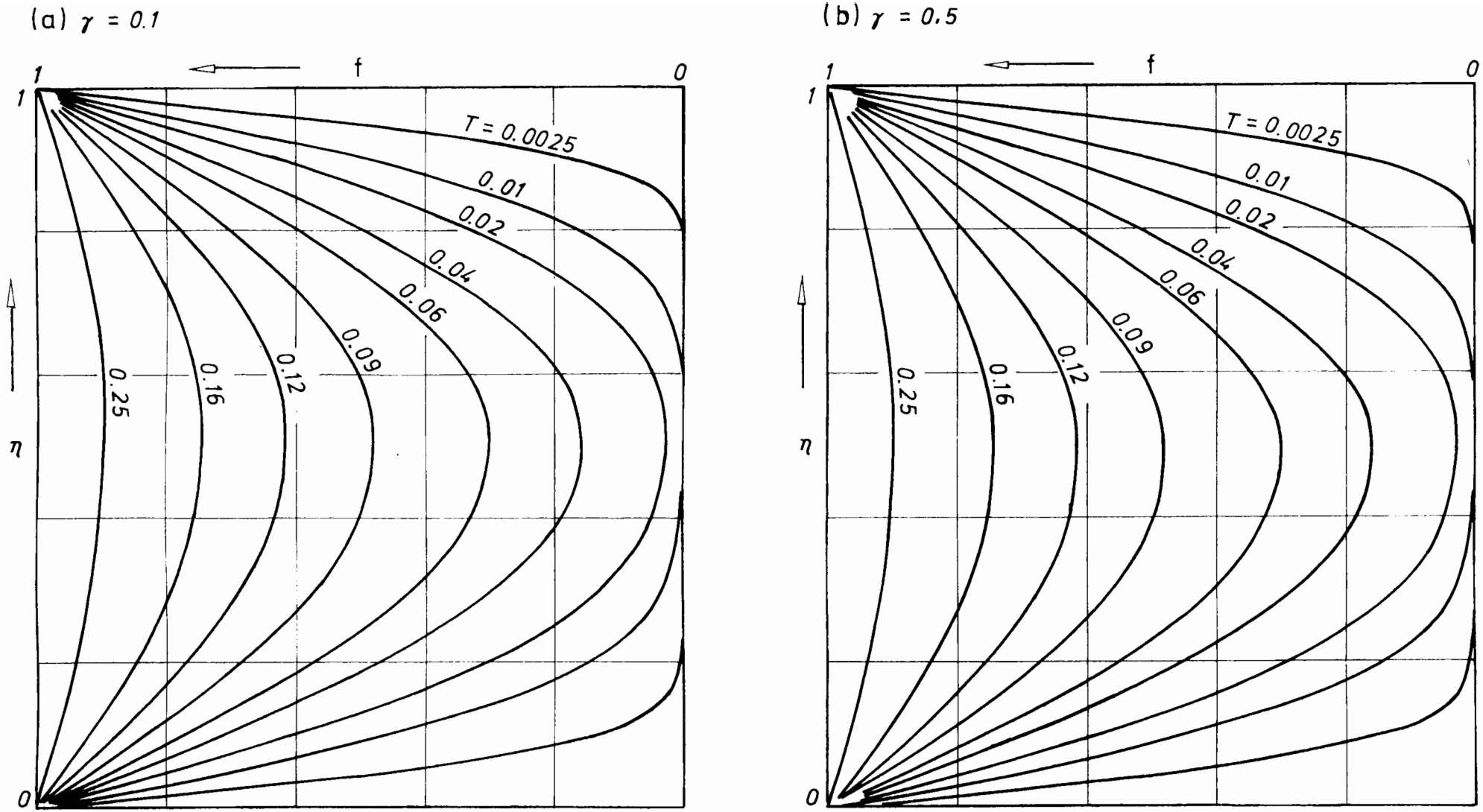

FIG. 6.8 Isochrones of the local degree of consolidation in a normally consolidated stratum under a step loading

(c) $\gamma = 1$

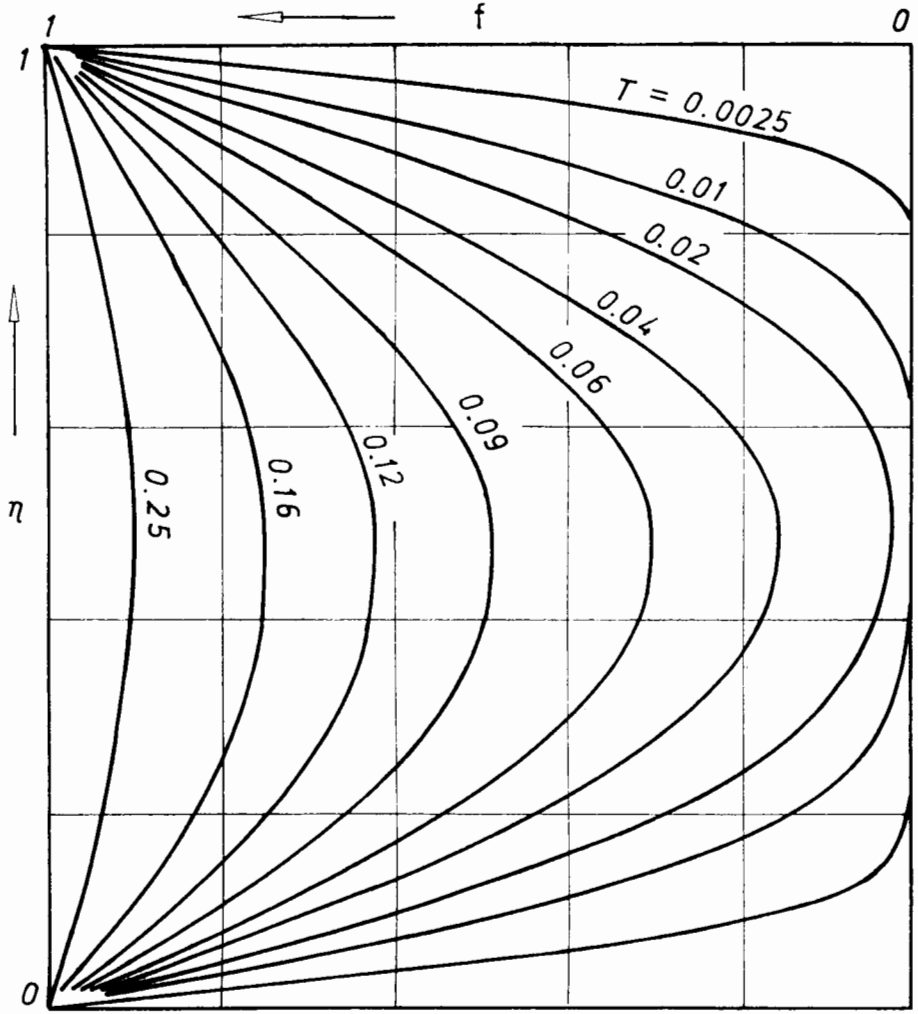

(d) $\gamma = 2$

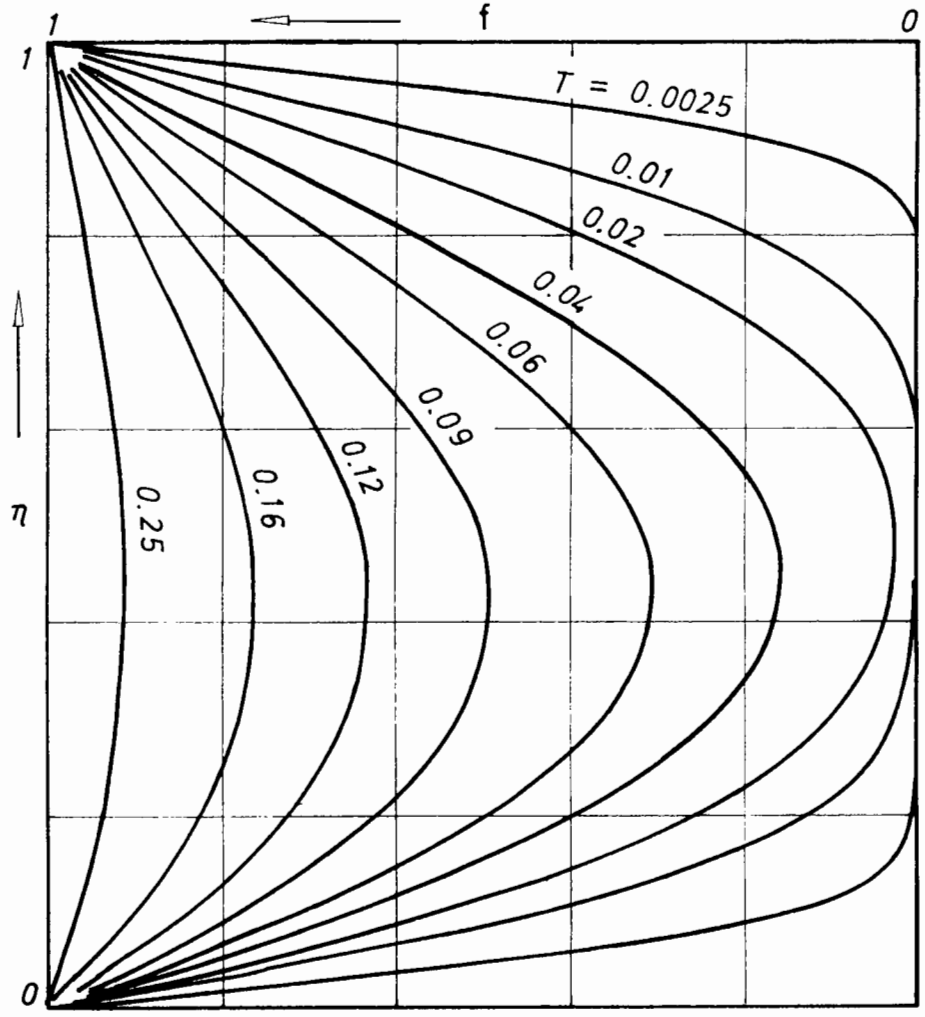

FIG. 6.8 (continued)

which the isochrones are symmetric to the mid-plane ($\eta = 0.5$) as a well known result. Such symmetry, however, is not found in the present solution as it can be seen that the isochrones are skewed with the peak below the mid-layer. The effect is more pronounced with larger γ . It can also be seen that the upper part of the stratum is better consolidated than predicted by the thin layer idealization (i.e. in the upper part the isochrones stay to the left of that of the thin layer) , while in the lower part the consolidation is less than that of the thin layer. It can be noticed that the no-flow-planes (i.e. the plane within the stratum with no excess pore pressure gradient, which can be seen in the figure as the peak in the isochrone) are located below the mid-layer, and move downwards as consolidation proceeds. In the thin layer this no-flow-plane is fixed to the mid-layer throughout the consolidation. Detailed drawings of the isochrones for each γ are presented in Fig.6.8 from which further evidences to support the above observations can be found.

The Single Drainage Boundary

Fig.6.9 shows the progress of the degree of settlement with the square root of the time factor for both surface and base drain cases. In the surface drain the trend is similar to the double drainage case in that faster consolidation is achieved with larger γ . However, the opposite is observed in the base drain case where larger γ will produce a slower consolidation. The thin layer solution is also included in this figure where there is only one solution for both surface and base drain cases. The difference between this and the present solution is greater than the double drainage case. It can be seen that the consolidation with base drain is always slower than the thin layer, while the surface drain will always be faster. This can be linked to the observation made in the isochrones of the double drainage case where the upper part of the stratum always consolidates faster and the lower part is always slower than the thin layer. The difference in the consolidation rate is probably a result of the different magnitudes of the void ratio changes required and the differences in permeability in each boundary.

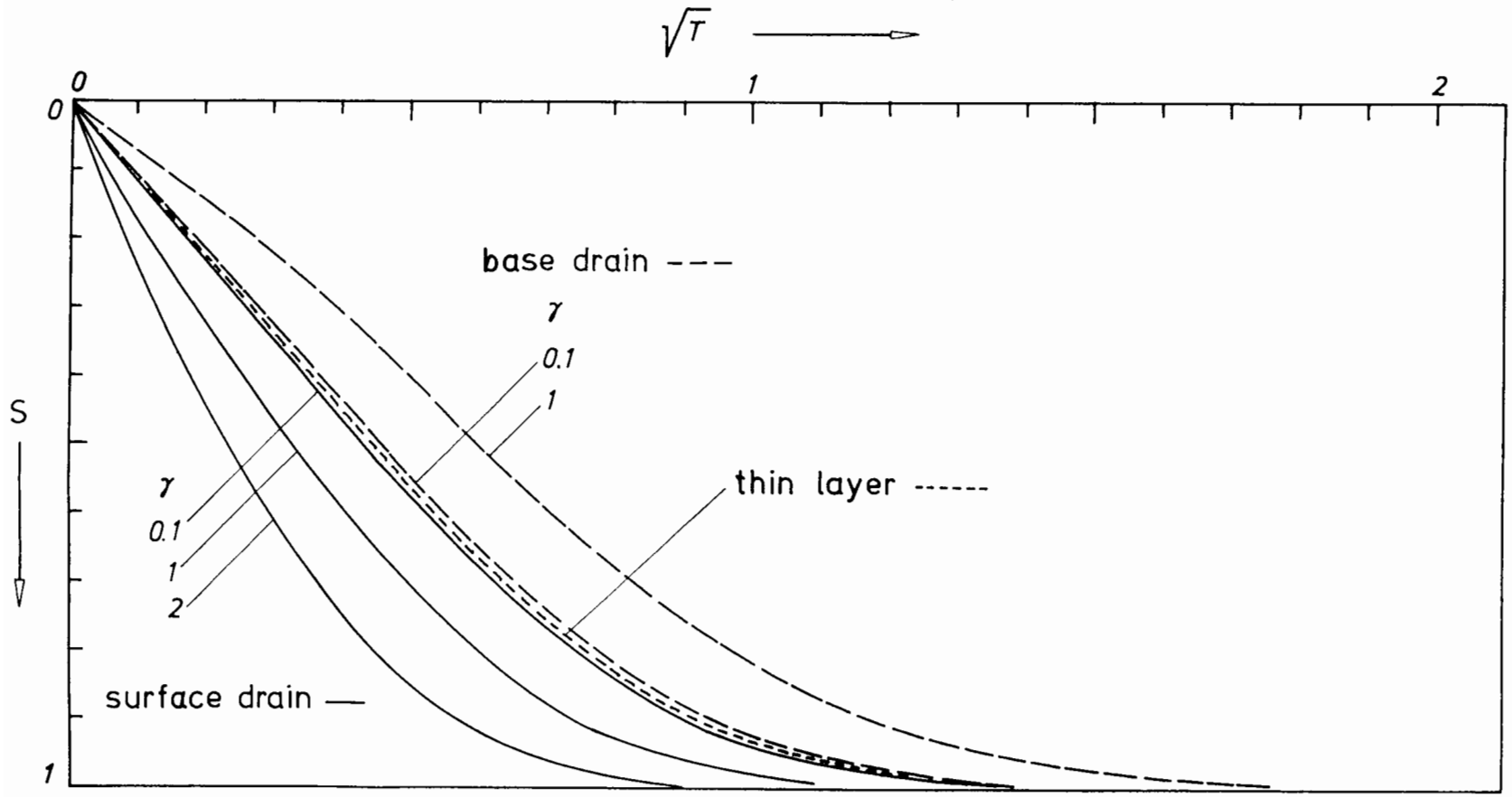

FIG.6.9 The degree of settlement versus the square root of the time factor for a normally consolidated stratum under a step loading with single drainage boundary.

The isochrones of the local degree of consolidation for each case are shown in Fig.6.10 for $\gamma = 0.1, 1$. The thin layer solution has also been included in this figure as broken lines for comparison. It is seen that the difference between this and the present solution is larger than in the double drainage case.

The calculation of the solution in the base drain case has been found difficult for large γ because of the elimination of the first characteristic root of eq(6.85) mentioned before. This causes the consolidation to be extremely slow, and an explanation is that in such situations the void ratio change in the base triggered by the surface loading is too small to initiate the consolidation of the whole stratum. This problem is largely theoretical as in practice not only does a perfect impervious surface not exist but also it is always possible to improve the surface drainage condition to accelerate its consolidation.

It is therefore concluded that in the consolidation of a normally consolidated stratum under a step loading both the consolidation rate and the variation of the local consolidation state will depend to a certain extent on the stratum coefficient γ. In most cases it is seen that the stratum will consolidate faster than predicted by the thin layer or the classical Terzaghi theory. And greater error will result when these two theories are applied to a thick, soft stratum which is associated with larger γ. In particular, the present theory predicts entirely different consolidation behaviour in the case of a single drain (either base or surface) from that predicted by the thin layer or Terzaghi theory. The very slow consolidation rate of the base drain case in comparison to the surface drain case indicates the importance of provisions for a good surface drainage in engineering practice for an earlier consolidation to be achieved.

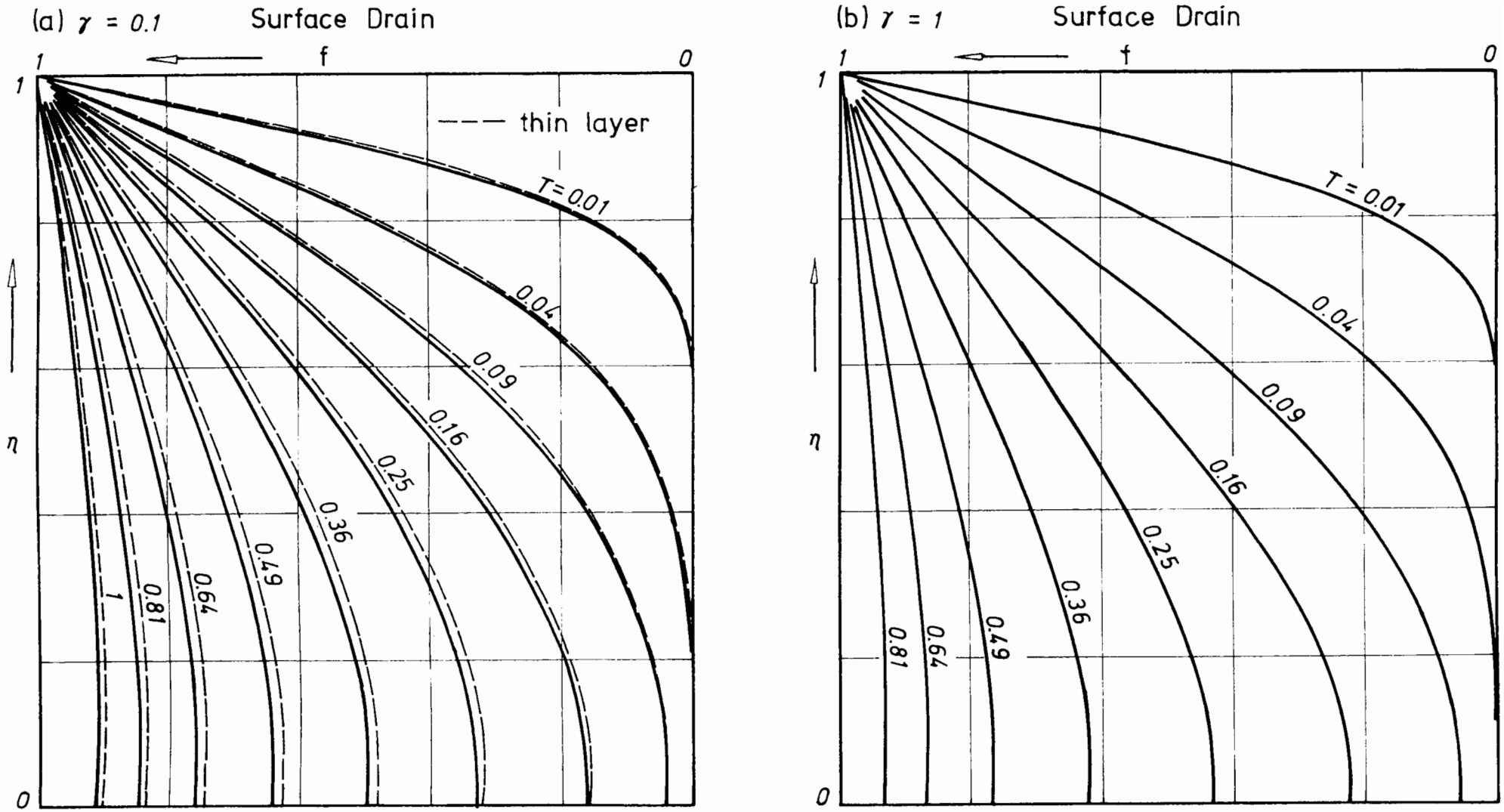

FIG. 6.10 Isochrones of local degree of consolidation in a normally consolidated stratum under a step loading

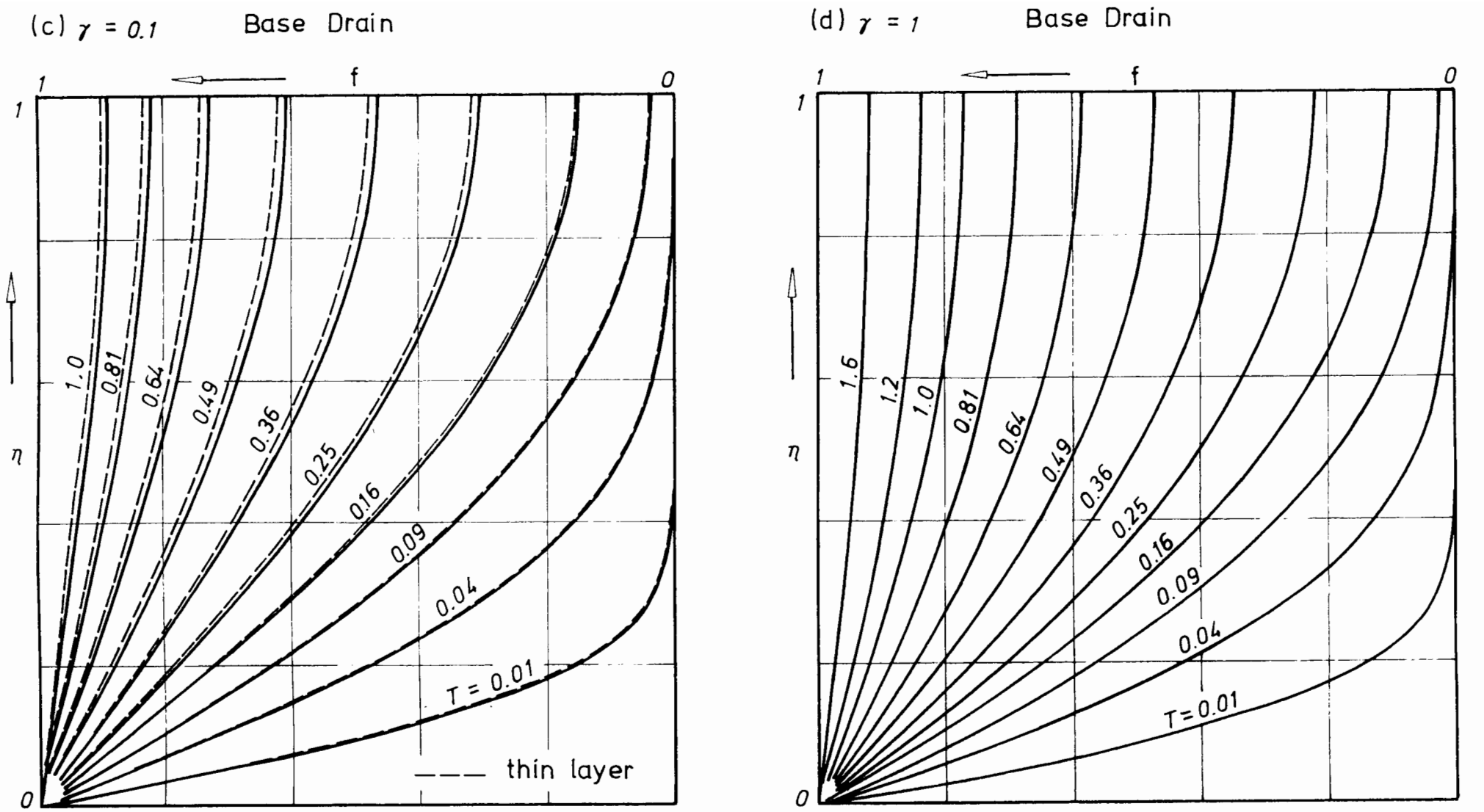

FIG.6.10 Isochrones of the local degree of consolidation in a normally consolidated stratum under a step loading.

(continued)

5. CONSOLIDATION WITH A TIME DEPENDENT LOADING

In practice the actual loading that a soil stratum experiences will vary with time, and the variation is usually so complicated that some degree of idealization and approximation must be applied. The step loading just considered is a highly idealized one, and only in rare circumstances can a real loading be approximated by this. When the variation of the surface loading has been estimated or specified, two approaches can be used :

(1) Approximate the loading history by a simple function to which a solution can be obtained.

(2) Break the loading history into steps (staircase). Within each step the consolidation is caused by a step loading with an initial condition determined by the previous stage and a solution can be obtained.

These two approaches will be treated seperately in this section. The general solution corresponding to each case is developed first. These solutions are then applied to the very important case of a linear ramp loading at the end of this section.

General Solutions

The governing equation of consolidation in the present theory uses void ratio as the dependent variable. However, in common engineering practice it is the stress boundary condition, i.e. the variation of surface loading with time, that is specified. For the purpose of analysis it is necessary to convert this stress boundary condition into a strain boundary condition by the stress-strain relationship. In the present case, once the loading function $P(t)$ is specified the corresponding void ratio function $b(t)$ in the base (assuming free drainage) is then :

$$b(t) = e_b \exp[-\frac{\alpha}{C_F} P(t)] \tag{6.90}$$

This equation is obtained from the stress-strain equation of the nonlinear model, eq(6.3). A similar expression can also be obtained for the void ratio in the surface.

It is seen from eq(6.90) that, a simple loading function may not result in a simple boundary condition. This point should be borne in mind when selecting an approximation to the actual loading history in practice.

(a) The double drainage boundary

The governing equation is,

$$\frac{\partial q}{\partial T} = \frac{\partial^2 q}{\partial \eta^2} - \gamma \frac{\partial q}{\partial \eta} \qquad 0 \leq \eta \leq 1 \ , \quad T \geq 0 \qquad (6.29)$$

where η is the normalized material coordinate and T is the time factor.

The initial and boundary conditions are :

$$q(\eta,0) = 0 \qquad (6.28)$$

$$q(0,T) = a(T) = e_b - b(T) \qquad (6.91)$$

$$q(1,T) = a(T)\exp(\gamma) \qquad (6.92)$$

Applying the Laplace transform to the equation yields :

$$\bar{q}(\eta,p) = \bar{a}(p)\exp\left[\frac{\gamma}{2}(\eta+1)\right] \frac{\sinh\left[\eta\sqrt{\left(\frac{\gamma^2}{4}+p\right)}\right]}{\sinh\sqrt{\left(\frac{\gamma^2}{4}+p\right)}}$$

$$- \bar{a}(p)\exp\left(\frac{\gamma}{2}\eta\right) \frac{\sinh\left[(\eta-1)\sqrt{\left(\frac{\gamma^2}{4}+p\right)}\right]}{\sinh\sqrt{\left(\frac{\gamma^2}{4}+p\right)}} \qquad (6.93)$$

where $\bar{q}$ and $\bar{a}$ are respectively the Laplace transform of q and a .
The inverse transform is aided by a standard pair (Erdelyi 1954) and the convolution thoerem and it is found that :

$$q(\eta,T) = 2 \sum_{1}^{\infty} n\pi \left[1-(-1)^n exp\left(\frac{\gamma}{2}\right)\right] sin(n\pi\eta) \; exp\left[-\left(n^2\pi^2 + \frac{\gamma^2}{4}\right)T + \frac{\gamma}{2}\eta\right]$$

$$\int_0^T a(\tau) exp\left[\left(n^2\pi^2 + \frac{\gamma^2}{4}\right)\tau\right] d\tau \qquad (6.94)$$

It is possible to define the degree of settlement from the final equilibrium condition $q(\eta,\infty)$:

$$q(\eta,\infty) = a(\infty) exp(\gamma\eta) \qquad (6.95)$$

where $a(\infty)$ is the final void ratio change in the base.

Hence,

$$S(T) = \frac{\int_0^1 q(\eta,T)d\eta}{\int_0^1 q(\eta,\infty)d\eta} = \frac{\gamma}{a(\infty)[exp(\gamma)-1]} \int_0^1 q(\eta,T)d\eta \qquad (6.96)$$

In the present case,

$$S(T) = \frac{2\gamma}{exp(\gamma)-1} \sum_{1}^{\infty} \frac{n^2\pi^2}{n^2\pi^2 + \frac{\gamma^2}{4}} \left[1-(-1)^n exp\left(\frac{\gamma}{2}\right)\right]^2 exp\left[-\left(n^2\pi^2 + \frac{\gamma^2}{4}\right)T\right]$$

$$\int_0^T \frac{a(\tau)}{a(\infty)} \; exp\left[\left(n^2\pi^2 + \frac{\gamma^2}{4}\right)\tau\right]d\tau \qquad (6.97)$$

(b) Surface drain

In this case the undrained boundary condition is the same as the step loading case, see eq(6.64). The boundary condition in the surface is given by eq(6.92). Applying the Laplace transform and the transformed solution is found to be :

$$\bar{q}(\eta,p) = \bar{a}(p)\exp\left[\frac{\gamma}{2}(\eta+1)\right]\frac{\sqrt{\left(\frac{\gamma^2}{4}+p\right)}\cosh\left[\eta\sqrt{\left(\frac{\gamma^2}{4}+p\right)}\right] + \frac{\gamma}{2}\sinh\left[\eta\sqrt{\left(\frac{\gamma^2}{4}+p\right)}\right]}{\sqrt{\left(\frac{\gamma^2}{4}+p\right)}\cosh\sqrt{\left(\frac{\gamma^2}{4}+p\right)} + \frac{\gamma}{2}\sinh\sqrt{\left(\frac{\gamma^2}{4}+p\right)}} \tag{6.98}$$

The inverse transform of part of this expression can be obtained using the result of the Appendix A as :

$$\mathcal{L}^{-1}\left\{\frac{\sqrt{\left(\frac{\gamma^2}{4}+p\right)}\cosh\left[\eta\sqrt{\left(\frac{\gamma^2}{4}+p\right)}\right] + \frac{\gamma}{2}\sinh\left[\eta\sqrt{\left(\frac{\gamma^2}{4}+p\right)}\right]}{\sqrt{\left(\frac{\gamma^2}{4}+p\right)}\cosh\sqrt{\left(\frac{\gamma^2}{4}+p\right)} + \frac{\gamma}{2}\sinh\sqrt{\left(\frac{\gamma^2}{4}+p\right)}}\right\}$$

$$= \frac{d}{dT}\quad\mathcal{L}^{-1}\left\{\frac{1}{p}\,\frac{\sqrt{\left(\frac{\gamma^2}{4}+p\right)}\cosh\left[\eta\sqrt{\left(\frac{\gamma^2}{4}+p\right)}\right] + \frac{\gamma}{2}\sinh\left[\eta\sqrt{\left(\frac{\gamma^2}{4}+p\right)}\right]}{\sqrt{\left(\frac{\gamma^2}{4}+p\right)}\cosh\sqrt{\left(\frac{\gamma^2}{4}+p\right)} + \frac{\gamma}{2}\sinh\sqrt{\left(\frac{\gamma^2}{4}+p\right)}}\right\}$$

$$= 2\sum_n \frac{(-1)^n\sqrt{\left(\beta_n^2+\frac{\gamma^2}{4}\right)}\left[\beta_n\cos\beta_n\eta + \frac{\gamma}{2}\sin\beta_n\eta\right]}{\beta_n + \frac{\gamma^2}{4\beta_n} + \frac{\gamma}{2\beta_n}}\exp\left[-\left(\beta_n^2+\frac{\gamma^2}{4}\right)T\right] \tag{6.99}$$

Therefore, from the convolution theorem,

$$q(\eta,T) = 2 \sum_n \frac{(-1)^n \sqrt{(\beta_n^2 + \frac{\gamma^2}{4})}\ [\ \beta_n \cos \beta_n\eta + \frac{\gamma}{2} \sin \beta_n\eta\ ]}{\beta_n + \frac{\gamma^2}{4\beta_n} + \frac{\gamma}{2\beta_n}} \exp[-(\beta_n^2 + \frac{\gamma^2}{4})T]$$

$$\int_0^T a(\tau)\exp[(\beta_n^2 + \frac{\gamma^2}{4})\tau]d\tau \qquad (6.100)$$

where β_n has the same meaning as in the step loading case, see eq(6.72).

From this, after some manipulation, follows the degree of settlement :

$$S(T) = \frac{2\gamma}{1-\exp(-\gamma)} \sum_n \frac{\beta_n \exp[-(\beta_n^2 + \frac{\gamma^2}{4})T]}{\beta_n + \frac{\gamma^2}{4\beta_n} + \frac{\gamma}{2\beta_n}} \int_0^T \frac{a(\tau)}{a(\infty)} \exp[(\beta_n^2 + \frac{\gamma^2}{4})\tau]d\tau$$

(6.101)

(c) Base drain

The boundary conditions in this case are given by eq(6.91) and eq(6.80). The technique used to solve this case is essentially similar to the previous case and the details will not be duplicated here.
It is found that :

$$q(\eta,T) = 2 \sum_n \frac{(-1)^n \sqrt{(\alpha_n^2 + \frac{\gamma^2}{4})}\ [\ \alpha_n \cos[\alpha_n(1-\eta)] - \frac{\gamma}{2} \sin[\alpha_n(1-\eta)]]}{\alpha_n - \frac{\gamma}{2\alpha_n} + \frac{\gamma^2}{4\alpha_n}}$$

$$\exp[-(\alpha_n^2 + \frac{\gamma^2}{4})T + \frac{\gamma}{2}\eta\ ] \int_0^T a(\tau)\exp[(\alpha_n^2 + \frac{\gamma^2}{4})\tau]d\tau \qquad (6.102)$$

and,

$$S(T) = \frac{2\gamma}{exp(\gamma) - 1} \sum_n \frac{\alpha_n exp[-(\alpha_n^2 + \frac{\gamma^2}{4})T]}{\alpha_n - \frac{\gamma}{2\alpha_n} + \frac{\gamma^2}{4\alpha_n}} \int_0^T \frac{a(\tau)}{a(\infty)} exp[(\alpha_n^2 + \frac{\gamma^2}{4})\tau]d\tau \quad (6.103)$$

The solutions developed in this section will prove useful in practical applications, and later on this will be applied to the very important case of a linear ramp loading. There are, however, situations where a staircase will be a better approximation to the real loading history. An example of such is a staged construction scheme. The next section is devoted to the solution of such cases.

Consolidation With A Staircase Loading

This situation is similar to the step loading case treated previously except that the initial condition will be a general function such as :

$$q(\eta,0) = f(\eta) \quad (6.104)$$

And in the drained boundary :

$$q(0,T) = \Delta e \quad (6.105)$$

$$q(1,T) = \Delta e\ exp(\gamma) \quad (6.106)$$

It is advantageous to use a new variable q_1 defined as :

$$q_1(\eta,T) = \Delta e\ exp(\gamma\eta) - q(\eta,T) \quad (6.107)$$

The governing equation in terms of this is,

$$\frac{\partial q_1}{\partial T} = \frac{\partial^2 q_1}{\partial \eta^2} - \gamma \frac{\partial q_1}{\partial \eta} \qquad (6.108)$$

with the initial condition :

$$q_1(\eta,0) = g(\eta) = \Delta e \exp(\gamma\eta) - f(\eta) \qquad (6.109)$$

and the simplified drainage boundary conditions :

$$q_1(0,T) = q_1(1,T) = 0 \qquad (6.110)a,b$$

(a) The double drainage boundary

The initial and boundary conditions in this case are given by eq(6.109,110a,b). It is seen the function :

$$q_1(\eta,T) = \sum_n s_n(T) \sin(n\pi\eta) \exp(\frac{\gamma}{2}\eta) \qquad (6.111)$$

satisfies the boundary conditions. This also satisfies the governing equation if the function $s_n(T)$ satisfies :

$$\frac{d}{dT} s_n + (n^2\pi^2 + \frac{\gamma^2}{4}) s_n = 0 \qquad (6.112)$$

Hence,

$$s_n(T) = b_n \exp[-(n^2\pi^2 + \frac{\gamma^2}{4})T] \qquad (6.113)$$

and,

$$q_1(\eta,T) = \sum_n b_n \sin(n\pi\eta) \exp[-(n^2\pi^2 + \frac{\gamma^2}{4}) + \frac{\gamma}{2}\eta] \qquad (6.114)$$

The coefficients b_n can be determined from the initial condition that :

$$q_1(\eta,0) = g(\eta) = \sum_n b_n \sin(n\pi\eta) \exp(\frac{\gamma}{2}\eta) \qquad (6.115)$$

Hence,

$$b_n = 2 \int_0^1 g(y)\sin(n\pi y)\exp(-\frac{\gamma}{2} y)dy \qquad (6.116)$$

And the required solution is,

$$q(\eta,T) = \Delta e \exp(\gamma\eta) - 2 \sum_n \sin(n\pi\eta)\exp[-(n^2\pi^2 + \frac{\gamma^2}{4})T + \frac{\gamma}{2}\eta] \int_0^1 g(y)\sin(n\pi y)\exp(-\frac{\gamma}{2} y)\, dy \qquad (6.117)$$

(b) Surface drain

The boundary conditions are given by :

$$q(1,T) = \Delta e \exp(\gamma) \qquad (6.106)$$

$$\frac{\partial q}{\partial \eta}(0,T) = \gamma q(0,T) \qquad (6.64)$$

Adopting the variable q_1 as in eq(6.107) it is found that :

$$\frac{\partial q_1}{\partial \eta}(0,T) = \gamma q_1(0,T) \qquad (6.118)$$

It is seen the function :

$$q_1(\eta,T) = \sum_n u_n(T)V_n(\eta)\exp(\frac{\gamma}{2}\eta) \qquad (6.119)$$

with the eigenfunctions,

$$V_n(\eta) = \beta_n \cos(\beta_n\eta) + \frac{\gamma}{2}\sin(\beta_n\eta) \qquad (6.120)$$

where,

$$\beta_n \cos\beta_n + \frac{\gamma}{2}\sin\beta_n = 0 \qquad (6.121)$$

satisfies the boundary conditions, eq(6.110b,6.118). It will satisfy the governing equation if the function $u_n(T)$ satisfies :

$$\frac{d}{dT} u_n + \left(\beta_n^2 + \frac{\gamma^2}{4} \right) u_n = 0 \qquad (6.122)$$

Therefore,

$$u_n(T) = c_n \exp\left[-\left(\beta_n^2 + \frac{\gamma^2}{4} \right) T\right] \qquad (6.123)$$

It follows that :

$$q_1(\eta,T) = \sum_n c_n V_n(\eta) \exp\left[-\left(\beta_n^2 + \frac{\gamma^2}{4} \right) T + \frac{\gamma}{2}\eta \right] \qquad (6.124)$$

From the initial condition,

$$g(\eta) = \sum_n c_n V_n(\eta) \exp\left(\frac{\gamma}{2}\eta \right) \qquad (6.125)$$

The following orthogonal condition for the functions V_n can be established by direct integration :

$$\int_0^1 V_m(y) V_n(y) dy = \begin{cases} 0 & m \neq n \\ \frac{1}{2}\left(\beta_n^2 + \frac{\gamma^2}{4} + \frac{\gamma}{2} \right) & m = n \end{cases} \qquad (6.126)$$

From this the coefficients c_n follow :

$$c_n = \frac{2}{\beta_n^2 + \frac{\gamma^2}{4} + \frac{\gamma}{2}} \int_0^1 g(y) V_n(y) \exp\left(-\frac{\gamma}{2} y\right) dy \qquad (6.127)$$

and the required solution is,

$$q(\eta,T) = \Delta e \exp(\gamma\eta) - \sum_n c_n V_n(\eta) \exp\left[-\left(\beta_n^2 + \frac{\gamma^2}{4} \right) T + \frac{\gamma}{2}\eta \right] \qquad (6.128)$$

(c) Base drain

The boundary conditions are given by eq(6.110)a and :

$$\frac{\partial}{\partial \eta} q_1(1,T) = \gamma q_1(1,T) \tag{6.129}$$

It is seen the function :

$$q_1(\eta,T) = \sum_n w_n(T)\, Y_n(\eta)\, exp(\frac{\gamma}{2}\eta) \tag{6.130}$$

where,

$$Y_n(\eta) = \alpha_n cos[\alpha_n(1-\eta)] - \frac{\gamma}{2} sin[\alpha_n(1-\eta)] \tag{6.131}$$

and,

$$\alpha_n cos\alpha_n - \frac{\gamma}{2} sin\alpha_n = 0 \tag{6.132}$$

satisfies the boundary conditions. It also satisfies the governing equation if the function $w_n(T)$ satisfies :

$$\frac{d}{dT} w_n + (\alpha_n^2 + \frac{\gamma^2}{4}) w_n = 0 \tag{6.133}$$

Therefore :

$$w_n(T) = d_n\, exp[-(\alpha_n^2 + \frac{\gamma^2}{4})T] \tag{6.134}$$

And the coefficients d_n are determined from the initial condition :

$$g(\eta) = \sum_n d_n\, Y_n(\eta)\, exp(\frac{\gamma}{2}\eta) \tag{6.135}$$

and the orthogonal condition of the functions $Y_n(\eta)$ which can be verified by direct integration :

$$\int_0^1 Y_m(y) Y_n(y)\, dy = \begin{cases} 0 & m \neq n \\ \frac{1}{2}(\alpha_n^2 + \frac{\gamma^2}{4} - \frac{\gamma}{2}) & m = n \end{cases} \tag{6.136}$$

Hence,

$$d_n = \frac{2}{\alpha_n^2 + \frac{\gamma^2}{4} - \frac{\gamma}{2}} \int_0^1 g(y)\ Y_n(y)\ exp(-\frac{\gamma}{2}y)\,dy \qquad (6.137)$$

And the required solution is,

$$q(\eta,T) = \Delta e\ exp(\gamma\eta) - \sum_n d_n\ Y_n(\eta)\ exp[-(\alpha_n^2 + \frac{\gamma^2}{4})T + \frac{\gamma}{2}\eta\ ] \qquad (6.138)$$

In the special case of a step loading, i.e. $f(\eta) = 0$, these solutions eq(6.117,128,138) have been seen to agree with the corresponding solutions developed in section 3.

An Analysis of the Consolidation Under A Linear Ramp Loading

This section will consider the very important case of a loading $P(t)$ applied to the surface of a normally consolidated stratum which increases linearly with time with a slope s' up to the time $t=t_0$, i.e.

$$P(t) = \begin{cases} s't & 0 \le t \le t_0 \\ s't_0 & t_0 \le t \end{cases} \qquad (6.139)$$

The corresponding void ratio change at the base of the stratum, assuming free drainage, is :

$$a(t) = \begin{cases} e_b[\,1 - exp(-\frac{\alpha}{C_F}\,s't)] & 0 \le t \le t_0 \\ e_b[\,1 - exp(-\frac{\alpha}{C_F}\,s't_0)] & t_0 \le t \end{cases} \qquad (6.140)$$

In order that the solutions in the previous sections can be applied, the above equations are rewritten in terms of the time factor T as:

$$P(T) = \begin{cases} sT & 0 \leq T \leq T_o \\ sT_o & T_o \leq T \end{cases} \qquad (6.139)a$$

and,
$$a(T) = \begin{cases} e_b[\,1 - exp(-\frac{\alpha}{C_F} sT)] & 0 \leq T \leq T_o \\ e_b[\,1 - exp(-\frac{\alpha}{C_F} sT_o)] & T_o \leq T \end{cases} \qquad (6.140)a$$

with a relationship between the coefficients s and s' :

$$s' = \frac{s\, C_F}{z_o^2} \qquad (6.141)$$

Substituting the function $a(T)$ into the solution, eq(6.94,97,100-103) and making use of the identity :

$$\int_0^T a(\tau)\, exp[(n^2\pi^2 + \frac{\gamma^2}{4})\tau]d\tau$$

$$= e_b \left\{ \frac{exp[(n^2\pi^2 + \frac{\gamma^2}{4})T] - 1}{n^2\pi^2 + \frac{\gamma^2}{4}} - \frac{exp[(n^2\pi^2 + \frac{\gamma^2}{4} - \frac{\alpha}{C_F} s)T] - 1}{n^2\pi^2 + \frac{\gamma^2}{4} - \frac{\alpha}{C_F} s} \right\} \qquad (6.142)$$

the solution during the loading period $0 \leq T \leq T_o$ is found to be :

For double drainage boundary :

$$q_d(\eta,T) = 2e_b \sum_n n\pi\, [1-(-1)^n exp(\frac{\gamma}{2})]sin(n\pi\eta)\, exp(\frac{\gamma}{2}\eta)\, \{ \frac{1}{n^2\pi^2 + \frac{\gamma^2}{4}}$$

$$[1-exp[-(n^2\pi^2 + \frac{\gamma^2}{4})T] - \frac{1}{n^2\pi^2 + \frac{\gamma^2}{4} - \frac{\alpha}{C_F} s} [exp(-\frac{\alpha}{C_F} sT) - exp[-($$

$$n^2\pi^2 + \frac{\gamma^2}{4})T]]\} \qquad (6.143)$$

$$S_d(T) = \frac{2\gamma}{(\exp(\gamma) - 1)[1 - \exp(-\frac{\alpha}{C_F} sT_o)]} \sum_n \frac{n^2\pi^2 [1-(-1)^n \exp(\frac{\gamma}{2})]}{n^2\pi^2 + \frac{\gamma^2}{4}} \{$$

$$\frac{1}{n^2\pi^2 + \frac{\gamma^2}{4}} [1 - \exp[-(n^2\pi^2 + \frac{\gamma^2}{4})T]$$

$$- \frac{1}{n^2\pi^2 + \frac{\gamma^2}{4} - \frac{\alpha}{C_F} s} [\exp(-\frac{\alpha}{C_F} sT) - \exp[-(n^2\pi^2 + \frac{\gamma^2}{4})T]]\} \quad (6.144)$$

For surface drain

$$q_s(\eta, T) = 2e_b \exp[\frac{\gamma}{2}(\eta+1)] \sum_n \frac{(-1)^{n+1} \sqrt{(\beta_n^2 + \frac{\gamma^2}{4})} [\beta_n \cos(\beta_n \eta) + \frac{\gamma}{2} \sin(\beta_n \eta)]}{\beta_n + \frac{\gamma^2}{4\beta_n} + \frac{\gamma}{2\beta_n}}$$

$$\{\frac{1}{\beta_n^2 + \frac{\gamma^2}{4}} [1 - \exp[-(\beta_n^2 + \frac{\gamma^2}{4})T]$$

$$- \frac{1}{\beta_n^2 + \frac{\gamma^2}{4} - \frac{\alpha}{C_F} s} [\exp(-\frac{\alpha}{C_F} sT) - \exp[-(\beta_n^2 + \frac{\gamma^2}{4}) T]]\} \quad (6.145)$$

$$S_s(T) = \frac{2\gamma}{(1-\exp(-\gamma))\left[1-\exp\left(-\frac{\alpha}{C_F}sT_o\right)\right]} \sum_n \frac{\beta_n^2}{\beta_n^2 + \frac{\gamma^2}{4} + \frac{\gamma}{2}} \cdot \left\{\frac{1}{\beta_n^2 + \frac{\gamma^2}{4}}\left[1-\exp\left[-\left(\beta_n^2 + \frac{\gamma^2}{4}\right)T\right]\right] - \frac{1}{\beta_n^2 + \frac{\gamma^2}{4} - \frac{\alpha}{C_F}s}\left[\exp\left(-\frac{\alpha}{C_F}sT\right) - \exp\left[-\left(\beta_n^2 + \frac{\gamma^2}{4}\right)T\right]\right]\right\}$$

(6.146)

For base drain :

$$q_b(\eta,T) = 2e_b\exp\left(\frac{\gamma}{2}\eta\right) \sum_n \frac{(-1)^n\sqrt{\left(\alpha_n^2 + \frac{\gamma^2}{4}\right)}\left[\alpha_n\cos(\alpha_n(1-\eta)) - \frac{\gamma}{2}\sin(\alpha_n(1-\eta))\right]}{\alpha_n + \frac{\gamma^2}{4\alpha_n} - \frac{\gamma}{2\alpha_n}}$$

$$\left\{\frac{1 - \exp\left[-\left(\alpha_n^2 + \frac{\gamma^2}{4}\right)T\right]}{\alpha_n^2 + \frac{\gamma^2}{4}} - \frac{\exp\left(-\frac{\alpha}{C_F}sT\right) - \exp\left[-\left(\alpha_n^2 + \frac{\gamma^2}{4}\right)T\right]}{\alpha_n^2 + \frac{\gamma^2}{4} - \frac{\alpha}{C_F}s}\right\}$$

(6.147)

$$S_b(T) = \frac{2\gamma}{(\exp(\gamma)-1)\left[1-\exp\left(-\frac{\alpha}{C_F}sT_o\right)\right]} \sum_n \frac{\alpha_n^2}{\alpha_n^2 + \frac{\gamma^2}{4} - \frac{\gamma}{2}}$$

$$\cdot \left\{\frac{1 - \exp\left[-\left(\alpha_n^2 + \frac{\gamma^2}{4}\right)T\right]}{\alpha_n^2 + \frac{\gamma^2}{4}} - \frac{\exp\left(-\frac{\alpha}{C_F}sT\right) - \exp\left[-\left(\alpha_n^2 + \frac{\gamma^2}{4}\right)T\right]}{\alpha_n^2 + \frac{\gamma^2}{4} - \frac{\alpha}{C_F}s}\right\}$$

(6.148)

In these expressions the subscripts d, s and b are used to indicate double drainage, surface drain and base drain respectively. The parameter $\frac{\alpha}{C_F}$ appearing in the expressions is related to the stratum coefficient γ by :

$$\frac{\alpha}{C_F} = \frac{\gamma}{z_o(\rho_s - \rho_f)} \qquad (6.149)$$

where $z_o(\rho_s - \rho_f)$ is the part of the effective stress in the base caused by the weight of the soil in the stratum. This is related to the total additional loading sT_o by a loading factor m defined as :

$$sT_o = m\,[\,z_o(\rho_s - \rho_f)\,] \qquad (6.150)$$

It can therefore be shown that the above solutions will depend on the two additional parameter m and T_o as well as the stratum coefficient γ. The loading factor m is a measure of the magnitude of loading and T_o is a measure of the loading speed. Hence, the solutions, eq(6.143-148) can be rewritten in these parameters, although the resulting expressions are still rather lengthy and will not be produced here. The degree of settlement has been calculated for $m = 0.1, 1, 2$ and $T_o = 0.05, 0.1, 0.2$ 0.5 for the double drain, this is shown in Fig.6.11 for $\gamma = 0.1, 1$. The single drainage cases have also been calculated with $m = 0.1, 1, 2$ and $T_o = 0.1, 0.2, 0.5, 1$ for $\gamma = 1$. These are shown in Fig.6.12.

Perhaps the quantity of most interest to the engineer is the degree of settlement of the stratum at the completion of loading. This is a function of γ, m and T_o as :

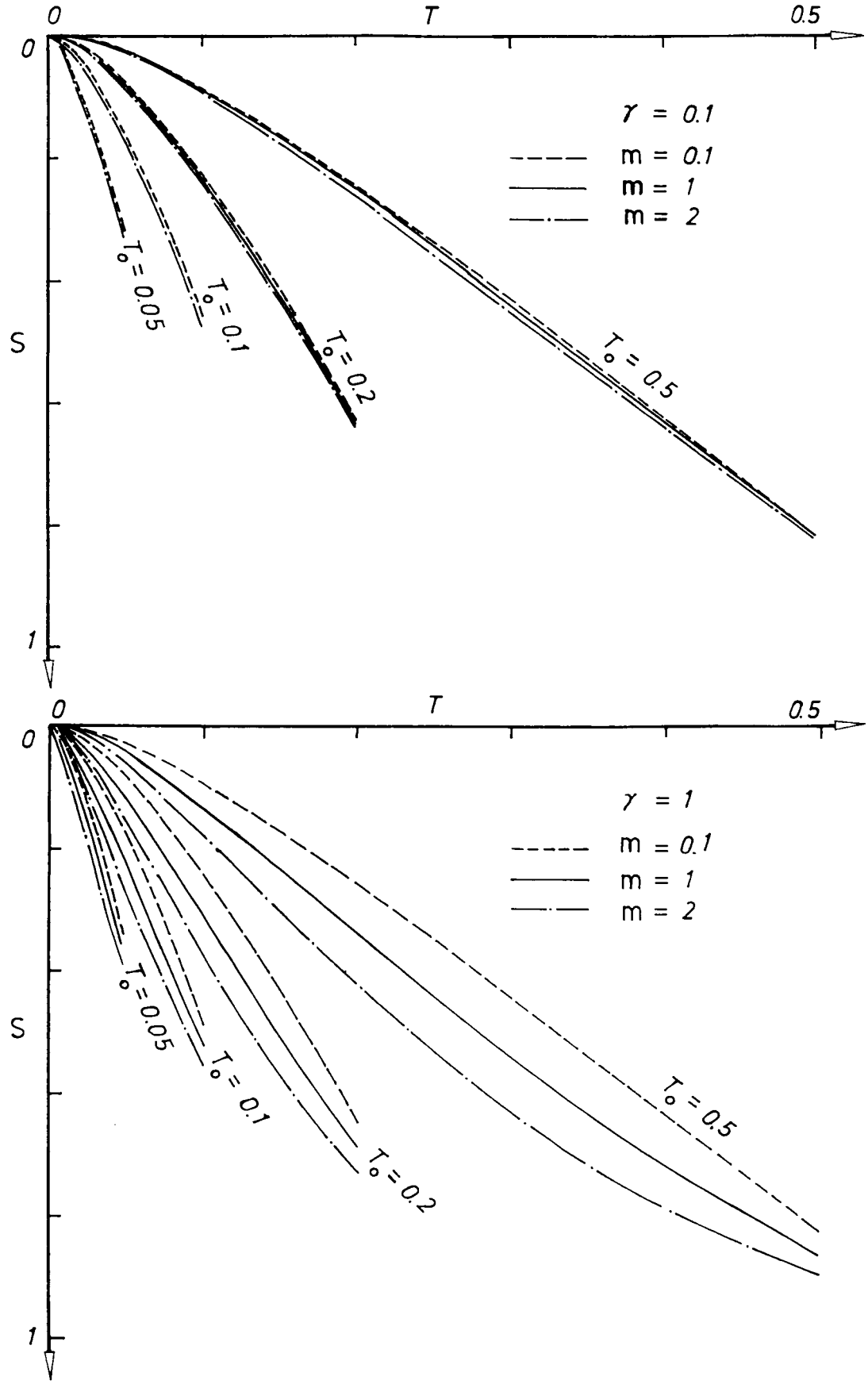

FIG. 6.11 Consolidation under a linear ramp loading, double drainage.

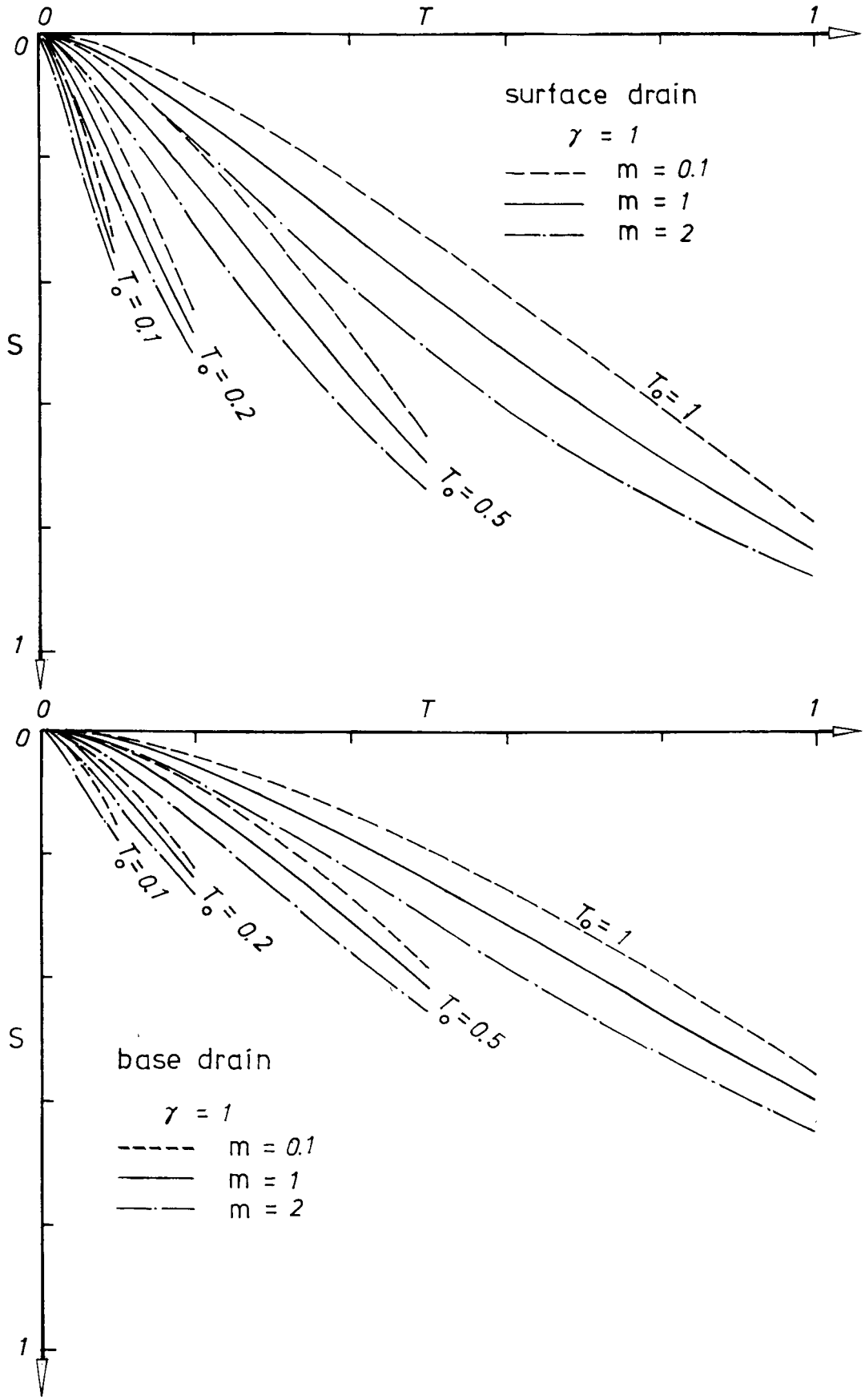

FIG. 6.12 Consolidation under a linear ramp loading, single drainage.

$$S_d(T_o) = \frac{2\gamma}{(\exp(\gamma)-1)[1-\exp(-m\gamma)]} \sum_n \frac{n^2\pi^2 [1-(-1)^n \exp(\frac{\gamma}{2})]^2}{n^2\pi^2 + \frac{\gamma^2}{4}}$$

$$\cdot \{ \frac{1 - \exp[-(n^2\pi^2 + \frac{\gamma^2}{4})T_o]}{n^2\pi^2 + \frac{\gamma^2}{4}} - \frac{[\exp(-m\gamma) - \exp[-(n^2\pi^2 + \frac{\gamma^2}{4})T_o]]}{n^2\pi^2 + \frac{\gamma^2}{4} - \frac{m\gamma}{T_o}} \}$$

(6.151)

$$S_s(T_o) = \frac{2\gamma}{(1-\exp(-\gamma)[1-\exp(-m\gamma)]} \sum_n \frac{\beta_n^2}{\beta_n^2 + \frac{\gamma^2}{4} + \frac{\gamma}{2}}$$

$$\cdot \{ \frac{1 - \exp[-(\beta_n^2 + \frac{\gamma^2}{4})T_o]}{\beta_n^2 + \frac{\gamma^2}{4}} - \frac{\exp(-m\gamma) - \exp[-(\beta_n^2 + \frac{\gamma^2}{4})T_o]}{\beta_n^2 + \frac{\gamma^2}{4} - \frac{m\gamma}{T_o}} \}$$

(6.152)

$$S_b(T_o) = \frac{2}{(\exp(\gamma)-1)[1-\exp(-m\gamma)]} \sum_n \frac{\alpha_n^2}{\alpha_n^2 + \frac{\gamma^2}{4} - \frac{\gamma}{2}}$$

$$\cdot \{ \frac{1 - \exp[-(\alpha_n^2 + \frac{\gamma^2}{4})T_o]}{\alpha_n^2 + \frac{\gamma^2}{4}} - \frac{\exp(-m\gamma) - \exp[-(\alpha_n^2 + \frac{\gamma^2}{4})T_o]}{\alpha_n^2 + \frac{\gamma^2}{4} - \frac{m\gamma}{T_o}} \}$$

(6.153)

where the subscripts d, s and b have the same meaning as before. These have been calculated and prepared as charts for $m = 0.1, 0.5, 1,2$

and $\gamma = 0.1, 0.5, 1, 2$. These are shown in Fig.6.13 for the double drain and in Fig.6.14 and Fig.6.15 for the surface drain and base drain respectively. These chart can be used to estimate the relative magnitude of settlement that has been completed at the end of construction by estimating the stratum coefficient γ, the loading factor m and the loading period in terms of the time factor T_o and using these values to interpret the degree of settlement $S(T_o)$ from these charts.

The consolidation that follows the completion of construction can be calculated by substituting the solutions at the completion of construction as the initial condition $f(\eta)$ of the staircase loading for which solutions have been developed in this section. This results in very long expressions and will not be produced here.

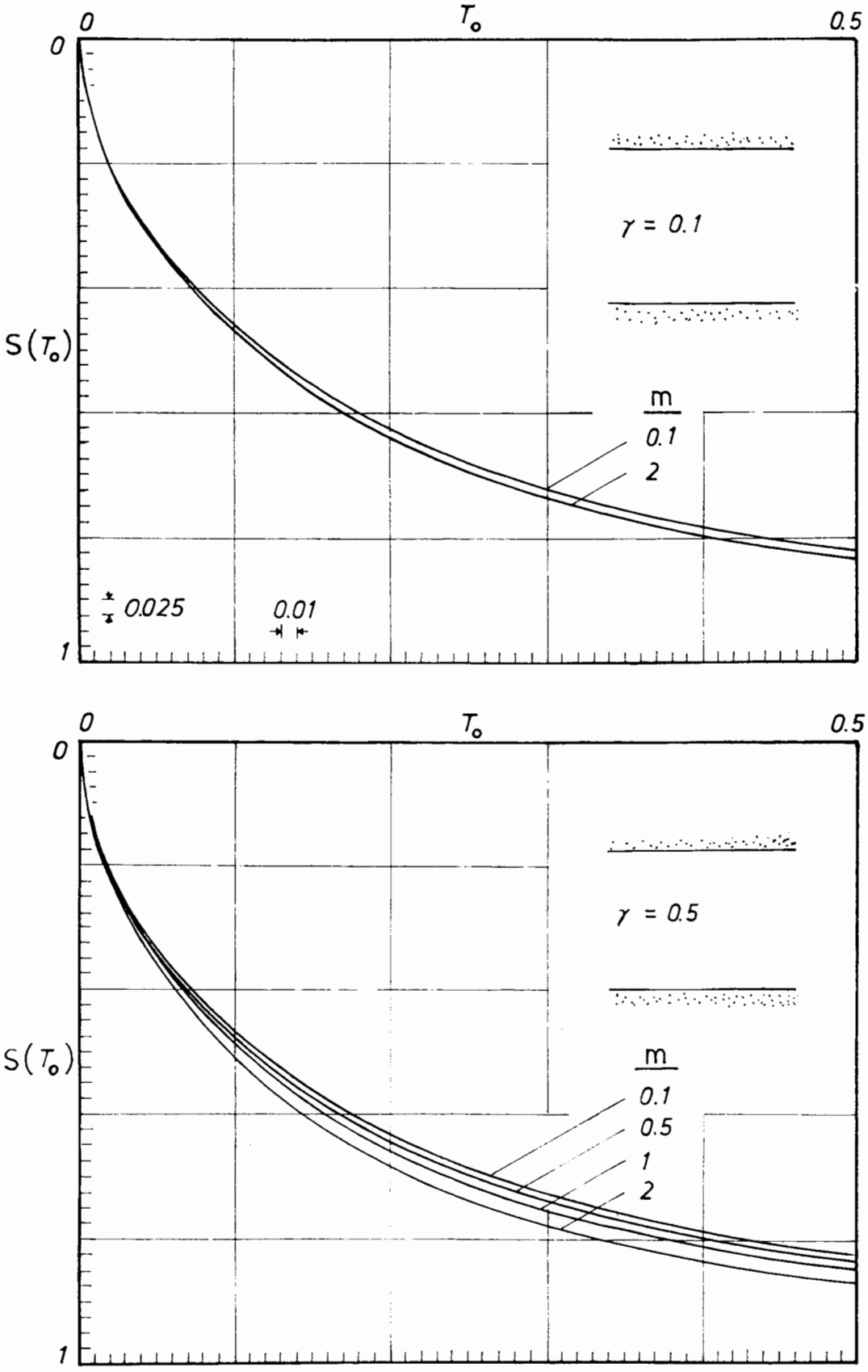

FIG.6.13 Degree of settlement at the completion of a linear ramp loading, double drain.

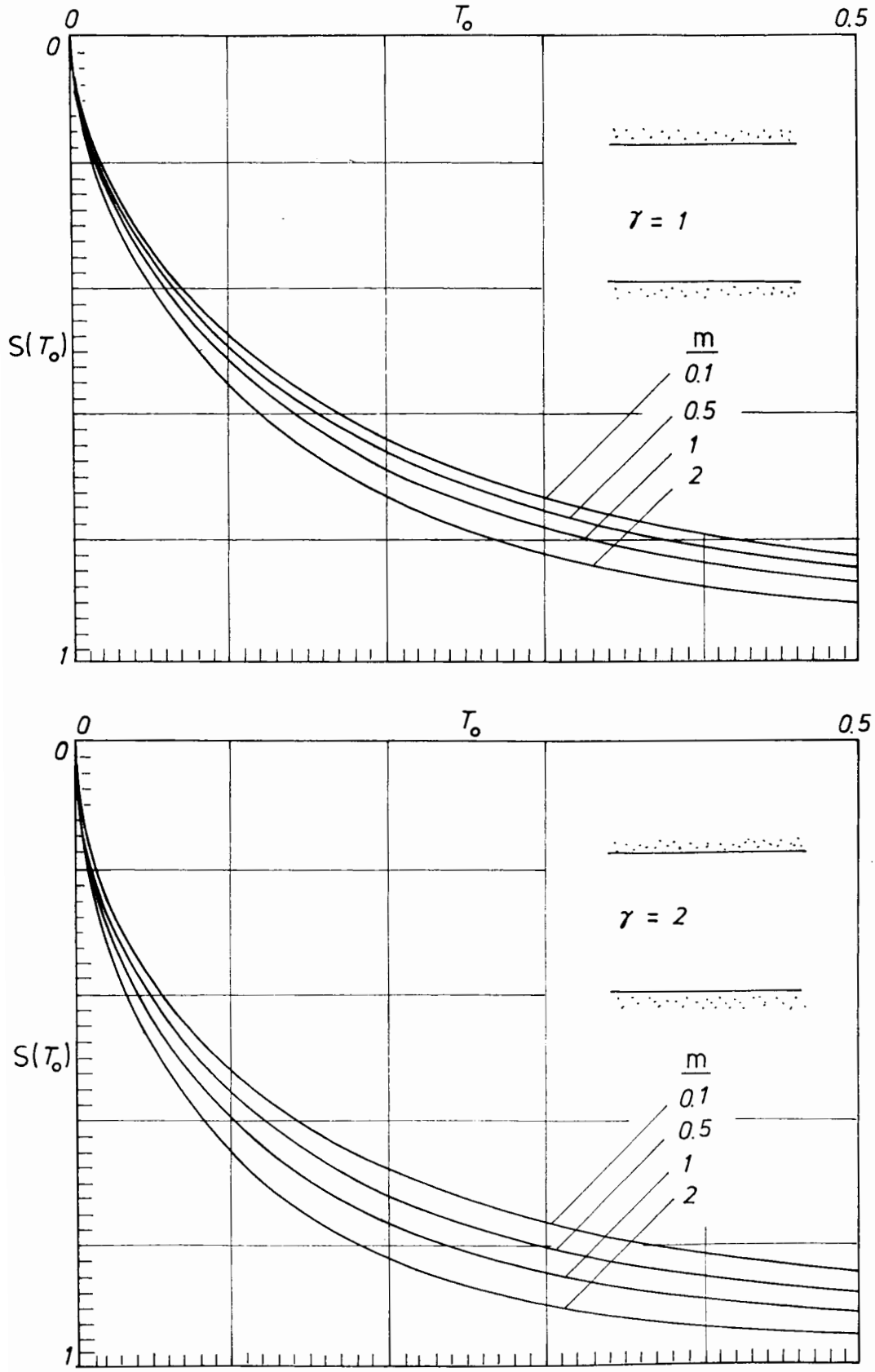

FIG.6.13 (continued)

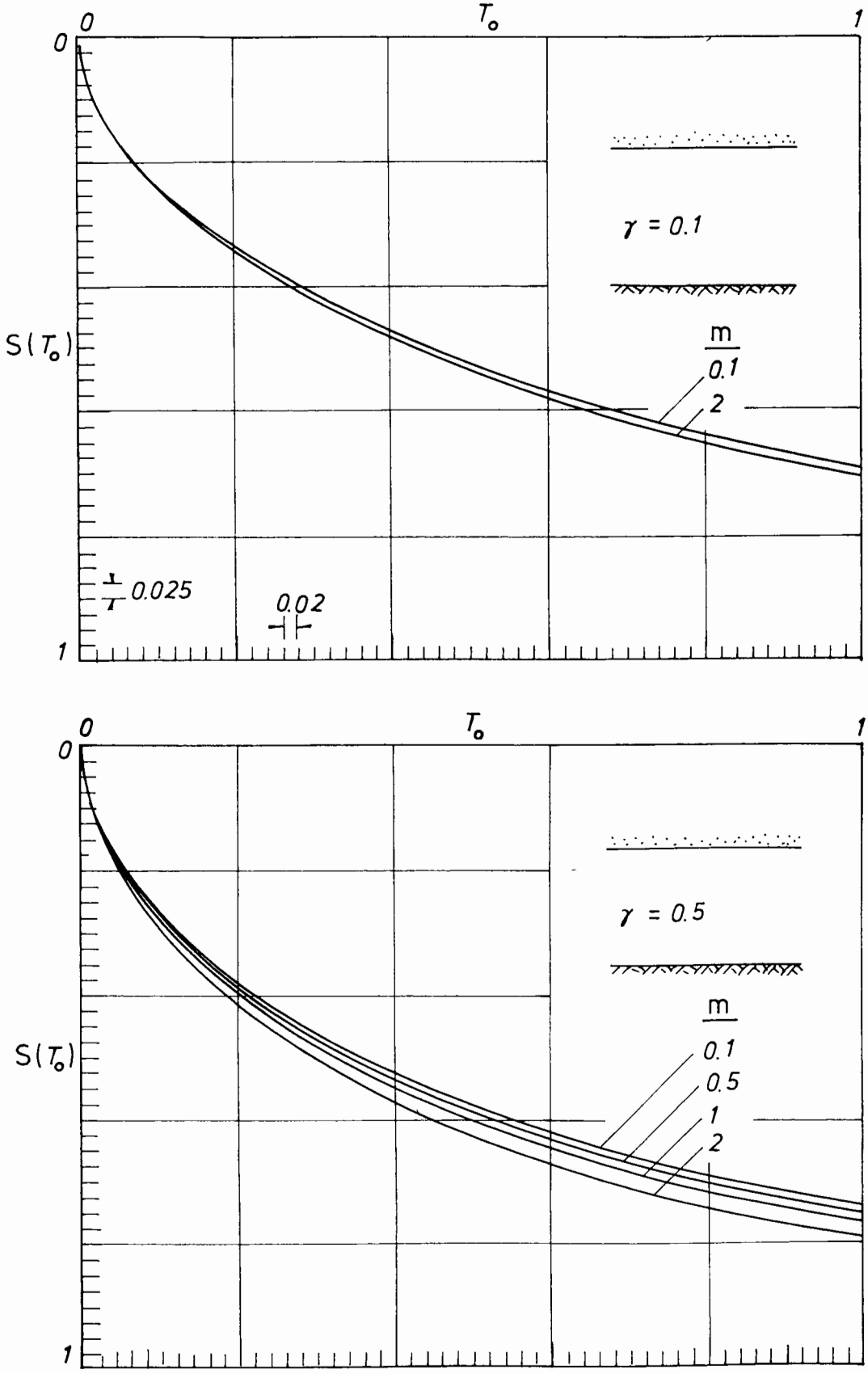

FIG.6.14 Degree of settlement at the completion of a linear ramp loading, surface drain

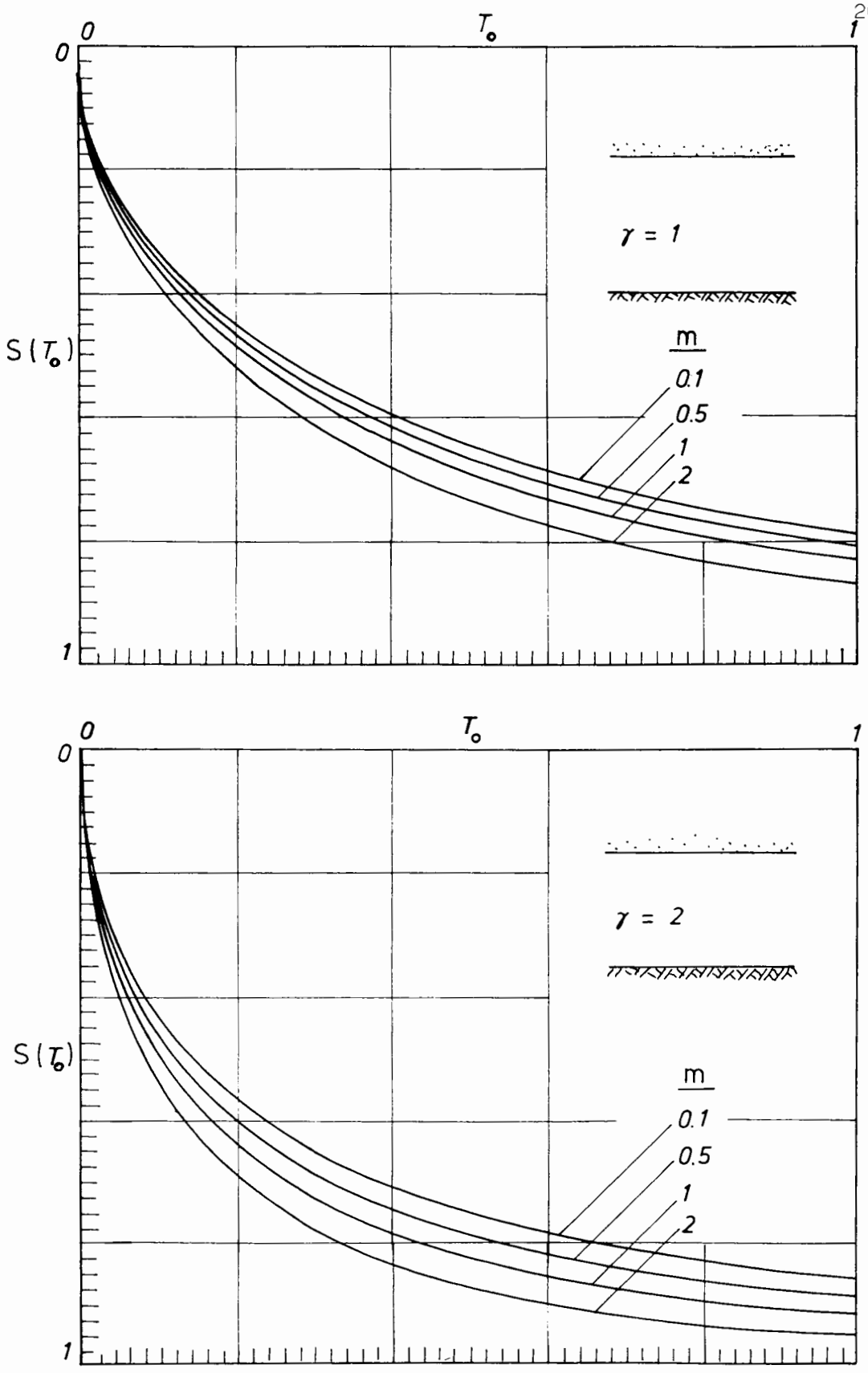

FIG.6.14 (continued)

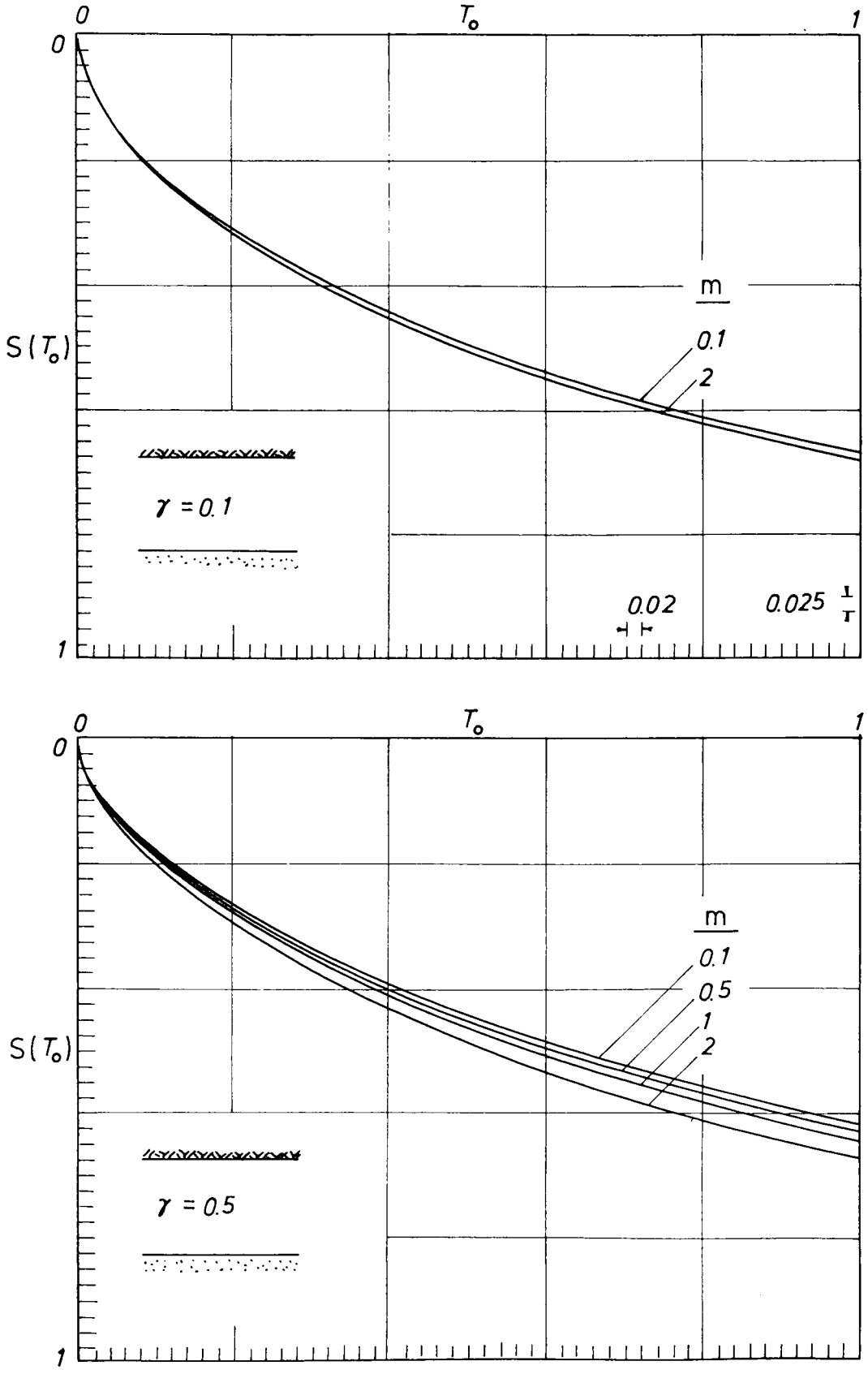

FIG.6.15 Degree of settlement at the completion of a linear ramp loading, base drain.

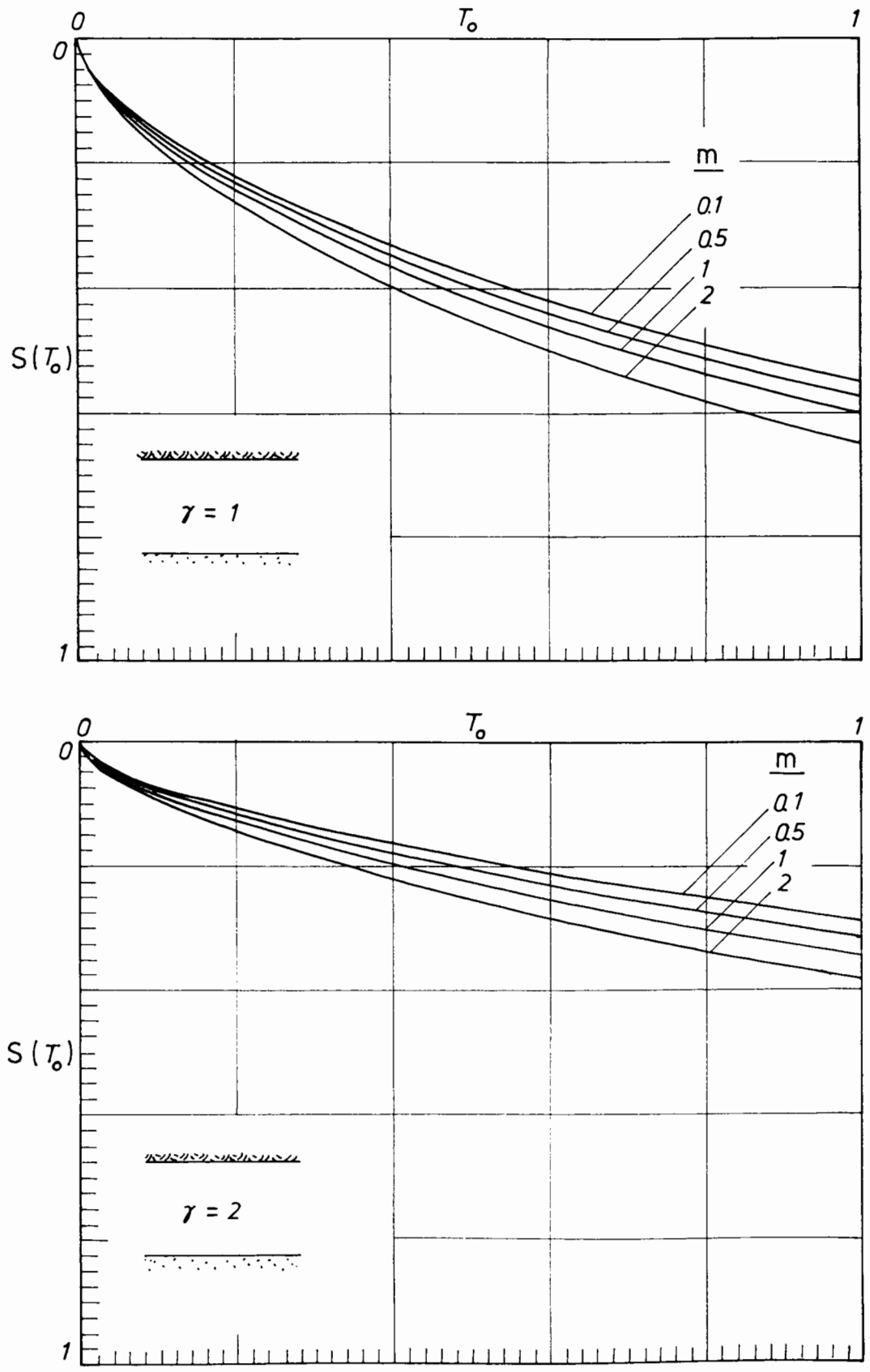

FIG. 6.15 (continued)

PART II THE CONSOLIDATION OF A DREDGED FILL UNDER ITS OWN WEIGHT

In this Part a dredged fill of a uniform density is considered. Consolidation of this is caused by the weight of the soil and proceeds until the normally consolidated state is achieved. Two cases will be considered here : the first is the double drainage boundary and the second is the surface drain. The possibility of a dredged fill with base drain only is excluded in the present study as it is unrealistic to assume an impervious surface to exist in practice.

6. DEVELOPMENT OF SOLUTIONS

The governing equation and the initial and boundary conditions have been given in section 2 of this chapter. The technique of developing the solutions in this section will be identical to the previous sections hence only a brief description will be given here.

The Double Drainage Boundary

The governing equation is given by eq(6.29) and the initial condition is given by eq(6.28). The boundary conditions are given by eq(6.25a,26a), and it can be shown that the final equilibrium condition i.e. when the stratum becomes normally consolidated, is :

$$q(\eta,\infty) = e_i \, [\, 1 - exp(\gamma(\eta-1))\,] \qquad (6.154)$$

The solution can simply be obtained by substituting the corresponding values of the boundary conditions into the general solution for the double drain, eq(6.46), where in this case $a = e_i exp(-\gamma)$

and $b = 0$. Thus,

$$q(\eta,T) = e_i \exp(-\gamma)\left\{\frac{1 - \exp[\gamma(\eta-1)]}{1 - \exp(-\eta)} - 2\sum_n \frac{n\pi \sin(n\pi\eta)}{n^2\pi^2 + \frac{\gamma^2}{4}}\right.$$

$$\left.\exp\left[-(n^2\pi^2 + \tfrac{\gamma^2}{4})T + \tfrac{\gamma}{2}\eta\right]\right\} \qquad (6.155)$$

From this and the final equilibrium condition eq(6.154) the degree of settlement follows,

$$S(T) = 1 - 2\sum_n \frac{\gamma(1-\exp(-\gamma)[1-(-1)^n\exp(\tfrac{\gamma}{2})]}{\gamma - 1 + \exp(-\gamma)} \left[\frac{n^2\pi^2}{n^2\pi^2 + \frac{\gamma^2}{4}}\right]^2 \exp\left[-(n^2\pi^2 + \tfrac{\gamma^2}{4})T\right]$$

(6.156)

An approximate solution in the early stages of consolidation can be obtained by the Laplace transform solution, which is :

$$\bar{S}(p) = \frac{\gamma(1-\exp(-\gamma))}{\gamma+\exp(-\gamma)-1}\left\{\frac{\gamma}{2p^2} + \frac{\sqrt{(\frac{\gamma^2}{4}+p)}}{p^2\tanh\sqrt{(\frac{\gamma^2}{4}+p)}} - \frac{\exp(\frac{\gamma^2}{2})\sqrt{(\frac{\gamma^2}{4}+p)}}{p^2\sinh\sqrt{(\frac{\gamma^2}{4}+p)}}\right\}$$

(6.157)

As $p \to \infty$, $\tanh\sqrt{(\frac{\gamma^2}{4}+p)} \to 1$ and $\sinh\sqrt{(\frac{\gamma^2}{4}+p)} \to \infty$

Hence,

$$S(p) \simeq \frac{\gamma(1-\exp(-\gamma)}{\gamma+\exp(-\gamma)-1}\left\{\frac{\gamma}{2p^2} + \frac{\sqrt{(\frac{\gamma^2}{4}+p)}}{p^2}\right\} \qquad p \to \infty \qquad (6.158)$$

The inverse transform of this is, approximately,

Time Factor	Degree of Settlement x 10^4		
	Exact Solution	Small Time Approximation	Large Time Approximation
0.0001	0195	0195	-
0.0025	0991	0991	-
0.0100	2026	2026	2028
0.0400	4233	4234	4232
0.0900	6487	6633	6487
0.1600	8263	-	8263
0.4900	9938	-	9938

TABLE 6.5 COMPARISON OF SMALL AND LARGE TIME APPROXIMATIONS WITH EXACT SOLUTION, DREDGED FILL, DOUBLE DRAIN

$$S(T) \simeq \frac{\gamma(1-\exp(-\gamma))}{\gamma+\exp(-\gamma)-1}\left\{ 2\sqrt{\left[\frac{T}{\pi}\right]} + \frac{\gamma}{2}T + \frac{\gamma^2}{6}\frac{1}{\sqrt{\pi}}\sqrt{(T)^3} \right\} \qquad (6.159)$$

This is compared with the exact solution in Table6.5. The large time approximation which also appears in this Table is obtained by using the first five terms from the series solution. In this example $\gamma = 1$.

Surface Drain

The boundary conditions in this case are given by eq(6.25a,30). Using the technique of Laplace transform it is found that :

$$\bar{q}(\eta,p) = e_i[1-\exp(\gamma(\eta-1))] - e_i\exp\left(\frac{\gamma}{2}\eta\right)\frac{\sinh[(1-\eta)\sqrt{\left(\frac{\gamma^2}{4}+p\right)}]}{p[\sqrt{\left(\frac{\gamma^2}{4}+p\right)}\cosh\sqrt{\left(\frac{\gamma^2}{4}+p\right)} + \frac{\gamma}{2}\sinh\sqrt{\left(\frac{\gamma^2}{4}+p\right)}]}$$

(6.160)

The second term is identical to half of the expression of eq(6.70) where the

inverse transform is obtained in Appendix A, from which it is found that :

$$q(\eta,T) = e_i \{(1-\exp(\gamma(\eta-1))) - 2\gamma \exp(\tfrac{\gamma}{2}\eta) \sum_n \frac{(-1)^n \sin[\beta_n(1-\eta)]\ \beta_n}{(\beta_n^2 + \frac{\gamma^2}{4})(\beta_n^2 + \frac{\gamma^2}{4} + \frac{\gamma}{2})}$$

$$\exp[-(\beta_n^2 + \tfrac{\gamma^2}{4})T]\} \qquad (6.161)$$

And the degree of settlement is,

$$S(T) = 1 + \frac{2\gamma^2 \exp(\frac{\gamma}{2})}{\gamma - 1 + \exp(-\gamma)} \sum_n \frac{(-1)^n \beta_n^2 \exp[-(\beta_n^2 + \frac{\gamma^2}{4})T]}{\sqrt{(\beta_n^2 + \frac{\gamma^2}{4})^3}(\beta_n^2 + \frac{\gamma^2}{4} + \frac{\gamma}{2})} \qquad (6.162)$$

In this case a simple approximate solution in small time is not available; however, it is found that the series in the exact solution eq(6.162) converges rapidly even at small values of time. This is shown in Table 6.6 for $\gamma = 1$ calculated to the 1st, 2nd, 3rd, 4th 5th and the 40th term of the series. It can be seen that a reasonable approximate solution valid for all values of time can be obtained by truncating the series solution after the third or the fifth term.

Time Factor	Degree of Settlement x 10^4					
	1st	2nd	3rd	4th	5th	40th
0.02	-0199	0282	0232	0237	0237	0237
0.03	0164	0544	0519	0519	0519	0519
0.04	0514	0815	0801	0801	0801	0801
0.05	0851	1089	1082	1082	1082	1082
0.1	2367	2441	2441	2441	2441	2441
0.2	4687	4694	4694	4694	4694	4694

TABLE 6.6 CONVERGENCY OF THE SERIES SOLUTION, EQ(6.162).

7 DISCUSSION OF SOLUTIONS

In the previous section the solutions have been developed for the void ratio change q and the degree of settlement S . The magnitude of strain that will occur when the consolidation is complete and the stratum becomes normally consolidated can be calculated from the initial and final void ratio distributions as :

initially, $e = e_i$

in the normally consolidated state : $e = e_i exp[\gamma(\eta-1)]$

The actual thickness (measured in space) of the stratum is :

initially, $h(0) = z \int_0^1 (1+e)d\eta = (1+e_i)z_o$

in the normally consolidated state,

$$h(\infty) = z_o \int_0^1 (1+e)d\eta = [\ 1 + \frac{e_i}{\gamma}(1-exp(-\gamma))]z_o$$

Hence the strain,

$$\varepsilon = \frac{h(0) - h(\infty)}{h(0)} = \frac{e_i}{1 + e_i}[\ 1 - \frac{1}{\gamma}\ (1-exp(-\gamma))]$$

which depends on both the initial void ratio e_i and the stratum coefficient γ . Since the degree of settlement depends on the stratum coefficient only, it follows that this is a strain-invariant solution. In Fig.6.16 this is plotted against the square root of time factor for the double drainage boundary. It can be seen that the settlement rate for larger γ is slower in the early stages, becoming faster in the later stages and eventually achieving full consolidation earlier. This behaviour is not observed in the case of surface drain, shown in Fig.6.17, where larger γ will always produce faster consolidation.

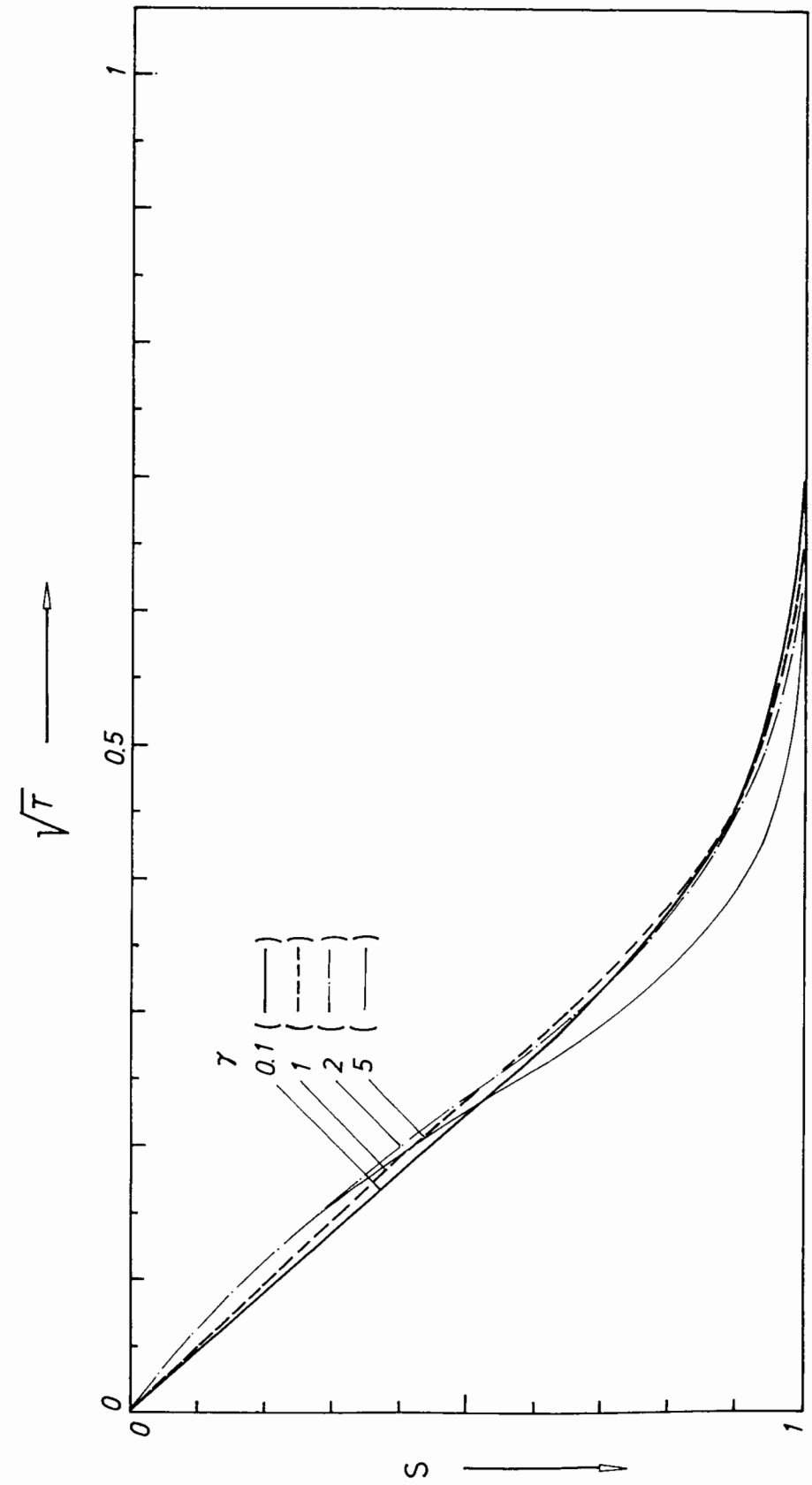

FIG. 6.16 Degree of settlement versus the square root of time factor , dredged fill, dorble drain.

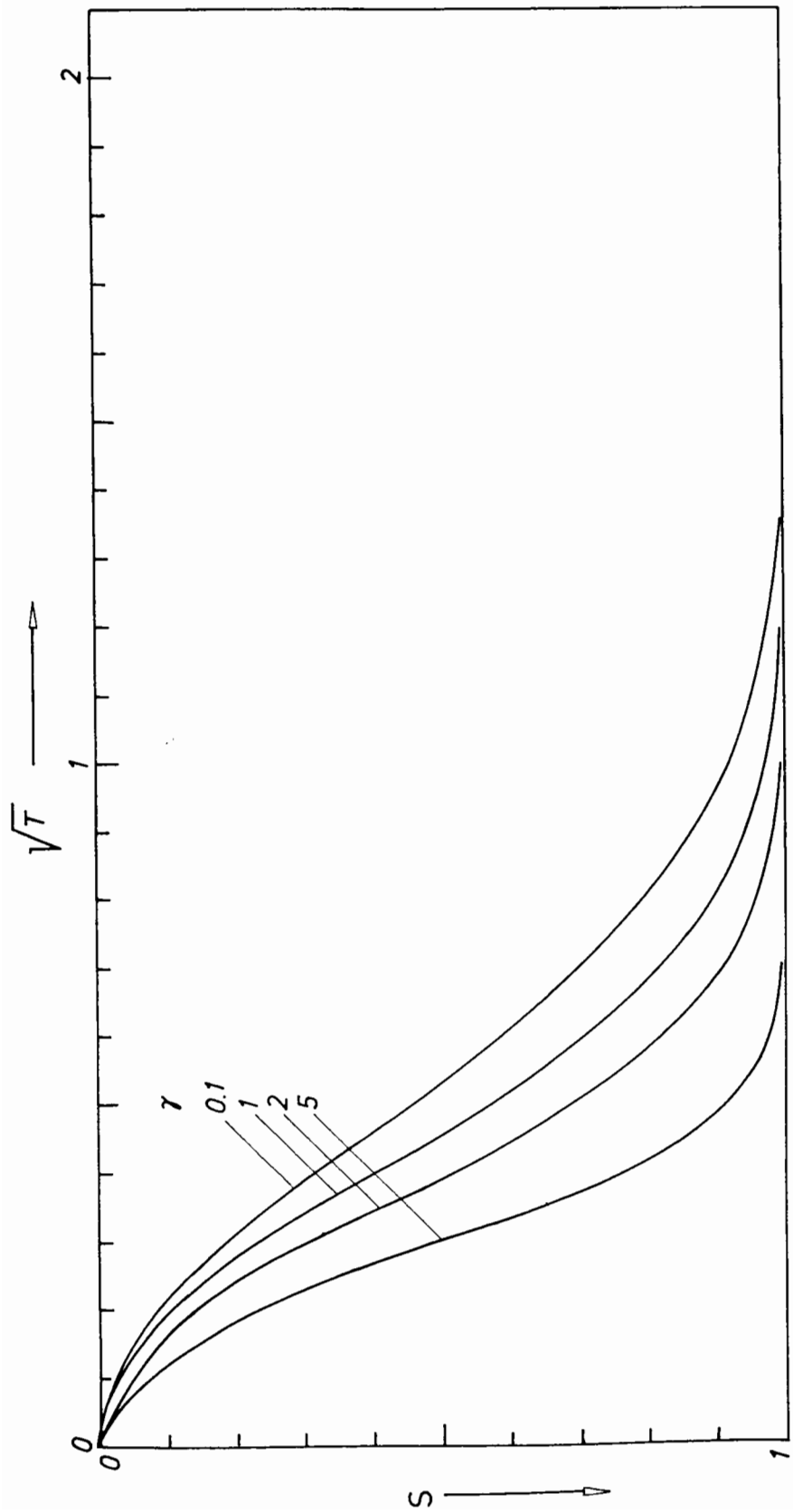

FIG. 6.17 Degree of settlement versus the square root of time factor, dredged fill, surface drain

The void ratio change q is dependent on both the initial void ratio e_i and the stratum coefficient γ. It is therefore desirable to use a normalized variable to remove the constraint from e_i. One of the many possibilities is to use the normalized void ratio change $\bar{q}$ defined as the ratio of the void ratio change at any particular point to the maximum void ratio change that could occur in the stratum, i.e.

$$\bar{q}\ (\eta,T) = \frac{q(\eta,T)}{e_i[1 - exp(-\gamma)]} \qquad (6.164)$$

This can be calculated from eq(6.155,161). The isochrones of this for the double drain are shown in Fig.6-18. It can be seen that the consolidation with larger γ in the early stages is not significantly faster than the small γ cases. This results in a comparable order of settlement, and hence the degree of settlement, which is the ratio of the current settlement to the final settlement, is smaller for larger γ in this stage as has been observed earlier. Further evidences of this can be found in Fig.6.19 -6.22 where isochrones for $\gamma = 0.1, 1, 2, 5$ are presented.

The isochrones for the surface drain are shown in Fig.6.23 where it can be seen that faster consolidation is associated with larger γ. These are shown seperately in Fig.6.24 -6.27 for each value of γ. It is difficult in these cases to judge the actual progress of consolidation from the positions of the isochrones because of the fact that the parameter is normalized to the largest void ratio change which will be different in each case. This is demonstrated by the difference in the final equilibrium state of each case, which has also shown in the figures by the curve marked with $T = \infty$. This difficulty then led to the consideration of the dissipation of the excess pore water pressure in the hope that more information could be obtained therefrom.

The excess pore water pressure u is related to the total stress σ, the effective stress σ' and the hydrostatic pore water pressure u_h by the equation :

$$u = \sigma - \sigma' - u_h \qquad (6.165)$$

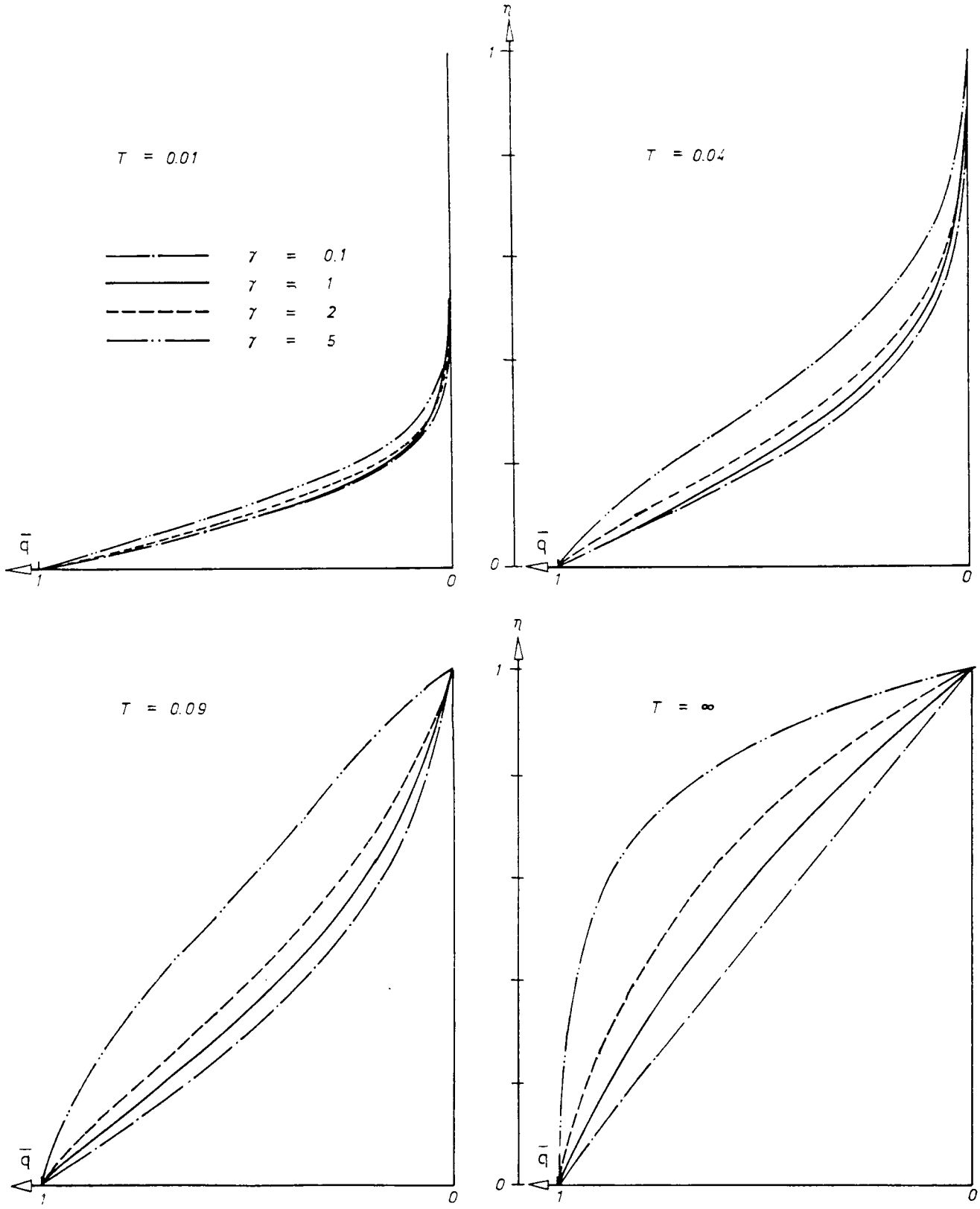

FIG. 6.18 Variations of the normalized void ratio change, dredged fill double drain.

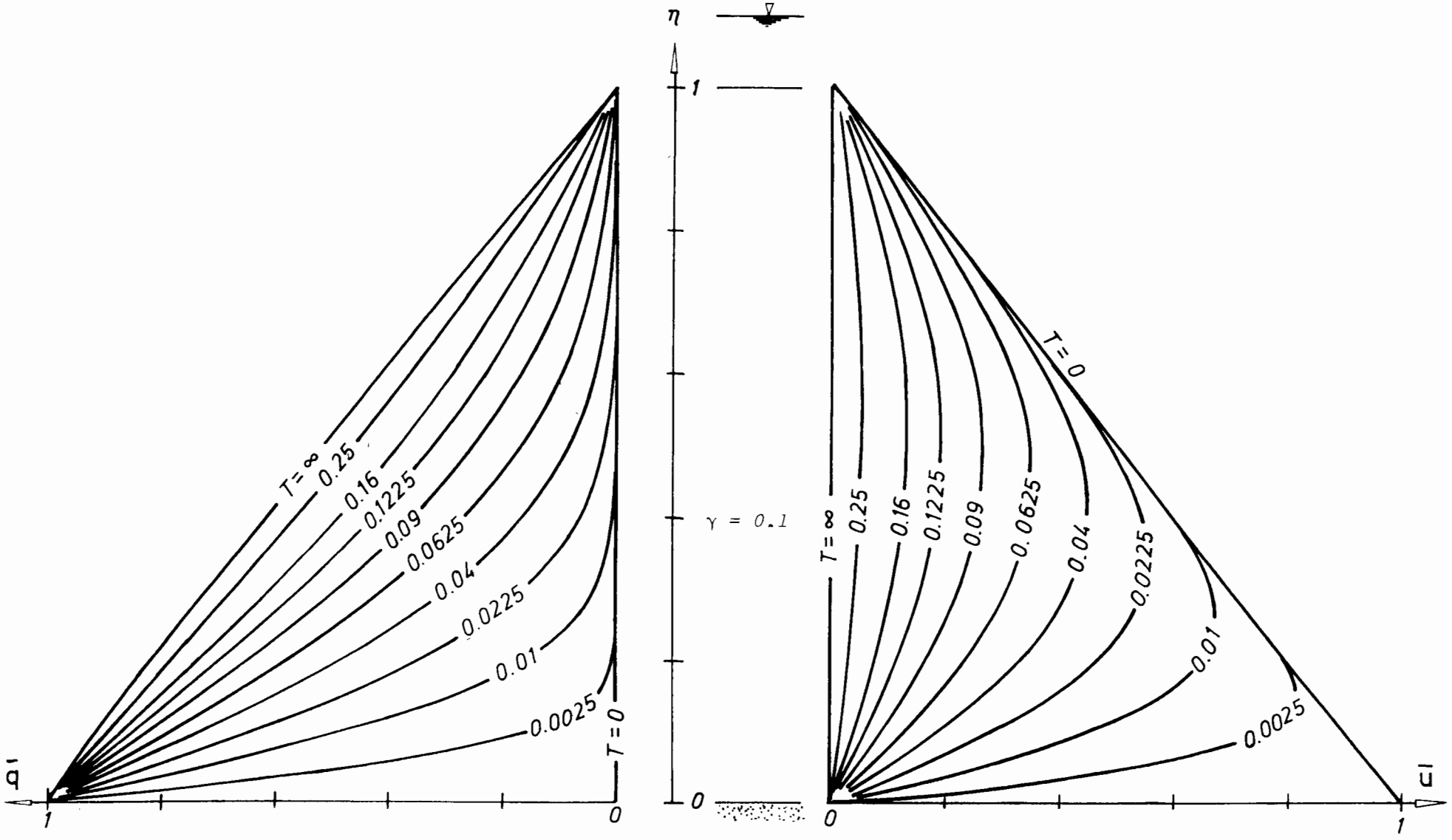

FIG. 6.19 Isochrones of the normalized void ratio change (left) and the normalized excess pore water pressure(right)

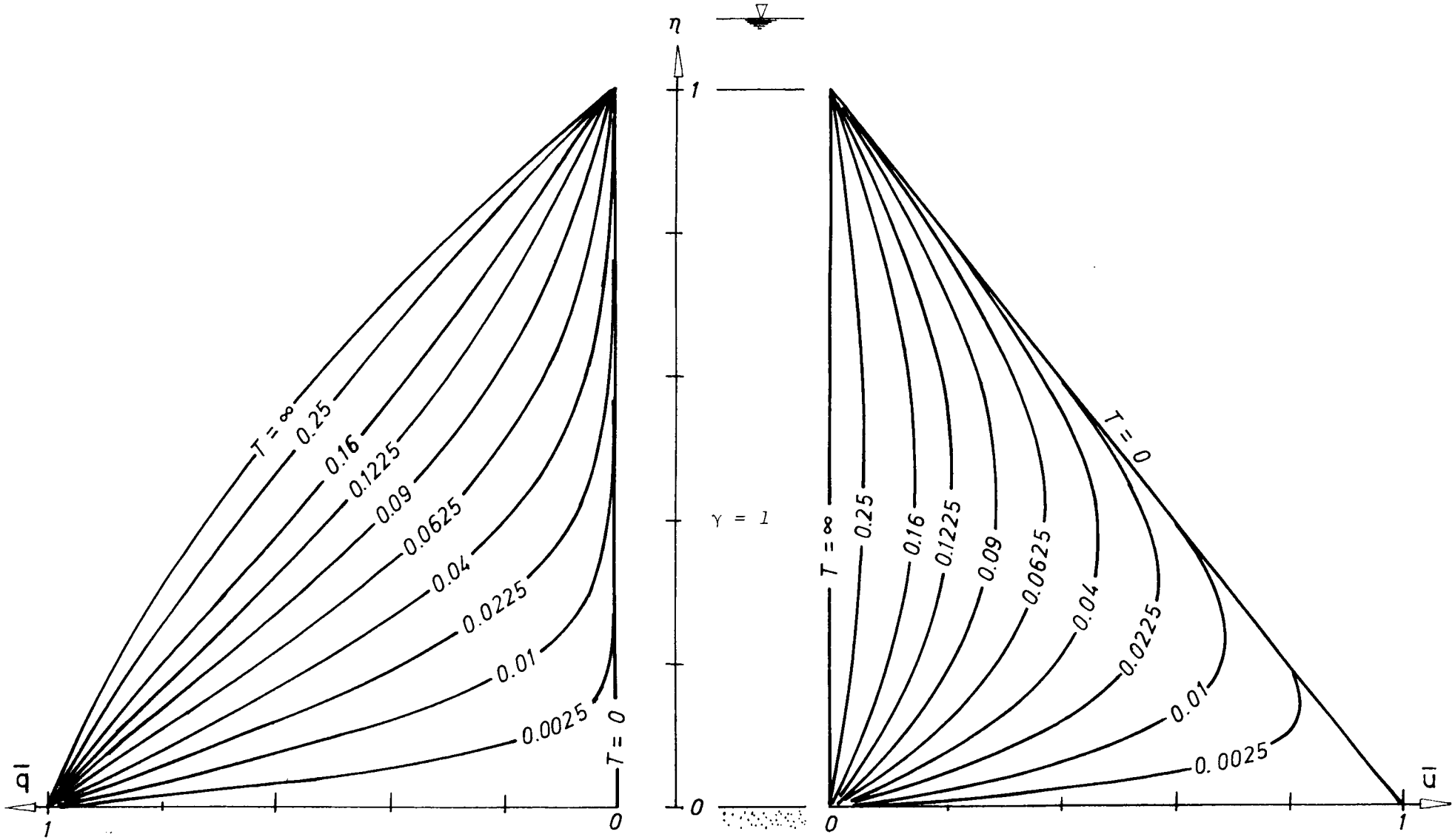

FIG. 6.20 Isochrones of the normalized void ratio change (left) and the normalized excess pore water pressure (right).

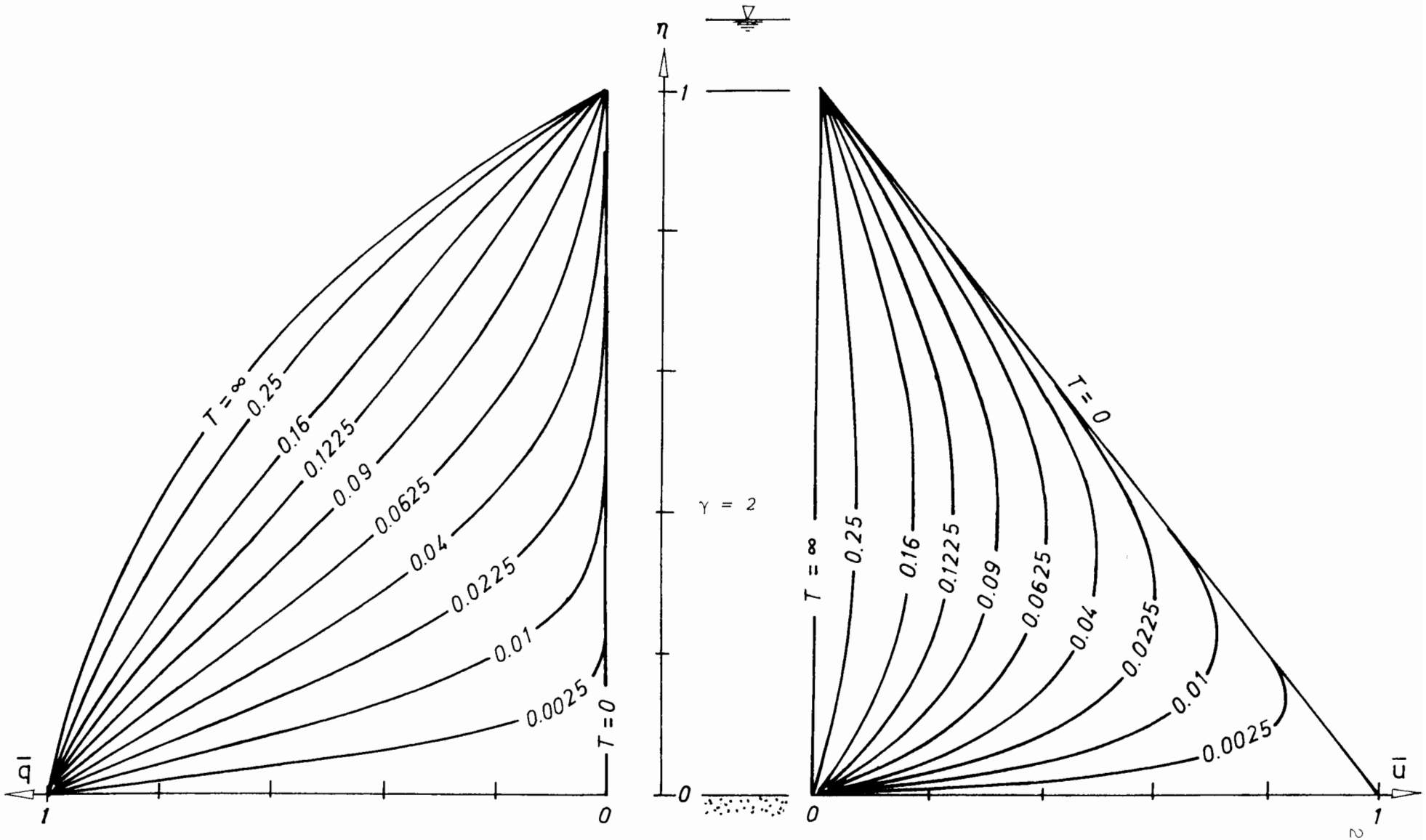

FIG. 6.21 Isochrones of the normalized void ratio change (left) and the normalized excess pore water pressure (right)

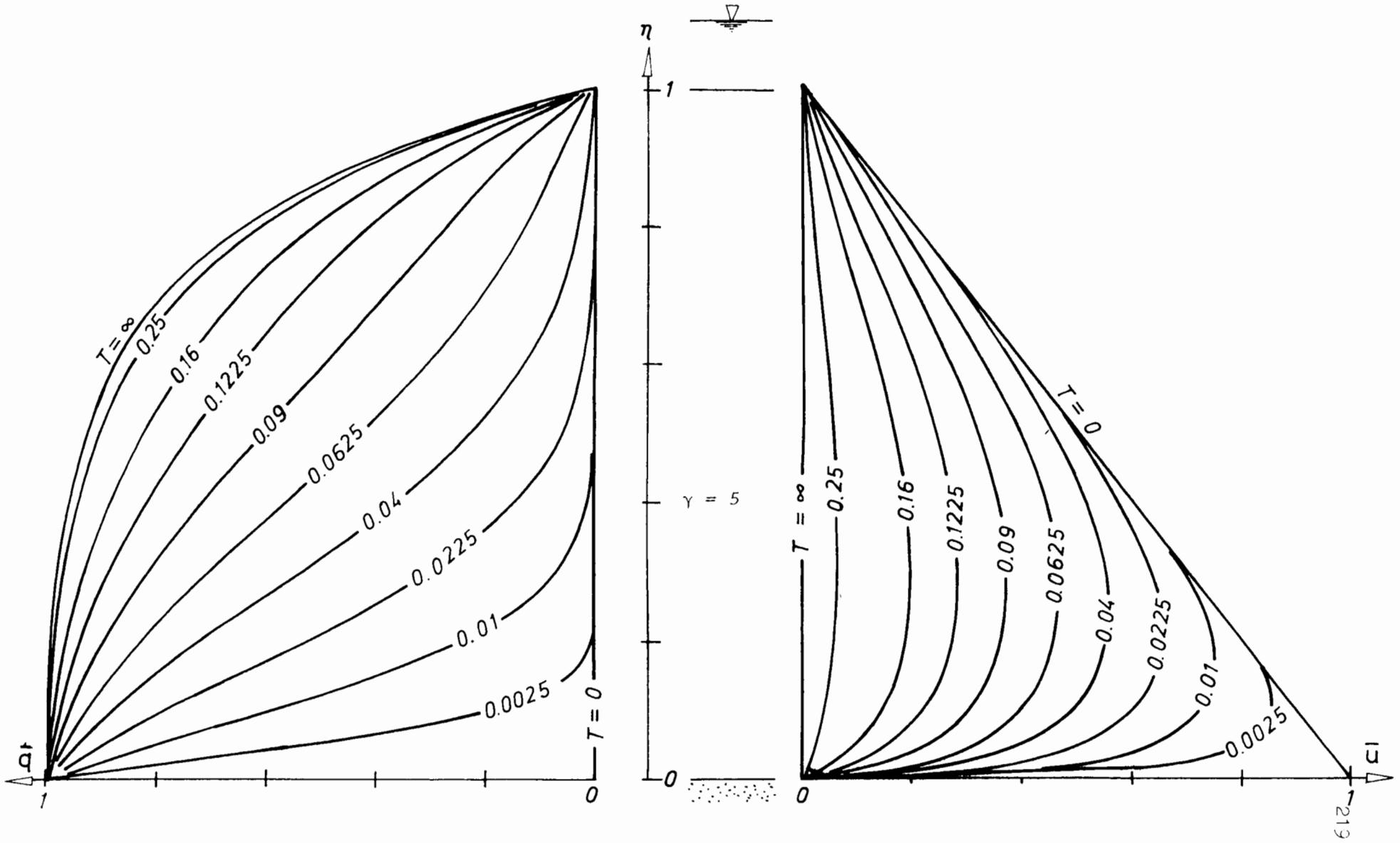

FIG. 6.22 Isochrones of the normalized void ratio change (left) and the normalized excess pore water pressure (right).

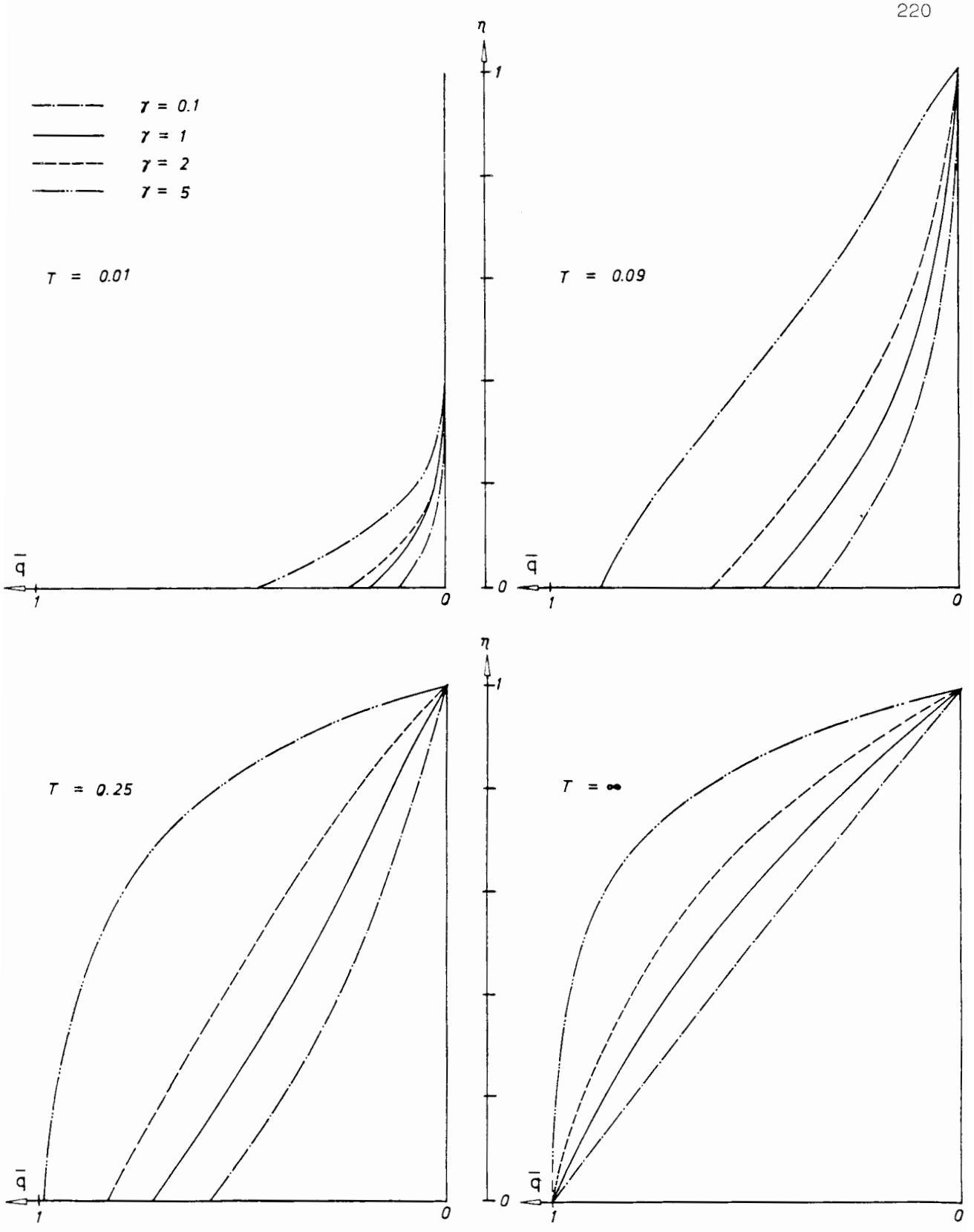

FIG.6.23 Variations of the normalized void ratio change, dredged fill surface drain

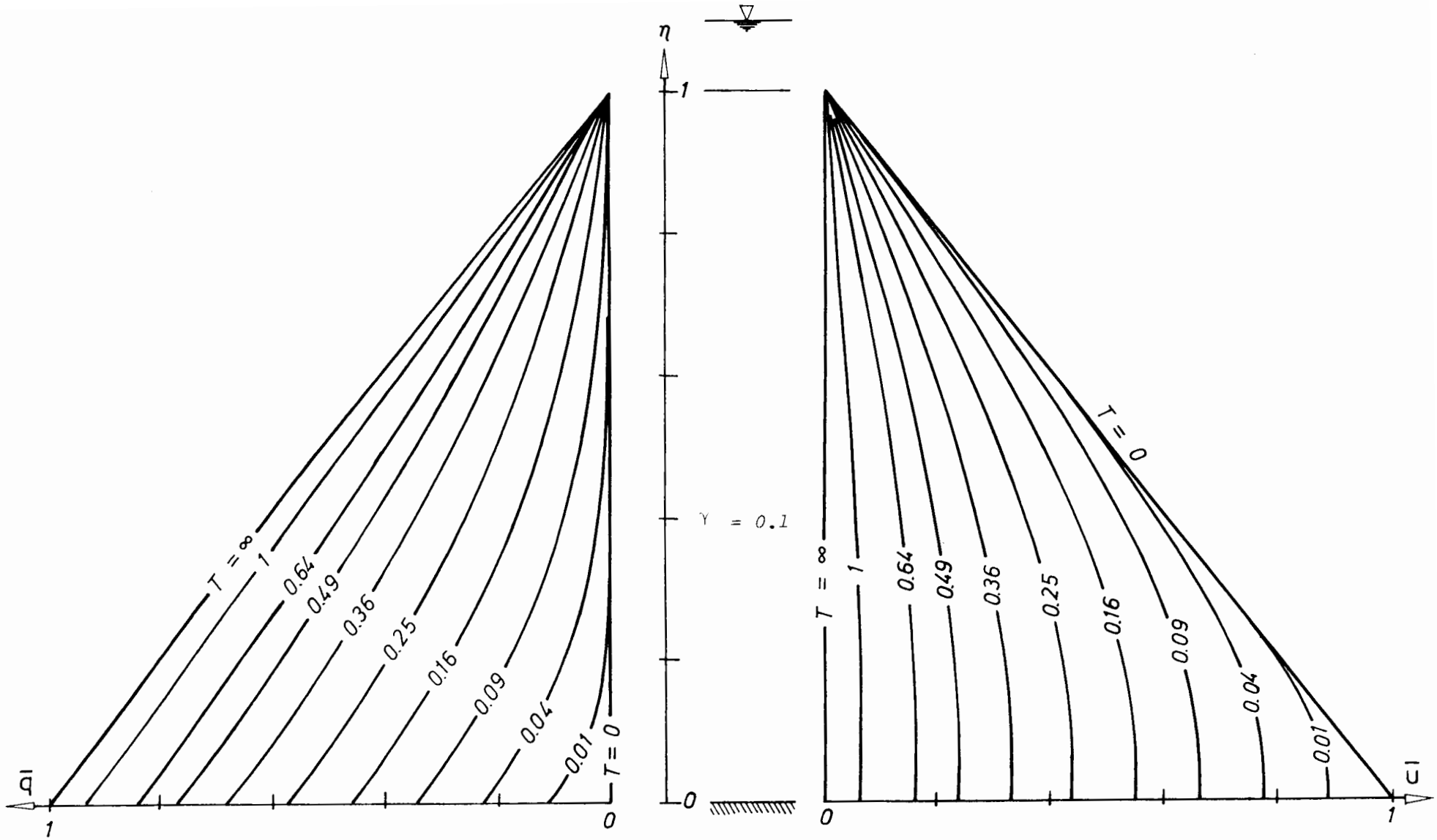

FIG.6.24 Isochrones of the normalized void ratio change (left) and the normalized excess pore water pressure (right)

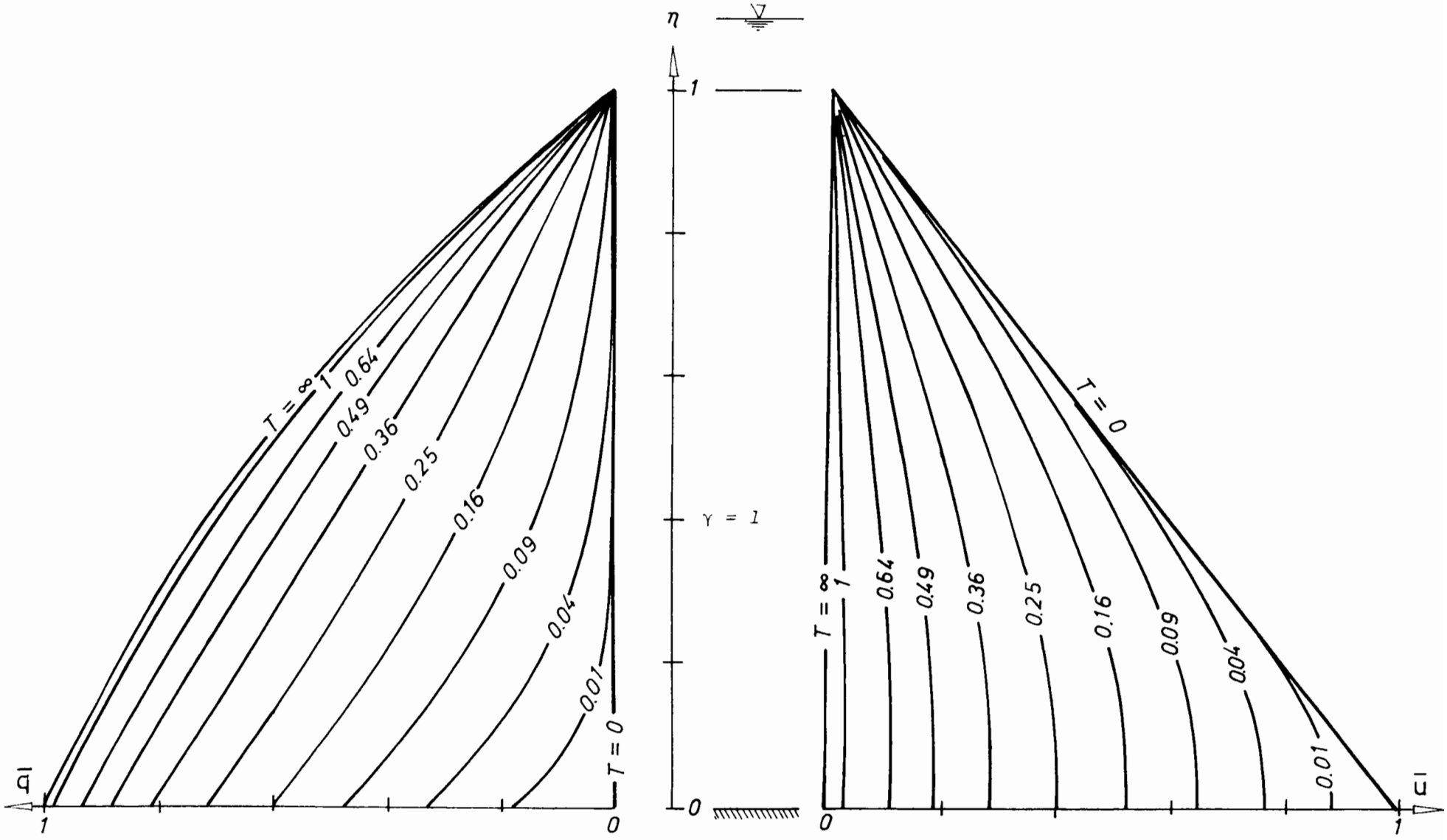

FIG.6.25 Isochrones of the normalized void ratio change (left) and the normalized excess pore water pressure (right)

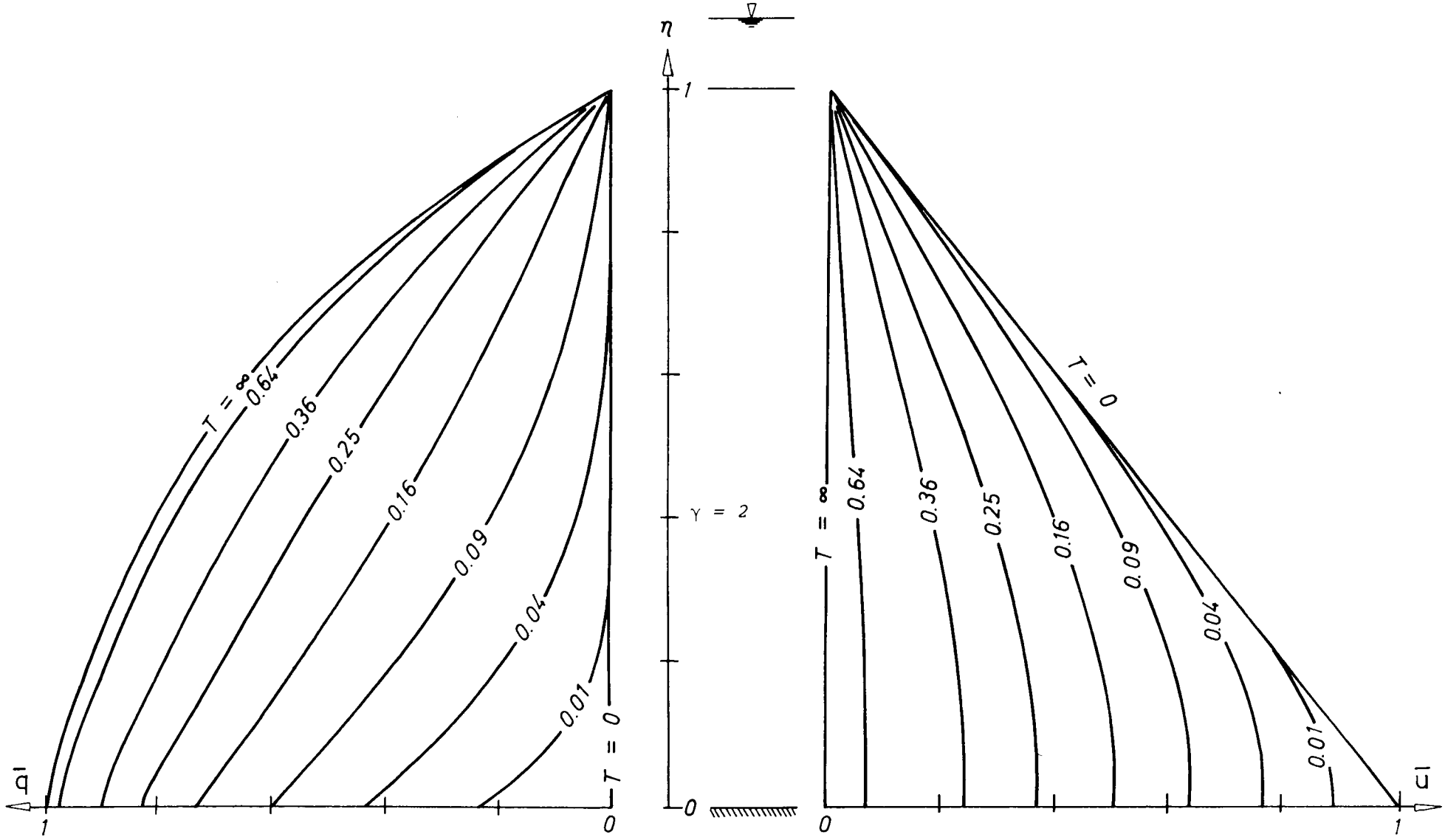

FIG.6.26 Isochrones of the normalized void ratio change (left) and the normalized excess pore water pressure (right)

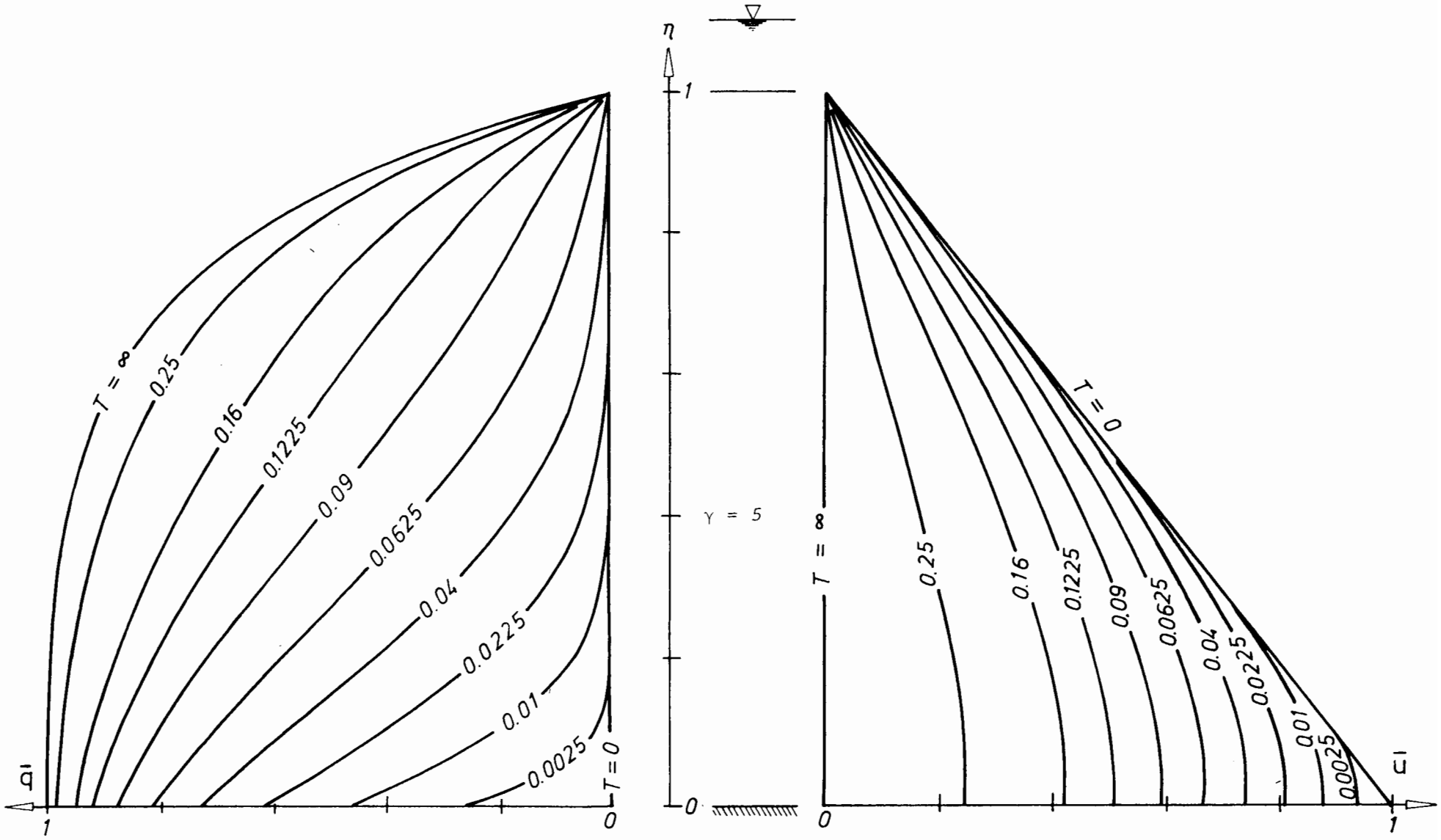

FIG.6.27 Isochrones of the normalized void ratio change (left) and the normalized excess pore water pressure (right)

The distribution of the total stress in terms of the material coordinate z is :

$$\sigma(z) = \int_{z}^{z_o} (\rho_s + \rho_f e) dz \qquad (6.166)$$

And the hydrostatic pore water pressure is :

$$u_h(z) = \rho_f \int_{z}^{z_o} (1+e) dz \qquad (6.167)$$

Eq(6.166,167) are obtained by assuming the ground water table remains in the surface of the fill.

The difference between the total stress and the hydrostatic pore water pressure is :

$$\sigma - u_h = (\rho_s - \rho_f)(z_o - z) \qquad (6.168)$$

Hence, initially,

$$\sigma' = 0, \quad u = (\rho_s - \rho_f)(z_o - z) \qquad (6.169)$$

and

$$u_{max} = (\rho_s - \rho_f) z_o \qquad (6.170)$$

which occurs at the base of the fill.

When the fill has become normally consolidated :

$$u = 0, \quad \sigma' = (\rho_s - \rho_f)(z_o - z) \qquad (6.171)$$

Therefore, during the consolidation stage :

$$u = (\rho_s - \rho_f)(z_o - z) - \sigma' \qquad (6.172)$$

The effective stress σ' can be calculated from the void ratio by the stress - void ratio equation :

$$\sigma' = A - (\rho_s - \rho_f) \frac{C_F}{\beta} ln(e) \qquad (6.173)$$

where,

$$A = (\rho_s - \rho_f) \frac{C_F}{\beta} ln(e_i) \qquad (6.174)$$

Therefore,

$$u = (\rho_s - \rho_f)(z_o - z) - (\rho_s - \rho_f) \frac{C_F}{\beta} ln(e_i) + (\rho_s - \rho_f) \frac{C_F}{\beta} ln(e)$$

This can be simplified to : (6.175)

$$u = (\rho_s - \rho_f) z_o [1 - \eta + \frac{1}{\gamma} ln(\frac{e}{e_i})] \qquad (6.176)$$

From which the normalized excess pore water pressure can be defined :

$$\bar{u} = \frac{u}{u_{max}} = 1 - \eta + \frac{1}{\gamma} ln(\frac{e}{e_i}) \qquad (6.177)$$

The only unknown involved in this expression is the term $\frac{e}{e_i}$, which is :

$$\frac{e}{e_i} = \frac{e_i - q}{e_i} = 1 - \frac{q}{e_i} \qquad (6.178)$$

which can be calculated from the solution q .

The isochrones of this for the double drain are shown in Fig.6.28. It is seen that for larger γ the dissipation of the excess pore water pressure is faster near the surface and slower near the base; this is probably a result of the very low permeability of the soil near the base. As γ is increased, the void ratio in the base is decreased exponentially according to the stress - void ratio law. Since the permeability decreases parabolically with the void ratio, the resulting permeability can be reduced to such an extent that the dissipation of

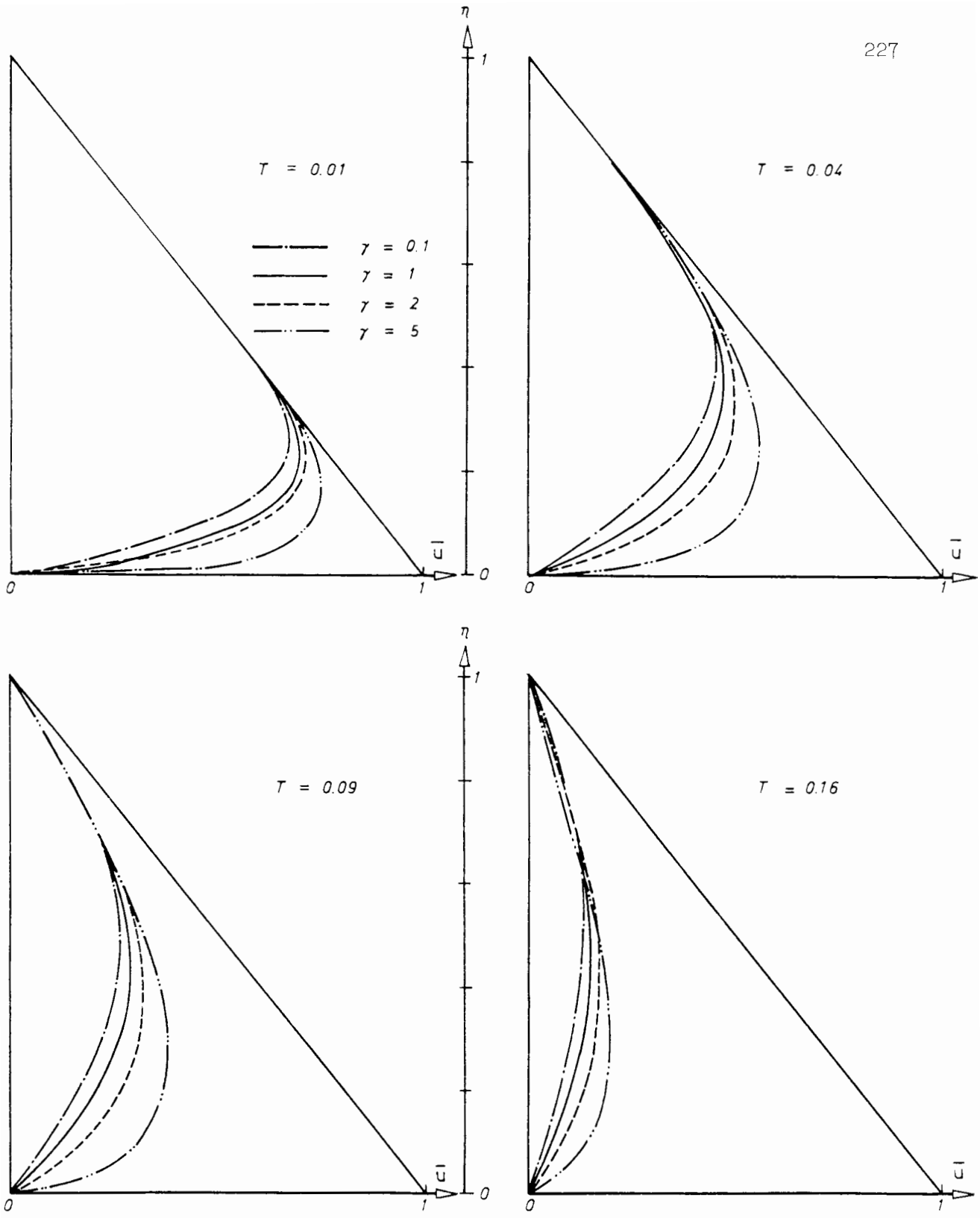

FIG.6.28 Variations of the normalized excess pore water pressure, dredged fill, double drain.

the excess pore water pressure is greatly retarded with larger γ . In the surface drain case shown in Fig.6.29, however, a different behaviour is observed. Here the dissipation of the excess pore water pressure is always faster with larger γ . This also agrees with the isochrones observed in the upper region in the double drain case. More details of the isochrones in each case are presented in Fig.6.19-22 and Fig.6.24-27.

Finally, the dissipation of the excess pore water pressure in the impervious base of the surface drain case is plotted against the square root of time factor in Fig.6.30 for different γ values. For most γ values it can be observed from this figure that there is a nearly linear region during the early stages of consolidation.

The analysis in this Part has been based on a rather unrealistic assumption, that is, the soil is assumed to be dumped on site instantaneously so that consolidation starts with an initially uniform density. In many applications, however, the time delay and the consolidation that occur during the filling operation can not be neglected. To account for these a deposition - consolidation situation will be more appropriate. The next chapter is devoted to such an analysis and considers the very important case of a constant rate of deposition.

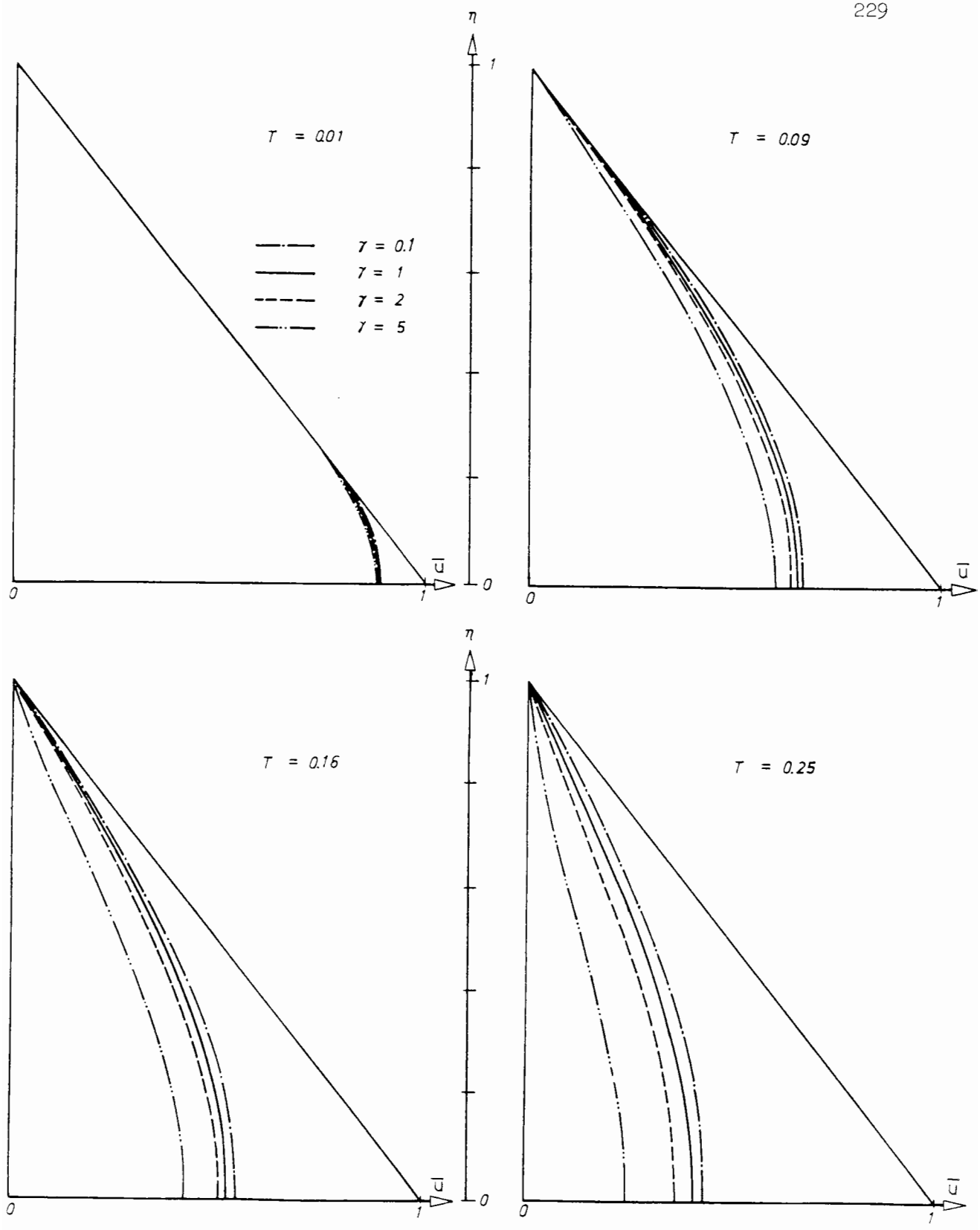

FIG.6.29 Variations of the normalized excess pore water pressure, dredged fill , surface drain.

APPENDIX A EVALUATING THE INVERSE LAPLACE TRANSFORM OF

$$\frac{1}{p}\,\frac{\sqrt{(a^2+p)}\cosh[x\sqrt{(a^2+p)}] + a\sinh[x\sqrt{(a^2+p)}]}{\sqrt{(a^2+p)}\cosh\sqrt{(a^2+p)} + a\sinh\sqrt{(a^2+p)}}$$

According to the inversion theorem (Carslaw and Jaeger, 1948) the inverse transform of this is given by :

$$\frac{1}{2\pi i}\int_{c-i\infty}^{c+i\infty}\frac{\sqrt{(a^2+p)}\cosh[x\sqrt{(a^2+p)}] + a\sinh[x\sqrt{(a^2+p)}]}{\sqrt{(a^2+p)}\cosh\sqrt{(a^2+p)} + a\sinh\sqrt{(a^2+p)}}\,\frac{\exp(pt)}{p}\,dp$$

The integrand is a single-valued function of p and there are poles at :

$$p = 0 \qquad \text{and} \qquad p = -(\beta_o^2 + a^2),\ -(\beta_1^2 + a^2),\ \ldots.$$

where $\pm\beta_o$, $\pm\beta_1$, ... are the zeroes of

$$x\cos x \pm a\sin x$$

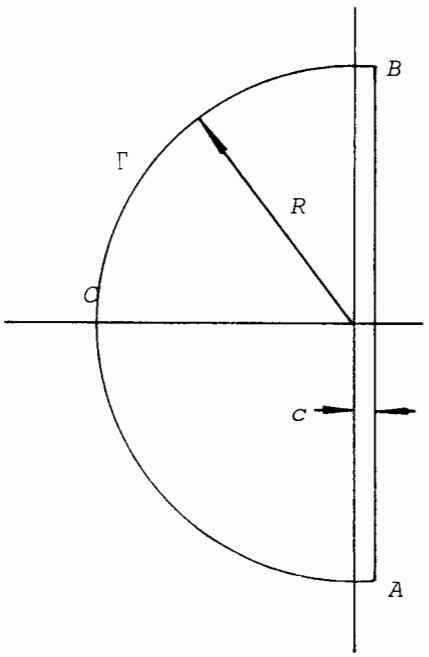

Consider the close contour $ABCA$ shown in the figure. AB is parellel to the imaginary axis at a distance c from it, in this case $c \to 0^+$. The circle Γ has a radius R equals to $(n^2\pi^2 + a^2)$, hence this will not pass through any pole of the integrand.

It can be proved that along the arc BCA :

$$\lim_{p\to\infty}\frac{\sqrt{(a^2+p)}\cosh[x\sqrt{(a^2+p)}] + a\sinh[x\sqrt{(a^2+p)}]}{\sqrt{(a^2+p)}\cosh\sqrt{(a^2+p)} + a\sinh\sqrt{(a^2+p)}} < \infty \quad , 0 \leq x \leq 1$$

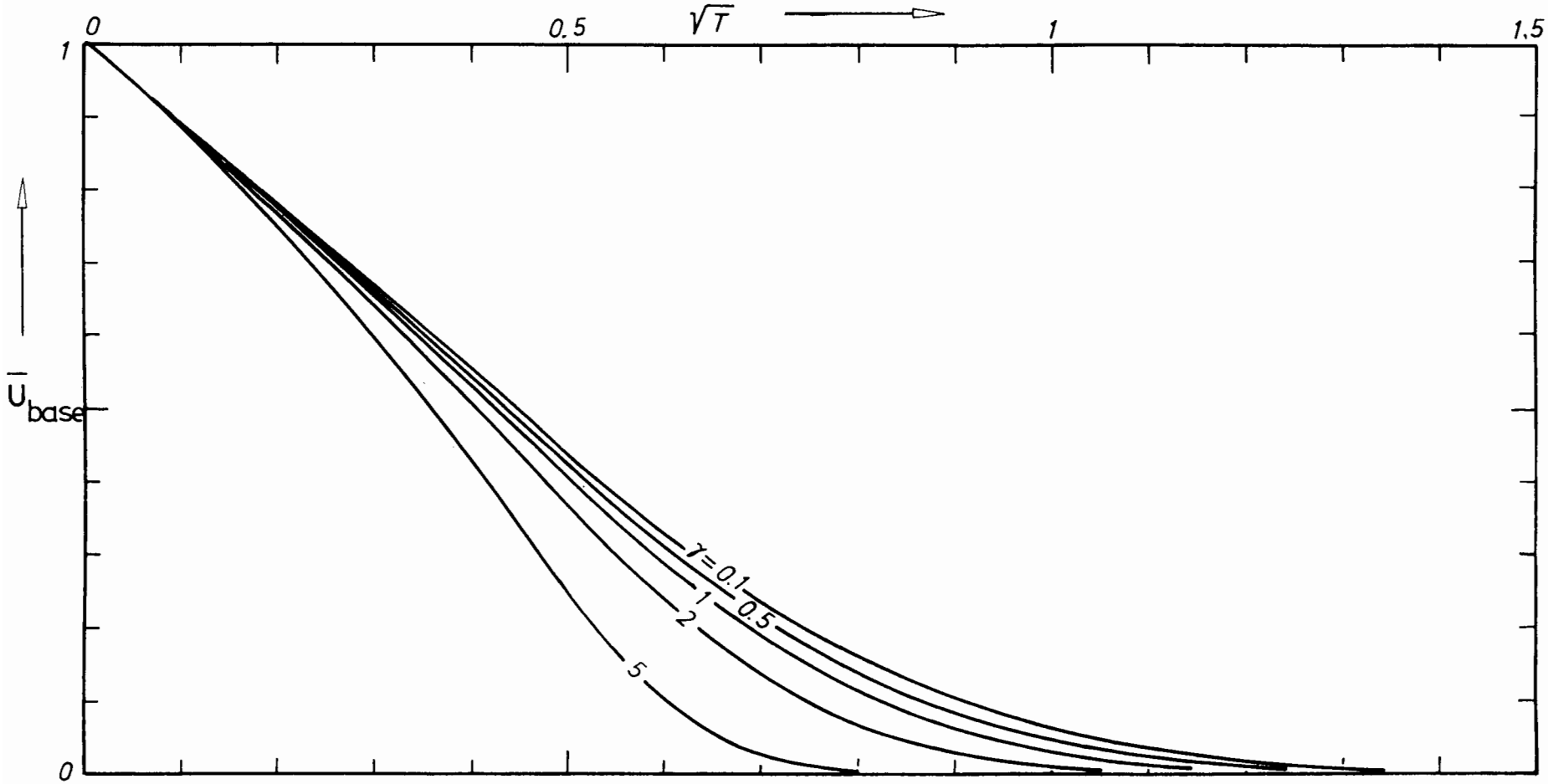

FIG.6.30 Dissipation of the normalized excess pore water pressure in the impervious base of a dredged fill with drainage from the surface.

CHAPTER SEVEN THE CONSOLIDATION DURING A CONSTANT RATE OF DEPOSITION OF A NONLINEAR SOIL

Thus, as $n\to\infty$ the integral over the arc BCA tends to zero (Carslaw and Jaeger, 1948). Consequently, the integral can be replaced by the integral over the closed contour $ABCA$ as $n\to\infty$. By Cauchy's theorem this is equal to the sum of the residues of the integrand at its pole.

The pole at $p=0$ gives $\dfrac{\cosh(ax) \pm \sinh(ax)}{\cosh(a) \pm \sinh(a)}$

and the pole at $p = -(\beta_n^2 + a^2)$ gives :

$$\left.\frac{\sqrt{(a^2+p)}\cosh[x\sqrt{(a^2+p)}] + a\sinh[x\sqrt{(a^2+p)}]}{\frac{d}{dp}[\sqrt{(a^2+p)}\cosh\sqrt{(a^2+p)} + a\sinh\sqrt{(a^2+p)}]}\right|_{p=-(\beta_n^2+a^2)}$$

this is :

$$-\frac{2(-1)^n\beta_n[\beta_n\cos(\beta_n x) \pm a\sin(\beta_n x)]}{\sqrt{(\beta_n^2+a^2)}[\beta_n^2+a(a\pm 1)]}\exp[-(\beta_n^2+a^2)t]$$

Thus the required inverse transform is :

$$\frac{\cosh(ax)\pm\sinh(ax)}{\cosh(a)\pm\sinh(a)} - 2\sum_n \frac{(-1)^n\beta_n[\beta_n\cos(\beta_n x)\pm a\sin(\beta_n x)]}{\sqrt{(\beta_n^2+a^2)}[\beta_n^2+a(a\pm 1)]}\exp[-(\beta_n^2+a^2)t]$$

ABSTRACT

The consolidation of a nonlinear soil during a constant rate of deposition is considered in this chapter. A new parameter, the deposition coefficient μ , is defined. This is a relative measure of the soil permeability to the rate of deposition, whose magnitude will determine the consolidation behaviour of the deposit.

The solutions are obtained numerically by discretizing in space using the finite element technique and a special variable step variable order (VSVO) algorithm for integration in time. Some preliminary studies, which also include the finite difference approximation and the Crank - Nicolson method, indicate that the solution in the later stages of deposition is very sensitive to the numerical procedure employed. The reason for this has not been fully established in the present study.

It is found that for both a pervious and an impervious base a larger deposition coefficient μ will correspond to a better consolidated deposit. The solutions also suggest that as μ tends to zero the present solutions converge to that of the linear soil. The role of μ in the present case is therefore comparable to that of the stratum coefficient γ in the theory of consolidation of an existing stratum, Chapter 6. This interesting observation appears to be a characteristic feature of the nonlinear soil discussed in this and the previous chapters.

1. INTRODUCTION

Following the development of the previous chapter, in this chapter the consolidation during a constant rate of deposition of a nonlinear soil will be considered. As would be expected, this problem is of considerably greater difficulty than its linear counterpart treated in Chapter 5, and numerical techniques will be applied.

The governing equation for the consolidation of the nonlinear soil is :

$$\frac{\partial e}{\partial t} = C_F \frac{\partial^2 e}{\partial z^2} - \beta \frac{\partial e}{\partial z} \tag{7.1}$$

The stratum is undergoing a continuous deposition at a constant rate m and hence the domain of the equation is :

$$0 \leq z \leq mt \ , \quad t \geq 0$$

On the surface the soil will remain at its initial void ratio e_i :

$$e(mt,t) = e_i \tag{7.2}$$

The boundary condition in an impervious base is given by :

$$\frac{\partial e}{\partial z}(0,t) = \frac{\beta}{C_F} e(0,t) \tag{7.3}$$

and in a pervious base this is,

$$e(0,t) = e_i \exp(-\frac{\beta}{C_F} mt) \tag{7.4}$$

If a time factor τ is defined as :

$$\tau = \frac{m^2 t}{C_F} \tag{7.5}$$

and a new variable y :

$$y = \frac{m}{C_F} z + \frac{\beta}{m} \tau \tag{7.6}$$

then the governing equation (7.1) becomes,

$$\frac{\partial \breve{e}}{\partial \tau} = \frac{\partial^2 \breve{e}}{\partial y^2} \tag{7.7}$$

where,

$$\breve{e}(y,\tau) = e(z,t) \tag{7.8}$$

The new equation (7.7) is defined in a moving domain,

$$\frac{\beta}{m} \tau \leq y \leq (1 + \frac{\beta}{m})\tau, \quad \tau \geq 0 \tag{7.9}$$

with the boundary conditions :

$$\breve{e}((1+\frac{\beta}{m})\tau , \tau) = e_i \tag{7.10}$$

and $$\breve{e}(\frac{\beta}{m}\tau , \tau) = e_i \exp(- \frac{\beta}{m}\tau) \quad \text{pervious base} \tag{7.11}$$

or : $$\frac{\partial \breve{e}}{\partial y}(\frac{\beta}{m}\tau ,\tau) = \frac{\beta}{m} \breve{e}(\frac{\beta}{m}\tau ,\tau) \quad \text{impervious base} \tag{7.12}$$

Using the method of generalized potential (see Appendix A of Chapter 5) eq(7.8-12) can be reduced to a system of Volterra equations which can be solved by successive approximation. However, the actual computation of this will require the development of a fairly sophisticated integration algorithm. For this reason this approach is not attempt any further at present.

An alternative approach is to define a variable x as :

$$x = \frac{z}{mt} \tag{7.13}$$

and the void ratio change q :

$$q(x,\tau) = e_i - e(x,\tau) \tag{7.14}$$

where $$e(x,\tau) = e(z,t) \tag{7.15}$$

and τ is the time factor already defined in eq(7.5). Eq(7.1-4) in terms of the new set of parameters become,

$$\frac{\partial q}{\partial \tau} = \frac{1}{\tau^2}\frac{\partial^2 q}{\partial x^2} - \frac{1}{\tau}(\mu - x)\frac{\partial q}{\partial x} \qquad 0 \leq x \leq 1, \quad \tau > 0 \tag{7.16}$$

$$\lim_{\tau \to 0} q(x,\tau) = 0 \tag{7.17}$$

$$q(1,\tau) = 0 \tag{7.18}$$

$$q(0,\tau) = 1 - exp(-\mu\tau) \qquad \text{pervious base} \tag{7.19}$$

$$\frac{\partial q}{\partial x}(0,\tau) = \mu\tau[q(0,\tau) - 1] \qquad \text{impervious base} \tag{7.20}$$

Note that eq(7.17) is an additional initial condition which does not exist in the original equations. The parameter μ appearing in the equations is the deposition coefficient defined as :

$$\mu = \frac{\beta}{m} \tag{7.21}$$

This gives the ratio of the soil permeability, which is characterized by β , and the deposition rate m . The product of this with the time factor τ is the stratum coefficient γ of the deposit at the corresponding time t during deposition, i.e. :

$$\mu\tau = \frac{\beta}{m}\frac{m^2 t}{C_F} = \left(\frac{\beta}{C_F}\right) mt \tag{7.22}$$

In the numerical work a new parameter $p(x,\tau)$ will be used instead of q, defined as :

$$p(x,\tau) = q(x,\tau) - [\, 1 - exp[-\mu\tau(1-x)]] \tag{7.23}$$

and the equations in terms of this will be :

$$\frac{\partial p}{\partial \tau} = \frac{1}{\tau^2}\frac{\partial^2 p}{\partial x^2} - \frac{1}{\tau}(\mu - x)\frac{\partial p}{\partial x} - \mu\, exp[-\mu\tau(1-x)] \tag{7.24}$$

$$\lim_{\tau \to 0} p(x,\tau) = 0 \tag{7.25}$$

$$p(1,\tau) = 0 \tag{7.26}$$

$$p(0,\tau) = 0 \qquad \text{pervious base} \tag{7.27}$$

$$\frac{\partial p}{\partial x}(0,\tau) = \mu\tau\, p(0,\tau) \qquad \text{impervious base} \tag{7.28}$$

This results in a simpler boundary condition and a slightly more complicated governing equation. The choice of either the variable p or q is therefore an individual preferrence, which also depends to a certain extent on the numerical algorithms available.

In analyzing the solutions, dimensionless parameters related to the state of consolidation of the deposit will be more useful, and two parameters have been chosen here. These are the local degree of consolidation f and the degree of settlement S defined as :

$$f(x,\tau) = \frac{\text{present void ratio change}}{\text{the required void ratio change for the fully consolidated state}}$$

$$= \frac{q(x,\tau)}{1 - exp[-\mu\tau(1-x)]}$$

$$= 1 - \frac{p(x,\tau)}{1 - exp[-\mu\tau(1-x)]} \qquad x \neq 1 \tag{7.29}$$

$$S(\tau) = 1 + \frac{\int_0^1 p(x,\tau)d\tau}{1 - \frac{1}{\mu\tau}[\,1 - exp(-\mu\tau)\,]}, \quad \mu\tau \neq 0 \qquad (7.30)$$

The governing equation will be discretized in space by the finite element method which results in a system of ordinary differential equations. This will be followed by a variable step variable order algorithm to perform the integration of the equations. These and the results of some preliminary numerical experiments will be described in the following section.

2. DEVELOPMENT OF NUMERICAL SOLUTIONS

Finite Element Discretization in Space

The coordinate x, now confined in the domain $(0,1)$, is divided into segments of arbitrary length with nodes x_i.

Let, $$0 = x_o < x_1 < \quad \ldots\ldots \quad < x_n = 1 \qquad (7.31)$$

and $$h_i = x_i - x_{i-1} \qquad (7.32)$$

be the nodes and lengths of each segment (element) respectively. The unknown function $p(x,\tau)$ at any time τ is approximated within each element by the Hermite piecewise cubic polynomials $V(x)$ and $W(x)$, i.e.:

$$p(x,\tau) \simeq P(x,\tau) = \sum_i [\, a_i(\tau)V_i(x) + b_i(\tau)W_i(x) \,] \qquad (7.33)$$

where

$$V_i(x) = \begin{cases} V((x-x_i)/h_{i+1}) & x \geq x_i \\ V((x-x_i)/h_i) & x \leq x_i \end{cases} \qquad (7.34)$$

$$W_i(x) = \begin{cases} h_{i+1}\, W((x-x_i)/h_{i+1}) & x \geq x_i \\ h_i\, W((x-x_i)/h_i) & x \leq x_i \end{cases} \qquad (7.34)$$

$$i = 0, 1, 2, \ldots, n \qquad h_o = h_{n+1} = 1$$

where,

$$V(x) = \begin{cases} 1 - 3x^2 + 2x^3 & 0 \leq x \leq 1 \\ 1 - 3x^2 - 2x^3 & -1 \leq x \leq 0 \\ 0 & \text{otherwise} \end{cases}$$

$$W(x) = \begin{cases} x\,(1-x)^2 & 0 \leq x \leq 1 \\ x\,(1+x)^2 & -1 \leq x \leq 0 \\ 0 & \text{otherwise} \end{cases} \qquad (7.35)$$

The basis functions $V(x)$ and $W(x)$ are shown in Fig.7.1 with the first and second derivatives. It can be seen from eq(7.33) that $a_i(\tau)$ is the function value $p(x,\tau)$ and $b_i(\tau)$ is the first derivative, $\frac{\partial p}{\partial x}$, at the node x_i. This type of approximation therefore ensures continuity of the approximate solution to the first derivative.

Since there are $(n+1)$ nodes in the discretization and in each node two unknowns a_i, b_i are to be determined, the total number of unknowns is $2(n+1)$. Two of these can be obtained from the boundary conditions, this leaves $2n$ unknowns to be determined.

The $2n$ unknowns a_i, b_i are determined in the present study by the collocation method, where the governing equation (7.24) is satisfied exactly at some specified points. This results in simpler implementation as well as more efficient computation in comparison with other methods. In their work Douglas and Dupont (1973) have shown that had the collocating points being chosen as the Gaussian points within each element, i.e. :

$$\zeta_{i,k} = \frac{1}{2}\,(x_{i-1} + x_i) + (-1)^k\, h_i\, \frac{1}{2\sqrt{3}}, \quad k=1,2 \qquad (7.36)$$

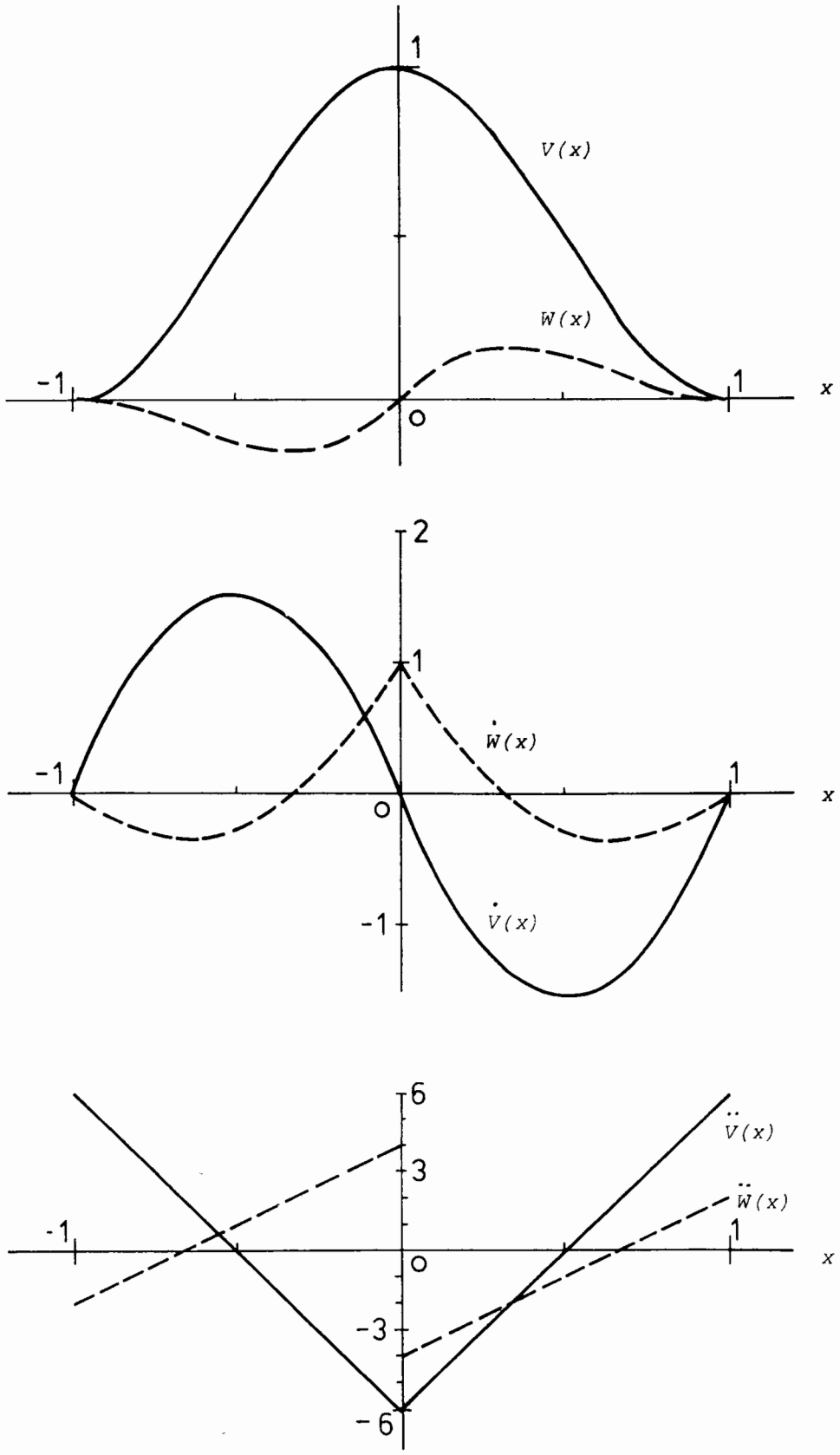

FIG.7.] *The basis functions V(x) and W(x) and their derivatives*

then this method should yield comparable accuracy with the Galerkin method, i.e. with a truncation error of $O(h^4)$ where h is the length of the largest element.

Since there are n elements in use, the number of collocating points is therefore $2n$. Satisfying the governing equation at each point then yields $2n$ equations for the $2n$ unknowns. Thus, the governing equation is approximated by :

$$\{\frac{\partial P}{\partial \tau} - \frac{1}{\tau^2}\frac{\partial^2 P}{\partial x^2} + \frac{1}{\tau}(\mu - x)\frac{\partial P}{\partial x} + \mu \exp[-\mu\tau(1-x)]\}(\zeta_{i,k}, \tau) = 0 \tag{7.37}$$

or :

$$\tilde{A}\frac{d\tilde{y}}{d\tau} = \tilde{B}\tilde{y} + \tilde{C} \tag{7.38}$$

in the matrix form, where $\tilde{y}$ is the solution vector of dimension $(2n)$. $\tilde{A}$ and $\tilde{B}$ are both pentadiagonal matrices of dimension $(2n \times 2n)$ whose coefficients are obtained from the finite element collocation via some pretty heavy algebra. $\tilde{C}$ is the coefficient vector. Alternatively, this equation can be written as :

$$\frac{d\tilde{y}}{d\tau} = \tilde{A}^{-1}\tilde{B}\tilde{y} + \tilde{A}^{-1}\tilde{C} \tag{7.39}$$

where $\tilde{A}^{-1}$ is the inverse matrix of $\tilde{A}$.

Note that in the pervious base case the boundary conditions give :

$$a_o(\tau) = a_n(\tau) = 0 \tag{7.40}$$

and the solution vector $\tilde{y}$ is thus :

$$\tilde{y} = [\, b_o , a_1 , b_1 , \ldots\ldots , a_{n-1} , b_{n-1} , b_n \,] \tag{7.41}$$

While in the impervious base case :

$$a_n(\tau) = 0 \tag{7.42}$$

and

$$b_o(\tau) = \mu\tau\, a_o(\tau) \tag{7.43}$$

hence the solution vector $\tilde{y}$:

$$\tilde{y} = [\, a_o\, ,\, a_1\, ,\, b_1\, ,\, \ldots\ldots\, ,\, a_{n-1}\, ,\, b_{n-1}\, ,\, b_n\,] \tag{7.44}$$

Accordingly, different arrangements of the matrices $\tilde{A}$ and $\tilde{B}$ will be required in each case.

Integration in Time

Eq(7.38) or eq(7.39) as derived from the finite element collocation are both systems of differential equations. The system can be written as :

$$\frac{d\tilde{y}}{d\tau} = \tilde{f}\,(\tau,\tilde{y}) \tag{7.45}$$

with initial condition :

$$\tilde{y}(0) = \tilde{0} \tag{7.46}$$

where $\tilde{0}$ is the null vector. The solution is therefore :

$$\tilde{y}(\tau) = \tilde{y}(0) + \int_0^{\tau} \tilde{f}(t,\tilde{y})\,dt \tag{7.47}$$

or, alternatively, a step by step solution :

$$\tilde{y}(\tau_{j+1}) = \tilde{y}(\tau_j) + \int_{\tau_j}^{\tau_{j+1}} \tilde{f}(t,\tilde{y})\,dt \tag{7.48}$$

which integrates in time with steps $(\tau_{j+1}-\tau_j)$. An integration scheme

which requires the knowledge of $\tilde{f}(\tau_{i+1},\tilde{y})$ is said to be implicit, with one example being the Crank - Nicolson method in which the trapezoidal rule is used for integration. An implicit scheme possesses the advantage of stability. However, if this is applied to the present situation then a great amount of computation will be required in the inversion of the matrix $\tilde{A}$ and the multiplication of matrices. Furthermore, the advantage associated with the banded structures of the matrices $\tilde{A}$ and $\tilde{B}$ will not be fully utilized. For this reason a semi-implicit VSVO algorithm is used instead of the fully implicit methods.

A detailed description of the VSVO algorithm is given by Gear (1971) which also lists a general purpose subroutine DIFSUB for stiff equations. This general purpose subroutine has been implemented in the NAG library as D02AEF which is available in the Oxford University Computing Centre.

Briefly, this algorithm approximates the integrand in eq(7.48) by a kth order polynomial from a knowledge of intermediate points that has been obtained in the previous steps. The starting solution is obtained by a predictor formula which initiates a correction (iterative) process. At the end of each iteration the convergence of the solution is checked with a prescribed error bound in a mixed sense (i.e. both the absolute and the relative errors depends on the magnitude of the solution). If the solution fails to converge after a predetermined number of cycles of iteration, then either a higher order formula or a reduced step size is automatically selected by the subroutine until the error bound is achieved.

During the execution of the subroutine $\tilde{f}(\tau,\tilde{y})$ must be evaluated given $\tilde{y}$ and τ . The major task at this stage of programming is therefore that of solving a system of simultaneous linear equations, eq(7.38), in which, due to the pentadiagonal structure of the matrices $\tilde{A}$ and $\tilde{B}$, a very efficient algorithm can be used (von Rosenberg 1969).

The numerical techniques outlined above have been written in a program which is listed at the end of this thesis. A brief description of this program is given in Appendix A of this chapter.

Some Preliminary Numerical Experiments

Before the bulk of the computation is commenced, some preliminary experiments with different time steps and element arrangements are performed to optimize the computing labour and accuracy. For the purpose of comparison the finite difference approximation and the Crank - Nicolson method have also been included. A pervious base is assumed , and a deposition coefficient of $\mu = 0.1$ is used, with the time steps so arranged that each step spans an equal interval on a logrithmatic time scale. The error bound within each step of integration (the local truncation error) is specified as 1×10^{-6}, which is recommended by the NAG library for a single precision arithmatic.

It has been found that the solution is insensitive to the actual size of the time step taken provided that the same error bound is used. The largest possible time step will therefore be preferred as not only is less computing labour involved but the possibility of accumulated error with each increment of time step is also reduced. In general, the present method of assigning the time step has been found satisfactory.

Thus, each decade of time factor is divided into ten roughly equal spans on the logrithmatic scale as 1, 1.25, 1.6, 2, 2.5, 3, 4, 5, 6.5, 8 and the integration starts at $\tau = 0.001$ since a singularity will occur at $\tau = 0$. It has been found that the effect of this starting time on the solution is negligible provided that a reasonably small magnitude is chosen.

The first type of element used is that of equal length, see

Fig.7.2(a). The solutions for 10 and 20 such elements are shown in column 1 and column 2 of Table7.1. It can be seen that these two give comparable results until $\tau=100$, after which the difference is magnified rapidly. This is also accompanied by a 'drop', i.e. the solutions decrease to a minimum value then increase upwards after which greater difference is found between the solutions.

Comparing the variation of the local degree of consolidation of the two solutions reveals that the difference between these two after $\tau=100$ is most noticeable in the upper half of the deposit. It was therefore decided to allocate more elements in this region and two possibilities have been considered. The first uses seven elements in the upper half and three elements in the lower half of the deposit, this is shown in Fig.7.2(b). The second method employes convergent elements such that the ratio of the lengths of adjacent elements is a constant, i.e. this forms a geometric progression with, in the present case, the ratio (scale factor) fixed as 0.9, see Fig.7.2(c). It has been found that these two arrangements yield solutions which are almost identical, and the latter is finally chosen for the discussion and the actual computation.

The solutions of 10 and 20 convergent elements are given in column 3 and column 4 of Table7.1 respectively. It can be seen that a considerable improvement has been achieved by using the convergent element, as column 3, which is the solution for 10 convergent elements, agrees better with column 2, which is obtained from 20 equal elements, than column 1, the 10 equal elements solution. Furthermore, no 'drop' is observed in the 20 convergent elements solution, column 4, up to $\tau=1000$.

The 'drop' observed in most of the solutions is curious behaviour, and Fig.7.3 compares the solutions from three different numerical procedures with $\mu=0.1$ and a pervious base. Curve 1 to 3 are

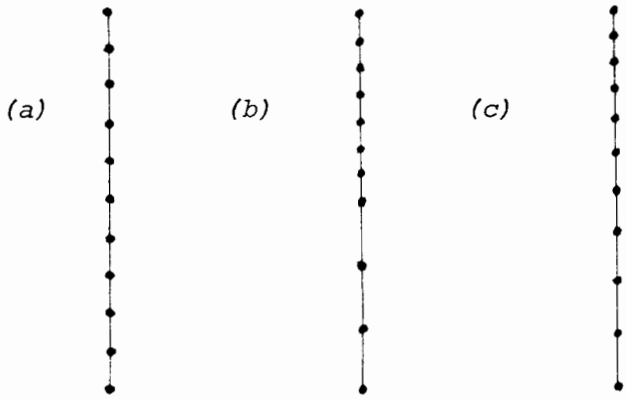

FIG.7.2 Three different methods of allocating elements.

Time Factor	Degree of Settlement x 10^6			
	1	*2*	*3*	*4*
0.125	979832	979832	979832	979832
0.2	968328	968328	968328	968328
0.5	926154	926156	926155	926156
1	866676	866683	866681	866683
2	774967	774987	774980	774987
5	608501	608562	608542	608562
10	470289	470406	470375	470411
20	346923	347158	347091	347161
50	229568	230171	229891	230159
100	175507	176714	175967	176669
200	141379	143685	142044	143714
500	122839*	117645	115876	118889
650	133901	113149	114970*	114345
800	155452	111598*	120213	111295
1000	195964	113892	135974	108429

TABLE 7.1 COMPARISON OF SOLUTIONS, PERVIOUS BASE,

1 -.10 equal elements *2* - 20 equal elements

3 - 10 convergent elements with scale factor 0.9

4 - 20 convergent elements with scale factor 0.9

* denotes minimum value recorded

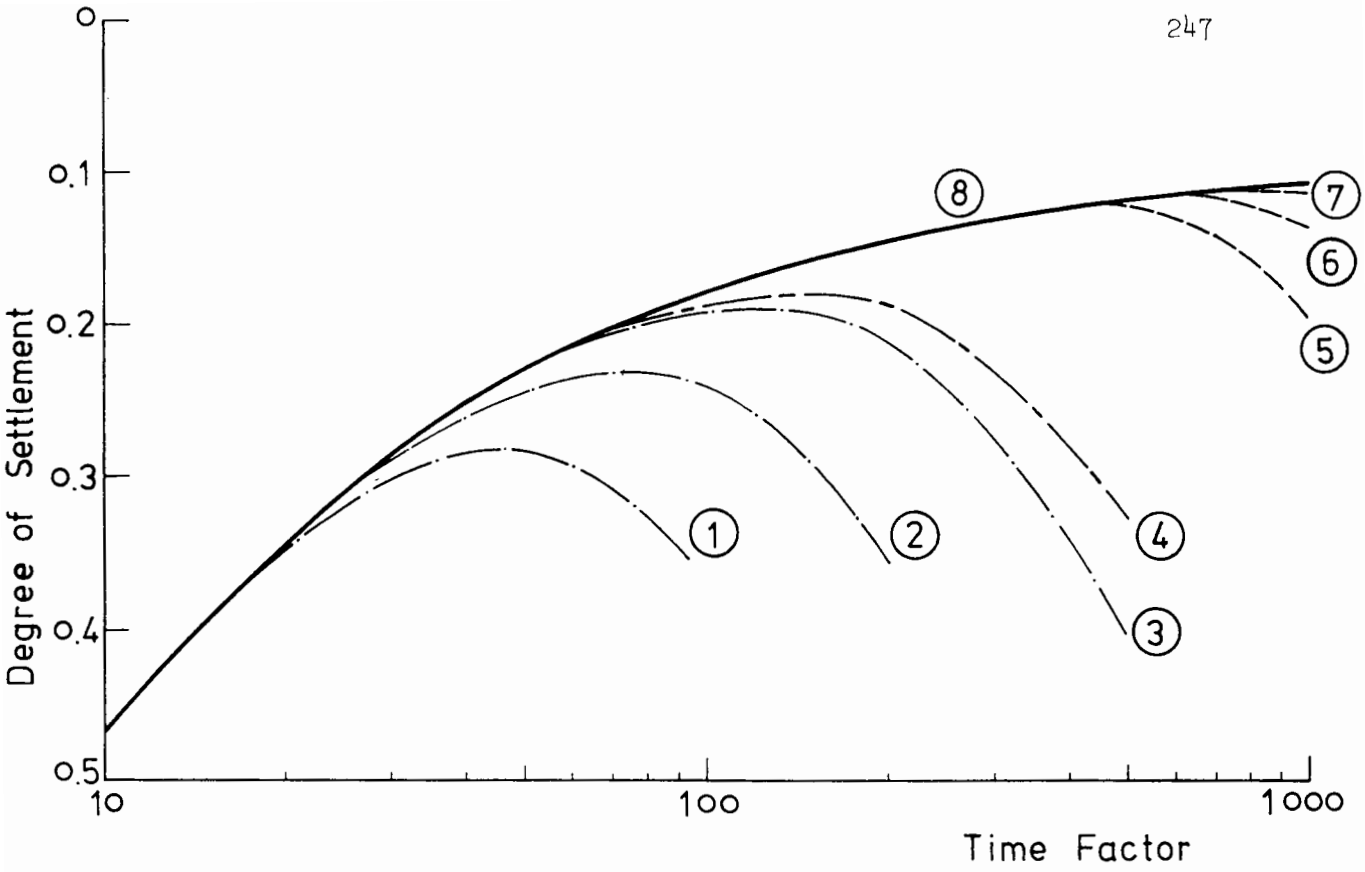

FIG.7.3 The occurrence of 'drop' in the solutions of different numerical procedures.

solutions obtained by using the finite difference approximation in space and the VSVO algorithm with 10, 20 and 40 space grids respectively. Curve 4 is obtained by combining a 20 space grid finite difference approximation with the Crank - Nicolson method which takes a time step four times smaller than that of the VSVO algorithm. Curves 5 to 8 correspond to the cases of column 1 to 4 of Table7.1, i.e. the finite element with VSVO algorithm. All except curve 8, which is obtained by using 20 convergent elements and the VSVO algorithm, show a 'drop' before the end of the program $\tau=1000$. It appears from this figure that these curves follow the 'best' solution, curve 8, till some stage before the seperation and the eventual drop.

Given the same time marching scheme, better agreement between a solution and curve 8 is associated with improved space discretization

method. The Crank - Nicolson also appears to be better than the VSVO algorithm when the finite difference approximation is used for space discretization. This is probably because in such a case the Crank - Nicolson does not require an iterative process which results in less roundoff and accumulated error as compared with the VSVO algorithm.

At present the cause that leads to the 'drop' has not been fully understood, and further work will be required. A different approach, such as solving the integral equation that arises in the method of generalized potential, will be most advantageous for this purpose.

The above discussions have been confined to the pervious base. Similar behaviour has also been observed in the impervious base and hence it will not be presented here.

Following the preliminary experiments the actual computation proceeded with the numerical technique developed in this section. In the following sections the solutions corresponding to a pervious and an impervious base will be discussed.

3. DEPOSITION ONTO A PERVIOUS BASE

The solutions are obtained by using 20 convergent elements with a scale factor 0.9. Integration starts at $\tau=0.001$ with each decade divided into 10 steps and the truncation error in each step is kept within 1×10^{-6} by the VSVO subroutine. Computation will proceed until $\tau=1000$ or an increase in the degree of settlement ('drop') is detected, whichever occurs first. Six cases have been computed with μ, the deposition coefficient, takes the value $0.1, 0.2(0.2)1.0$.

Fig.7.4 shows the relationship between the degree of settlement and the time factor. Also shown in this figure by a broken line is the solution corresponding to the linear soil developed in Chapter 5. It can be seen from this figure that the deposit is better consolidated with larger μ . This means that, for example, if two soils having the same coefficient of consolidation c_F are deposited at the same speed m, the more permeable one will have a larger value of μ and hence, according to the solutions, will consolidated faster. For a given μ , the state of consolidation of the deposit, represented by the degree of settlement , becomes worse with time, i.e. as deposition proceeds the deposit becomes less consolidated. A similar observation has been made before in the linear soil model, Chapter 5. Furthermore, the solutions suggest that, as μ tends to zero, the solution of the nonlinear soil will converge to that of the linear soil.

Except the $\mu=0.1$ and $\mu=0.2$ cases the solutions were not recorded to $\tau=1000$ as an increase in the degree of settlement is detected earlier than this. Every curve in Fig.7.4 is therefore drawn to the point of increase in the degree of settlement. It can be seen that with larger μ this point is reached earlier.

In section 1 of this chapter it has been pointed out that the stratum coefficient γ of the deposit is given by the product of the deposition coefficient μ and the time factor τ . The maximum value of γ that can be used in the nonlinear soil model would probably be 10 (in which case according to the theory the void ratio in the base of the stratum when this becomes fully consolidated will be 22026 times smaller than the void ratio in the surface !). Hence, it will be meaningless to record the solution to a time factor greater than that given by the limit $\mu\tau=10$. For example, when $\mu=0.1$ then $\tau=100$ will be the practical upper limit of the useful solution.

Bearing this in mind and noting that in Fig.7.4 all curves

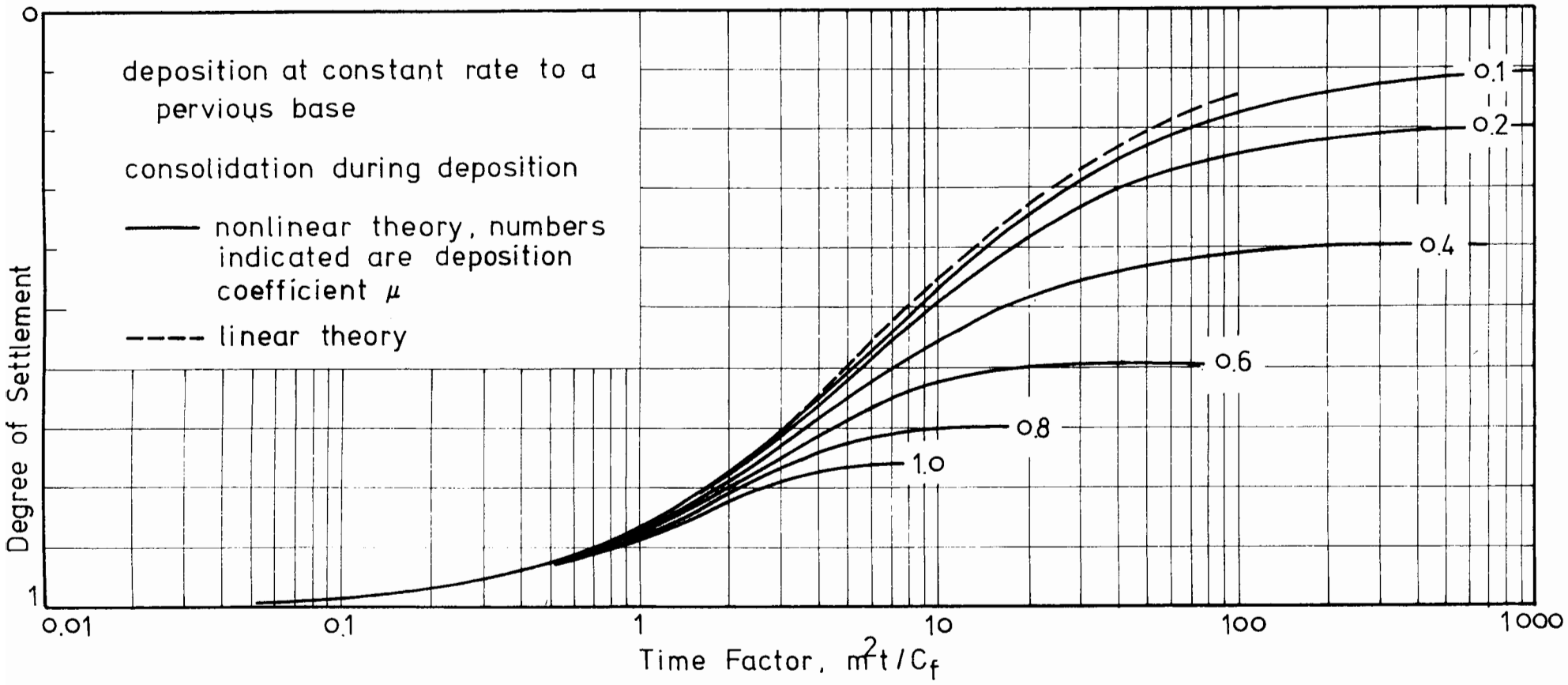

FIG.7.4 Degree of settlement versus the time factor for a deposit undergoing a constant rate of deposition.

except that of $\mu=1$ have the 'drop' occuring beyond the $\mu T=10$ limit, this drop that is observed in the solutions is in fact of little practical consequence.

The variation of the local degree of consolidation for each of the six cases considered is shown in Fig.7.5(a)-(f). It can be seen that the deposit has now become less consolidated with continuing deposition. However, at some stage depending on the deposition coefficient, the lower part of the deposit begins to be better consolidated (as the isochrones in this part move towards the right) while the consolidation state in the upper part is still decreasing. This is more noticeable in the cases of $\mu=0.2$, 0.4 and 0.6 . It can also be noticed that with increasing μ this 'inflection point' seems to move upward (in terms of the material coordinate). Discussion of these points will be provided in the next section when considering the impervious base.

In practical applications these isochrones can be used as a basis to calculate the void ratio and the excess pore pressure distribution in the deposit. The procedure will follow that outlined in the previous chapter of the dredged fill case and will not be described here.

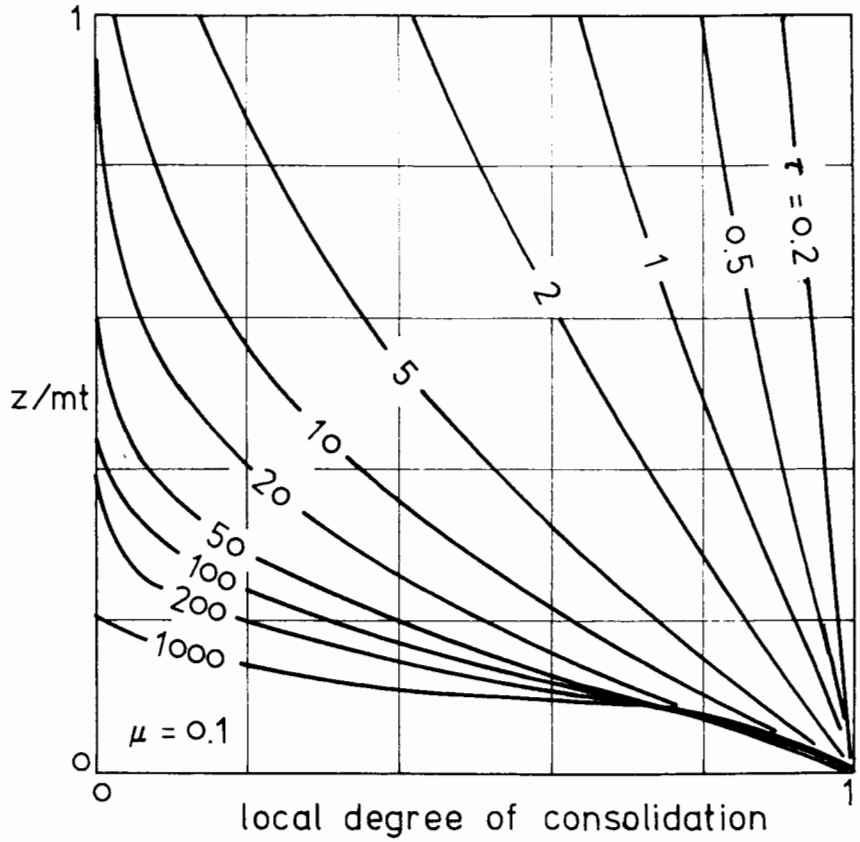

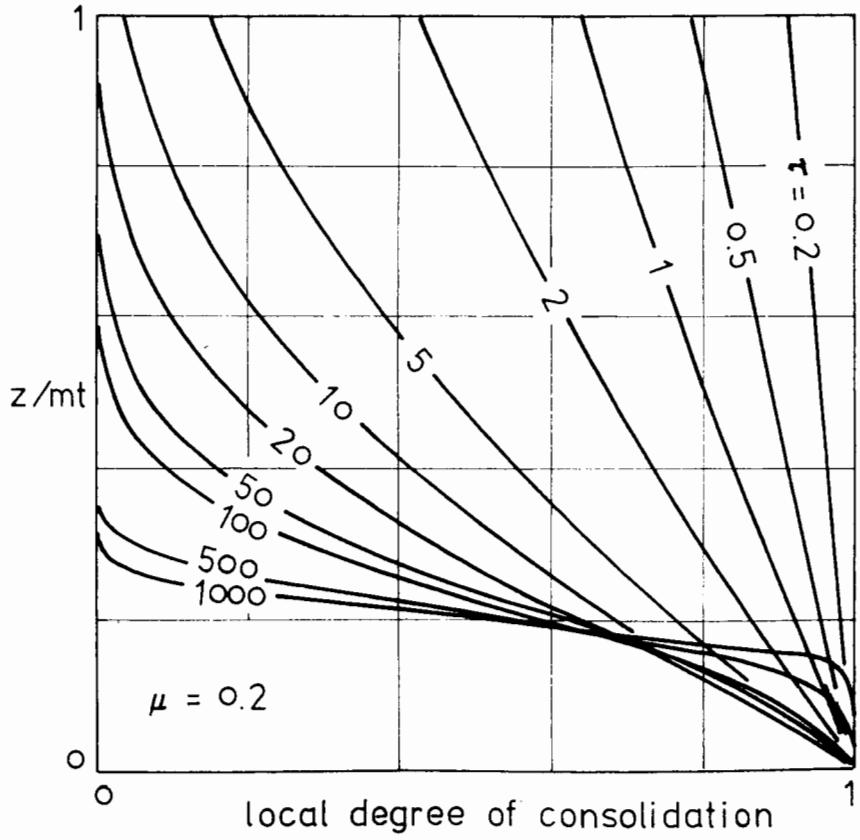

FIG.7.5 Variations of the local degree of consolidation, pervious base
(a) top, μ = 0.1 (b) above, μ = 0.2

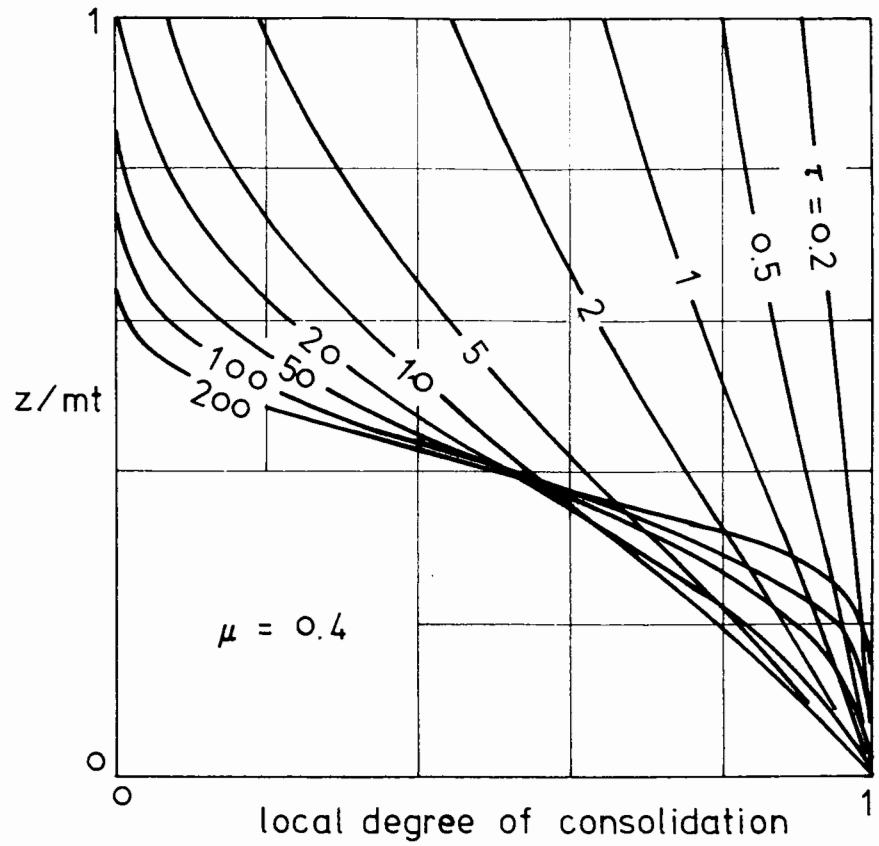

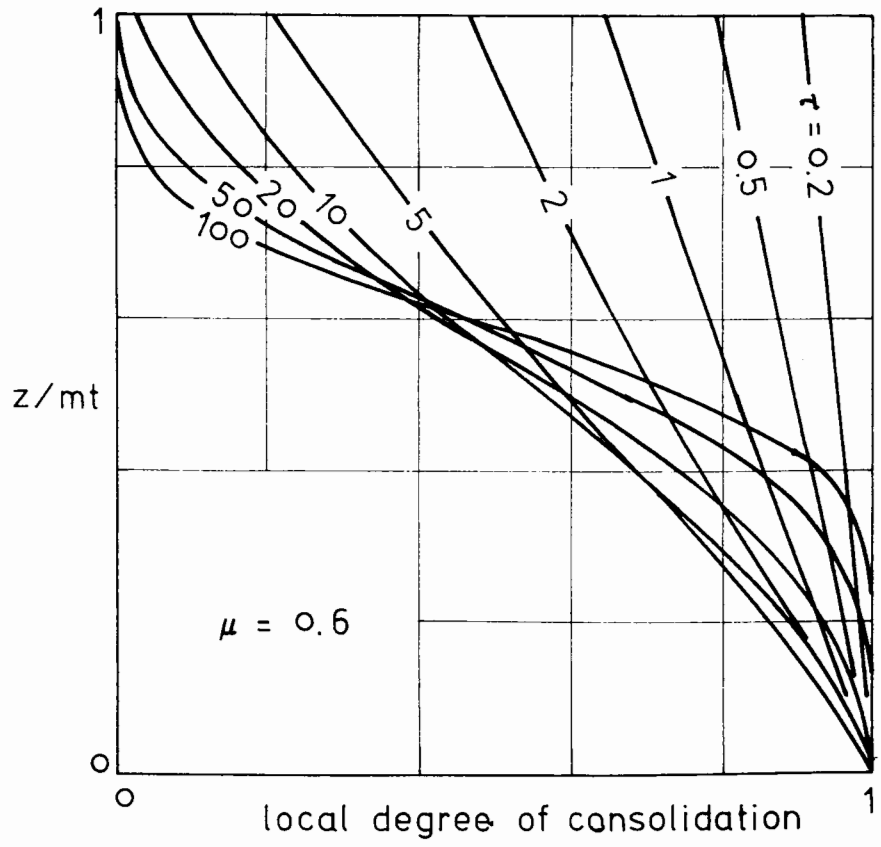

FIG.7.5 (continued) *(c) top, μ = 0.4* *(d) above, μ = 0.6*

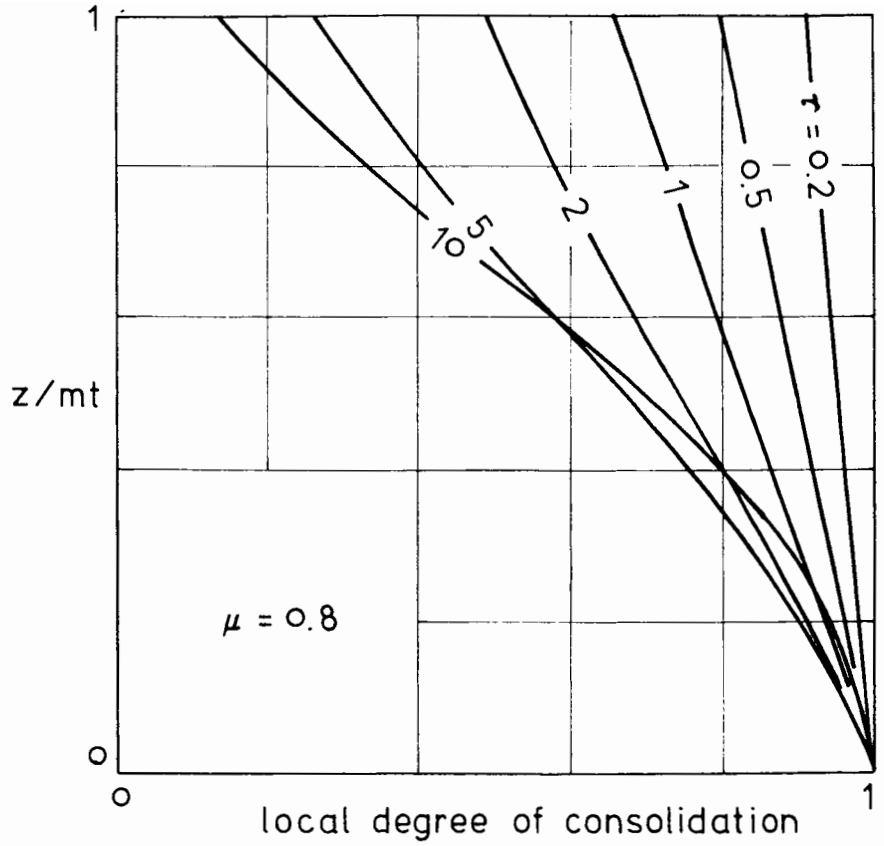

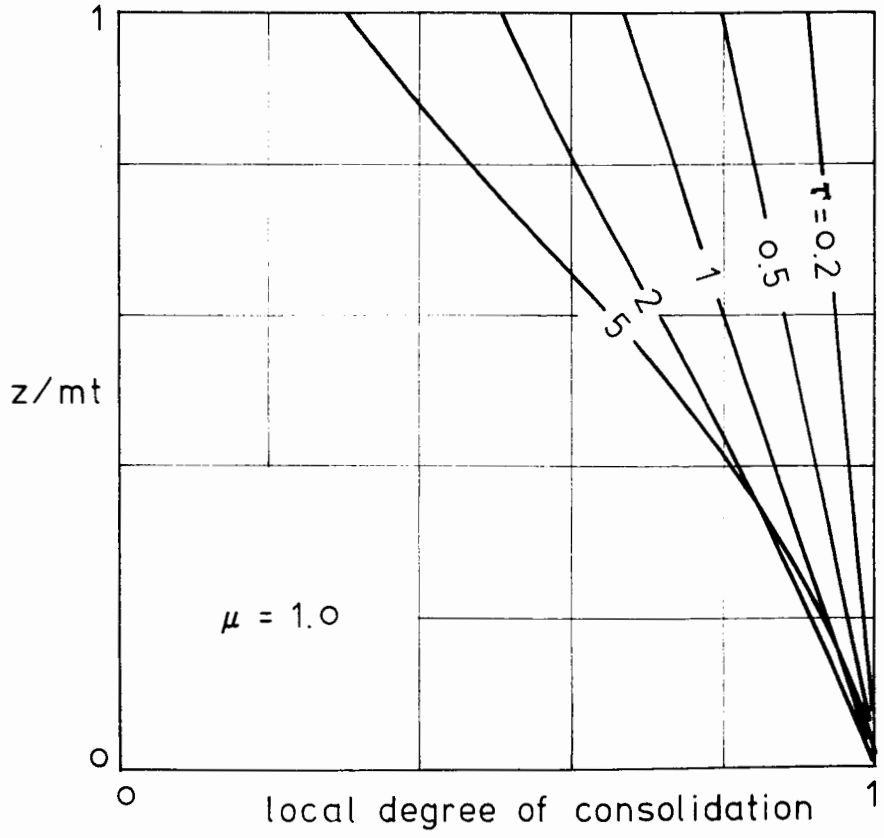

FIG.7.5 (continued) (e) top, μ = 0.8 (f) above, μ = 1

4. DEPOSITION ONTO AN IMPERVIOUS BASE

The space x is discretized into 20 convergent elements with scale factor 0.98. This value has been determined from the preliminary experiments not presented here. Integration in time starts at $\tau=0.001$ with each decade divided into 10 steps and the truncation error for integration and the termination criteria are identical to the pervious base case. Six values of μ , corresponding to 0.1,0.2(0.2)1.0 have also been considered.

The variation of the degree of settlement with the time factor is shown in Fig.7.6. It can be noticed that the solutions do not extend as far as the pervious base case, as a 'drop' has been detected earlier in the present case. Also included in this figure as a broken line is the solution of the linear soil, this again appears to be the limiting solution as μ, the deposition coefficient, tends to zero. In the present case the effect of the deposition coefficient μ on the consolidation of the deposit is similar to that of the pervious base case, i.e. consolidation improves with larger μ .

The variation of the local degree of consolidation at the impervious base of the deposit with the time factor is shown in Fig.7.7. A similar, but earlier drop is observed. This is compared with the degree of settlement in Fig.7.8(a)-(c) for $\mu=0.1$, 0.4 and 1.0. This drop is probably a result of the exponential stress - void ratio relationship of the nonlinear soil. To illustrate this, a point in the base of the deposit will be considered.

As deposition proceeds the weight of overburden at this point is increased, and it will become denser in its fully consolidated state, i.e. a smaller void ratio. Consequently a larger void ratio change from its initial state will be required. Because of the exponential stress - void ratio relationship of the nonlinear soil the

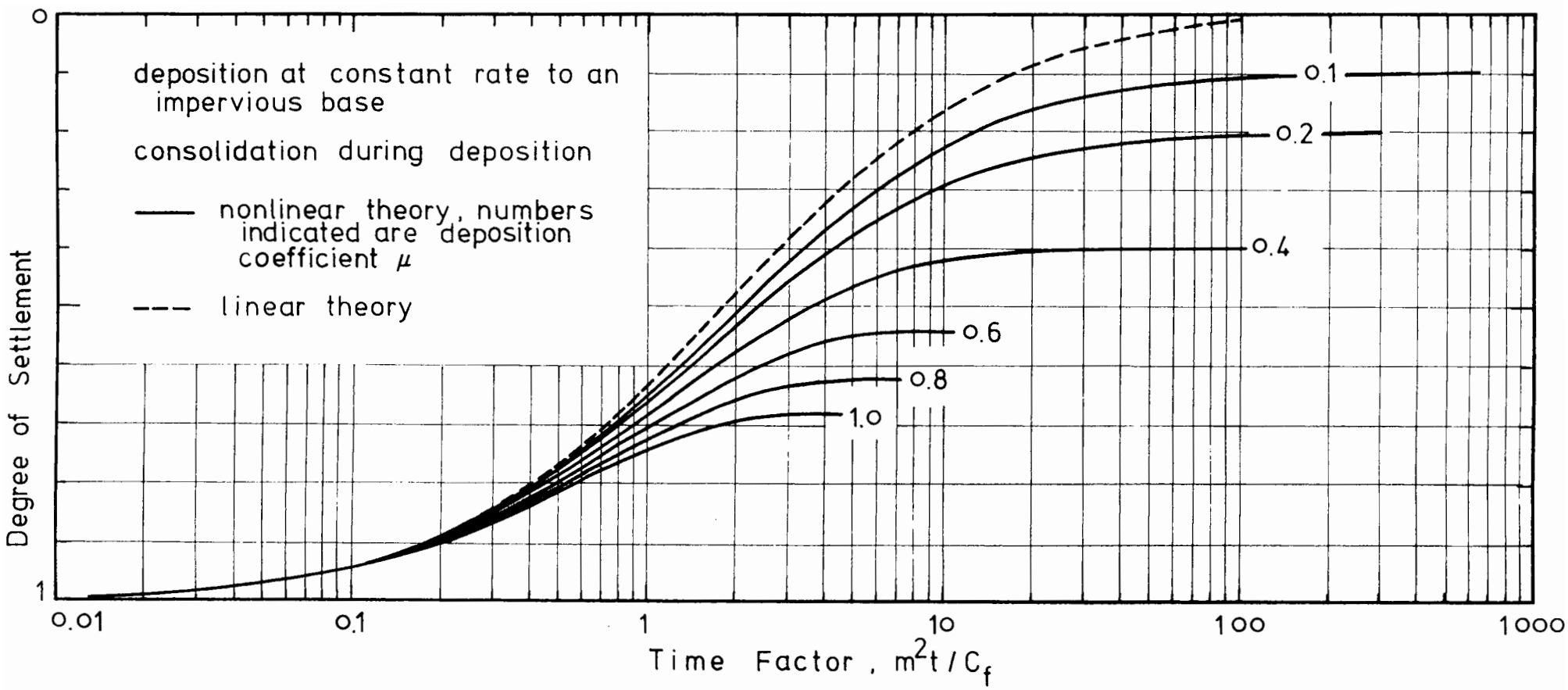

FIG.7.6 Degree of settlement versus the time factor for a deposit undergoing a constant rate of deposition.

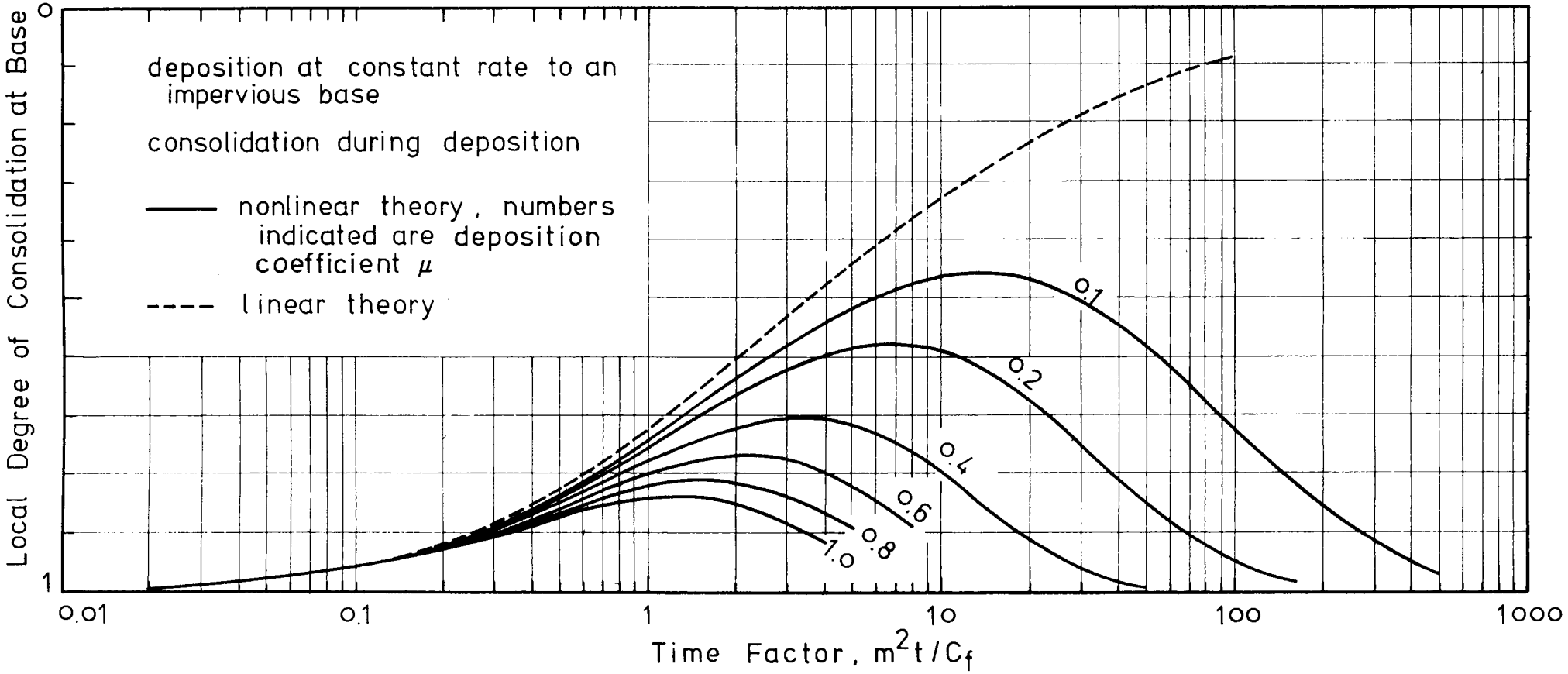

FIG.7.7 Local degree of consolidation at the impervious base of a deposit undergoing a constant rate of deposition.

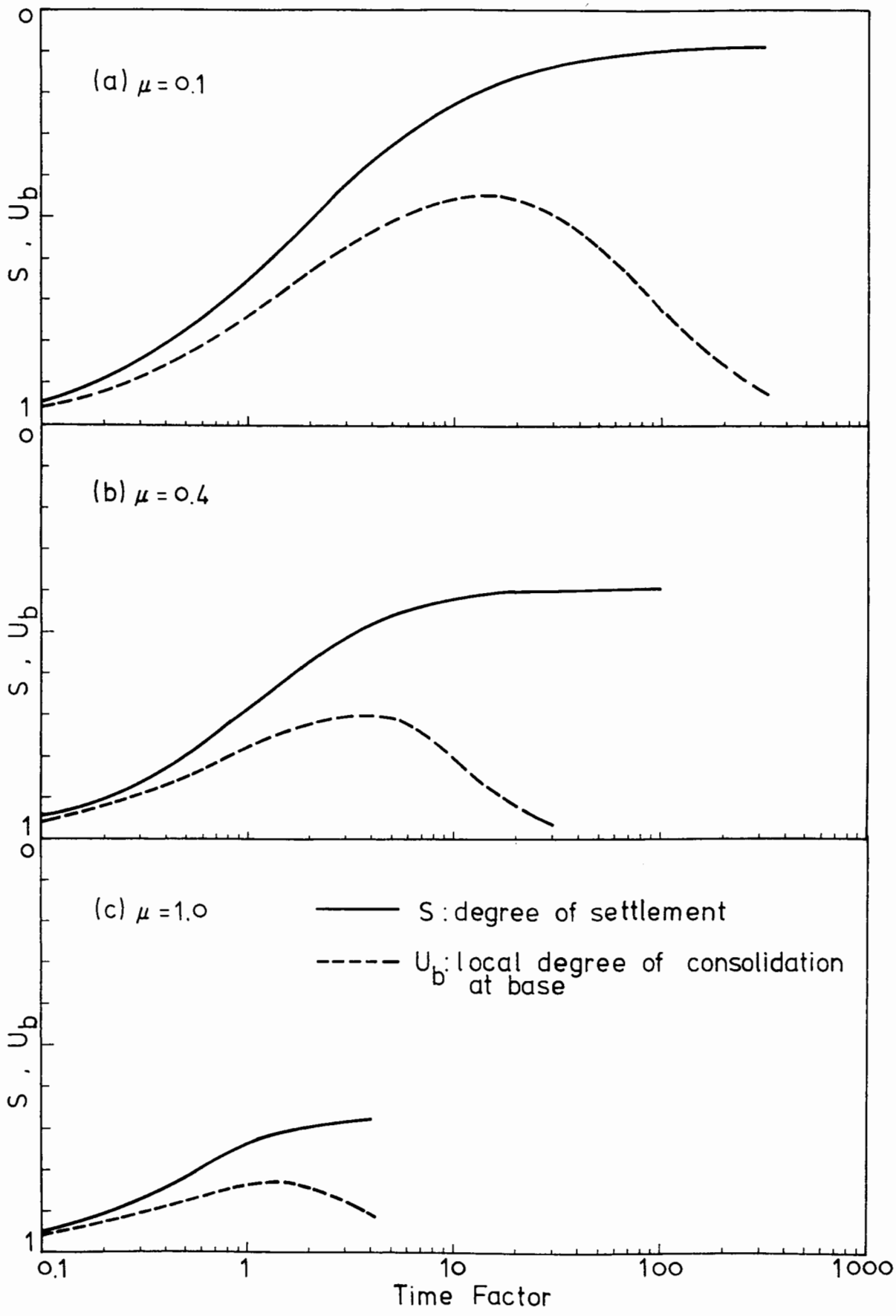

FIG.7.8 Comparison of the degree of settlement with the local degree of consolidation at the impervious base.

increase (from its previous state) of the required void ratio change will decay exponentially with added deposition. At the same time this point is undergoing a void ratio change as a result of consolidation caused by its previous and current overburden.

The local degree of consolidation in this point is, according to its definition eq(7.29), the ratio of the current void ratio change to that required in its fully consolidated state due to the current overburden. Thus, a decrease in the local degree of consolidation means that the rate of current void ratio change is slower than that of the void ratio change required to achieve full consolidation. This is what has been observed in the early stages of deposition. However, as the deposit becomes thicker and thicker the increase (rate) of the required void ratio change decays exponentially while the point in the base is still consolidating at a rate which may not give an exponential decrease of void ratio.

Thus, it is possible that there might exist a turnover stage when the deposit has become sufficiently thick and the rate of current void ratio change becomes faster than that of the required void ratio change, and an increase in the local degree of consolidation will be observed after this turnover stage.

The isochrones of the local degree of consolidation are shown in Fig.7.9(a) to (f). These can be used as a basis to calculate the void ratio and the excess pore pressure distribution in the deposit. It should be pointed out, however, that an increase in the local degree of consolidation at some stage during the deposition does not imply that the excess pore water pressure will ever be decreased. Because of the continuous deposition process the excess pore water pressure will always be increased as deposition proceeds.

Finally, it is interesting to compare the deposition coefficient μ with the stratum coefficient γ that appears in the consolidation

of an existing stratum, Chapter 6. A larger value of both these coefficients will result in faster consolidation (using the time factor for comparison). In Chapter 6 it is seen that as γ tends to zero the solution corresponding to the linear soil is recovered. The numerical solutions developed in this Chapter also suggest a similar tendency. The presence of, and the strong analogy between, the two coefficients when compared with the linear soil seems to be a distinguishing feature of the nonlinear soil, although further theoretical development will be required for a full justification.

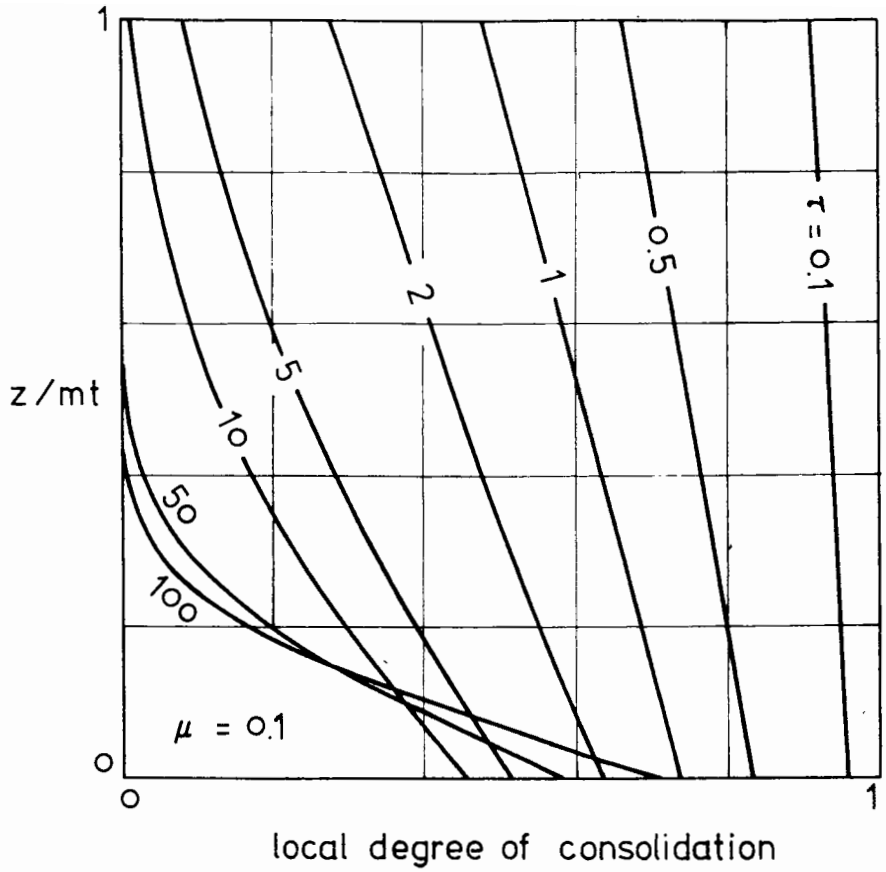

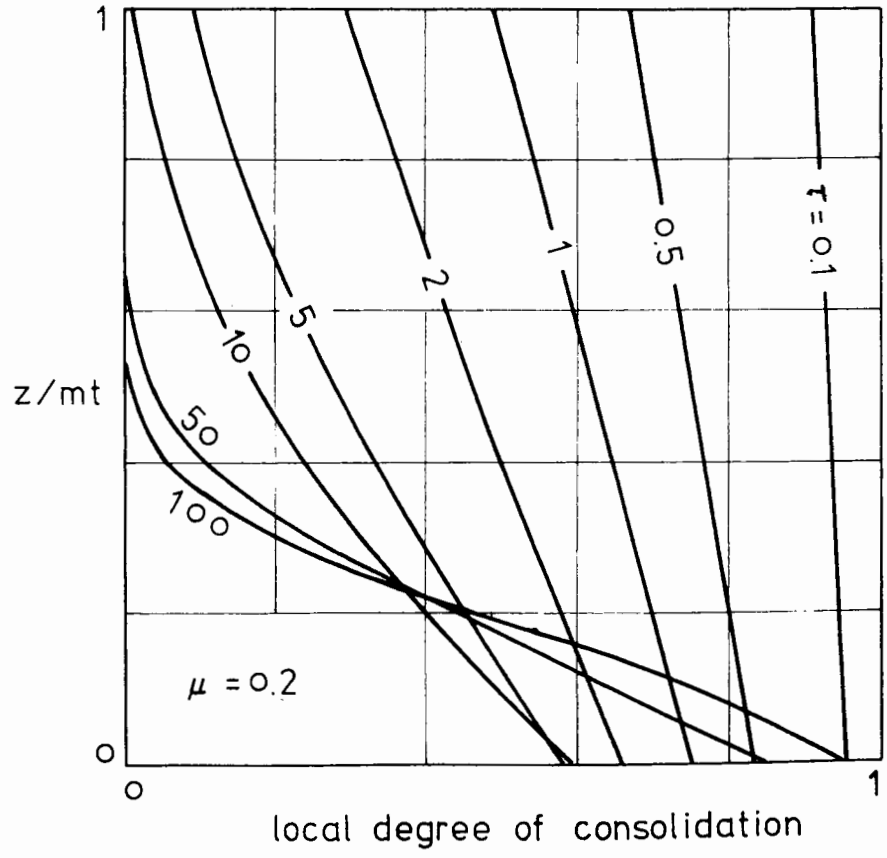

FIG.7.9 Variations of the local degree of consolidation, impervious base

(a) top, μ = 0.1 (b) above, μ = 0.2

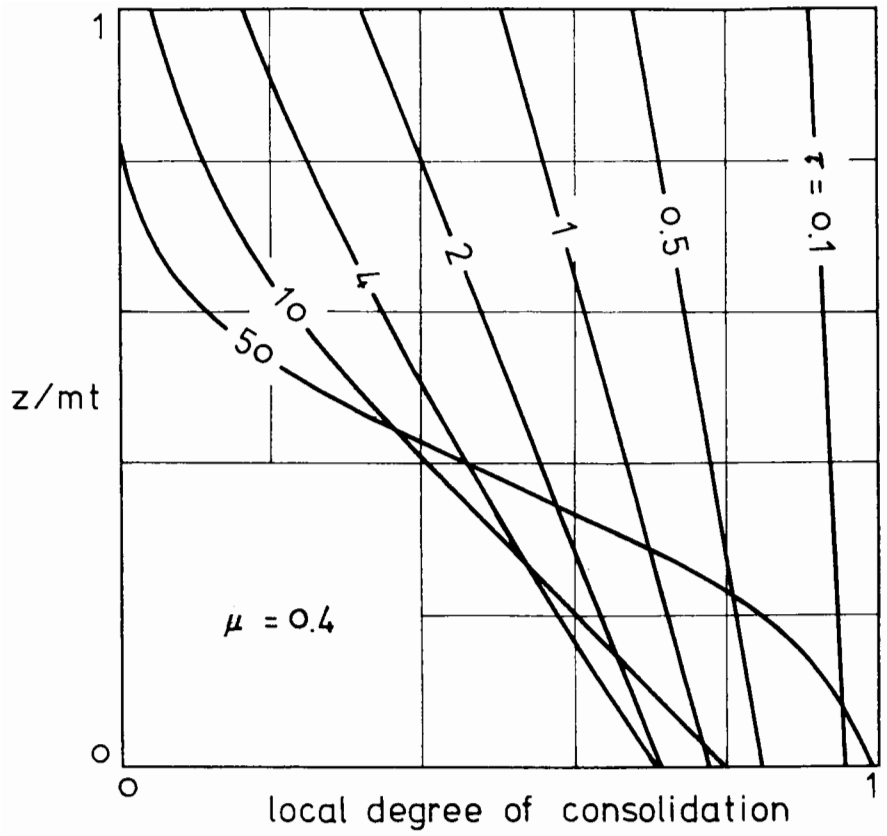

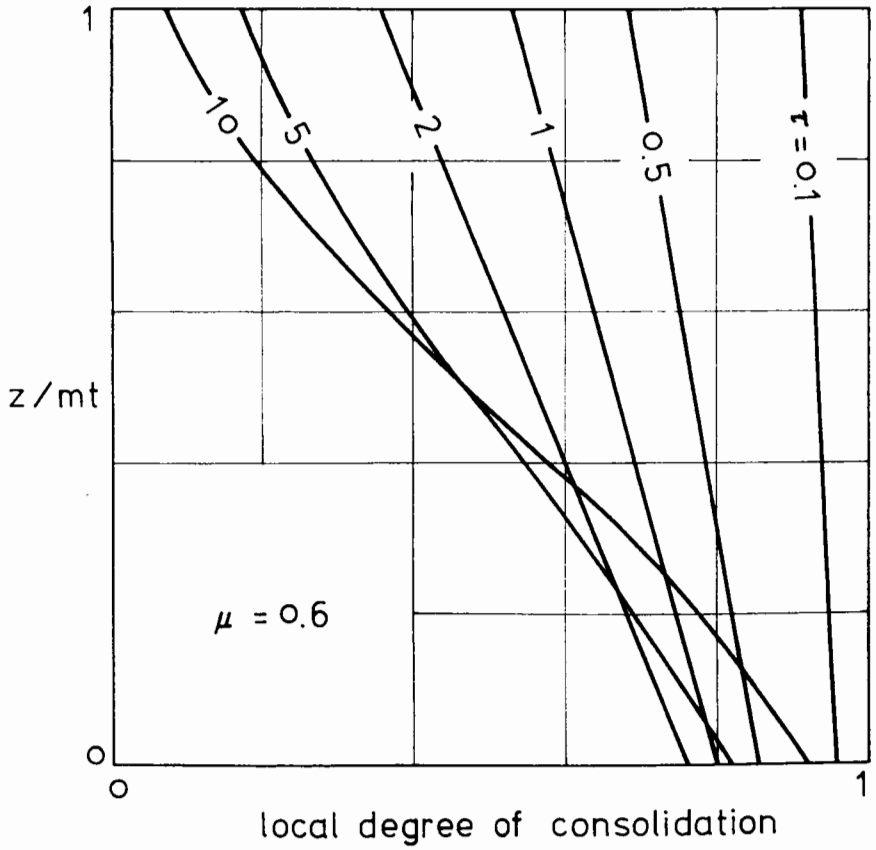

FIG.7.9 (continued) (c) top, μ = 0.4 (d) above, μ = 0.6

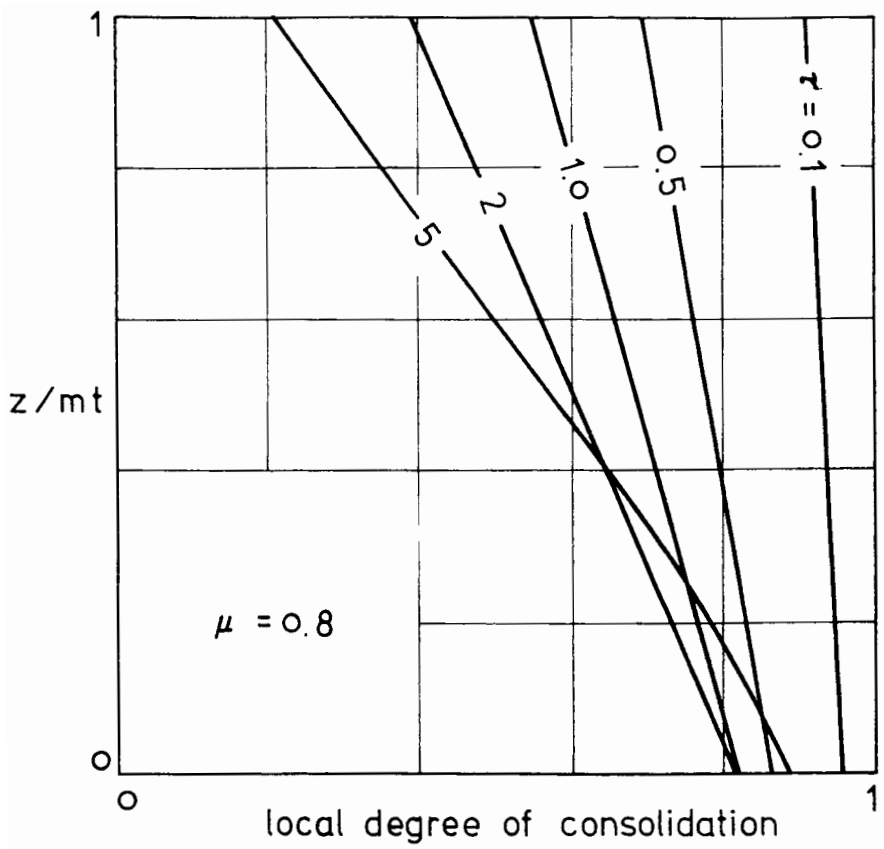

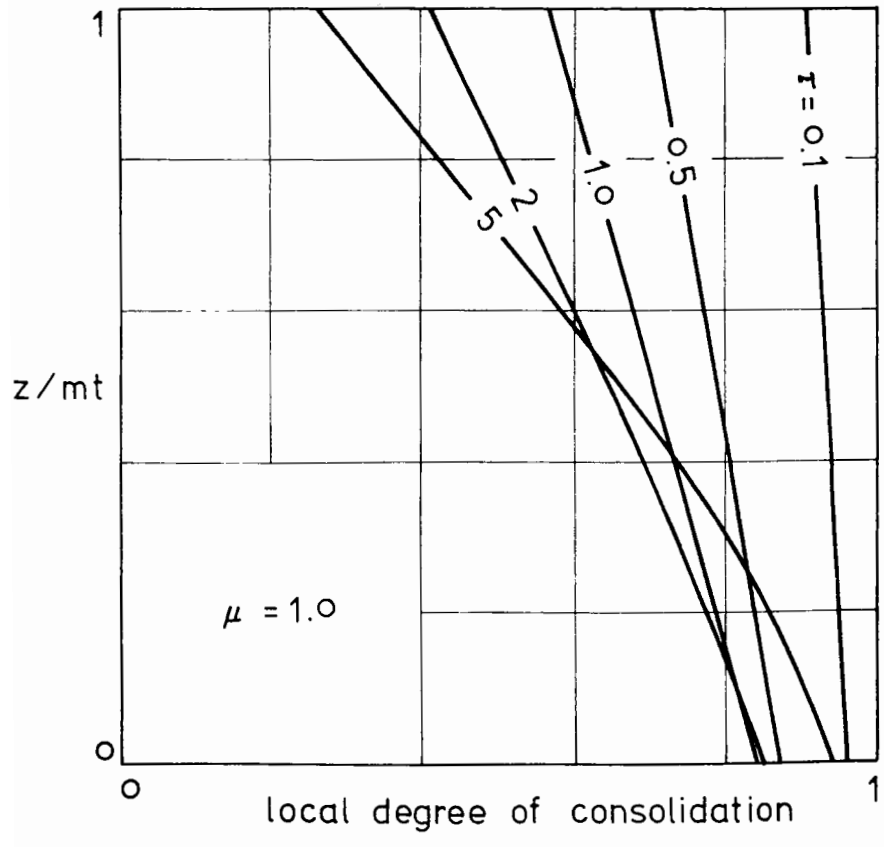

FIG.7.9 (continued) (e) top, μ = 0.8 (f) above, μ = 1.0

APPENDIX A A BRIEF DESCRIPTION OF THE FINITE ELEMENT COMPUTER PROGRAM

The program is based on the algorithms outlined in this chapter to calculate the consolidation of a nonlinear soil during and after a constant rate of deposition.

There are two versions of this program that are available, the DEPOSS is written for the case of a pervious base and the DEPO102 is written for the case of an impervious base. The difference between these two versions is in the internal setup of the matrices $\tilde{A}$ and $\tilde{B}$.

In both versions the main program is supported by 7 subroutines, these are :

AUX : a subroutine to calculate $\tilde{f}(\tau,\tilde{y})$ from given τ and $\tilde{y}$.

ASSEMBLE : a subroutine to assemble the coefficient matrices $\tilde{A}$,$\tilde{B}$ and $\tilde{C}$.

BASIS : a subroutine to allocate the collocation points within each element and to calculate its basis functions V_i , W_i .

DECOMP : a subroutine to decompose the matrix $\tilde{A}$ into its upper and lower triangular form.

D02AEF : a NAG subroutine for solving systems of ordinary differential equations using the VSVO method.

PRINT : a subroutine for the output of results.

XXLL : a subroutine for calculating the consolidation after deposition has terminated, this is supported by four functions F01(G01) to F04(G04).

Both versions of this program can be found in the List of Programs in this thesis. Since the program is not designed for general purpose application, the intended user is advised to contact the author before using this program.

CHAPTER EIGHT THE DEVELOPMENT OF A NEW OEDOMETER

ABSTRACT

A specially developed oedometer for consolidating a very soft specimen to a very large strain is described in this chapter. The basic design differs from the existing devices in that the loading is applied from underneath the specimen. This makes possible a precisely controlled stress, and yet another advantage is that the specimen can be prepared in situ which minimizes the disturbance.

The various instruments developed in conjunction with the oedometer are also described. These include a low range contact stress transducer, a self balancing volume change indicator and a dropometer which will measure both the volume change and the rate of volume change of the specimen.

Finally, the mode of operation and testing procedure are described. The experimental programme and discussion of results are deferred to the next chapter.

1. INTRODUCTION

The demand for adequate equipment to perform a consolidation test of very soft soil has been pointed out in Chapter 1 of this thesis. As traditional Soil Mechanics equipment is not suitable for this purpose, a specially designed oedometer has been developed in the present study. This will be described in this chapter and discussion of some of the experiment results made on this will be presented in the next chapter.

The oedometer has several advantages in use for investigating soil consolidation characteristics. There is a truly one-dimensional flow and deformation condition in the specimen, and both the stress and deformation boundary conditions can be controlled to a close degree. The only disadvantage is that of the wall friction, which has some uncertain effects on the specimen. This friction is a consequence of the mechanical configuration which has to produce a one-dimensional condition, and it appears that it would be impossible to eliminate this entirely.

There have been a number of efforts during the past to design oedometers for testing very soft soil. Leonard and Altschaeffl (1964) consolidated an artificially sedimented clay by a piston and weight system in a constant loading rate. Berry and Poskitt (1972) tested remoulded amorphous granular and fibrous peat in the Rowe consolidation cell, and the largest strain reported in that work is of the order of 40%. Monte and Krizek (1976) used a slurry oedometer to test a particular type of Kaolin (Hydrite 10). The loading steps were kept sufficiently small and thus the strain developed within each step is also very small. Although it is essential to provide instrumentation to assess the performance of the equipment, no mention was made of such instrumentation by these authors.

The design of the present oedometer is therefore based on the following considerations :

(1) It should be capable of accomodating a very soft specimen.

(2) It should cause as little disturbance to the specimen as possible in the assembly stage.

(3) It should be able to develop large strain in the specimen.

(4) It should give access to various instruments for monitoring and controlling the stress, strain and other parameters.

2. A BRIEF DESCRIPTION OF THE OEDOMETER AND ITS MODE OF OPERATION

Fig.8.1 shows a schematic diagram of the oedometer. This comprises a cell, a piston and its bearing, a base and a top platen. The specimen is confined between the piston and the top platen as can be seen in this figure. As opposed to the traditional design, in this oedometer the soil is sedimented into the cell to produce a very soft specimen and is loaded from underneath by the piston for least disturbance.

The mode of operation of the oedometer is shown schematically in Fig.8.2. In the initial stage, Fig.8.2(a), the cell is bolted to the base with the piston seated in the middle. The piston is instrumented with a contact stress transducer and a pore pressure probe. It is guided by a ram carrying the signal cables from the contact stress transducer, and the part of the piston protruding from the base of the cell has a dial gauge for measuring the movement of the piston. A plain bush seated in the base is used to guide the ram for a smooth and linear movement. The

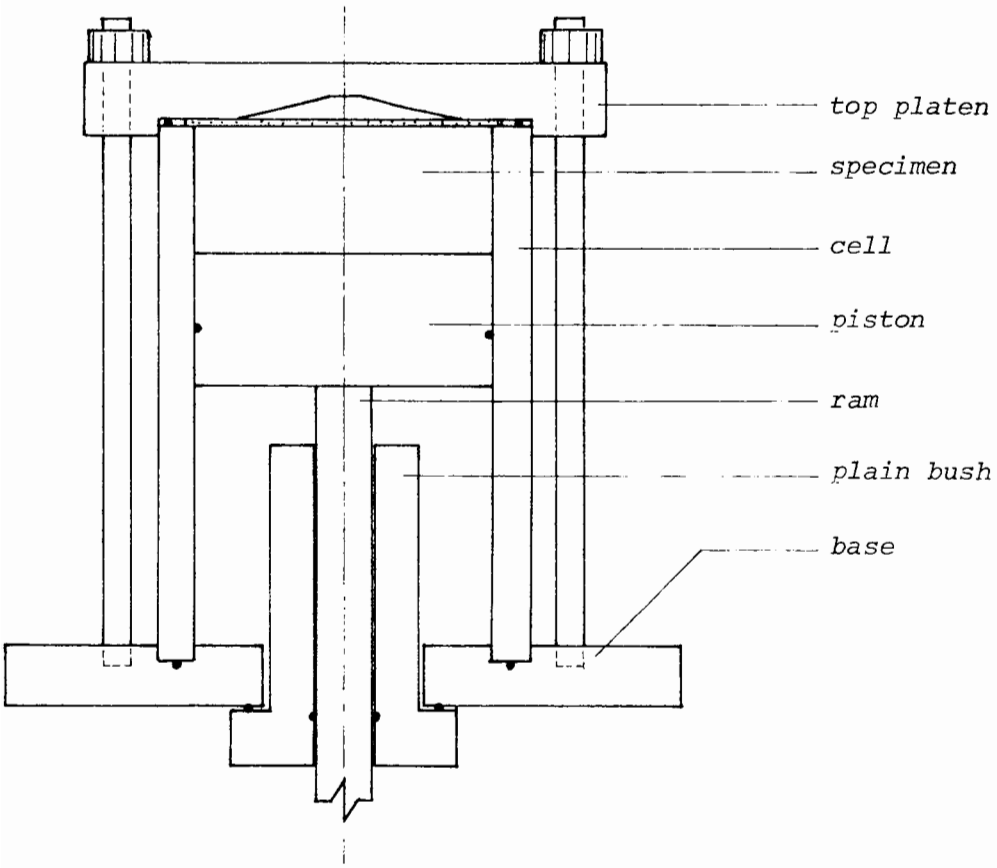

FIG.8.1 A schematic diagram of the oedometer.

part of the space in the cell underneath the piston is filled with water which connects through the base to an external pressure source used to drive the piston.

After the initial setup, an acrylic tube having the same internal diameter as the cell is installed on top of the cell, Fig.8.2(b). The space intended for the specimen is then filled up with de-aired water, and the soil, in the form of a dilute suspension, is poured into this using a syringe. This will take a day or two for the soil particles to settle out of the suspension and consolidate under their own weight.

The specimen thus formed will protrude slightly above the top of the cell, Fig.8.2(c). After removing the acrylic tube, the specimen is trimmed to be level with the top of the cell, see Fig.8.2(d). It is then covered with a thin sheet of porous membrane filter, followed by a sintered disc. Finally, the top platen is installed and bolted to the base, Fig.8.2(e)

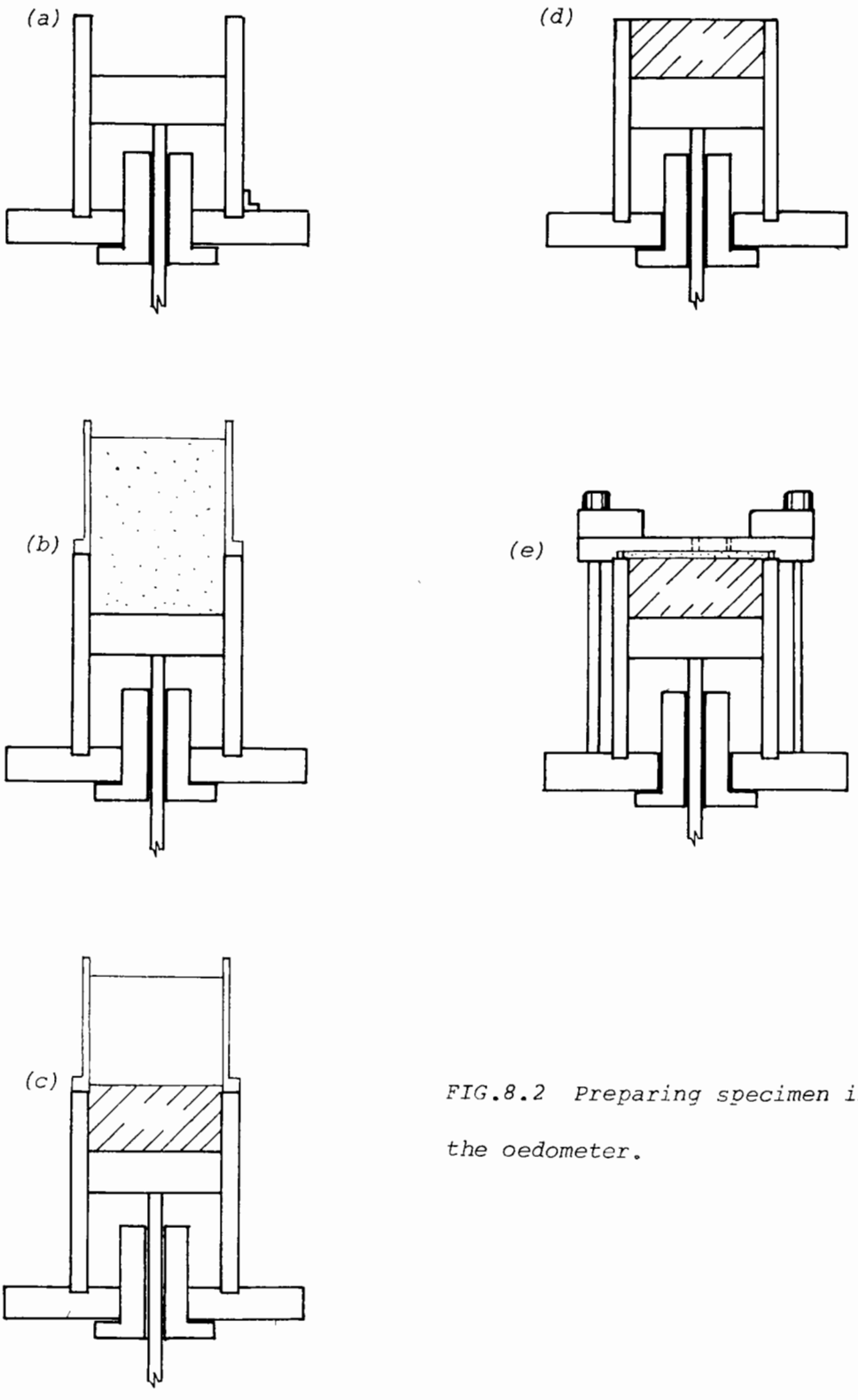

FIG.8.2 Preparing specimen in the oedometer.

The specimen end of the top platen is slightly domed to facilitate deairing which is carried out by flushing water through the two openings in the platen. Later these two openings are connected to the back pressure line and a pressure transducer.

3. THE OEDOMETER

A diagram of the oedometer is shown in Fig.8.3 in which each part has been numbered for identification. These numbers will be referred to in brackets when the corresponding parts are described in the following paragraphs. A photograph of the complete assembly is shown in Fig.8.4.

The Cell

The cell (1) is made out of a stainless steel tube 4" (101.6 mm) internal diameter with 0.5" (12.7mm) thick wall and 6" (152.4mm) high. Three brackets (2) 120° to each other are welded near the lower end of this, and these are used to bolt the cell onto the base in the initial setup stage.

The Base

The base (23) is machined from a 1" (25.4mm) thick stainless steel plate to an overall diameter of 9" (228.6mm). A 2" (50.8mm) hole is cut in the centre of this to accommodate the plain bush (16). Further out there is a concentric groove (3) cut to act as a recess to accept the cell, an O-ring groove (4) is also provided within this to seal against the cell pressure. Outside this groove there are three

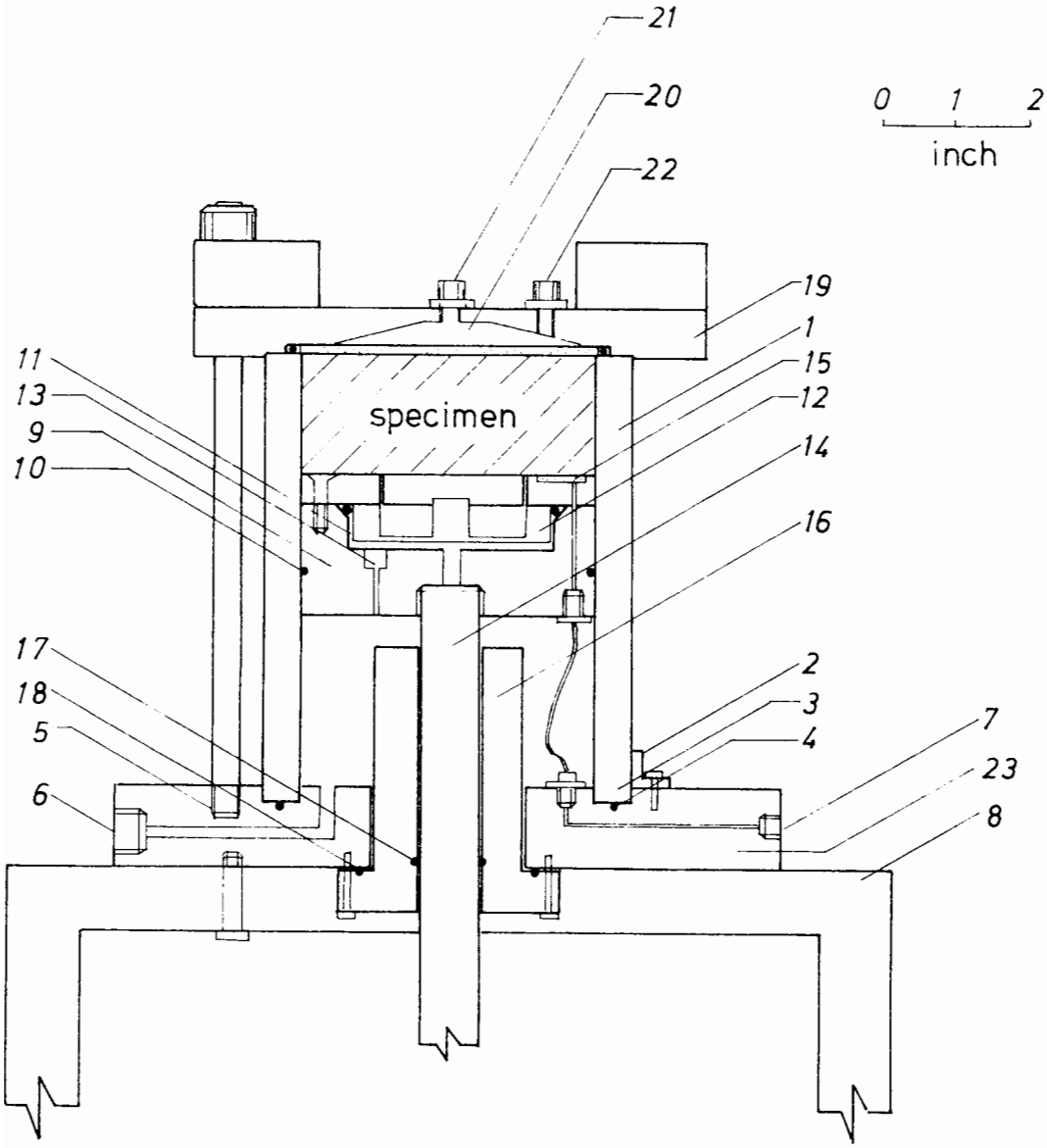

FIG.8.3 The oedometer.

1. *cell*
2. *bracket*
3. *recess*
4. *O-ring groove*
5. *threaded holes*
6. *cell pressure inlet*
7. *pore pressure probe outlet*
8. *main frame*
9. *piston*
10. *O-ring seal*
11. *recess*
12. *contact stress transducer*
13. *bleeding valve*
14. *ram*
15. *pore pressure probe*
16. *plain bush*
17. *O-ring seal*
18. *O-ring seal*
19. *top platen*
20. *domed space*
21. *drainage outlet*
22. *outlet to pressure transducer*
23. *base*

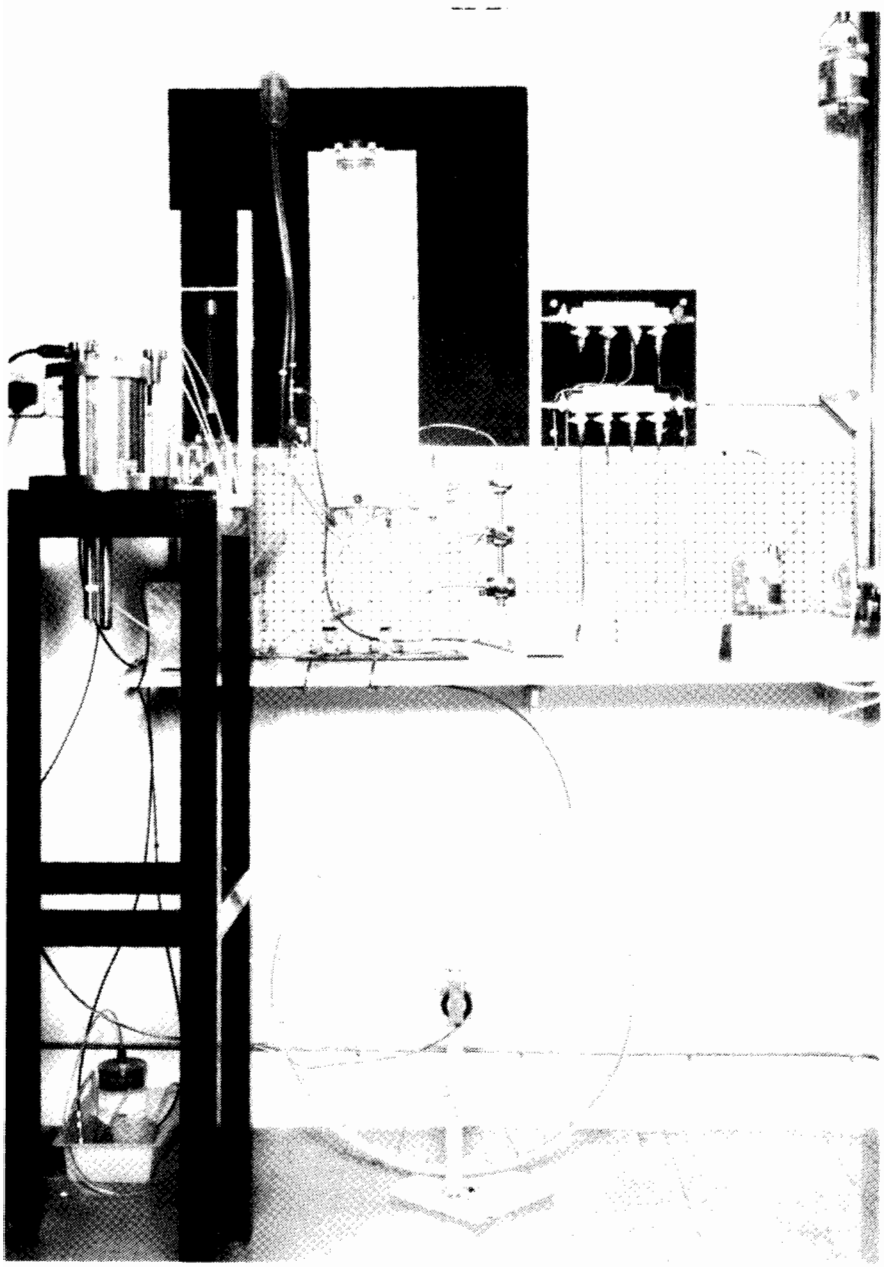

FIG.8.4 The oedometer

threaded holes to which the cell can be bolted, and there are also three larger threaded holes (5) which are used to bolt the top platen onto the base. Two outlets have been provided in the base, one for connecting to the cell pressure (6) and the other to the pore pressure transducer (7). The base is bolted to a main frame which is fixed to the floor.

The Piston

The piston (9) is machined from a solid block of brass to give a radial clearance of 0.005" (0.127mm) to the wall of the cell. Sealing of this piston is achieved by the use of an O-ring (10) which has a cross-sectional diameter of 0.139" (3.53mm). The O-ring groove is cut by successive trials till the O-ring just touches the cell in order to minimize the friction. On the specimen side of the piston there is a recess (11) 0.625" (15.87mm) deep and 2.75" (69.85mm) in diameter to house the contact stress transducer (12). A clearance hole 0.25" (6.35mm) in the centre of the recess is drilled through the piston to provide an outlet for the signal cables from the contact stress transducer. The bleeding valve (13) is made out of a 4.B.A screw through the piston and sealed by the use of a Downty seal. The edge of the recess is chamferred 30° to the vertical to accept the O-ring for sealing the recess against the specimen. Threaded connections are provided in the cell pressure side for connecting the ram (14) and the pore pressure probe (15).

The Ram and the Plain Bush

The ram (14) is made of a stainless steel tube of 0.75" (19.05mm) outside diameter with 0.125" (3.17mm) thick wall and an over-all length of 8" (203.2mm). This is guided by a plain bush (16) machined from a solid block of brass. The overall guided length of the bush is 3" (76.2mm) which has been precisely bored to a close

tolerance. Sealing against the cell pressure is achieved by an O-ring in the bore(17) and another O-ring (18) pressed between the base of the bush and the base of the cell, these two parts being jointed together by four bolts with adjustable position to reduce any possible misalignment in the assembling stage.

The Top Platen

The top platen (19) is made of a 0.5" (12.7mm) thick, 7" (177.8mm) diameter Perspex disc. The side facing the specimen (20) is domed 15° to horizontal from a base diameter of 3.5" (88.9mm). Two outlets are provided here for the initial deairing and connection to the back pressure (21) and pressure transducer (22) during the test.

4. INSTRUMENTATION

The Contact Stress Transducer

(a) The transducer

As shown in Fig.8.5 the transducer has the shape of a wheel with four thin webs connecting the central hub to the rim. In operation the hub is bolted to the active face which makes contact with the specimen, and the rim is fixed to the piston. Each web therefore acts as a double cantilever and the force applied to the active face is sensed by strain gauges in the webs. The present transducer is machined out of a solid block of dural, and four strain gauges attached to two opposite webs and wired in a full bridge configuration have been used. The strain gauges thus wired up are connected to an external circuit, Fig.8.6 , which provides the nulling and scaling

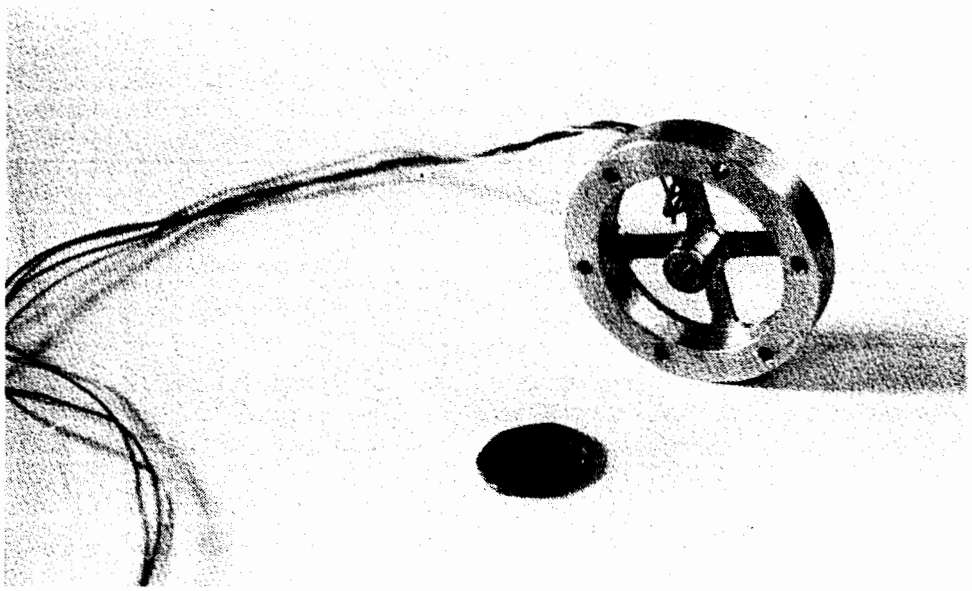

FIG.8.5 The transducer (above) photograph, (below) dimensional drawing

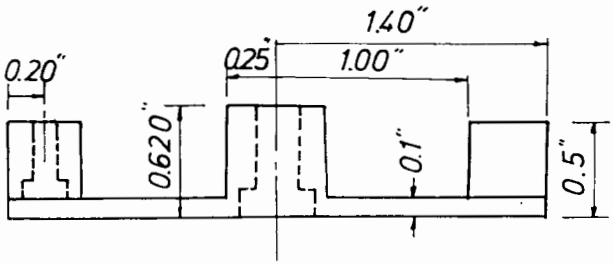

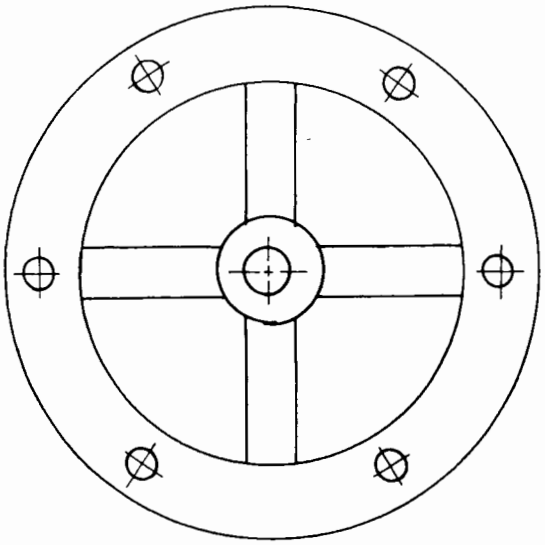

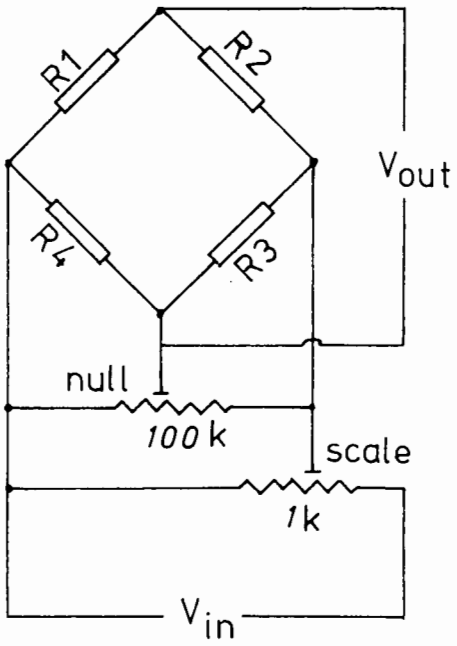

FIG.8.6

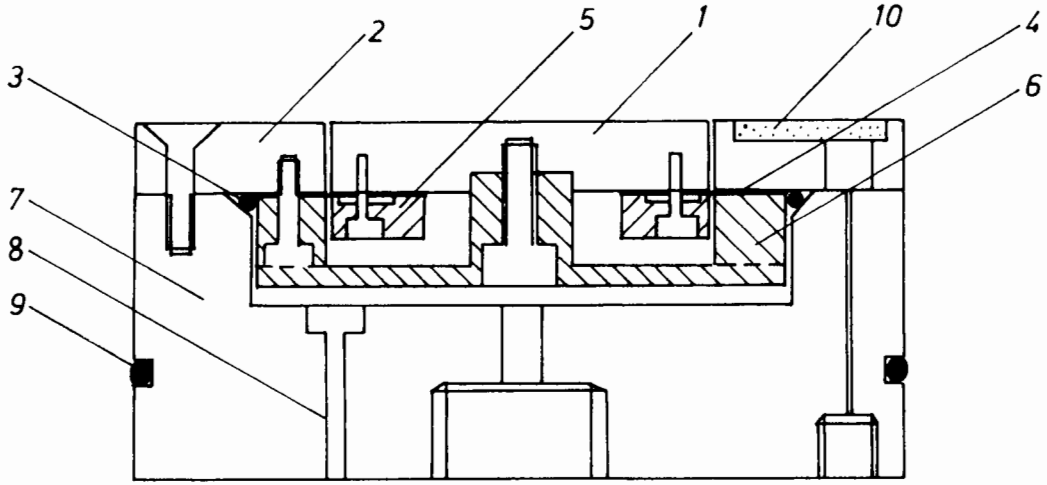

FIG.8.7 The contact stress transducer

1. active face
2. top platen
3. O-ring seal
4. rubber diaghragm
5. knife edge ring
6. transducer
7. piston
8. bleeding valve
9. O-ring seal
10. pore pressure probe

functions. These are adjusted to give 10mV output in 100 KN/m^2 for 10V excitation.

(b) Assembling and calibrating the transducer

The assembled diagram of the transducer is shown in Fig.8.7. The active face (1) is bolted to the transducer (6) to transmit the force. The rim of the transducer is bolted to the top platen (2) which is bolted to the piston (7).

To seal the transducer against the specimen, an O-ring (3) and a specially developed rubber diaphragm (4) have been used. The diaphragm is clamped to the active face by a knife edged ring (5), and to the top platen by the transducer. To prevent the diaphragm from causing jamming during the operation, the underside edges of the active face and the top platen are slightly chamferred, and the gap between these two parts is filled with silicon grease.

The bleeding valve (8) and the O-ring (9) on the side of the piston are also shown in this figure. In the top platen there is a recess to accomodate a sintered disc (10) which serves to transmit the pore water pressure to the Druck transducer. The Druck transducer, as will be described later, is used to calibrate the contact stress transducer. One set of calibration result is shown in Fig.8.8, from which it can be seen that the transducer response is very linear. However, under a constant pressure its output is found to creep in 24 hours to an order of 1 per cent higher than its initial reading. This is likely to be a result of the instability of the dural used.

The Pore Pressure Transducer

Two integrated silicon chip pressure transducers manufactured

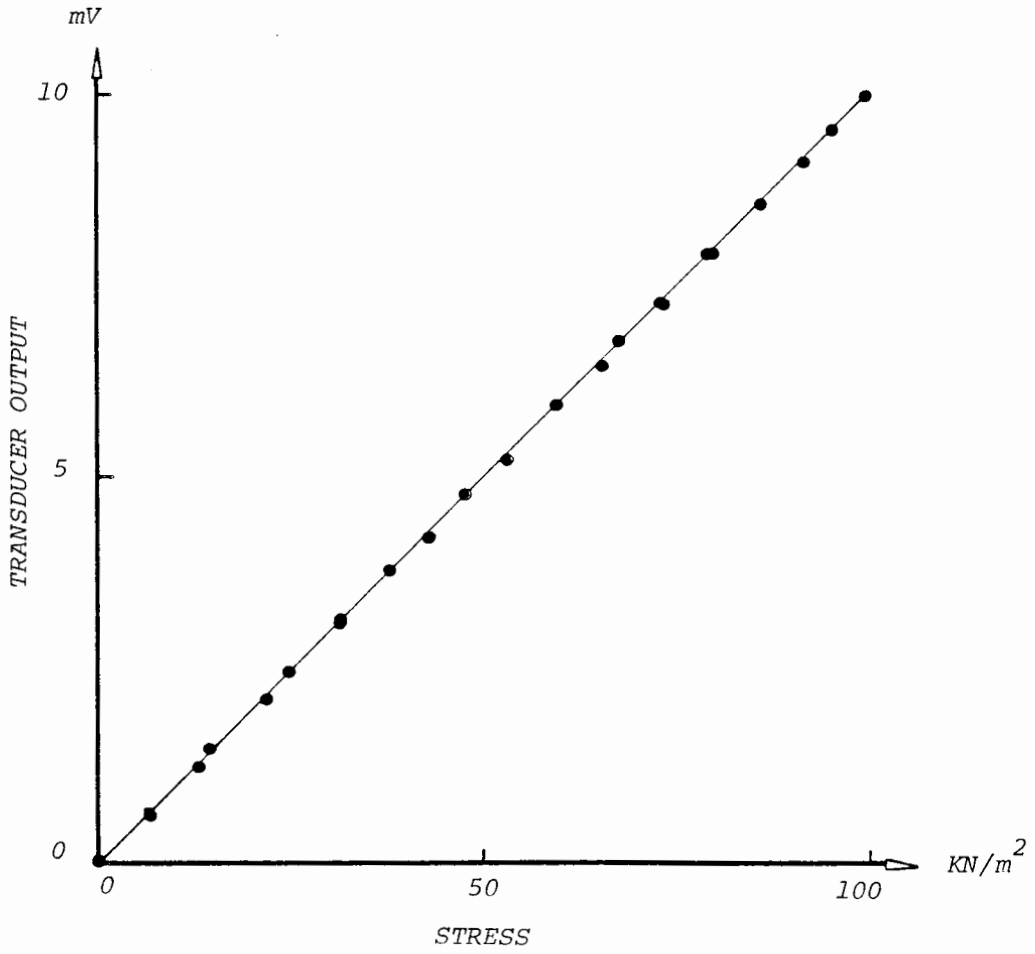

FIG.8.8 Calibration result of the contact stress transducer

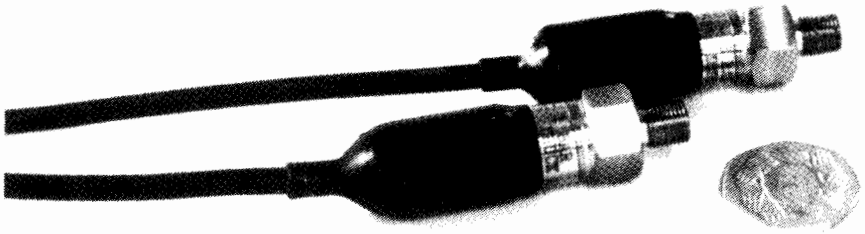

FIG.8.9 The druck Transducers

by Druck Limited have been used. These can be seen in Fig.8.9. One of these transducers, the PDCR10, has a range of 0 - 100 KN/m^2 and the combined nonlinearity and hysterisis is less than $\pm$ 0.1% off best straight line. The other transducer, the PDCR20, has a range of 0 - 300 KN/m^2 and the combined nonlinearity and hysterisis is less than $\pm$ 0.05% off best straight line.

Volume Change Measurement Devices

(a) A self - balancing volume change indicator

Borrowing an early idea from Bishop and Henkel (1962), this device makes use of the weight of mercury. A tube, partially filled with mercury, is mounted on a circular arc, which is free to rotate about its centre. Water passing through the tube displaces the mercury, and the resulting out of balance moment will drive the circular arc until the balance is restored. The rotation of the circle can thus be calibrated with the quantity of water flowing through it.

This device is shown schematically in Fig.8.10. The rotating part consists of a bicycle wheel (1) pivoted on a central shaft. This is supported on a metal frame (2) through two 0.25" (6.35mm) ball bearings (3). A 5mm i.d. polyethelene tube (4) to carry the water and the mercury (5) is wound around the bicycle rim. On both ends it is connected to smaller tubes (6) of 2mm i.d. by a special Nylon coupling (7). These smaller tubes provide the water inlet and outlet. The rotation is picked up by a potentiometer (8) fixed to one end of the bicycle shaft. The potentiometer has a continuous travel of 355 degrees with a quoted accuracy of $\pm$ 0.075% , about 0.27 degree. The calculated resolution of the present model, based on the size of wheel and tube used, is of the order of 0.03ml.

The device is calibrated against a standard burette, and the

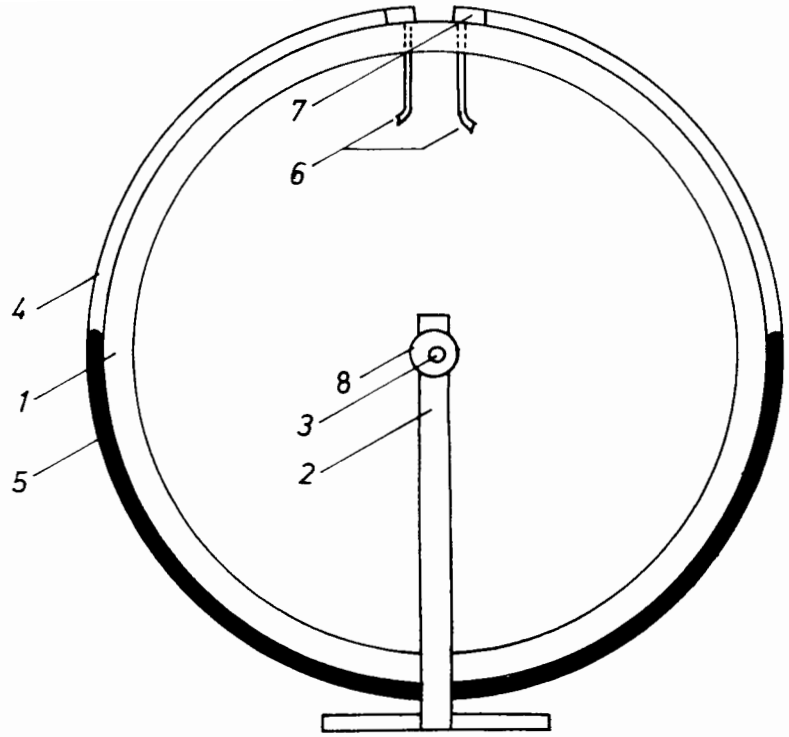

FIG.8.10 The self - balancing volume change indicator.

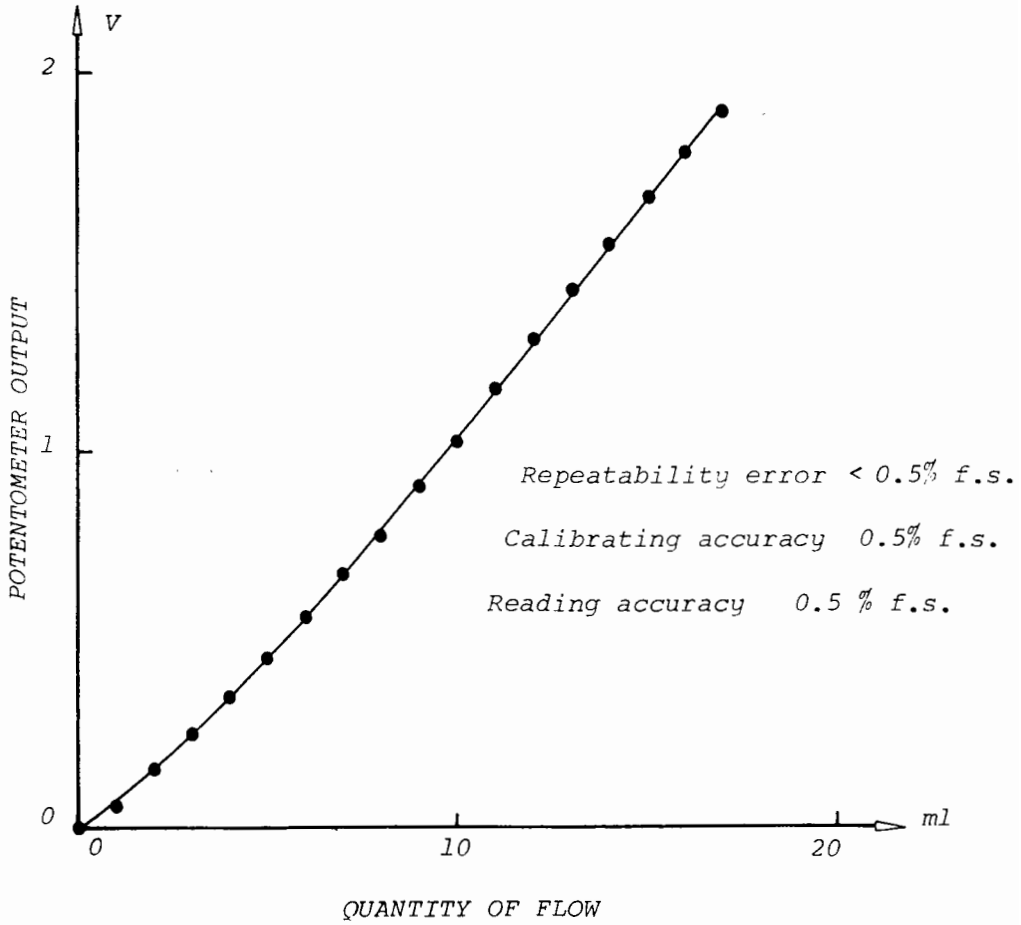

FIG.8.11 Calibration of the self - balancing volume change indicator.

results of ten runs are shown in Fig.8.11. The response, as can be seen, is weakly nonlinear; this is due to the stiffness of the outgoing tubes. The repeatability, which is the consistency of the results in ten runs, is better than 0.5%. This is compatible with the accuracy of the burette.

(b) The dropometer

In the self - balancing volume change indicator the resolution of the device is dependent upon the total capacity. The dropometer to be described here has a fixed resolution (accuracy) and a theoretically infinite capacity. This was originally intended for measuring volume change, but by using a different electronic circuit this can also be used for rate of volume change measurement.

The idea behind this device is that the outward water flow from the specimen is used to feed a syringe which has a hyperdemic needle fitted at its outlet. This flow will therefore come out as droplets which have a constant volume depending upon the size of the needle and the surface tension of the water. The size of the droplet is calibrated by an analytical balance which can measure down to 0.2 mg, this corresponds to a volume of 0.0002 ml. A set of such calibration results is shown in Fig.8.12 which shows a mean value of 0.0123 ml and a standard deviation of 0.0004 ml. This degree of accuracy is indeed more than adequate for most Soil Mechanics experiments.

Having thus made the outward water flow come out as droplets, the total amount of flow equals the total number of droplets and can be obtained by an optical method. Furthermore, due to the fact that the drop size is very small, a fairly accurate flow rate (rate of volume change) can be obtained by measuring the time period between two drops.

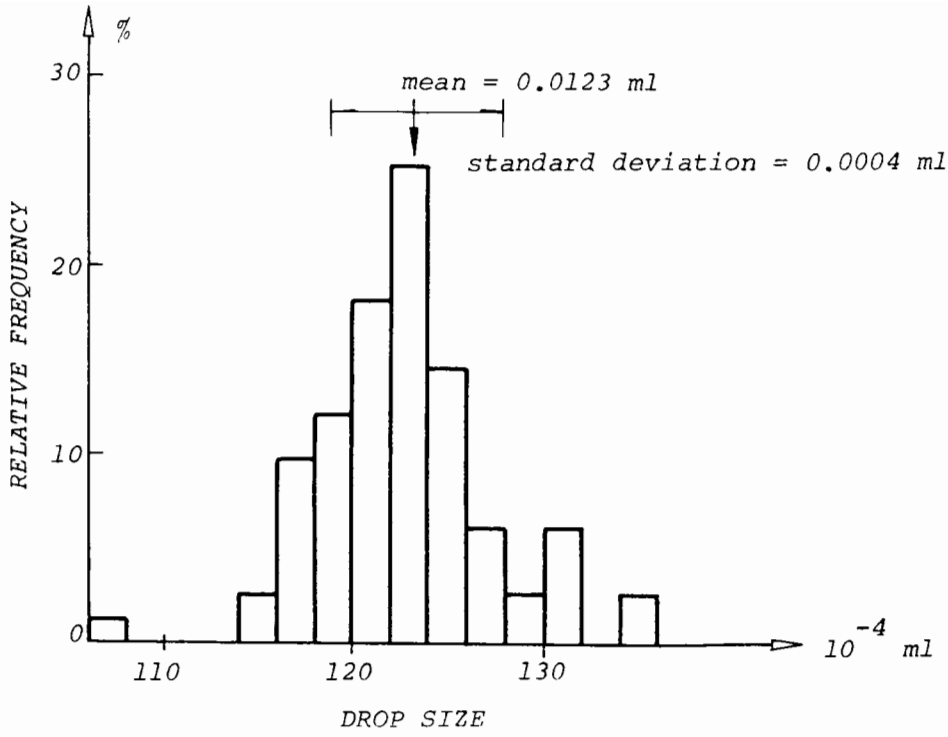

FIG.8.12 (above) Statistics of drop size from 83 consequetive measurements.

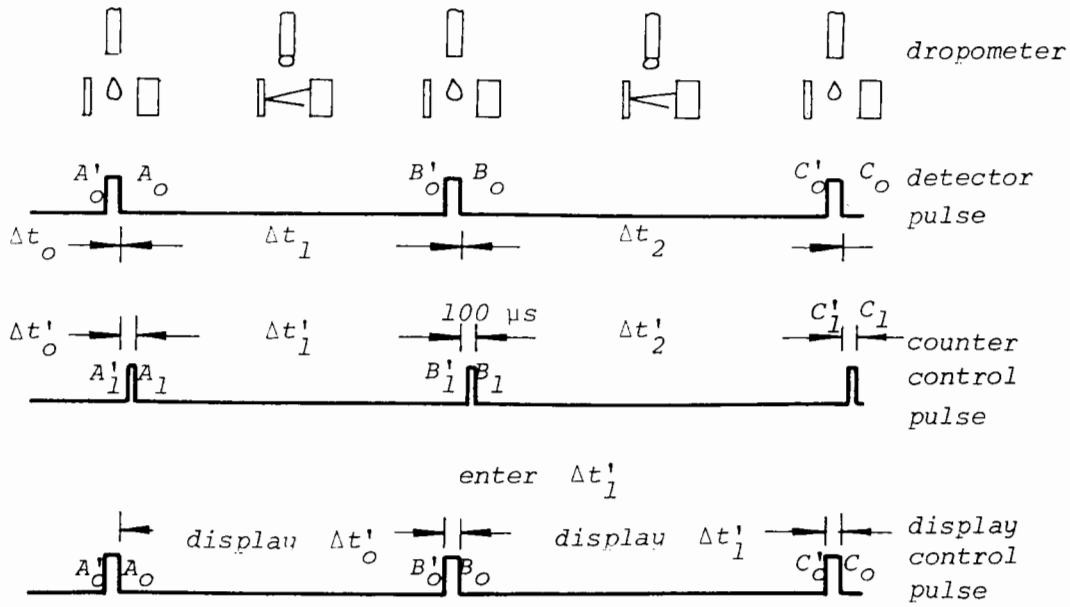

FIG.8.13 Operation of the time period measurement circuit of the dropometer.

The actual device used to detect the droplet is a system of an infra red light source and a sensor arranged as a reflective object detector. This is obtained as a ready made component from RS Component Ltd.. In front of this is a reflective metal surface, and the droplet is fed through the gap between this surface and the detector. As soon as a droplet passes through this gap the infra red light beam is blocked, which is sensed by a circuit emitting a pulse to activate the counting circuit or the time period measurement circuit.

The operation of the time period measurement circuit is illustrated in Fig.8.13. The counter is fed with a 50 Hz clock signal derived from the mains supply. As soon as a droplet is detected, i.e. at A'_o , B'_o or C'_o in this figure, the circuit will respond in the following steps :

(1) The counter display is set to the enter mode, i.e. it now erases the previous display and displays the total number of 50 Hz clock signals it received during the previous period $\Delta t'_o$ or $\Delta t'_1$.

(2) After this number is entered in the display, i.e. at A_o , B_o or C_o , the display is then frozen until the next droplet is detected so that a manual reading can be taken at this period, say, between A_o and B'_o or between B'_o and C'_o .

(3) The counter is reset to zero and starts counting the clock signals.

It can be seen from Fig.8.13 that the actual time period measured is from A_1 to B_o ($\Delta t'_1$) instead of the true time period of from A_o to B_o (Δt_1). The difference is of the order of 100 microseconds. This is the time required between freezing the display and resetting the counter. However, this is negligible in comparison with the accuracy of the system clock, which is 20 milliseconds for 50 Hz signal.

The corresponding circuit diagram is shown in Fig.8.14.

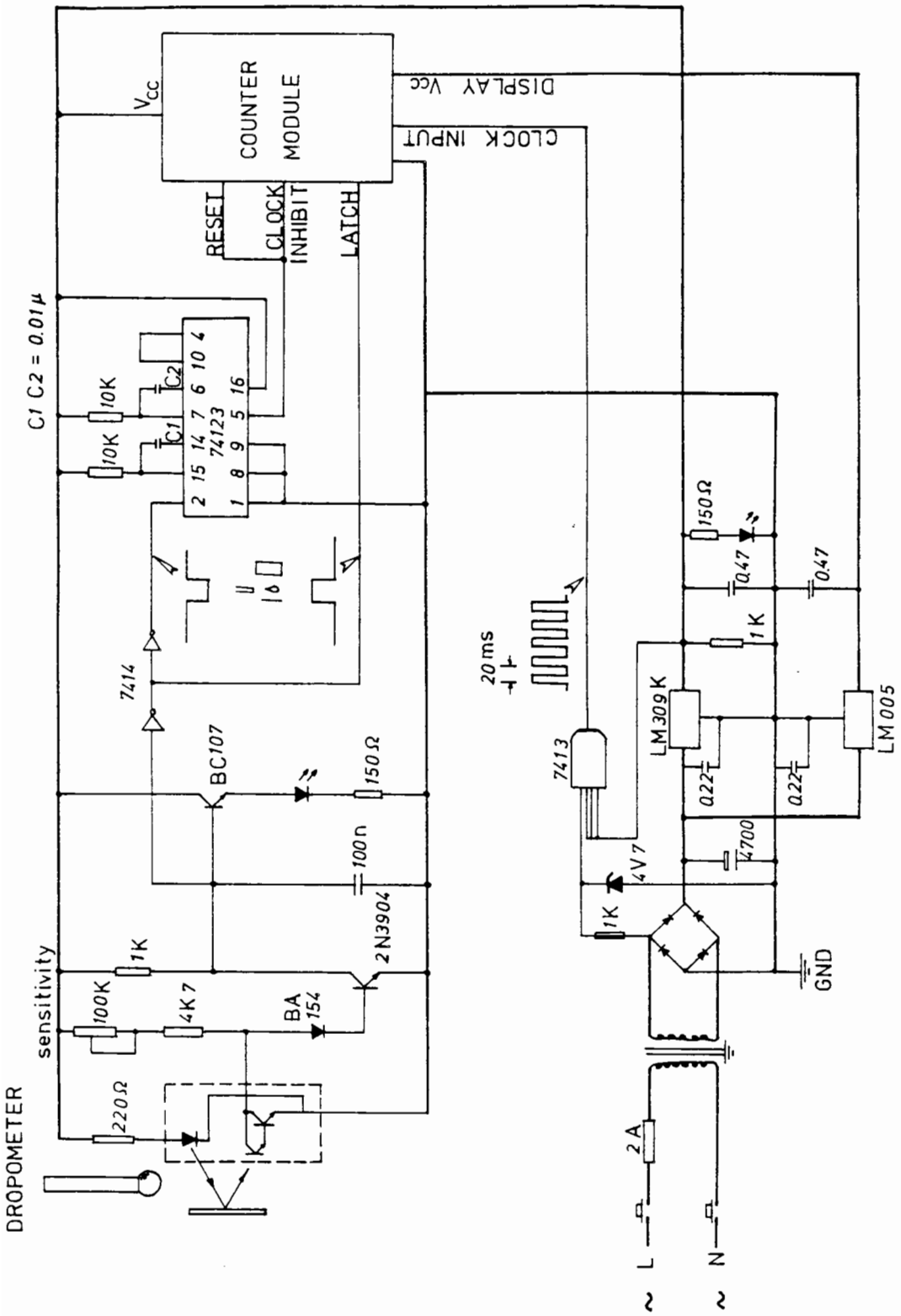

FIG.8.14 Time period measurement circuit for the dropometer.

5. MISCELLENEOUS DEVICES

The Pressure System

The initial design of the pressure system uses the self compensating mercury pot for both the cell pressure and the back pressure sources. However, it was discovered in the preliminary tests that this is unable to maintain a constant pressure during the early stages of consolidation because of the very large flow rate required during this stage. A set of results measured by the contact stress transducer is shown in Fig.8.15(a). It can be seen that as soon as the drainage valve is opened and the specimen starts consolidating there is an immediate drop in the stress applied to the specimen due to a similar drop in the cell pressure source. As the specimen consolidates and the flow rate is reduced this pressure will gradually rise back to its initial level.

To minimize this effect, an oxygen bottle with a pressure regulator is then used for the cell pressure. The result is shown in Fig.8.15(b) where it can be seen that a much smaller initial drop and a faster recovery are achieved.

The Filter

It has been pointed out in a previous work (Lee, 1977) that the use of a good filter is essential in the consolidation test. The requirements are that it should be permeable enough not to impede the flow and that it should have a small pore size to avoid clogging during an experiment. These requirements are achieved by the use of a very thin plastic membrane with precisely controlled pore size and porosity manufactured by Minipore Ltd.. The particular type finally chosen is a prefilter which is 0.005" (0.127mm) thin and is made by coating a

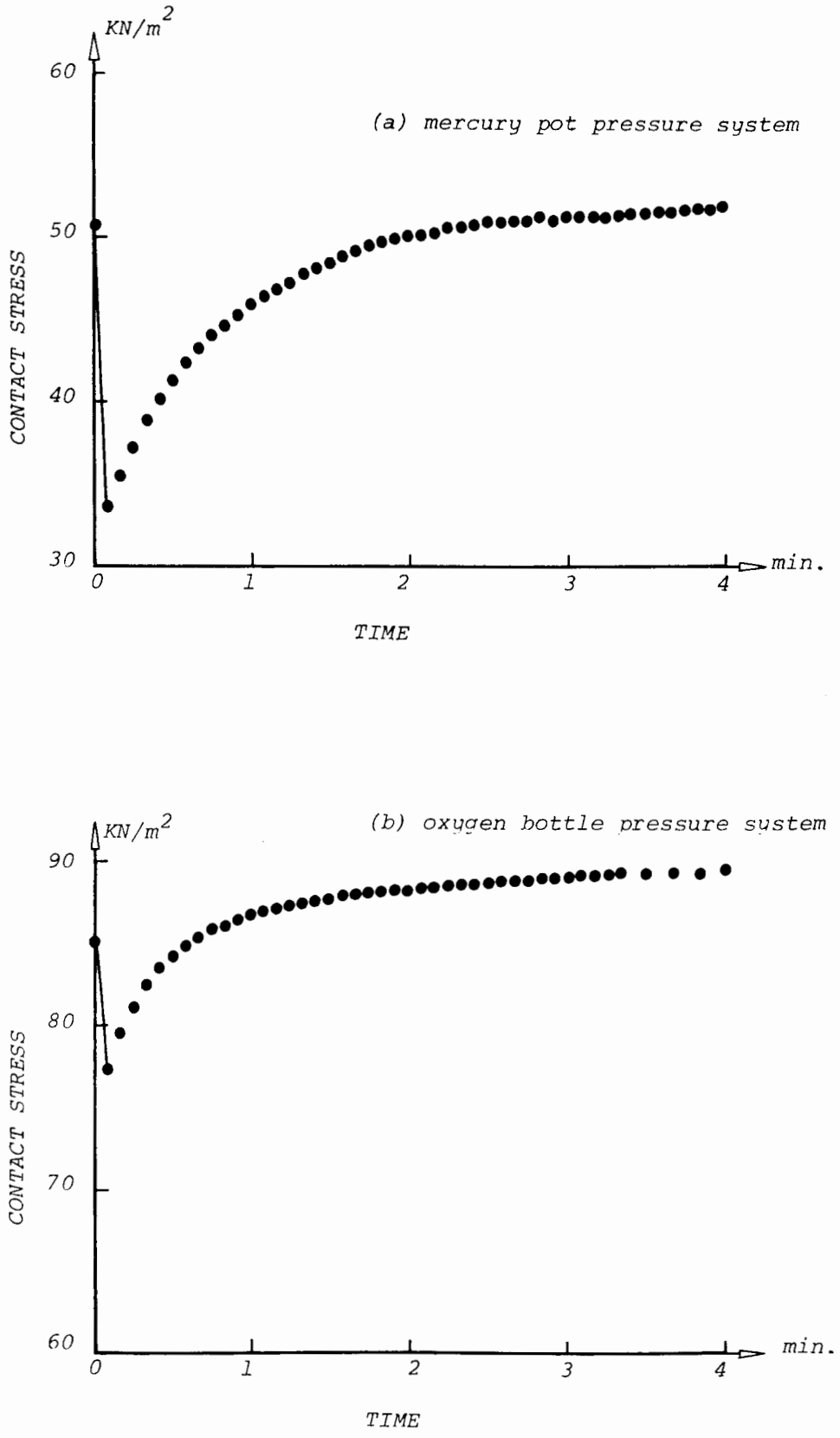

FIG.8.15 Responses of two pressure systems during the first four minutes of a consolidation test.

CHAPTER NINE ANALYSIS AND DISCUSSION OF EXPERIMENTAL RESULTS

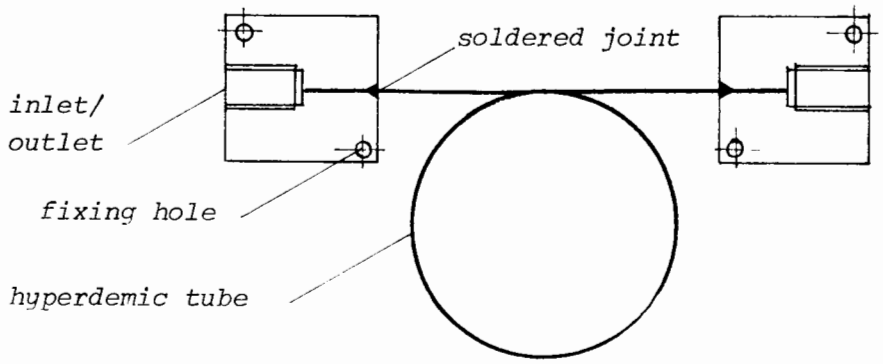

FIG.8.16 The flow restrictor.

very thin layer of plastic membrane filter with 0.2 - 0.45 micron pore onto an ordinary paper filter.

The Flow Restrictor

The flow restrictor is a length of fine bore hyperdemic tube which has both ends soldered into brass blocks for external connections, see Fig.8.16. The flow thus passing therefore depends on the differential pressure existing between its two ends. This is used in the present study to preconsolidate the specimen to eliminate the disturbances caused during the preparation stage, and this is also used in a special experiment in which the rate of consolidation is delayed artificially by connecting this to the drainage line.

6. FINAL ASSEMBLY AND TESTING PROCEDURE

A general layout of the final assembly is shown in Fig.8.17. The oxygen bottle (7) is used as the pressure source for the cell pressure. This is regulated by a pressure regulator (8) and transmitted

to the cell water by an oxygen-oil-water interface (6). This can be monitored by the Druck transducer (10) and read out by the DVM.

The back pressure to the specimen is maintained by the self compensating mercury pot (4) with the dropometer (5) connected in its outlet. The flow restrictor (2) is connected in parallel to the drainage line from the specimen with a series of on/off valves.

The preparation of the specimen follows that outlined in section 2 of this chapter. After this has been assembled in the oedometer and connections have made, the drainage line is closed and the cell pressure is introduced by adjusting the regulator until the required stress is registered in the contact stress transducer. The specimen is then allowed to drain and readings of the contact stress, the pore water pressure in the undrained and drained faces are taken from the DVM. The compression of the specimen is monitored by the dial gauge (3) attached to the ram of the piston and in some experiments the rate of volume change is monitored by the dropometer. Except for the preconsolidation stage and the special flow restrictor test, these readings are taken at intervals appropriate to plotting as the square root of time in the first three hours. The specimen is then left for 16 to 24 hours before the application of the next loading. The experimental programme and the results will be discussed in the next chapter.

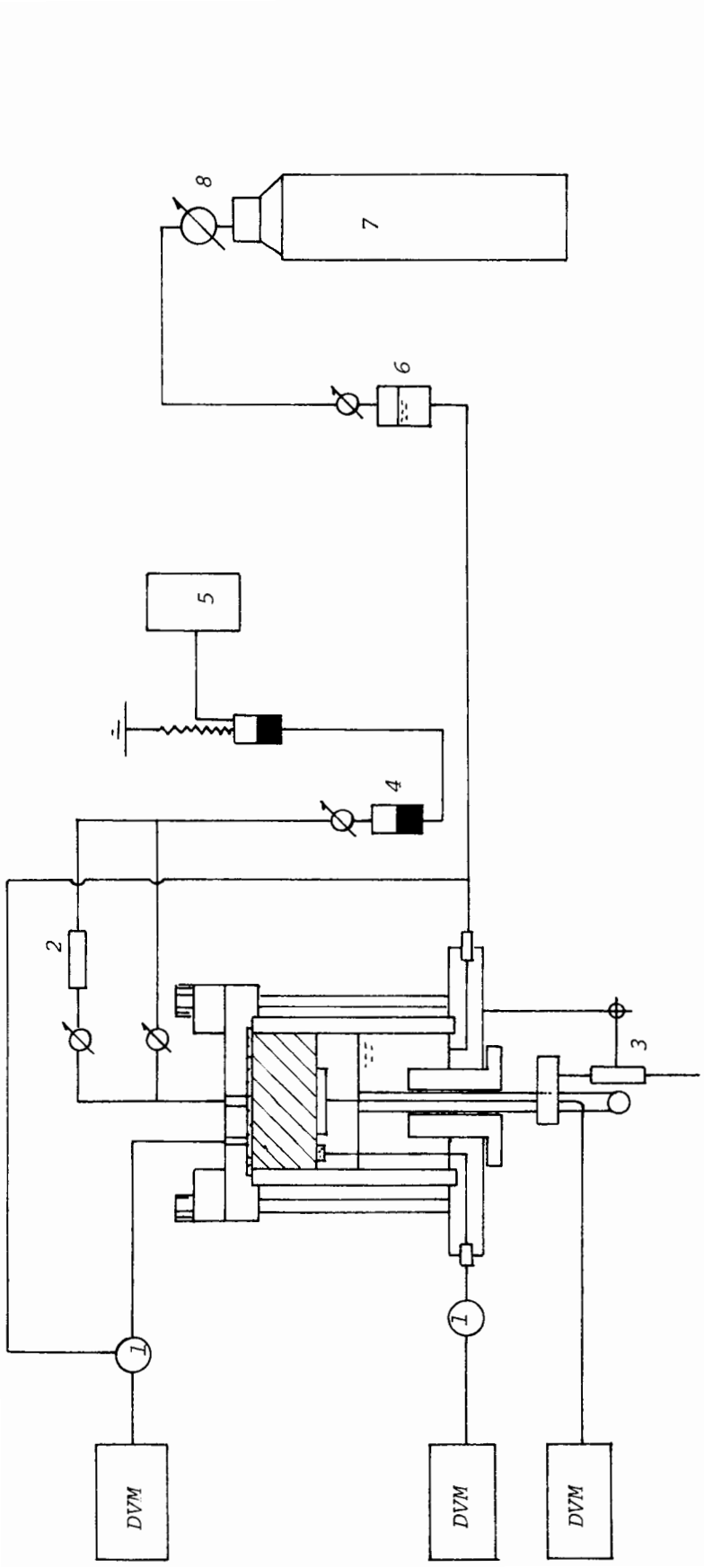

FIG.8.17 A general layout of the final assembly in the experiment.

ABSTRACT

The results of five step loading tests on Bridgewater Bay Silt are discussed in this chapter. It is found that the settlement of the specimen behaves linearly with the square root of time in the early stages of consolidation. This is used to determine the coefficient of consolidation C_v and C_F, and the result shows C_v to be more constant than C_F. The analysis of settlement is carried out by normalizing the settlement by dividing by its final value, and the time is also normalized to the square of the initial specimen thickness. This procedure thus absorbs some of the difference in the deformation and specimen thicknesses between these tests, and a comparison of these indicates that the behaviour is strain - dependent. Based on these results it is postulated that the particular type of soil used in this study will be better described by the C_v constant model. This postulation is further supported by comparing the theoretical settlement curves with the experimental results.

The stress-strain relationship is then interpreted from the experimental results using the C_v constant theory. This is compared with that obtained in a special step loading test having a flow restrictor in the drainage line. The results from this special test are also used to calculate the permeability and coefficient of consolidation.

Finally, based on these experimental findings a scheme for improving the present oedometer is proposed.

1. INTRODUCTION

The oedometer and its associated instrumentation described in the previous chapter have been the results of several modifications based on a number of preliminary experiments in the development stage. In this chapter the results of five step loading tests made in the final version of the oedometer will be analysed and discussed. A special step loading test, incorporating a flow restrictor in the drainage line, has also been carried out. This will be described in the later part of this chapter.

The soil used in this study is the Bridgewater Bay Silt recovered from 4" cores obtained in the Bristol Channel by gravity sampling. The core material is fairly dense and contains a considerable portion of fine sand and coal dust. In order to achieve a uniform and reproduceable specimen the core material is pretreated by wet sieving through B.S. no.200 (75 microns) sieve to remove the coarser partcles and heated so as to eliminate the bacteria that exist in the seabed. The resulting material is bluish-grey with approximately 30% clay content, it has a specific gravity of 2.665 and a liquid limit of 46% and plastic limit of 22%. The experimental programme and soil characteristics are summarized in Table 9.1.

The scope of the present study is thus limited to one particular type of soil with a special boundary and loading condition, and only the large strain cases will be considered here. The analysis and discussion will be mainly concerned with the settlement behaviour of the specimen, in which a comparison with the theory will be provided. Measurements of total stress and pore pressure are used for an indication of the quality of the experiment, and some discussion will be devoted to the interpretation of the stress-strain relationship from these measurements.

Destination		Loading Increment, KN/m^2	Initial Specimen Thickness mm	Strain, %	Particle Composition, %				C_F, $10^{-4} cm^2/sec$		C_v, $10^{-4} cm^2/sec$	
					Silt			clay				
					coarse	medium	fine		(1)*	(2)**	(1)*	(2)**
SL11		0 - 48	21.82	50.0					11.1		4.7	
SL2	SL21	0 - 15	28.64	56.3	30	24	12	34	12.0		4.8	
	SL22	15 - 52		14.7					5.4		4.4	
	SL23	52 - 105		8.9					4.9		4.4	
SL4	SL41	0 - 20	32.72	55.7	27	24	14	35	10.6	9.7	3.9	3.6
	SL42	20 - 52		12.4					5.5	4.9	4.7	4.1
SL5	SL51	0 - 60	29.16	57.7	30	31	11	28	15.2	12.1	5.3	4.2
	SL52	71 - 106		7.2					4.5	5.0	4.1	4.6
SL61		0 - 80	21.18	61.1	28	26	12	34	16.0	15.4	5.1	4.9
IF1		0 - 140	22.08	66.0	25	27	18	30				

TABLE 9.1 SUMMARY OF EXPERIMENTAL PROGRAMME AND RESULTS.

** determined from settlement measurements ** determined from rate of settlement measurements*

2. A BRIEF REVIEW OF RELEVENT THEORIES

The oedometer specimen is effectively a thin layer, the consolidation theory of which has been discussed in Chapter 3 of this thesis and several earlier works are also available, see the review in Chapter 1. The most important prediction made by the theory is that the settlement of the specimen is proportional to the square root of time in the early stages of consolidation regardless of the magnitude of strain. This is proved theoretically by McNabb (1960) on the general assumption that the effective stress and permeability are functions of void ratio only, and supported by a large number of analytical and numerical solutions (Mikasa (1963), Gibson, England and Hussey (1967) and Chapter 3 of this thesis).

An essential feature of the thin layer consolidation theory is its dependence on the coefficient of consolidation. For example, Chapter 3 shows that the consolidation behaviour of the specimen is determined to a large extent by the variation of this coefficient and the final magnitude of strain. Among the solutions developed the most useful ones are the constant C_F and the constant C_v cases. The constant C_F case results in a strain invariant solution, and in the constant C_v case the larger strain case will consolidate faster, where comparisons are made on the basis of the same time factor. In both constant C_v and constant C_F cases approximate analytical expressions are available for the early settlement behaviour, and these can be used to obtain the coefficient of consolidation C_v or C_F . This will be discussed in section 4 and a detailed analysis is given in Appendix A of this chapter.

3. GENERAL EXPERIMENTAL OBSERVATIONS

A typical experimental result is shown in Fig.9.1. The upper part of this graph shows the total stress applied to the specimen measured on the contact stress transducer and the pore pressures in the drained and undrained faces of the specimen. The lower part of this graph shows the settlement and rate of settlement of the specimen.

It can be seen from this figure that there is a considerable variation in the total stress applied to the specimen, despite the fact that the cell pressure has been maintained fairly constant. This variation is most likely to be caused by the piston friction. It can be seen that immediately after the specimen starts consolidating there is a sudden increase in the total stress which may be a result of the piston movement causing the friction to be reduced. The total stress will reach a steady value in a period of two to three hours. However, at the end of an experiment this total stress will have dropped a few kilonewtons per square metre from this stabilized value, which is probably a result of friction build up in the piston as its movement ceases.

The pore water pressure measured in the same face as the contact stress transducer (the undrained face) follows the same pattern of variation in the early stages. Note that this pore water pressure starts dissipating at a fairly late stage of the total consolidation. In the example shown here it can be seen that by the time this occurs some more than 60% of the total settlement has already taken place. This suggests that the soil in its very soft state, as is the present case, can be strained without appreciable effective stress change. This particular aspect will be further discussed in section 6.

The pore water pressure in the drained face does not drop immediately to the back pressure level as soon as the consolidation starts, see Fig.9.1. This is possibly a result of the hydraulic resistance existing in the back pressure line despite all the connecting

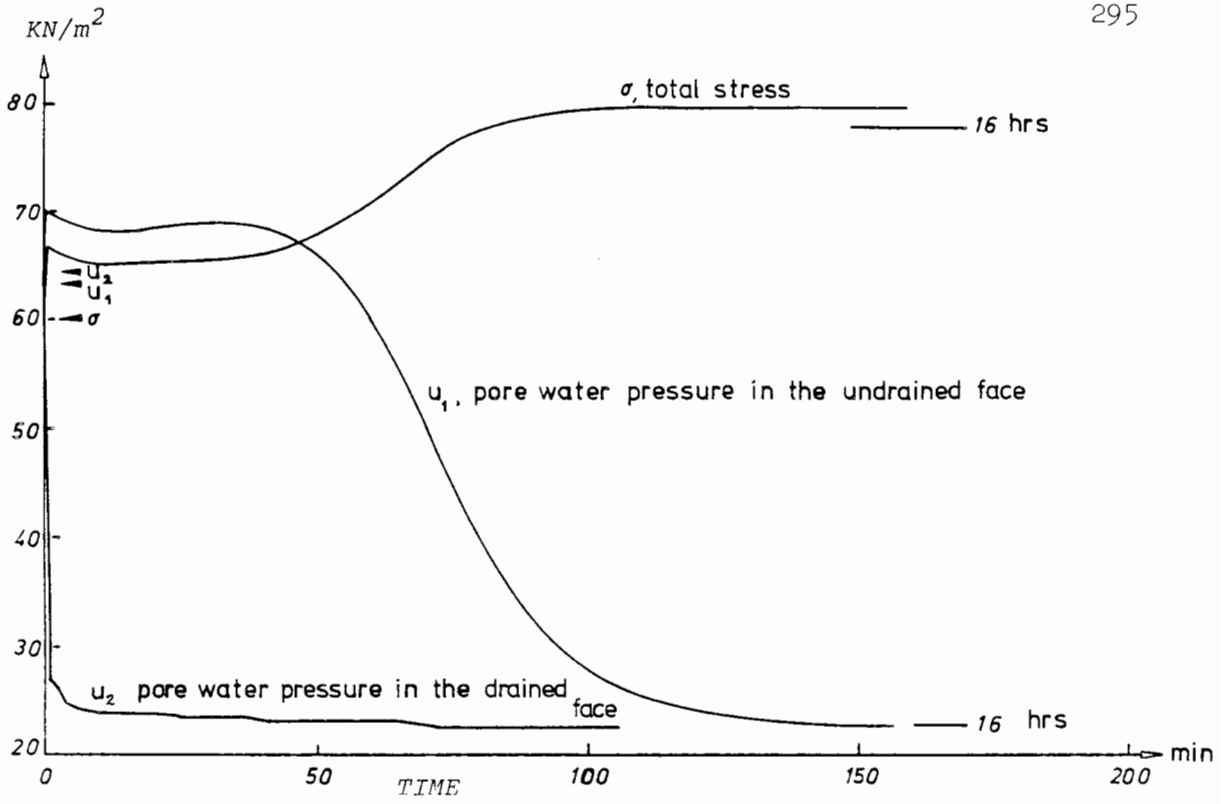

TEST SL51 INITIAL SPECIMEN THICKNESS = 29.16 mm

FINAL STRAIN = 57.7 %

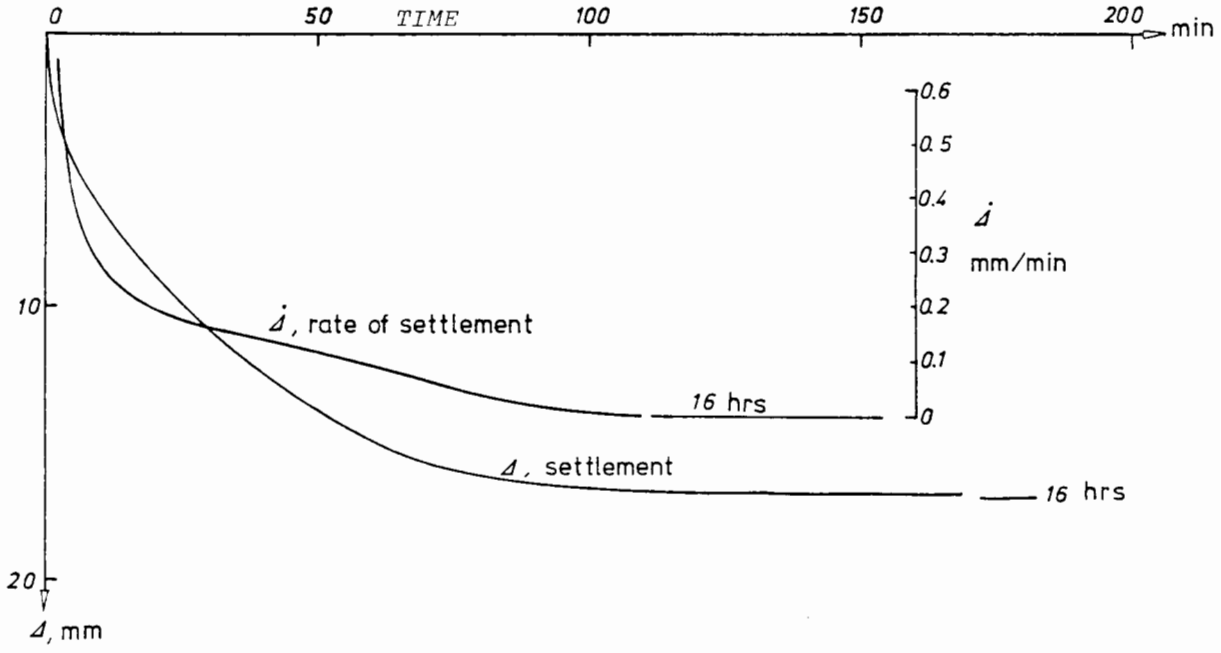

FIG.9.1 A typical experimental result

tubes being kept as short as possible. In the previous chapter a similar, but more marked effect has been observed in the cell pressure line when the mercury pot was used as the pressure source.

Despite the fact that the performances of the total stress and the drainage condition are not ideal, the settlement behaviour of the specimen correlates well with the theory. The settlement of Fig. 9.1 is plotted against the square root of time in Fig.9.2, and a well defined initially linear region can be seen in this graph. This is further supported by the rate of settlement measurement. In Fig.9.3 the rate of settlement as measured in the dropometer is plotted against the reciprocal of the square root of time and a linear region can again be observed. This linear property will be used in interpreting the coefficient of consolidation in the next section.

4. DETERMINATION OF THE COEFFICIENT OF CONSOLIDATION

In order to interpret the experimental result it is necessary to adopt some assumptions regarding the variation of the coefficient of consolidation c_v or c_F . Since the assumptions are made before the actual variation of c_v and c_F are known, the most reasonable way would be assuming that either c_v or c_F remains constant within each step loading. Hence the values of c_v or c_F can be interpreted from the initially linear region of the settlement - square root time curve or the rate of settlement measurement. Detailed description of this method is given in Appendix A of this chapter.

In the case of interpreting from the settlement measurement, this method consists of extending the initially linear region of the settlement - square root time curve to intercept with the final settlement, see Fig.9.2. The time coordinate of the intercept is denoted

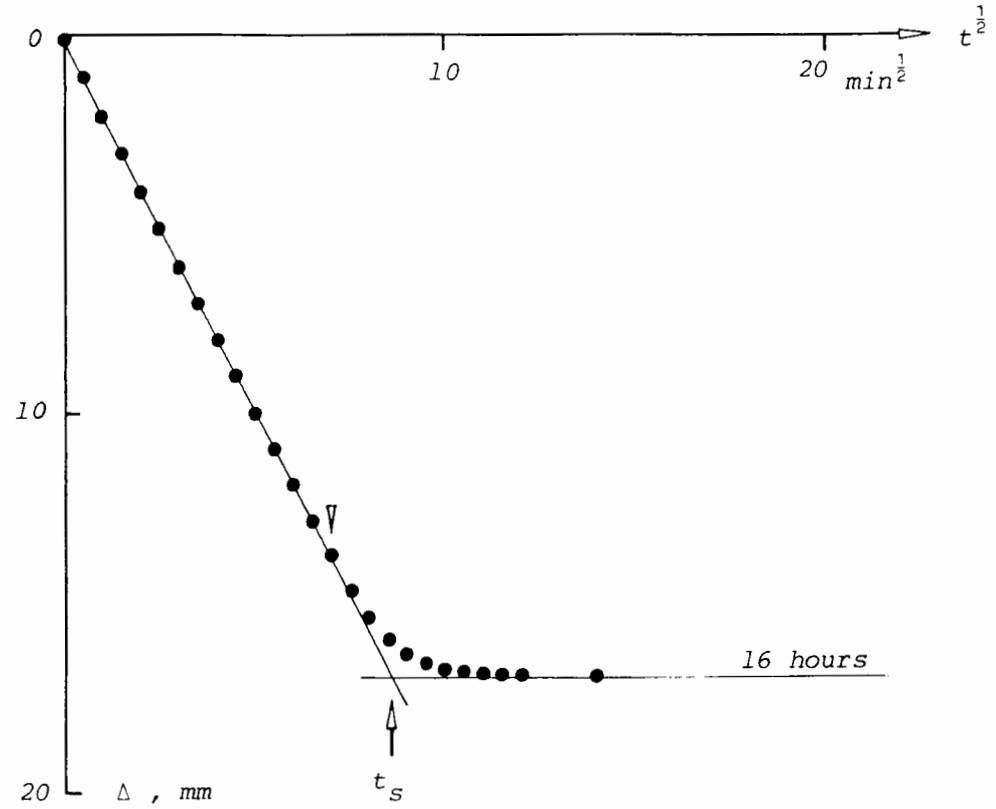

FIG.9.2 Settlement versus the square root of time for test SL51

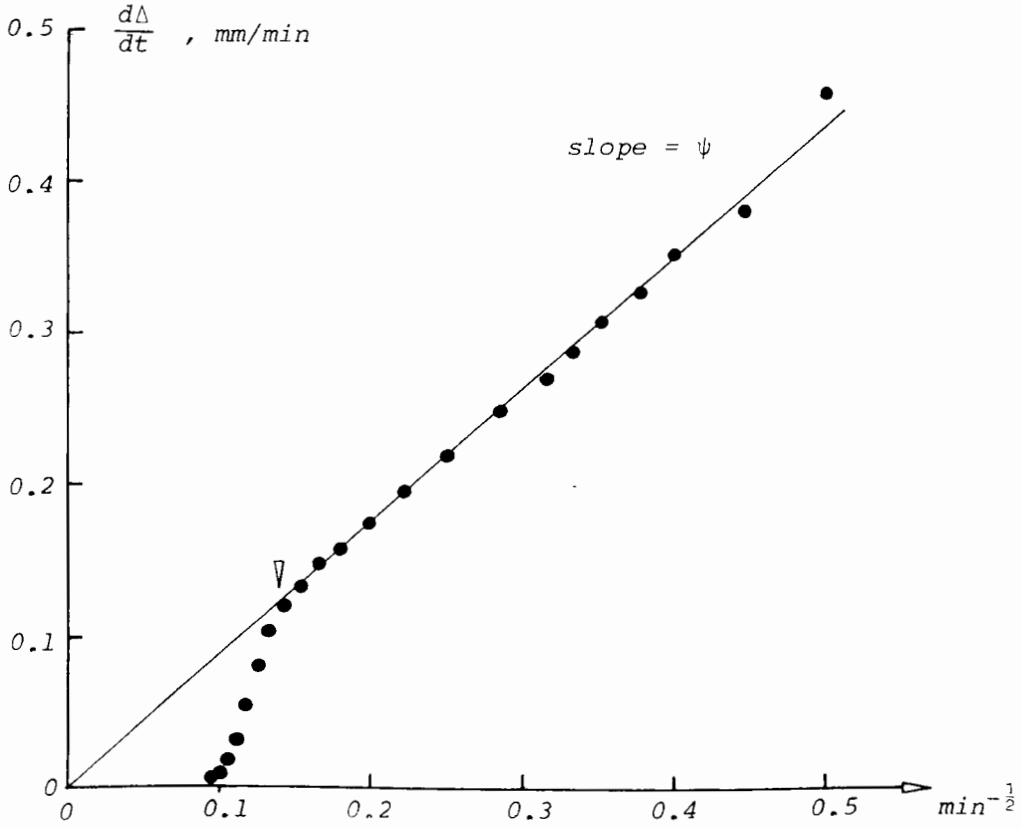

FIG.9.3 Rate of settlement versus the reciprocal of the square root of time for test SL51.

by t_s and the coefficient of consolidation is calculated from the equation :

$$C_v \text{ , } C_F = h_o^2 \frac{T_s}{t_s} \qquad (9.1)$$

where h_o is the initial specimen thickness. The details can be found in Appendix A.

The method using the rate of settlement curve requires a slightly more complicated equation as :

$$C_v \text{ , } C_F = [\frac{2\psi}{\beta \lambda}]^2 \qquad (9.2)$$

where λ is the final (Lagrangian) strain and ψ is the slope of the linear region in the rate of settlement - reciprocal of square root of time curve, see Fig.9.3, β is a constant whose values are given in Appendix A.

The calculated C_v and C_F determined by these methods are shown in Table 9.1. It can be seen that in the large strain cases (SL11, SL21, SL41, SL51 and SL61) there is a very large difference between the C_v and C_F values so interpreted. This is because the values of T_s and β used are very different in the two cases with large strain. In subsequent loading where the strain is fairly small the difference between C_v and C_F also becomes smaller for the same reason. It can be noticed that the C_v constant theory gives in this case more compatible values of C_v in subsequent loading than the C_F constant theory.

5. TIME - SETTLEMENT BEHAVIOUR

In the present experimental programme specimens of different thickness have been used with different loading increments. Thus, in

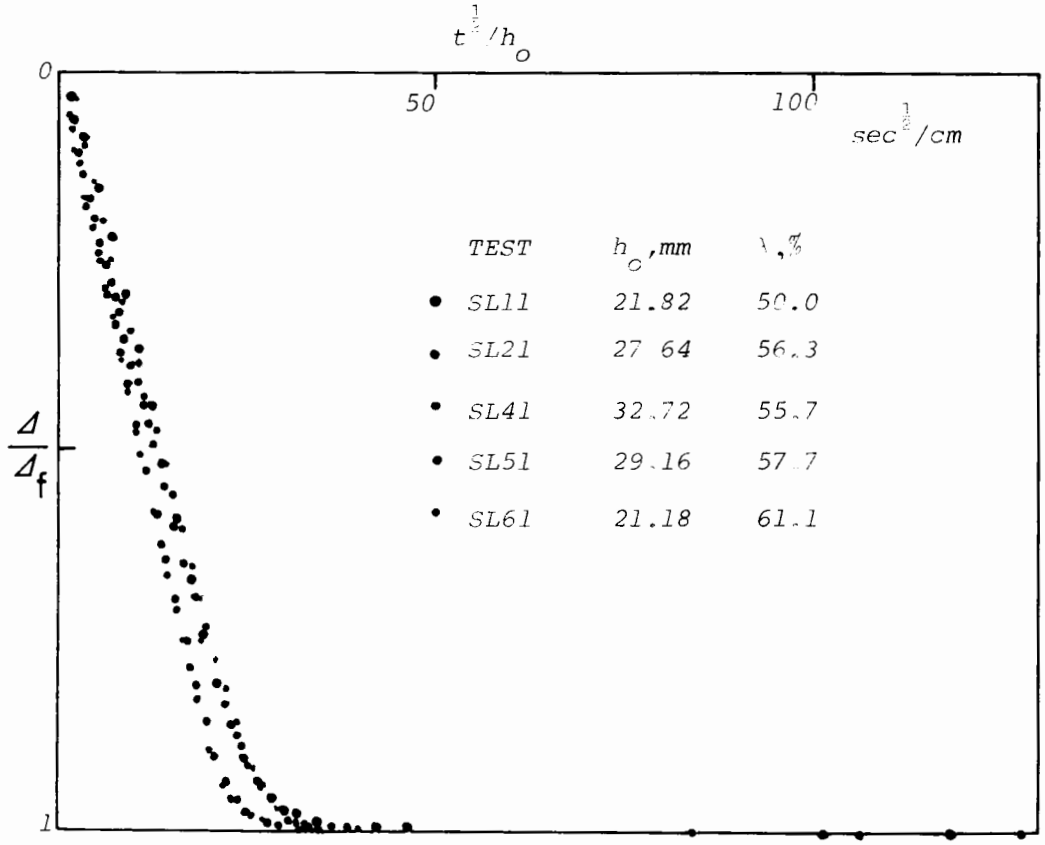

FIG.9.4 The degree of settlement versus the square root of the tranformed *time for five large strain tests.*

order to analyse the settlement behaviour the settlement is normalized by dividing by its final value, which results in the degree of settlement which has been used in the theoretical analysis. The time is normalized with respect to the square of the initial specimen thickness, and the result t/h_o^2 is then proportional to the time factor which is defined as $C_v t/h_o^2$ in Chapter 3 or $C_F t/h_o^2$ by Gibson et.al.(1967).

The normalized results of the five large strain tests are plotted in Fig.9.4 where the square root time axis has been used. It can be seen that regardless of the difference in specimen thickness and loading increment between each test, the results so normalized all fall into a fairly narrow band. The slight difference between these results can be related to the magnitude of strain. The slowest consolidation, in terms of the normalized time t/h_o^2 occurs with SL11 which has the smallest strain (50%), and the fastest consolidation occurs

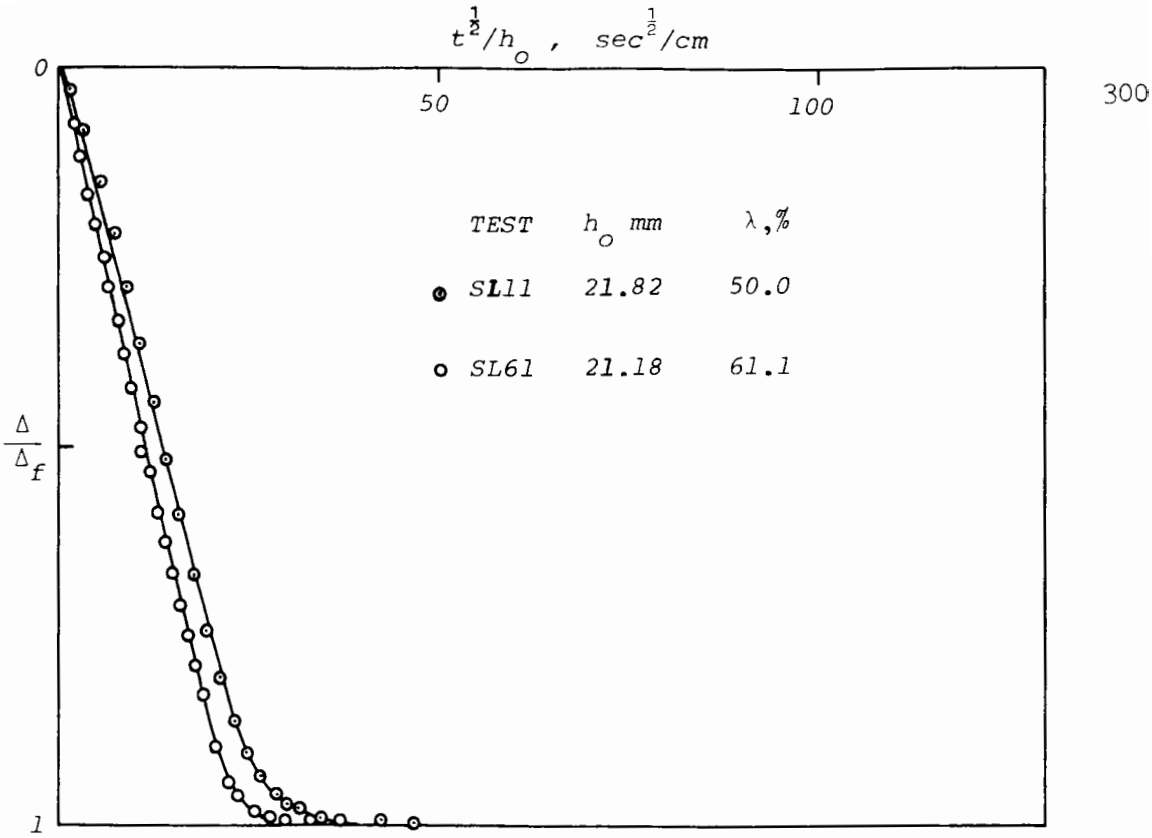

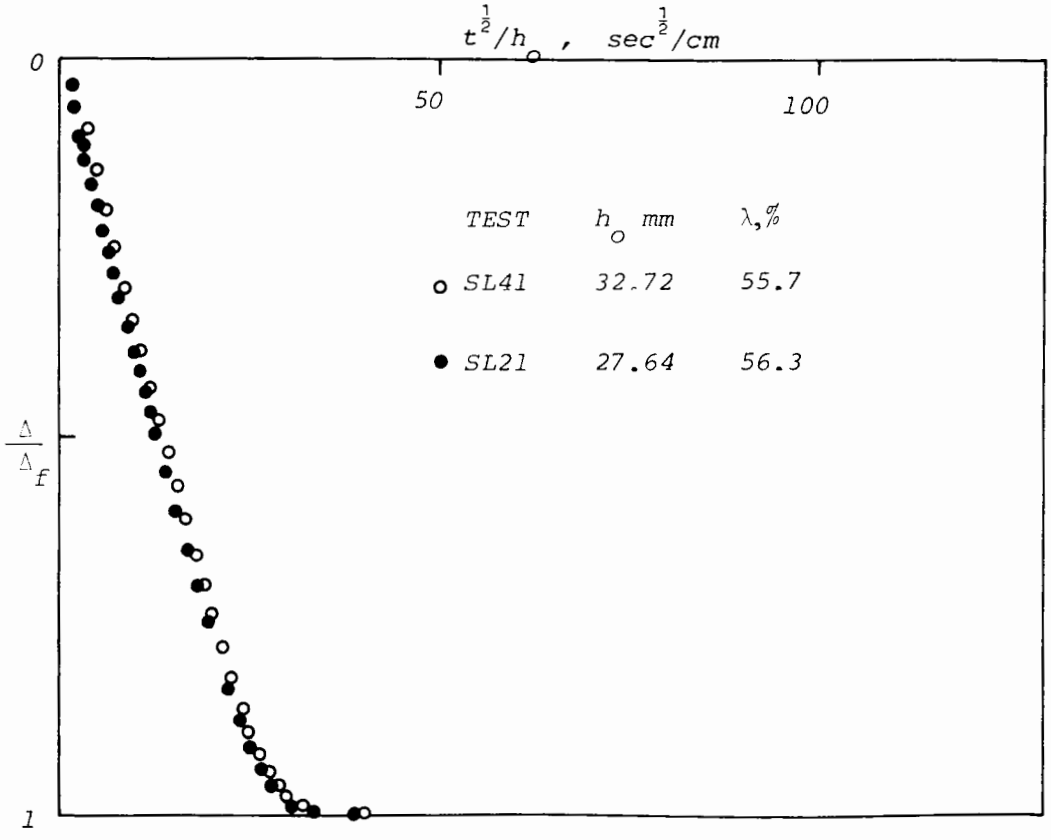

FIG.9.5 (top)

FIG.9.6 (above)

with SL61 which has the largest strain (61%). These two cases are compared in Fig.9.5 for clarity. This behaviour is also supported by comparing the results of SL21 and SL41. These two cases have similar magnitude of strain (56.3% for SL21 and 55.7% for SL41) and different specimen thickness (27.64mm for SL21 and 32.72mm for SL41). Their results, when normalized to take into account the different thickness and final settlement, are very close to each other. This is shown in Fig.9.6.

A further comparison between the large and small strain cases is provided in Fig.9.7 which shows the results of three subsequent loading steps SL21, SL22 and SL23. Here again the normalization procedure has been applied to account for the very substantial change in thickness

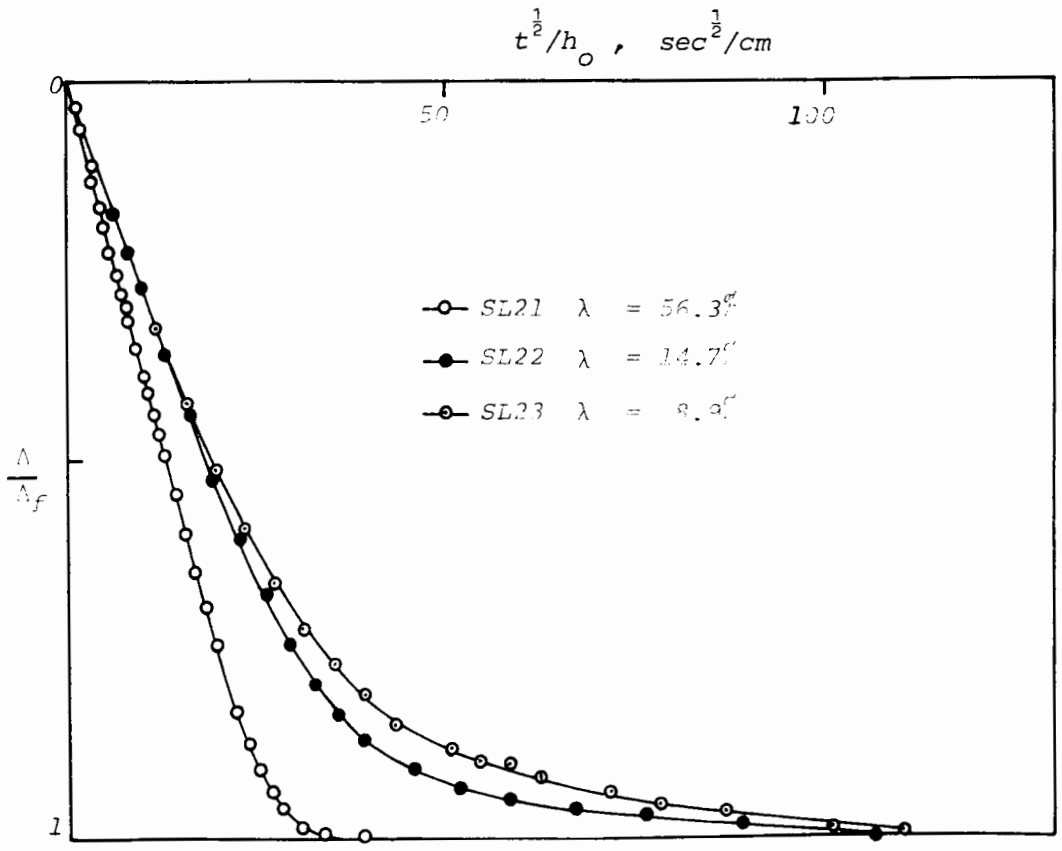

FIG.9.7 Normalized results of three subsequent loading steps.

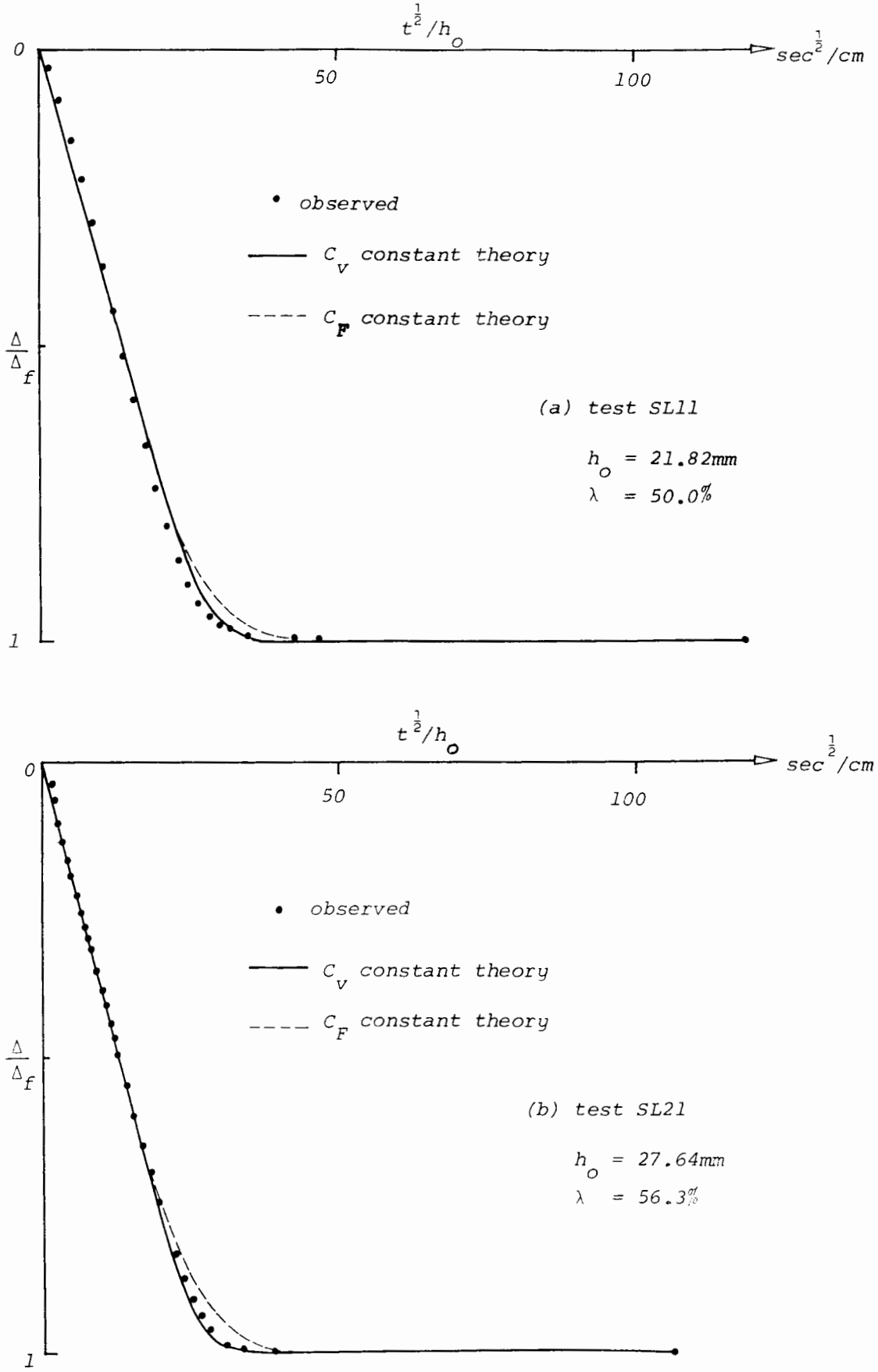

FIG.9.8 Comparison of theoretical and observed time - settlement behaviour of step loading tests with large strains.

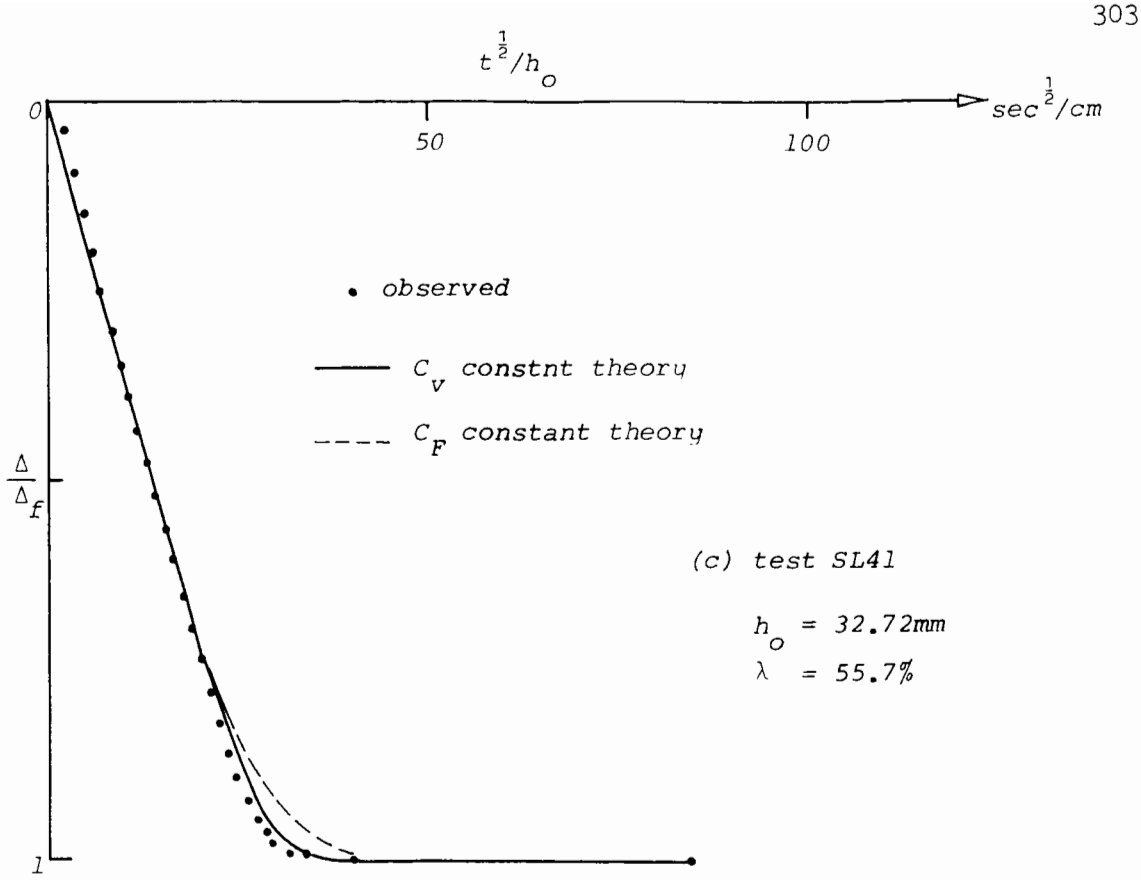

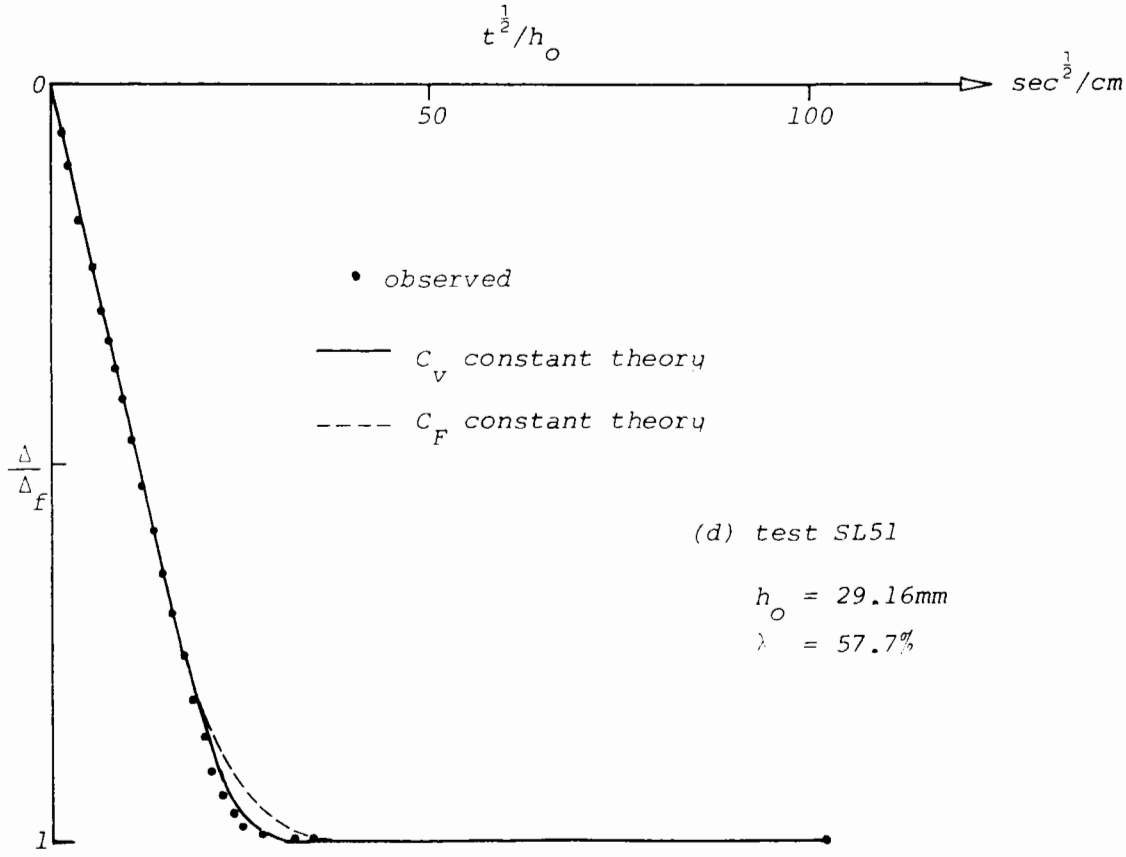

FIG.9.8 (continued)

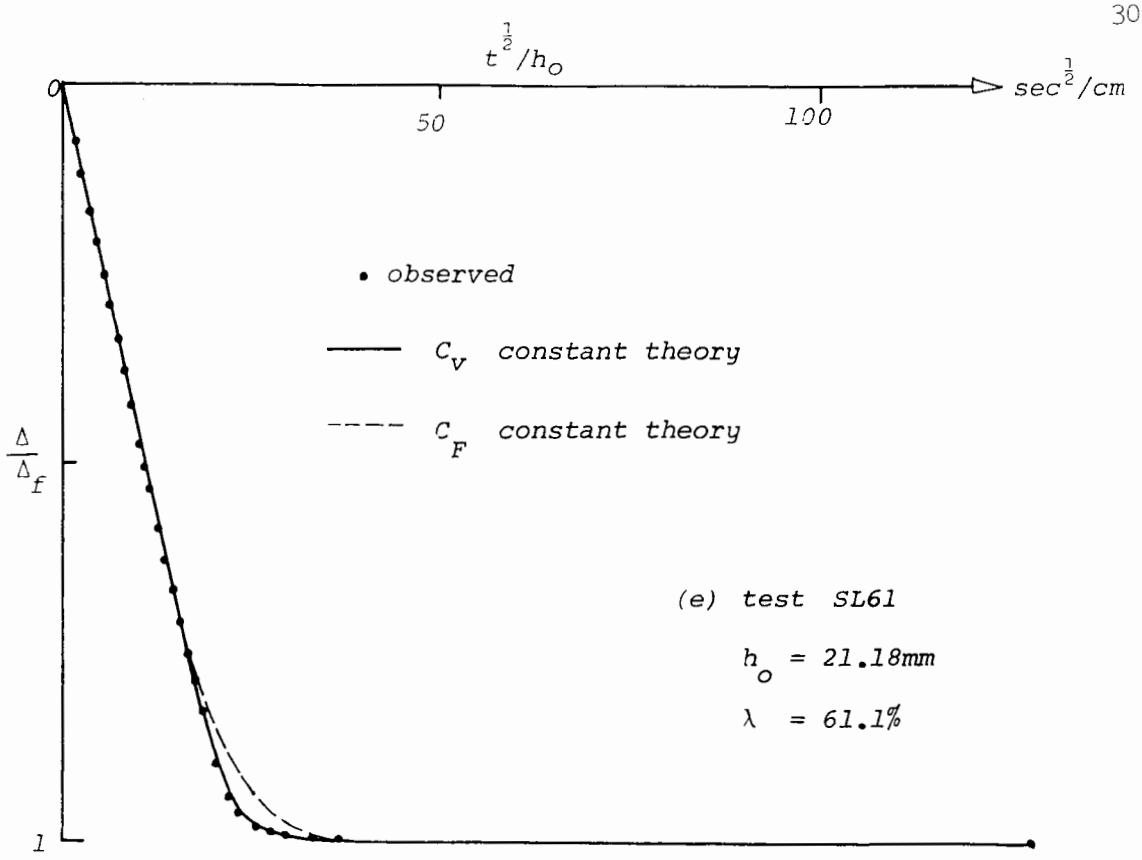

FIG.9.8 (continued)

in between loading steps. The trend that larger strain consolidates faster (with respect to t/h_o^2) is clearly demonstrated in this example. Referring to the theory developed in Chapter 3, the trend suggests that the C_v constant model would be more adequate for the particular type of soil used in the present programme. The fact that more consistent values of C_v have been achieved in the last section also supports this point of view.

To pursue this discussion further, the theoretical time - settlement relationship has been calculated using the coefficient of consolidation C_v and C_F obtained in the last section. These are shown in Fig.9.8 in which only the large strain cases are analysed. The full lines are those calculated by the C_v constant theory using the numerical technique developed in Chapter 3, and the broken lines are those obtained from the C_F constant theory. It can be seen that better agreement with experiment is obtained with the C_v constant theory (although in fact the agreement with C_F constant theory is quite reasonable).

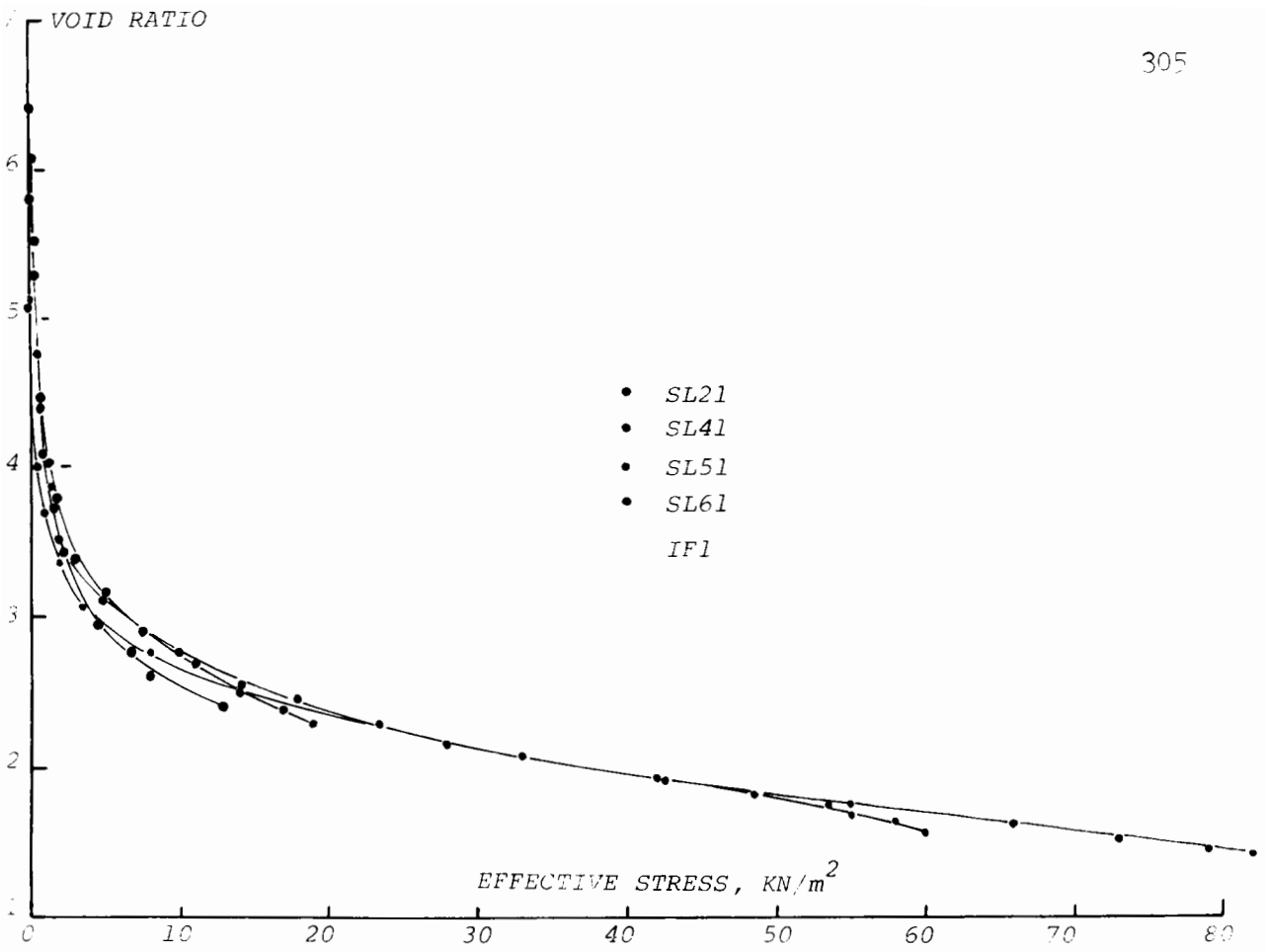

FIG.9.9 The interpreted effective stress - void ratio relationship.

6. THE STRESS - STRAIN RELATIONSHIP

The development of effective stress in the undrained face is obtained from the total stress and pore water pressure readings taken during the experiment. The corresponding void ratio can be calculated from the theory, and the C_v constant theory is used for this purpose owing to its great success in correlating with the settlement behaviour as shown in the previous section. The stress - strain relationship interpreted by this method is shown in Fig.9.9 for the five large strain cases. There is a slight scattering in between the results because of the difference between the theory and experiment. However, the trend shows that the stiffness (or void ratio) of the soil changes considerably in the first ten kilonewtons per square metre, within which the soil can be deformed without much increase in effective stress. In general, these results also agree favorably with that obtained by

the flow restrictor test also shown in this figure. The flow restrictor test will be explained in the next section.

7. CONSOLIDATION WITH FLOW RESTRICTOR

In a previous work (Lee,1977) the effect of an imperfect filter on the consolidation of an oedometer specimen has been studied within the framework of small strain Terzaghi theory. An imperfect filter will act like a flow restrictor in the drainage outlet of the specimen. As a result, the pore water pressure in the drainage face of the specimen will be higher than the back pressure level and will dissipate slowly according to the flow rate. This general statement can also be applied to the large strain case, and the purpose of introducing a flow restrictor in the drainage line is to decrease the pore pressure gradient across the specimen. If the gradient is sufficiently small, the soil specimen will be almost uniform and measurement made at one face will be close to the average value obtaining throughout the thickness.

To illustate this, Fig.9.10 shows schematically a specimen with a flow restrictor connected to the back pressure source. During the experiment the following parameters are measured :

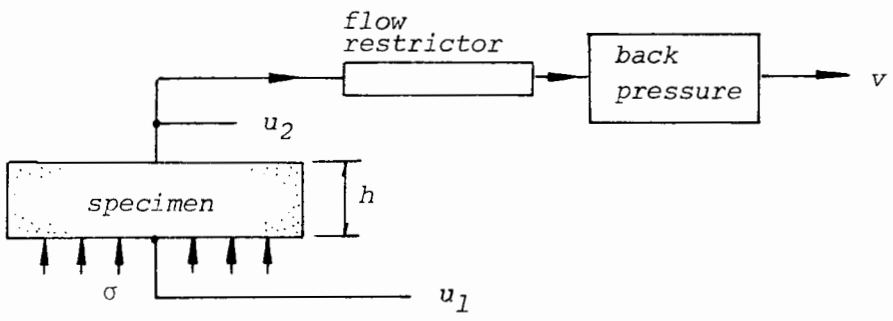

FIG.9.10 Schematic diagram of the layout of a flow restrictor test.

(1) outward flow rate from the specimen v

(2) thickness of the specimen h

(3) total stress applied to the specimen σ

(4) pore water pressure on the undrained face of the specimen u_1

(5) pore water pressure on the drained face of the specimen u_2

Accordingly the following parameters can be calculated :

(1) average void ratio of the specimen e

(2) average effective stress in the specimen $\sigma - \frac{1}{2}(u_1+u_2)$

(3) average hydraulic gradient across the specimen $i = (u_1-u_2)/(h\rho_f)$

(4) average permeability of the specimen $k = \frac{v}{i}$

(5) coefficient of consolidation $$C_v = -\frac{k}{\rho_f}(1+e)\frac{d\sigma'}{de}$$

$$C_F = -\frac{k}{\rho_f}\frac{(1+e_o)}{(1+e)}\frac{d\sigma'}{de}$$

The results of an experiment carried out (IF1) are shown in Fig.9.11. It can be seen that the difference between the pore water pressures in the undrained and drained face of the specimen is very small for most of the times. The interpreted stress - strain relationship which has already been shown in Fig.9.9 is reproduced in greater details in Fig.9.12. In this figure the data are bounded by an estimated error bound which represents the error that may have been introduced in assuming that the average effective stress corresponds to the average void ratio. The interpreted permeability is shown in Fig.9.13, and the variation of C_v and C_F are shown in Fig.9.14. There is a considerable scatter in the C_v and C_F values, which is caused by a similar scatter in the permeability and also to a less extent by the numerical differentiation process to obtain $d\sigma'/de$. The scatter in the permeability is likely to be a result of inaccuracies in the pore pressure and flow rate measurements. At present no attempt has been made to smooth the data by numerical techniques. However, despite the scatter of the C_v and C_F values, the results suggest that C_v is more likely than C_F to have a constant value. This provides a further

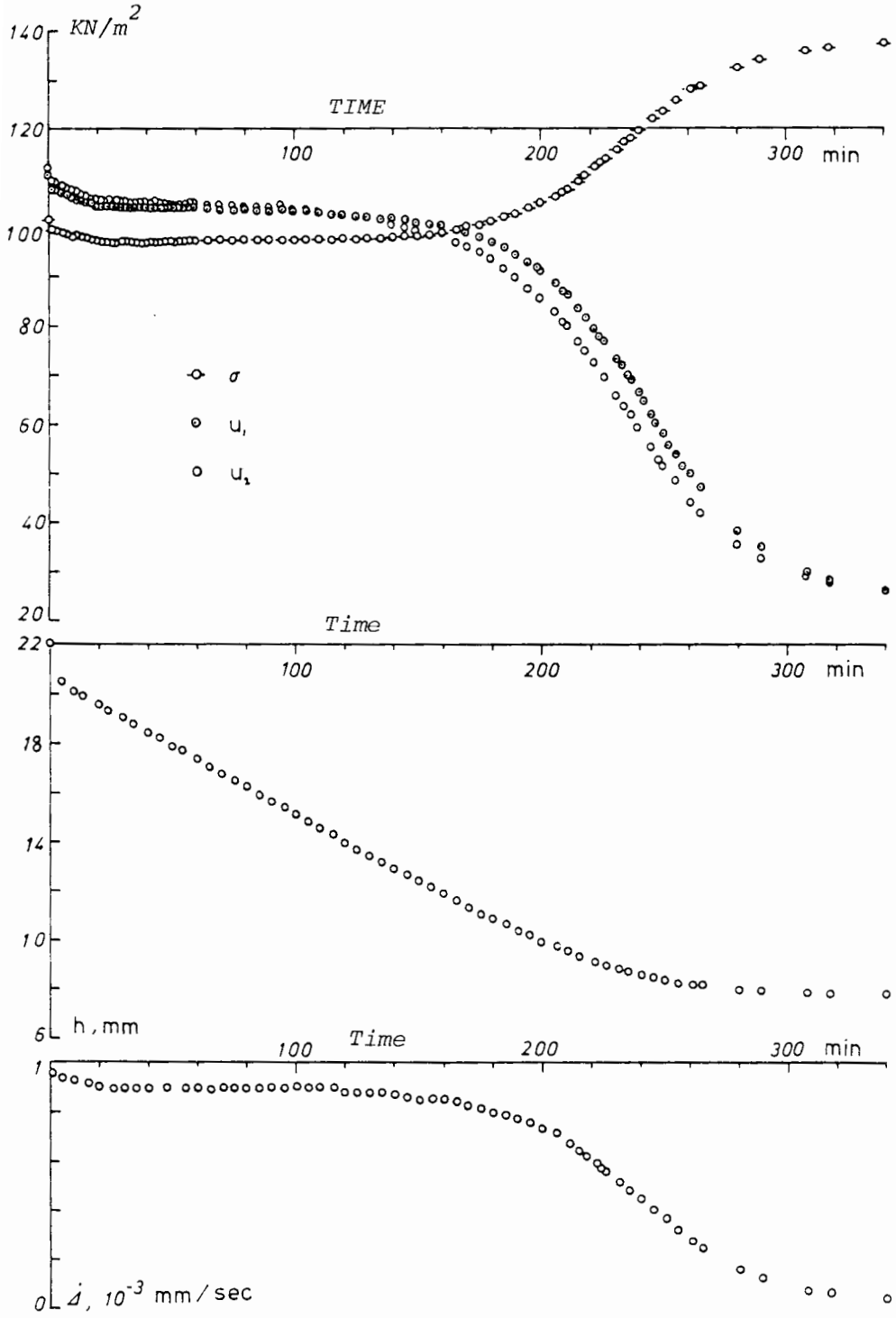

FIG.9.11 Experimental result of the flow restrictor test

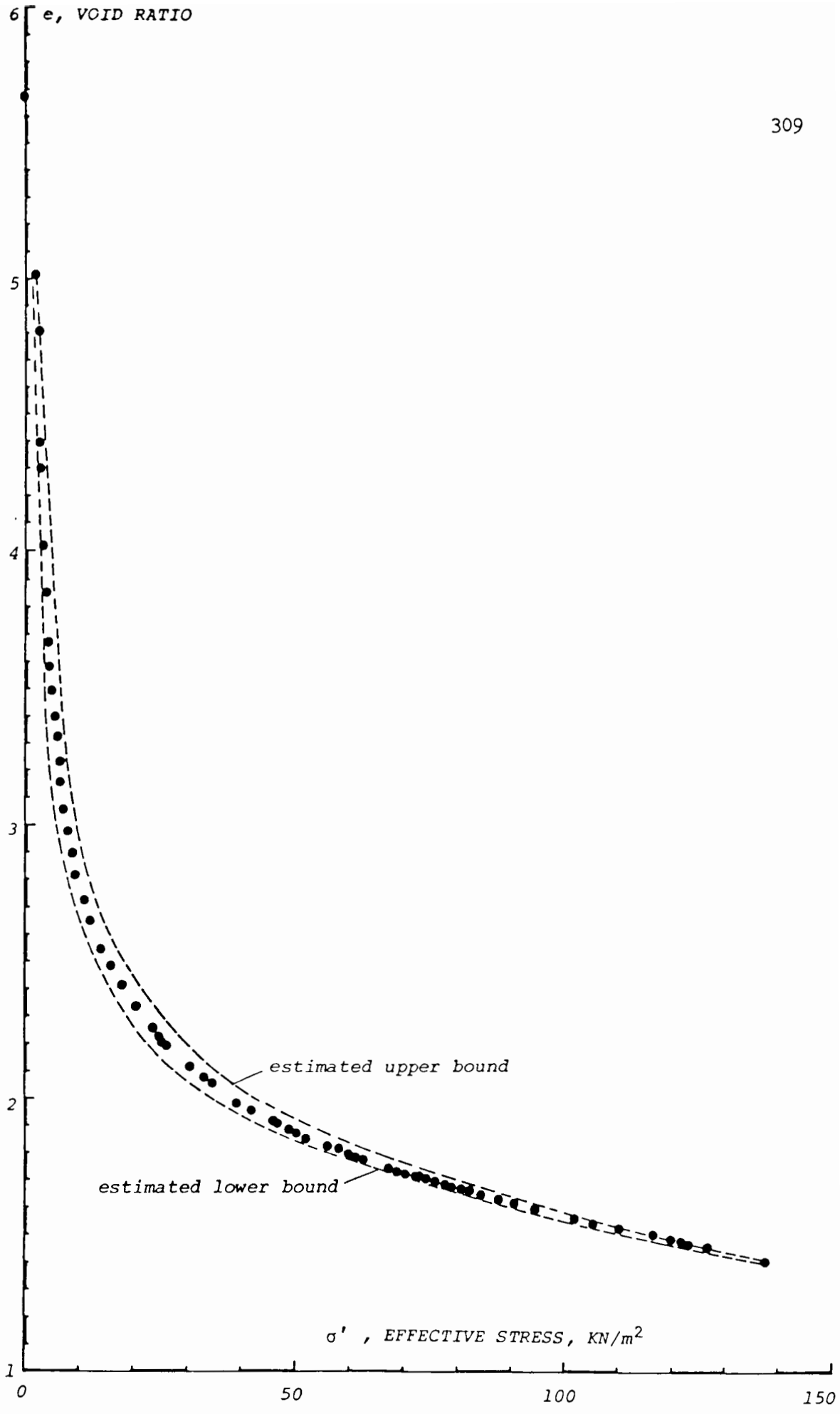

FIG.9.12 Interpreted effective stress - void ratio relationship.

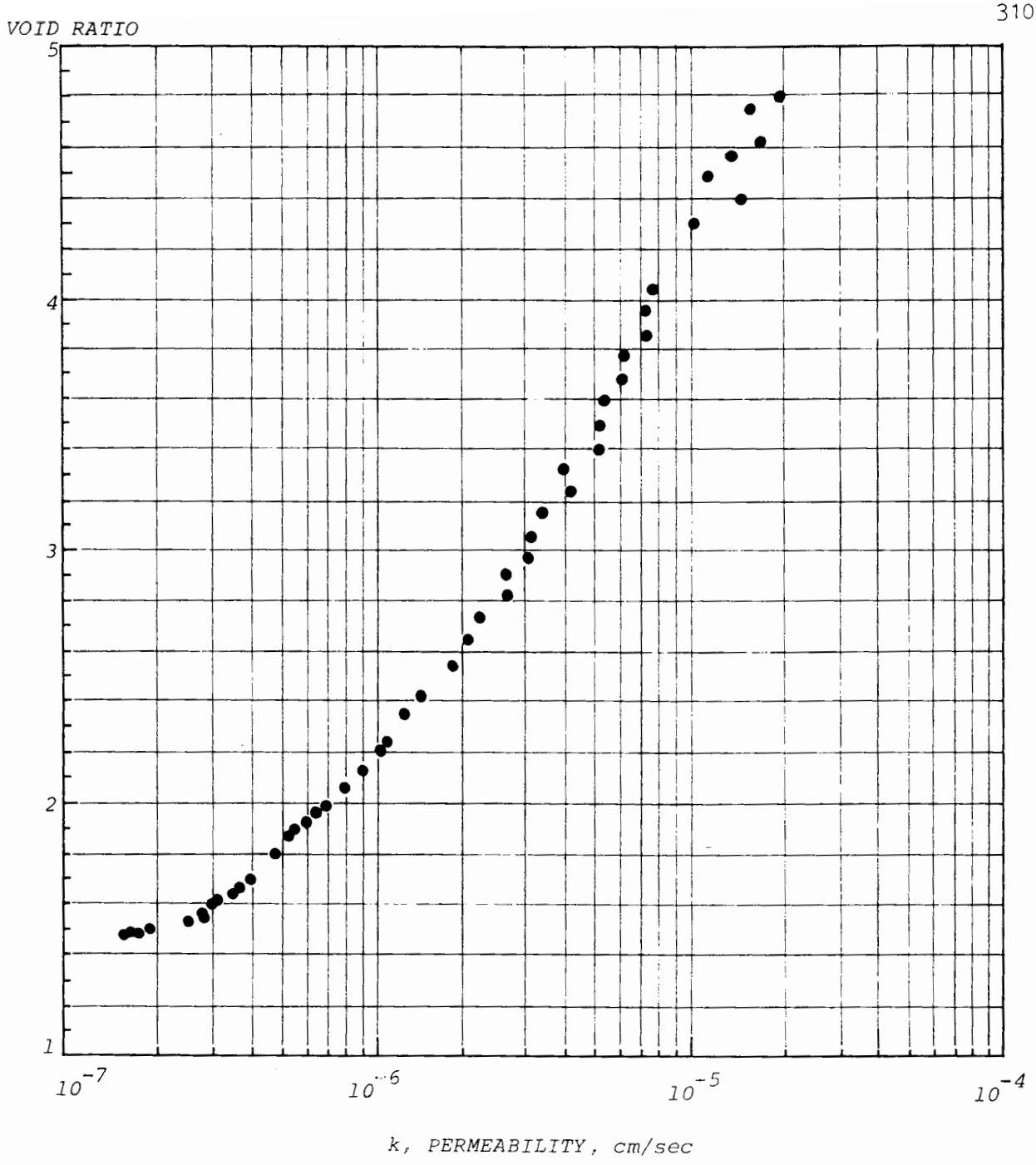

FIG.9.13 Interpreted permeability - void ratio relationship.

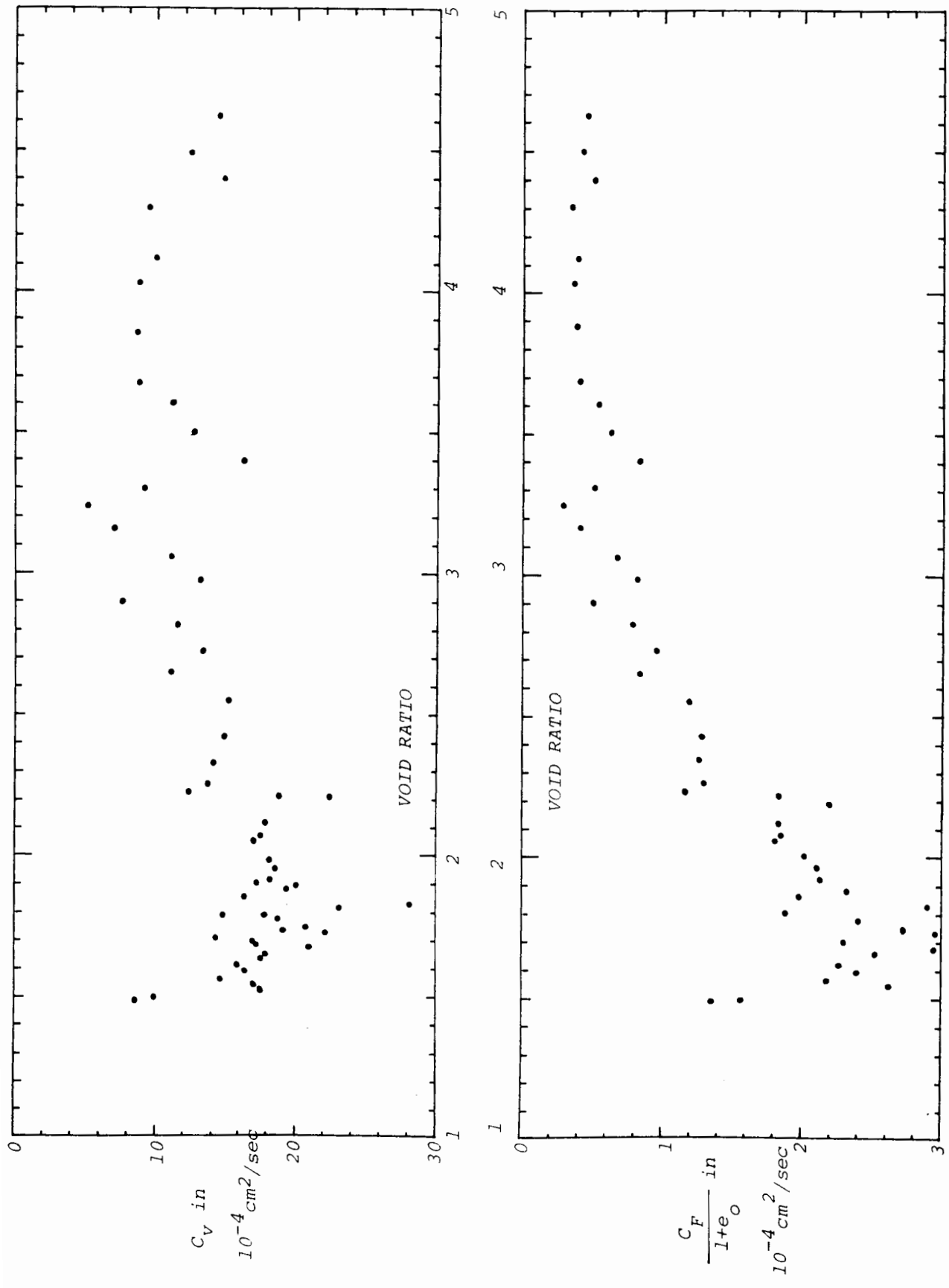

FIG.9.14 Interpreted coefficient of consolidation C_v and C_F.

support to the use of the c_v constant model for this particular type of soil.

Finally, it is noted that there is a difference in the mean c_v value obtained in this experiment and those obtained from the step loading tests.

8. CONCLUDING REMARKS

The purpose of the experimental study reported in this chapter are :

(1) To provide an assessment for the theory.

(2) To investigate the consolidation characteristics of a very soft soil where large strain occurs.

and these two goals have been achieved with some success. In the early part of this chapter the inadequacy of the present oedometer to produce an ideal theoretical boundary condition has been pointed out. Nevertheless the settlement behaviour of the specimen correlates surprisingly well with the theory, and invaluable information has been obtained in this study regarding the consolidation characteristics of the soil.

In general, it has been established qualitatively that the particular type of soil used in the study behaves closely to the c_v constant model. Further research will be required to confirm this at a quantitative level. This will involve an improvement of the present oedometer to produce a near ideal boundary condition, and also the development of a better flow restrictor and new techniques for direct measurement of soil consolidation characteristics. A proposed scheme for improving the oedometer is given in the following section, and other aspects of further development will be discussed in the next chapter.

9. FURTHER DEVELOPMENT

The most undesirable feature of the present oedometer is the variation of the total stress applied to the specimen as a result of piston friction. This can be overcome either by adjusting the cell pressure to compensate for the piston friction or by a different mechanical design to eliminate this friction. It is proposed that the latter approach be adopted, and a new piston design will be outlined below.

Fig.9.15 shows schematically the proposed new design. The piston can be made of sintered bronze which has an exceptionally good bearing property and very low friction. In this arrangement the pore water from the specimen is communicating with the cell chamber, which is connected to the back pressure source. Since it is not required to seal the piston the only possible source of friction comes from the scraper ring on top of the piston, and it is possible to design this ring with suitable material to achieve a very low friction. A further advantage of this arrangement is that the actual amount of flow communicating with the back pressure source is very small, and depends on the size of the ram used, and hence the drainage boundary condition can be close to ideal.

It is proposed to actuate the piston by an air cylinder using a bellofram type of seal which has a very low friction. The total combination thus should give a friction figure much smaller than the present oedometer. Furthermore, should this very small friction cause any concern it can easily be compensated by servoing the back pressure to maintain a truly constant total stress.

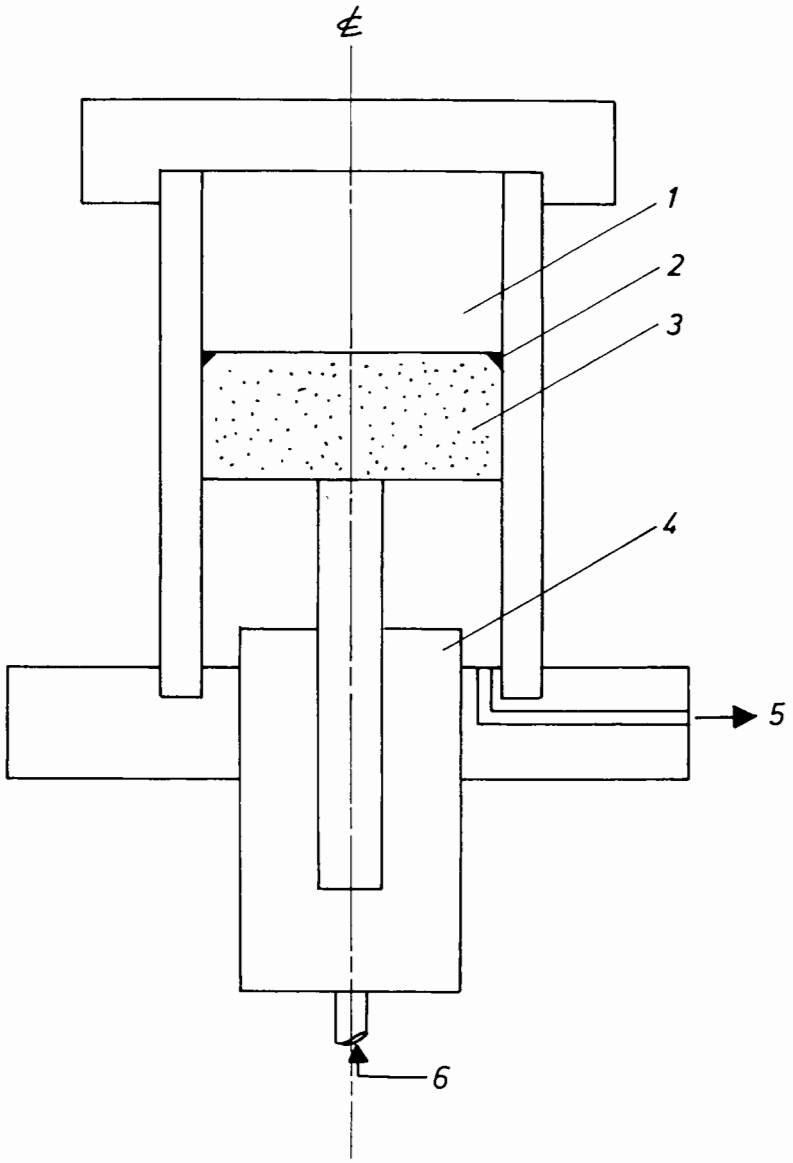

FIG.9.15 Proposed new oedometer design.

1. *specimen*
2. *scraper ring*
3. *porous piston*
4. *bellofram type air cylinder*
5. *back pressure outlet*
6. *air pressure inlet*

APPENDIX A DETERMINATION OF THE COEFFICIENT OF CONSOLIDATION FROM EXPERIMENTAL RESULTS

It is known from Chapter 3 that during the early stages of consolidation the degree of settlement is given approximately by :

$$S = \beta\sqrt{T} \tag{A.1}$$

where S is the degree of settlement, T is the time factor defined as $C_v t/h_o^2$ or $C_F t/h_o^2$. β is a constant which in the C_F constant theory equals $2/(\sqrt{\pi})$ or 1.1284, and in the C_v constant theory this will depend on the magnitude of strain. Its numerical value is given in Table3.1 and is reproduced graphically in Fig.A.1 here.

The theoretical T_s corresponds to $S=1$ using eq(A.1) is :

$$T_s = \frac{1}{\beta^2} \tag{A.2}$$

which in the C_F constant theory equals $\pi/4$ or 0.7854 and in the C_v constant theory this can be calculated. This is shown in the following Table and Fig.A.2 for a quick reference.

λ	0.0	0.1	0.2	0.3	0.4	0.5
0.00	0.7854	0.6872	0.5928	0.5023	0.4159	0.3337
0.01	0.7754	0.6776	0.5836	0.4935	0.4075	0.3258
0.02	0.7654	0.6680	0.5744	0.4847	0.3991	0.3178
0.03	0.7556	0.6585	0.5652	0.4759	0.3908	0.3099
0.04	0.7457	0.6490	0.5562	0.4673	0.3825	0.3031
0.05	0.7359	0.6396	0.5471	0.4586	0.3743	0.2943
0.06	0.7260	0.6302	0.5380	0.4499	0.3661	0.2866
0.07	0.7164	0.6208	0.5291	0.4414	0.3579	0.2789
0.08	0.7066	0.6114	0.5201	0.4328	0.3498	0.2713
0.09	0.6969	0.6021	0.5112	0.4243	0.3417	0.2637

TABLE A.1 NUMERICAL VALUES OF T_s

Having thus determined the theoretical T_s and the experimental t_s the coefficient of consolidation can be obtained by the following equation :

$$T_s = \frac{C_v\ t_s}{h_o^2} \quad or \quad \frac{C_F\ t_s}{h_o^2} \tag{A.3}$$

or : $$C_v\ ,\ C_F = h_o^2\ T_s\ /\ t_s \tag{A.4}$$

which is eq(9.1).

Diffrentiating eq(A.1) leads to :

$$\frac{dS}{dT} = \frac{\beta}{2}\ T^{-\frac{1}{2}} \tag{A.5}$$

Since, $$T = \frac{C_v\ t}{h_o^2} \quad or \quad \frac{C_F\ t}{h_o^2}$$

and, $$S = \frac{h_o - h}{h_o - h_f} = \frac{\Delta}{\Delta_f}$$

eq(A.5) can be rearranged to give :

$$\frac{d\Delta}{dt} = \frac{1}{2}\beta\lambda\ \sqrt{(\frac{C_v}{t})} \tag{A.6}$$

where λ is the final (Lagrangian) strain Δ_f/h_o. The term on the right hand side of eq(A.6) $\frac{1}{2}\beta\lambda\ \sqrt{C_v}$ is the slope measured in the linear portion of the rate of settlement $\frac{d\Delta}{dt}$ against the reciprocal of the square root time $t^{-\frac{1}{2}}$ curve denoted by ψ , see Fig.9.3.

Hence, $$\psi = \frac{1}{2}\beta\lambda\ \sqrt{C_v} \tag{A.7}$$

or : $$C_v = [\frac{2\psi}{\beta\lambda}]^2 \tag{A.8}$$

which is eq(9.2).

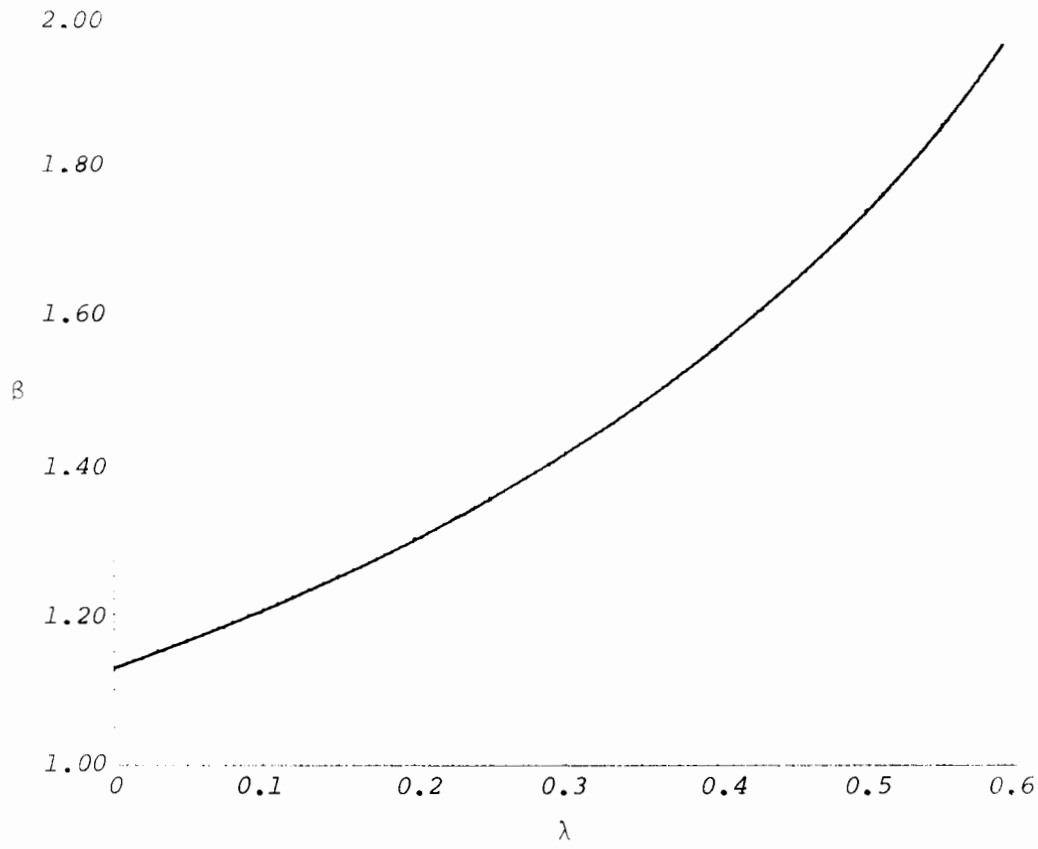
2.00
1.80
1.60
β
1.40
1.20
1.00
0
0.1
0.2
0.3
0.4
0.5
0.6
λ

FIG.A.1

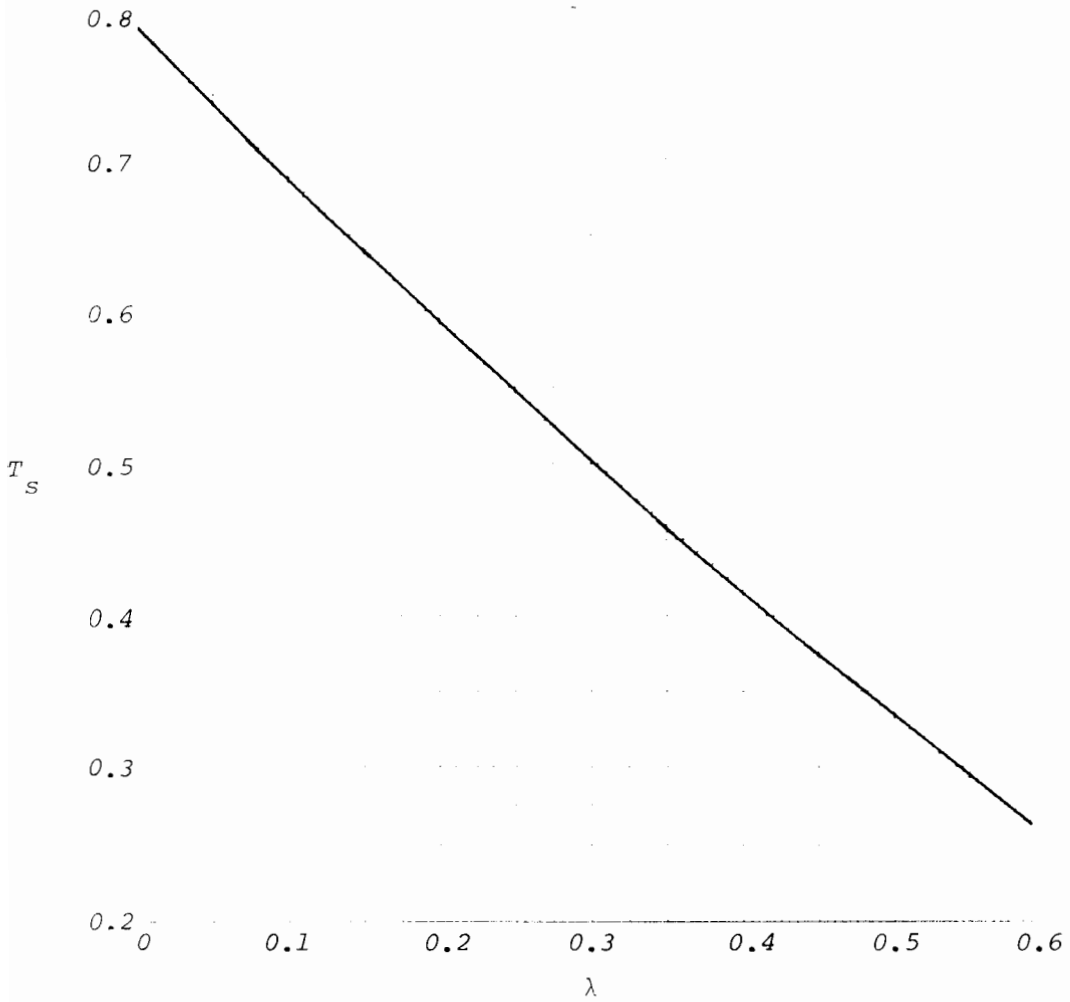
0.8
0.7
0.6
T_s
0.5
0.4
0.3
0.2
0
0.1
0.2
0.3
0.4
0.5
0.6
λ

FIG.A.2

CHAPTER TEN IN CONCLUSION : CONTRIBUTION OF THIS THESIS AND AN OUTLINE OF FUTURE WORK

1. CONTRIBUTION OF THIS THESIS

The Consolidation of a Thin Soil Layer

The thin layer consolidation has been a subject of intensive research in Soil Mechanics. There has been, however, confusion in recent years over large strain consolidation theories as several theories have claimed to be suitable for the case of large strain and yet the coordinate system has not been specified. The present work, particularly Chapter 2 and Chapter 3 of this thesis, may help clarify the situation : that there are two coordinate systems, the space (Eulerian) and the material (Lagrangian) coordinate; in the former case the problem is a moving boundary problem and not only must this be included in the theoretical framework but also special numerical algorithms must be applied.

In view of this, this particular piece of the present work is of considerable importance as it shows how a theory based on the space coordinates can be formulated as well as how the solution can be obtained. For practical applications the c_v constant solution developed in Chapter 3, especially the small time approximate solution, offers a new possibility of interpreting oedometer test results. The results in Chapter 9 show that a more compatible c_v can be obtained by this new method. Further work will be required before this can become accepted practice, and it suffices to conclude here that the future work will prove to be fruitful.

The Consolidation of a Normally Consolidated Stratum

The thin layer is an idealization of a real soil stratum : it assumes that the effect of self weight is negligible in comparison

with that of the consolidation loading. The validity of this assumption must therefore depend on the particular situation involved. Unfortunately, this point of view is very often overlooked in practice, and the acceptance of this assumption has become a rule rather than an exception in current practice. This is partly due to the historical development of consolidation theory and partly due to the complications of taking into account the effect of self weight, for which no such analysis has previously been available.

Chapter 4 and Chapter 6 of this thesis therefore contribute to the present state of knowledge on this particular aspect. The main contributions are summarized as follows :

(1) Whether a stratum can be approximated as a thin layer depends on its stratum coefficient : the smaller this coefficient is, the better will be the approximation.

(2) There will be a difference in consolidation behaviour between the double drainage and the single drainage cases. A stratum with a surface drain will consolidate faster than that with a base drain, and this is most pronounced in a thick, soft stratum.

(3) Although the thin layer theory might, in circumstances where the stratum coefficient is small, closely approximate the total settlement behaviour of a real stratum, this is not so when local consolidation behaviour is concerned. Thus, interpretation of the piezometer or settlement plate reading may not be satisfactory using the thin layer theory. In this case a theory including the effect of self weight is recommended.

The Consolidation of a Dredged Fill and a Deposit Undergoing Continuous Sedimentation

These subjects have not been studied in the case of large strain, so that solutions in this thesis are thus obtained for the

first time. The most interesting point observed in the consolidation of a dredged fill is the effect of drainage boundary conditions. The difference in consolidation rates between the cases with and without a base drain is larger than one might have expected. It is hoped that the availability of these solutions will initiate an experimental and field study, and the provision of a good base drainage condition can be incorporated into standard practice.

In the consolidation of a deposit undergoing continuous sedimentation analytical and numerical solutions have been obtained for the linear and nonlinear soil model respectively. Based on these solutions it is now not only possible to explain the consolidation behaviour of a deposit, but also future predictions can be made. One example of the application of the solutions is given in Chapter 5.

2. IN CONCLUSION

The contribution of this thesis, as described above, is mainly theoretical. Soil consolidation is a very complicated process : the complexity is amply demonstrated in the solutions developed in this thesis. As such, these solutions would have little practical values without simplification. In an effort to achieve this, a number of approximate solutions have been developed and the feasibility of using a simpler theory - such as the thin layer or the linear soil model - is extensively discussed in this thesis. Furthermore, the trends indicated by the solutions have been discussed - which is likely to be more helpful than the equations to the engineers. For example, the effect of the location of the drainage boundary on the consolidation of a stratum has been studied. It can be anticipated, therefore, that

the availability of these solutions to the engineer as a result of the present study will lead to an improvement of the current practice.

Having achieved these, one might ask what should be done in the immediate future. The vast amount of theoretical solutions developed in this thesis calls for an equal amount of experimental and field work. This has been accomplished to a limited extent in the present experimental study, and there is still a great deal of work that has to be done. An outline of some of the possible future developments will be the subject of the next section.

3. FUTURE WORK

The Oedometer Test

A scheme for improving the present oedometer has been proposed in Chapter 9. The author intends to carry out this improvement in the near future. Hopefully, this will produce a near ideal step loading condition so that the result can be compared quantitatively with the theory.

A prerequisite for a quantitative study is that the stress - strain and permeability characteristics of the soil must be determined from direct measurement. The stress - strain characteristic can be determined either by the step loading test or by the flow restrictor test. The determination of permeability is more difficult, especially with very soft clay, and new testing methods will be required. A suitable method will now be described in the following section.

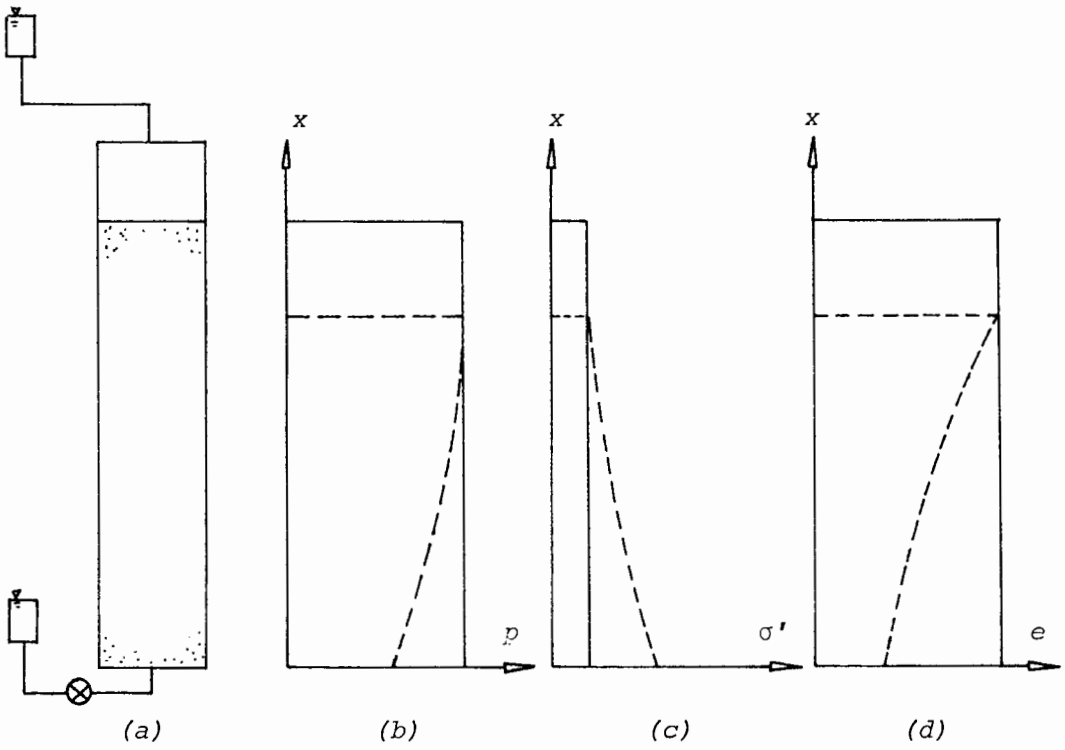

FIG.10.1 The seepage consolidation test

The Seepage Consolidation Test

The proposed method uses seepage force to consolidate a soil column. This is illustrated by considering a conventional constant head permeability test as shown in Fig.10.1(a). A soil column with an initially uniform density is connected at its upper end to a higher pressure source, and its lower end is connected by a tap to a constant head tank. Referring to Fig.10.1(b), the solid line indicates the pore water pressure in the soil column before the tap is opened, where the hydrostatic gradient and the weight of the soil are omitted here for simplicity. Some time after opening the tap a steady state seepage will be established in the soil column, and the pore water pressure in this state is now given schematically by the dotted line of Fig.10.1(b). The change in pore water pressure causes a corresponding change in effective stress (since the total stresses are unchanged). Thus, the process in reaching the final steady state is a consolidation process. The variation in effective stress and void ratio within the soil column

is shown schematically in Fig.10.1(c),(d).

The final equilibrium condition depends on the permeability and the stress - strain characteristics of the soil. Since in this condition there is a steady state seepage, thus by Darcy's law :

$$\frac{k}{\rho_f}\frac{du}{dx} = v = constant \qquad (10.1)$$

Knowing the final pore pressure distribution by measurement at points throughout the column, and the seepage velocity, it is then possible to calculate the permeability within the soil column according to eq(10.1). If the void ratio distribution can be measured at the same time then the required permeability - void ratio relationship is obtained. Furthermore, referring to Fig.10.1(c), since the effective stress is uniquely linked to the pore water pressure, the above information also yields the stress - strain characteristic of the soil.

The equipment for performing this experiment is now in its final development stage. The column is built from a four inch diameter acrylic tube, 500mm high, with 12 pore pressure probes installed in the side. These probes are connected to manifold blocks which are in turn connected to a pressure transducer. The top of the column will be connected to a pressure regulator, and the base of the column is connected to a conventional constant head tank. The void ratio of the soil will be accurately determined using X-ray techniques developed at Oxford.

REFERENCES

Abramovitz, M., and Stegun, I.A. , 1961
'Handbook of mathematical functions'
U.S. Government Printing Office, Washington,D.C.

Berry, P.L., and Poskitt, T.J., 1972
'The consolidation of peat'
Geothchnique 22:1:27-52

Biot, M.A., 1935 'Le probleme de la consolidation des matieres argileuses sous une charge'
Annales de la Societe Sci de Bruxelles
Ser. B55, 110-113

Bishop, A.W., and Henkel, D.J., 1962
'The measurement of soil properties in the triaxial test'
Edward Arnold, London (2nd edition)

Carslaw, H.S., and Jaeger, J.C., 1948
'Operational methods in applied mathematics'
Oxford University Press, London. (2nd edition)

Carslaw, H.S., and Jaeger, J.C., 1959
'Conduction of heat in solid'
Oxford University Press, Oxford

Cox, D.R., and Miller, H.D., 1965
'The theory of stochastic processes'
Chapman Hall, London

Crank, J., 1970 'Mathematics of diffusion'
Oxford University Press, Oxford, (2nd edition)

Crank, J., and Gupta, R.S., 1972a
'A moving boundary problem arising from the diffusion of oxygen in absorbing tissue'
J. Inst. Maths. Applics., 10:19-33

Crank, J., and Gupta, R.S., 1972b
'A method for solving moving boundary problems in heat flow using cubic splines or polynomials'
J. Inst. Maths. Applics., 10:296-304

D'Elia, B., and Grisolia, M., 1974
'On the behaviour of a partially floating foundation on normally consolidated silty clays'
Proc. Conf. on the Settlement of Structures
Pentech Press, pp.91-98

De Simone, P., and Viggiani, C., 1976
'Consolidation of thick bed of clay'
Proc. 2nd Int. Conf. Numerical Method in Geomechanics, 1:1067-1081

Douglas, J.J., and Dupont, T., 1973
'A finite element collocation method for quasilinear parabolic equations'
Mathematics of Computation, 27:121:17-28

Erdelyi, A., (editor) 1954
'Table of integral transforms'
Vol. 1, Bateman Manuscript Project
McGraw-Hill, N.Y.

Feller, W., 1966
'An introduction to probability theory and its application'
John Wiley & Sons, N.Y. (2 volumes)

Fox, E.N., 1948
'The mathematical solution for the early stages of consolidation'
Proc. 2nd Int. Conf. Soil Mech., 1:41-42

Gear, C.W., 1971
'Numerical initial value problems in ordinary differential equations'
Prentice Hall, New Jersey

Gibson, R.E., 1958
'The progress of consolidation in a clay layer increasing in thichness with time'
Geotechnique, 8:2:171-182

Gibson, R.E., England, G.L., and Hussey, M.J.L., 1967
'The theory of one dimensional consolidation of saturated clays. I. Finite nonlinear consolidation of thin homogeneous layers'
Geotechnique, 17:3:261-273

Girault, P., 1072 'Settlement of some piled foundations in Mexico' Proc. Conf. Performance of Earth and Earth Supported Structures, 2:1185-1205

Goodwin, E.T., 1949 'The evluation of integrals of the form $\int_{-\infty}^{\infty} f(x)e^{-x^2}dx$' Proc. Cam. Phil. Soc., 45:241

Holmgren, E., 1908 Arkiv fur Matematik, 4:18:8-12

Ladd, C.C., 1972 'Test embankment on sensitive clay' Proc. Conf. Performance of Earth and Earth Supported Structures, 1:101-128

Lebedev, N.N., 1965 'Special functions and their applications' Prentica Hall, N.Y.

Lee, K., 1977 'Consolidation with imperfectly permeable drainage boundary' Paper submitted for the British Geotechnical Society Cooling Prize Competition, September, 1977

Leonard, G.A., and Altschaeffl, A.G., 1964 'Compressibility of clays' Proc. ASCE, 90:SM5:133-156

Mikasa, M., 1963 'Consolidation of soft clay' Kashima Shappan-Kai Publishing Co., Tokyo

Mitchell, A.R., Wait, R., 1977 'The finite element method in partial differential equations' John Wiley & Sons, London

Monte, J.L., and Krizek, R.J., 1976 'One dimensional mathematical model for large strain consolidation' Geotechnique, 26:3:495-510

Murray, W.D., and Landis, F., 1959
'Numerical and machine solutions of transient heat conduction problems involving melting or freezing. Part I Method of analysis and sample solutions'
J. Heat Transfer, Trans. ASME
Vol. 81, Series C, 2:106-112

McNabb, A., 1960 'A mathematical treatment of one dimensional soil consolidation'
Q. Appl. Maths., 17:4:337-347

Ockendon, J.R., and Hodgkins, W.R., (editors) 1975
'Moving boundary problems in heat flow and diffusion'
Oxford University Press, Oxford

Poskitt, T.J., 1969 'The consolidation of saturated clay with variable permeability and compressibility'
Geotechnique, 19:2:234-252

Rubinstein, L., 1967 'The Stefen problem'
Trans. Math. Monogrphs 27, American Mathematical Society

von Rosenberg, D.U., 1969
'Method for the numerical solution of partial differential equations'
American Elsevier Publishing Co. Inc., N.Y.

Sanglerat, G., Girousse, L., and Gielly, J., 1974
'Unusual settlements of a building at Nantua (France)'
Proc. Conf. Settlement of Structures
Pentech Press, pp123-131

Sills, G.C., 1972 'Coupled and uncoupled theories of soil consolidation and their relevance in practice'
Ph.D. thesis, London University

Smirnov, V.I., 1964 'Integral equations and partial differential equations' in Vol. 4 of 'A course of higher mathematics'
Pergamon Press, Oxford

Squire, W., 1970 'Integration for engineers and scientists' American Elsevier Publishing Co., Ltd., N.Y.

Taylor, H.T., and Buchignani, A.L., 1972 'Field test of debris fill over soft soil' Proc. Conf. Performance of Earth and Earth Supported Structures, 1:395-413

LIST OF PROGRAMS